

## Doctoral Thesis

# Isolation and *ex-vivo* Activation of Adipose-derived Cells

submitted in satisfaction of the requirements for the degree of  
Doctor of Natural Sciences  
at the Vienna University of Technology, Faculty of Technical Chemistry  
under the supervision of

Univ. Prof. Dipl.-Ing. Dr. Heinz Redl  
Institute of Chemical, Environmental and Bioscience Engineering

submitted by:

Julia Maier, MSc

Matriculation Number: 01556383

Study Index: E 791 800

Julius-Raab-Straße 19, 4040 Linz

I faithfully declare, that I have written this thesis independently and without outside help. I have only used the sources which are quoted in the reference and I have marked the pages taken, either directly or as regards content from the sources.

The thesis was in this or similar style never shown to another board of examiners nor it was published.



.....  
Julia Maier

Vienna, September 2019

‘Science is about knowing;  
Engineering is about doing.’

Henry Petroski

I want to thank Heinz Redl for giving me the opportunity to do my PhD thesis at the LBI Trauma and for believing in me that it will be a successful project. My gratitude goes to Susanne Wolbank for her support during the course of the PhD project and to all members at the LBI, who contributed to make this possible, especially to my team at the LBI Linz.

Special thanks to Eleni Priglinger for pushing my limits, for always making me go further and for enabling me to reach beyond my boundaries.

And last but not least many thanks to my beloved family and friends, especially my parents and Sandra Rutzetschin, for standing by my side and supporting me in every situation during the PhD project, for not judging me and dealing with my mood swings.

Finally, yet importantly: Thank you to all the people who made it possible for me to write this thesis!

## I. Abstract

In recent years stem cell research has become increasingly important for regenerative medicine and tissue engineering. The isolation of stem cells from adipose tissue evades ethical concerns with which embryonic stem cells and induces pluripotent stem cells (iPS) are afflicted, because of its declaration as clinical waste material. Tumescence liposuction is a minimally invasive procedure providing high amounts of adipose tissue rich in therapeutically relevant cells within a short time. The isolated stromal vascular fraction (SVF) and the adipose derived stromal/stem cells (ASC) contained therein show a high regenerative potential and have been successfully used in many clinical studies. Maintaining SVF cells in their natural environment and therefore providing the maximum possible regenerative potential of adipose tissue-derived cells is a prerequisite for successful autologous clinical application. With an improved gentle and fast isolation process by minor manipulation it is possible to obtain a therapeutically relevant cell population. A physical stimulus already used in clinics is the extracorporeal shockwave therapy (ESWT), shockwaves are characterized by their high rise in pressure within a very short time followed by cavitation wave with a negative amplitude. By applying low-energy ESWT on freshly obtained human liposuction material and isolated SVF cells (*in vitro*) we aimed to equalize and enhance stem cell properties and their functionality. We were able to show an increased adenosine tri-phosphate (ATP) concentration after applying ESWT on adipose tissue as well as a significantly increased expression of single mesenchymal and vascular surface markers in comparison with the untreated group. Additionally, the protein secretion of insulin-like growth factor 1 (IGF-1) and placental growth factor (PLGF) was significantly enhanced. Further it was investigated if there is the same beneficial effect when applying ESWT on the adipose tissue harvest site before liposuction to improve cell properties *in situ*. We showed a significantly enhanced viability, ATP concentration and population doublings after 3 weeks in culture for cells isolated from ESW treated adipose tissue harvest site. Further the expression of mesenchymal and endothelial/pericytic markers was elevated collaborating with the increased angiogenic differentiation potential as well as the increased secretion of certain angiogenic proteins after ESWT *in situ*. Besides ESWT the effect of another physical stimulus on SVF/ASC cells was tested - Low level laser therapy (LLLT) has already shown beneficial effects. Therefore, we investigated effects of pulsed blue (475nm), green (516nm) and red (635nm) light from light-emitting diodes (LEDs) applied on freshly isolated SVF cells. Cells had a stronger capacity to vascular tube formation after exposure to green and red light concomitant with an increased concentration of vascular endothelial growth factor (VEGF) in the secretome. In a side project during the PhD program the hormone-related women's disease lipedema was investigated. The SVF cell properties of healthy and lipedema patients were investigated and a significant enhancement in cell yield as well as a reduction in adipogenic differentiation capacity of lipedema SVF cells was revealed. Within this work different physical forces applied on adipose tissue and adipose tissue-derived cells were presented as well as an improved isolation method and characteristics of degenerated adipose tissue. This are promising applications for the clinical use in the field of regenerative medicine and tissue regeneration.

## II. Kurzfassung

In den letzten Jahren gewann die Stammzellforschung immer mehr an Bedeutung für die regenerative Medizin und im Bereich Tissue Engineering. Die Isolation von Stammzellen aus humanem Fettgewebe umgeht ethische Probleme mit welchen embryonale und induzierte pluripotente Stammzellen (iPS) behaftet sind durch ihre Deklaration als klinisches Abfallmaterial. Die Tumescenzliposuktion ist ein minimal invasiver Eingriff mit welchem eine große Menge Fettgewebe reich an therapeutisch relevanten Zellen innerhalb kurzer Zeit gewonnen werden kann. Die daraus isolierte stromale vaskuläre Fraktion (SVF) und die darin enthaltenen Stammzellen (adipose derived stromal/stem cells – ASC) weisen ein sehr hohes Regenerationspotential auf und wurden bereits in mehreren klinischen Studien erfolgreich eingesetzt. Die Voraussetzung für eine erfolgreiche klinische Anwendung von autologen Zellen aus dem Fettgewebe ist das höchst mögliche Regenerationspotential der SVF, welches durch den Verbleib der ASC in ihrer natürlichen Umgebung erreicht werden kann. Mit einer verbesserten, sanften und schnellen Isolation kann diese therapeutisch relevante Zellpopulation unter minimaler Manipulation gewonnen werden. Ein physikalische Stimulationsmethode, welche bereits klinisch angewendet wird, ist die extrakorporale Stoßwellen Therapie (ESWT). Das charakteristische Stoßwellenprofil zeichnet sich durch ihren sehr schnellen und starken Druckanstieg, gefolgt von einer Kavitationswelle mit einer negativen Amplitude, aus. Durch die Anwendung von niedrig-energetischer ESWT auf frisches Liposuktionsmaterial sowie isolierte SVF Zellen (*in vitro*) haben wir versucht deren Stammzeleigenschaften und Funktionalität anzugleichen und zu verbessern. Wir konnten eine erhöhte Adenosin Tri-Phosphat (ATP) Konzentration sowie eine signifikant erhöhte Expression von einzelnen mesenchymalen und vaskulären Oberflächenmarkern im Vergleich mit der Kontrollgruppe nach einer ESWT Behandlung zeigen. Zusätzlich war die Sekretion der Proteine Insulin-ähnlicher Wachstumsfaktor (IGF-1) und des Plazenta-Wachstumsfaktors (PLGF) signifikant erhöht. Des Weiteren haben wir untersucht ob diese positiven Effekte bezüglich zellulärer Eigenschaften ebenfalls auftreten, wenn die Liposuktionsstelle vor der Absaugung einer ESWT unterzogen wird (*in situ*). Wir konnten ein signifikant erhöhte Zellviabilität, ATP Konzentration und Populationsverdopplungen nach 3 Wochen in Kultur zeigen bei Zellen, welche aus *in situ* behandeltem Gewebe isoliert wurden. Weiters war die Expression von mesenchymalen und endothelialen/perizyten Oberflächenmarkern erhöht, was wiederum mit einem erhöhten adipogenen Differenzierungspotential und einer erhöhten Sekretion von angiogenen Proteinen nach einer ESWT *in situ* einhergeht. Neben der ESWT wurde eine weitere physikalische Zellstimulationsmethode getestet – die Low Level Laser Therapie (LLLT), welche bereits positive Effekte gezeigt hat. Wir haben den Effekt von gepulstem blauen (475nm), grünem (516nm) und rotem (635nm) Licht von Licht-emittierenden Dioden (LEDs) auf frisch isolierte SVF Zellen untersucht. Zellen zeigten eine stärkere Kapazität zur vaskulären Gefäßneubildung nach der Behandlung mit grünem und rotem Licht, parallel mit einer erhöhten Konzentration des vaskulären endotheliale Wachstumsfaktors (VEGF) im Sekretom. In einem Nebenprojekt wurde die hormonbedingte Frauenkrankheit Lipödem untersucht. Bei der Untersuchung der SVF Zelleigenschaften von gesunden und Lipödem Zellen hat sich eine signifikant erhöhte Zellausbeute sowie eine Reduktion des

adipogenen Differenzierungspotentials bei Lipödem SVF Zellen gezeigt. Im Zuge dieser Arbeit wurden verschiedene physikalische Stimulationsmethoden für Fettgewebe und deren Zellen vorgestellt, sowie eine verbesserte Isolationsmethode und Charakterisierung von entartetem Fettgewebe. Diese Arbeit zeigt vielversprechende Anwendungen für den klinischen Einsatz in der regenerativen Medizin sowie im Tissue Engineering.

### III. Table of Content

I. Abstract .....	IV
II. Kurzfassung .....	V
III. Table of Content .....	VII
1. Introduction .....	9
1.1. General Introduction .....	9
1.1.1. Stem Cells .....	9
1.1.2. Adult Stem Cells .....	11
1.1.3. Adipose Tissue – An Abundant Source for Adult Stem Cells .....	13
1.1.4. Stromal Vascular Fraction (SVF) .....	15
1.2. Specific Introduction .....	17
2. Aim of This Study .....	20
3. Methods .....	21
3.1. Cell Isolation .....	21
3.2. Extracorporeal Shockwave Therapy (ESWT) .....	21
3.3. Low Level Light Therapy .....	21
3.4. Cell Yield and Viability .....	21
3.5. Surface Marker Profile Analysis .....	22
3.6. Cellular Adenosine Tri-Phosphate (ATP) .....	22
3.7. Cytotoxicity .....	23
3.8. Proliferation, Clonogenic Potential and Morphology .....	23
3.9. Secretory Profile Analysis .....	24
3.10. Vascularization Potential .....	24
3.11. Differentiation Potential .....	25
3.12. Immunofluorescence Staining .....	25
3.13. Histological Staining .....	25
3.14. <i>In Vivo</i> Analysis .....	26
4. Summary of Publications .....	27
4.1. Adipose Tissue-Derived Therapeutic Cells in Their Natural Environment as Novel Autologous Cell Therapy Strategy: The Microtissue-Stromal Vascular Fraction .....	27
4.2. Improvement of Adipose Tissue-Derived Cells by Low-Energy Extracorporeal Shockwave Therapy .....	29
4.3. Extracorporeal Shock Wave Therapy <i>in situ</i> – A Novel Approach to Obtain an Activated Fat Graft .....	31

4.4.	<b>Photobiomodulation of Freshly Isolated Human Adipose Tissue-Derived Stromal Vascular Fraction Cells by Pulsed Light-Emitting Diodes for Direct Clinical Application</b> .....	33
4.5.	<b>The Adipose Tissue-Derived Stromal Vascular Fraction Cells from Lipedema Patients: Are They Different?</b> .....	35
4.6.	<b>Conference Talks and Poster Presentations</b> .....	37
5.	<b>Discussion</b> .....	38
IV.	<b>List of Figures</b> .....	XL
V.	<b>List of Tables</b> .....	XL
VI.	<b>Abbreviations</b> .....	XL
VII.	<b>Literature</b> .....	XLII
VIII.	<b>Appendix</b> .....	LII



# 1. Introduction

## 1.1. General Introduction

The general introduction is focusing on the properties und functionality of stem cells especially of the stromal vascular fraction (SVF) and adipose derived stromal/stem cells (ASC).

### 1.1.1. Stem Cells

Stem cells are significant for the genesis and maintenance of an organism. They have the ability to stay in quiescence (unspecialized until differentiation) and/or self-renew simultaneously. This self-renewed daughter cell is necessary to maintenance the stem cell pool. The differentiated daughter cell (progenitor cell) is determined to proliferate in order to form a larger pool of specialized cells or differentiate into a more specialized precursor cell, which are committed to differentiate into a distinct cell lineage. For example, hematopoietic precursor cells can only differentiate towards the hematopoietic lineage. When cells are injured, mutated or in a senescent state within an organism they need to be replaced. This is a natural process in an organism where these injured, mutated or senescent cells undergo the programmed cell death (apoptosis) and have to be replaced by new cells. Figure 1 illustrates the self-renewal and differentiation potential of a stem cell [1-3].

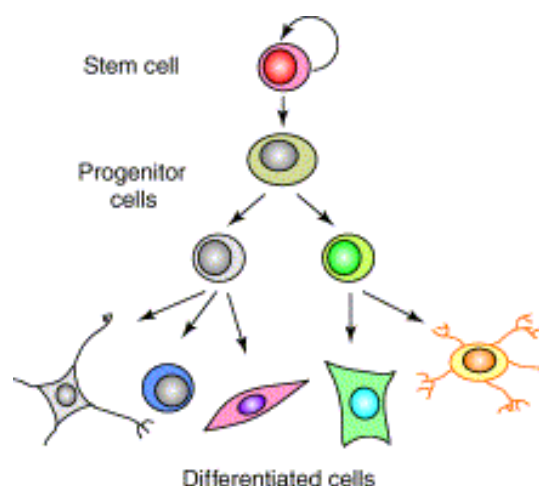


**Figure 1. Self-renewal and differentiation potential of a stem cell [2].**

*A stem cell is able to self-renew and/or differentiate. In a first step progenitor cells are formed, further giving rise to precursor cells, which become in the end terminally differentiated cells.*

For maintaining stem cells properties, they need a proper, specific and individual microenvironment: The stem cell niche, which is a dynamic and complex system communicating through either cellular or acellular substances. After an injury, this microenvironment induces self-renewal and differentiation in cells to form new tissues. As every stem cell has other requirements to its niche, a variety of components for the niche are necessary, for example, soluble factors, a vascular network, stromal cells, an extracellular matrix, cell adhesion components and the stem cell itself among others [4-6]. Figure 2 illustrates the concept of a stem cell niche.

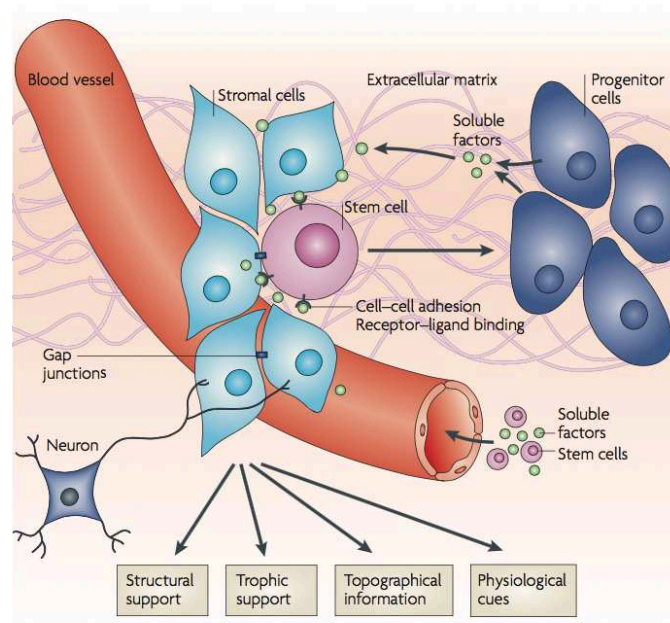


**Figure 2. Components and functions of stem cell niches [4].**

*A stem cell niche is a complex structure - some elements are necessary other components are optional, but every stem cell has its own demands for its niche. Elements of a stem cell niche are: Extracellular matrix components, stromal cells, progenitor cells, soluble factors, receptor binding sites, blood vessels and neurons. Within the niche, stem cells are maintaining their unique properties and functions accomplished by structures and factors building the niche and surrounding the stem cells.*

Due to the different requirements, origin and capacities of stem cells during embryogenesis and their lifecycle, stem cells are divided into different groups. Embryonic stem cells (ESC) can give rise to all cell types (they are totipotent) and are found in the embryo. After completing the genesis of an organism, the remaining stem cells are termed adult stem cells and are tissue specific. Adult stem cells have the ability to self-renew and/or differentiate and they are committed to a specific lineage. For example, adult stem cells with hematopoietic origin are able to renew all cell types in the blood. Adult stem cells are accountable for the regeneration of injured and damaged tissue in addition to tissue homeostasis. Besides ESC and adult stem cells, there are induced pluripotent stem cells (iPS), which are used for research purposes [7-

9]. The group of Yamanaka and colleagues were the first who could reprogram fibroblasts and dedifferentiate them into stem cells by retroviral induction of four genes (Oct3/4, Sox2, c-Myc, and Klf4) [7].

### 1.1.2. Adult Stem Cells

Stem cell research still is the most controversial topic in research [10]. ESC and iPS are tormented with many ethical, legal and political concerns. ESC used in stem cell research are donated by women undergoing *in vitro* fertilization (IVF) [11]. In Austria the research on human embryos is prohibited (FMedG StF: BGBl. Nr. 275/1992 (NR: GP XVIII RV 216 AB 490 S. 69. BR: AB 4255 S. 553.)). The genome needs to be manipulated to generate cells with the ability to differentiate into more cell types, which is another drawback afflicted with concerns [7]. To elude these concerns, the focus was set on adult stem cells. Sabin showed 1932 that there are cells with the ability to recover the hematopoietic system after radiation in the adult human body. The regeneration potential on lymph nodes and lymphocytes besides bone marrow (BM) and red blood cells was shown [12]. In the 1950`s, Thomas et al. first described hematopoietic stem cells from BM. Thomas and colleagues destroyed the BM from rodents with a lethal dose of radiation and intravenously injected cellular suspensions of BM afterwards. Their results clearly suggested the presence of stem cells with the ability to reinstate hematopoiesis [13]. In 1966, Friedenstein and colleagues described a new adult stem cell type within the BM. Besides the already known hematopoietic stem cells, they found BM-mesenchymal stromal/stem cells (BM-MSC). These BM-MSC have the capacity to self-renew, adhere on plastic surfaces and differentiate into the mesodermal lineages (including fat, cartilage, bone, tendon and muscle), which is illustrated in Figure 3 [14-17].

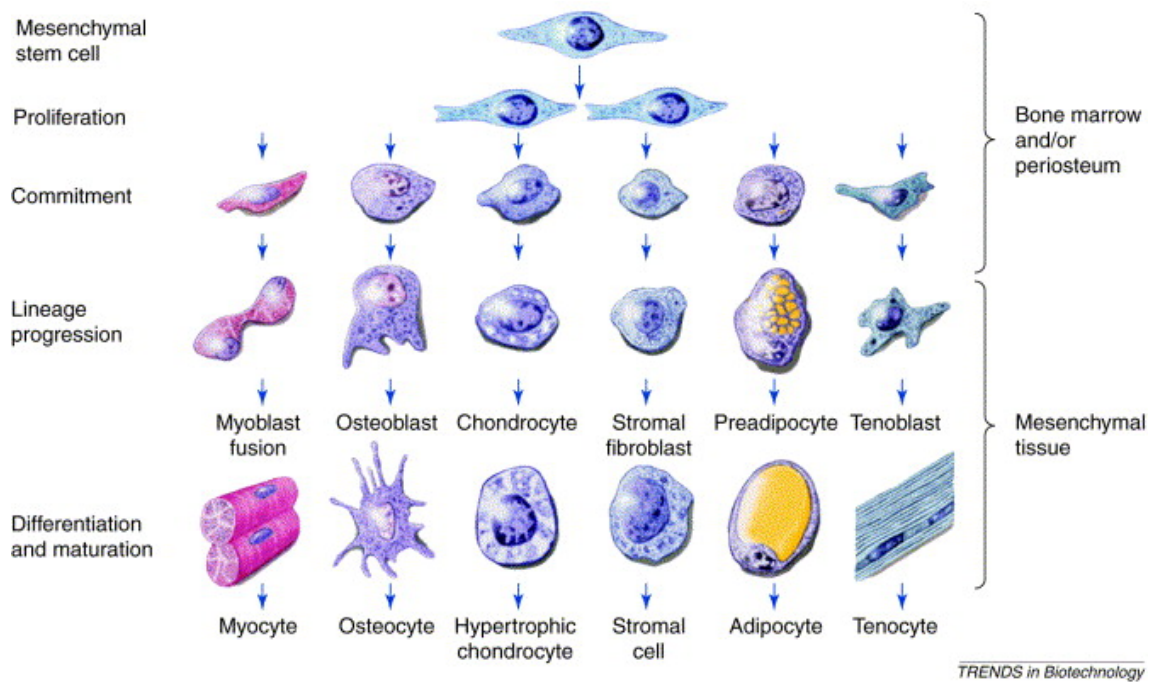


**Figure 3. The mesengenic process [18].**

The mesengenic process of mesenchymal stem cells (MSC) involves cell proliferation, commitment, lineage progression, differentiation and maturation. MSC are capable to differentiate into different cell types from the mesodermal lineage like myocytes, osteocytes, hypertrophic chondrocytes, stromal cells, adipocytes and tenocytes, therefore they are able to form muscle, bone, cartilage, marrow, fat and tendon.

BM-MSC are referred as the golden standard for MSC and have been extensively used for stem cell research and tissue engineering since their discovery [15, 16, 19, 20]. Harvesting BM is an invasive procedure and, therefore, arguable as a source for MSC. As an alternative to BM, more MSC sources were found in numerous tissue types like muscle, skin, placenta, blood, cord blood, connective tissue, adipose tissue, periosteum, perichondrium or synovium [16, 21-34]. Figure 4 illustrates the differentiation potential of stem cells derived from different sources.

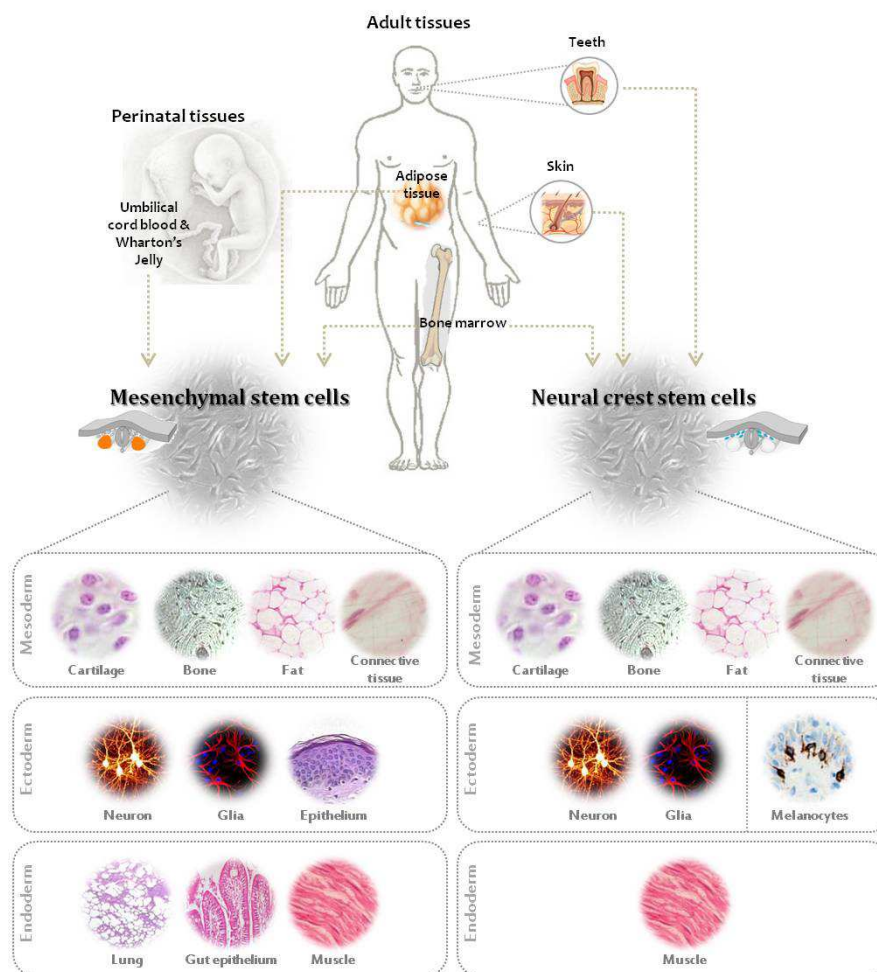


**Figure 4. Different sources of adult stem cells and their differentiation potential towards the meso-, ecto-, and endodermal lineage [35].**

Adult stem cells obtained from adipose tissue, bone marrow or umbilical cord blood are able to differentiate into the mesodermal lineage (cartilage, bone, fat and connective tissue). Furthermore, these stem cells can also differentiate to cells from the ectodermal lineage (neurons, glia cells and epithelium) and the endoderm (cells from the lung, gut epithelium and muscle cells). Neural crest stem cells from teeth and skin can also differentiate towards the mesodermal lineage (cartilage, bone, fat and connective tissue), ectoderm (neurons, glia cells and melanocytes) and endoderm (muscle).

### 1.1.3. Adipose Tissue – An Abundant Source for Adult Stem Cells

Adipose tissue is organized in subcutaneous and visceral depots all over the human body with a complex shape. It is separated into brown and white adipose tissue with distinct functions and localizations. The distribution of brown and white adipose tissue depends on various factors including age, sex, nutritional status, and it is genetically determined [36]. White adipose tissue is recognized for its function in energy storage, the transport of lipids and glucose, synthesis and mobilization of fatty acids, regulation of insulin sensitivity and for its endocrine function by secreting adipokines. Energy is stored in form of triglycerides by white adipose tissue. The accumulation of fat is either attained by the uptake of fatty acids or by

lipogenesis (formation of fatty acids from glucose) [37, 38]. Brown adipose tissue is maintaining the body temperature by converting energy to heat in a process called non-shivering thermogenesis [39, 40]. Adipose tissue is a connective tissue consisting of adipocytes, a heterogeneous cell mixture (the stromal vascular fraction - SVF) and extracellular matrix components. Due to its adipokine and leptine secretion it is defined as an endocrine organ [41-43]. Adipose tissue is involved in biological processes like homeostasis regulation, energy metabolism and has immune- and neuroendocrine functions. Besides its function in energy storage and release, it is communicating with distant organs including the central nervous system. Due to the expression of receptors, adipose tissue can respond to signals from the hormone system as well as the central nervous system [41, 44-46].

In 2001, Zuk et al. were the first who discovered adipose tissue as a new promising source for adult stem cells. These stem cells are called adipose derived stromal/stem cells (ASC) and have similar characteristics and differentiation potential like BM-MSC [47] and the cell proliferation rate is higher in comparison with BM-MSC [48]. Adipose tissue as a source for stem cells evades ethical concerns because it is usually discarded as clinical waste material. Besides that, the increasing number of liposuction procedures for cosmetic reasons without general anesthesia [49] makes the application of adipose tissue-derived cells for reconstructive and regenerative medicine even more appealing. At the beginning, lipoaspirate was used as a filler in plastic and reconstructive surgery. Later, the application of adipose tissue as autologous fat graft for the treatment of various tissue defects surfaced. Soft tissue defects can be caused by trauma, congenital anomalies, tumor extirpation or simply by aging. In 1938 Neuber et al. reported the first corrections of soft tissue defect by fat grafting [50-55] and its beneficial effect could be partially proven for adipose tissue atrophy, rejuvenation, body contour improvement and breast augmentation after mastectomies [56-63]. But until now the long-term survival rates of fat grafts vary to high degrees [51-54, 64]. Despite the constantly further development of fat grafting procedures, there are certain drawbacks such as fat resorption, limited survival of grafts leading to partial necrosis, fibrosis and calcification [65]. For targeting the earlier mentioned drawbacks, the survival rate of the transplanted fat graft has to be improved by guaranteeing a sufficient nutrition supply due to an early and abundant vascularization and the integration inside the surrounding tissue [62, 66-70]. Fat grafts enriched with therapeutically relevant cells derived from the adipose tissue can improve the long-term survival rate. This method, where adipose tissue combined with cells derived thereof and then transplanted, is called cell assisted lipotransfer (CAL) [71]. It has already been shown that CAL enhances angiogenesis of the fat grafts [58, 60, 62, 72-74] and it can reduce postoperative atrophy in breast augmentations [75]. Adipose tissue and its therapeutically relevant cells are a promising tool for reconstructing and regenerating diseased or damaged tissue when common therapy fails. ASC have shown regenerative potential *in vitro*, in animal models and in clinical studies for several applications like cardiovascular diseases, gastrointestinal diseases, neurological diseases, diabetes and the treatment of immune diseases as well as soft tissue reconstruction and bone and cartilage regeneration with variable

success [76, 77]. Therefore, adipose tissue and the cells derived thereof are a very promising source in the field of regenerative medicine and tissue engineering.

### 1.1.4. Stromal Vascular Fraction (SVF)

The stromal vascular fraction (SVF) isolated from adipose tissue is a heterogeneous cell population consisting of MSC, which are named ASC, hematopoietic stem cells and endothelial progenitor cells. Additionally, endothelial cells, erythrocytes, fibroblasts, lymphocytes, monocyte/macrophages, pericytes and further cell types are included. Figure 5 illustrates the composition of adipose tissue and the SVF [78, 79].

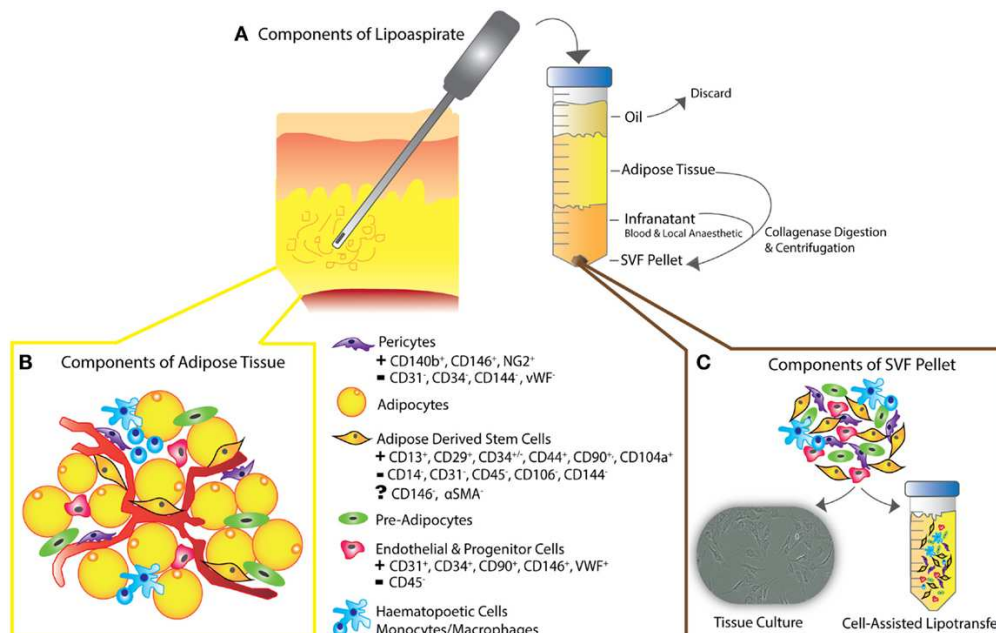


**Figure 5. Composition of adipose tissue and the stromal vascular fraction (SVF) [80].**

When adipose tissue or lipoaspirates are collected and centrifuged, a separation of the fatty portion, liquid portion and a pellet is obtained. The cell pellet is called stromal vascular fraction (SVF) and is a heterogeneous mixture of cells – containing mature (adipocytes, fibroblasts, smooth muscle-, endothelial- and blood cells), progenitor (endothelial progenitor cells, preadipocytes, vascular progenitors and hematopoietic progenitor cells) and stem cells (mesenchymal stem cells, hematopoietic stem cells, pericytes and supra-adventitial cells) among others.

ASC can be isolated from the SVF by *in vitro* cultivation on plastic surfaces. This results in the accumulation of cells characterized by their self-renewal potency and their ability to give rise to at least the adipocytic, osteoblastic and chondrocytic lineages [47]. SVF and ASC could prove their regenerative potential by treating soft tissue defects [63, 71, 81, 82], immune disorders [83, 84], gastrointestinal lesions [85], bone defects [86, 87], neurological injuries [88] and cardiovascular diseases [89].

To obtain a uniform nomenclature and characterization of cells isolated from adipose tissue, the International Federation for Adipose Therapeutics and Science (IFATS) in cooperation with the International Society for Cellular Therapy (ISCT) established a document with the purpose to define SVF and ASC. IFATS is a non-profit scientific society, with their aim to establish collaborations within in the field of adipose tissue research. ISCT is a global association with the focus to translate cell-based research into clinical therapies improving the patient's life. For the definition of SVF and ASC, IFATS and ISCT postulated characteristics such as differentiation potential and immunophenotype. ASC are expected to have the capacity to differentiate into adipocytes, chondrocytes and osteocytes. For the immunophenotypic characterization, distinct cell surface markers (cluster of differentiation / CD) should be positive or negative in a defined combination and expression level for identifying SVF and ASC [78]. Selected surface marker profiles of SVF and ASC is depicted in Table 1.

**Table 1. Surface marker profile for SVF and ASC [78, 90].**

*The most important surface markers for SVF and ASC are shown. There is a defined combination of positive and negative markers.*

surface marker	SVF	ASC
<b>CD31</b> (a classical marker for endothelial cells and their progenitors)	+/-	+/-
<b>CD34</b> (stem cell/progenitor cell marker in hematopoietic lineage and endothelial cells)	+	+/-
<b>CD45</b> (cells from hematopoietic origin except for red blood cells)	+	-
<b>CD73</b> (stromal cell marker, mesenchymal marker)	+/-	++
<b>CD90</b> (stem cell progenitor maker, mesenchymal marker, stromal cell marker)	+/-	++
<b>CD105</b> (mesenchymal marker)	+/-	++
++ = > 70%, + = > 30-70%, +/- = >2-30%, - =<2%		



## 1.2. Specific Introduction

Over the last two decades, adipose tissue has become more and more attractive as easily obtained and autologous source of adult stem cells with regenerative potential in the field of tissue engineering and regenerative medicine [91]. The interaction of cells from inside the fat grafts and the surrounding tissue triggers repair mechanisms by the release of cytokines, growth factors and immunomodulatory proteins. For example, ASC are able to migrate to damaged areas of the body where they are facilitating tissue repair [76, 92-101]. Its immunomodulatory and angiogenic potential is underlined by their induction of a local regulatory, pro-regenerative immune cell phenotype and the recruitment of vessels by the SVF (reviewed by [102]).

In the last years there has been a shift towards using the total SVF cell population, following the concept of an intraoperative procedure and bringing autologous cells back into the patient without further processing. In terms of CAL, the addition of SVF has successfully been established in fat grafting with the effect of enhancing long-term graft stability [58, 60]. Providing a clinical grade product is a critical requirement for the application of ASC or SVF. In contrast to SVF, ASC depend on *in vitro* selection/expansion, which is associated with encounters such as the loss of stemness or possible cell transformation risks [103-106]. Standard procedures in clinical trials using ASC are cultivation, purification and differentiation of the cells, but it still remains challenging to meet the requirements of regulatory agencies for translating stem cells into clinics. It is not considered an advanced therapy medicinal product (ATMP) to use SVF cells within the same surgical procedure in an autologous and homologous way [107].

Different cell isolation protocols, methods and closed automated isolation devices bring up cell populations with variable content of potentially therapeutically relevant cells within the SVF or the fat graft [108]. Additionally, a reduction in reproducibility and efficacy may be caused due to donor variability resulting in a highly heterogeneous cell composition and functionality which is accompanied with the risk of transplanting low-potency cells into the patient [78, 108].

To increase therapeutic cell potency, numerous strategies have been evaluated for the activation of cells or cell material. The efficiency of ASC transplants was improved by addition of growth factors [109] or activated platelet-rich plasma (PRP) [58, 110] but also different forms of physical stimulation employing low level laser therapy (LLLT) [111-113], photobiostimulation [114] or radio electric asymmetric conveyers [115] were tested.

One approach to improve stem cell properties and reduce donor variability is to apply mild mechanical stimulation using extracorporeal shockwave therapy (ESWT). Extracorporeal shockwaves are sonic pulses, characterized by an initial rise, reaching a positive peak of up to 100 MPa within 10 ns, followed by a negative amplitude of up to -10 MPa and a total life cycle of less than 10  $\mu$ s. Biological responses are thought to be triggered by the high initial pressure, followed by a tensile force and the resulting mechanical stimulation [116]. For several decades now, ESWT has been applied in the clinics and it has demonstrated beneficial effects.

ESWT accelerates impaired wound healing in different clinical circumstances [117-121]. However, the mechanisms underlying the beneficial effects of shock waves have not been fully revealed yet. One known mechanism is that, ESWT triggers adenosine tri-phosphate (ATP) release in an energy- and pulse number- dependent manner. This shockwave treatment induced ATP release, increases the purinergic signaling of the Erk1/2 and p38 MAPK pathways and further enhances proliferation in different cell types [122, 123]. Beneficial effects of ESWT were not only determined when applying on SVF cells or directly on the lipoaspirate but also when applying ESWT on the adipose tissue harvest side. ESWT has also been applied in cosmetic and aesthetic medicine or the treatment of patients with cellulite, lipedema and lymphedema [124-128]. Applying ESWT in cellulite and lipedema patients, their biomechanic skin properties were significantly improved, leading to a smoothening of the dermis and hypodermis surface [124]. This effect is amongst others caused by a remodeling collagen in the regions treated with ESWT [129] or by stimulating microcirculation [130].

Similar effects on wound healing processes were shown by applying LLLT. Cellular functions, such as angiogenesis, collagen deposition, fibroblast proliferation, macrophage activation and tissue repair were beneficially influenced by LLLT [131]. By now, other clinical applications of LLLT include pain relief, treatment of neurological and chronic joint disorders and reducing inflammation [132]. Several studies already aimed to investigate the effects of LLLT on a cellular level on stem cells and showed that low level laser stimulation on MSC cultures derived from bone marrow or adipose tissue *in vitro* and *in vivo* increased cell proliferation, viability, osteogenic differentiation and tissue regeneration [133-135]. Until now LLLT is mainly performed with laser light, however light-emitting diodes (LEDs) are representing an appropriate alternate. Lasers have disadvantages like local heat production, a narrow beam width and high costs compared to LEDs as well as the necessity of special safety measures. Comparative studies using lasers and LEDs showed that no significant differences were detectable in association with angiogenesis, proliferation and wound healing [136-138].

As a side project, cell properties from healthy and lipedema patients were compared. In brief, lipedema is a progressive disease characterized by subcutaneous bilateral deposition of adipose tissue in the extremities and buttocks [139, 140]. A genetic background with familial predisposition was described in 60% of lipedema cases [141]. The increase in fatty tissue is the consequence of adipocyte hypertrophy and hyperplasia [142] emphasized by alterations of the connective tissue [143]. Furthermore, the enhanced growth of adipocytes leads to enhanced capillary permeability and an insufficient lymphatic backflow, which is accompanied by hematoma [144]. Lipedema disease is mainly affecting women, is hormone-related and its onset is in puberty, after pregnancy or during menopause [145]. Estrogen is responsible therefore because of its contribution in decreasing lipolysis in the gluteal compared to abdominal region due to a distinct pattern of estrogen receptors [146]. Additionally, estrogen regulates bone morphogenetic protein (BMP) 2, which could be shown to stimulate adipogenesis. At the same time it inhibits adipogenesis by knockdown peroxisome proliferator-activated receptor gamma 2 (PPAR $\gamma$ 2), thus PPAR $\gamma$ 2 may play a role in BMP induced adipogenesis [147]. However, the exact etiopathogenesis of this disorder is still largely unknown. Analysis of adipose tissue of lipedema patients revealed differences in adipocyte

morphology. The infiltration of macrophages and the presence of necrotizing adipocytes was observed when analyzing adipose tissue of lipedema patients. In parallel proliferation capacity of adipose-derived stem/progenitor/stromal cells (Ki67<sup>+</sup>/CD34<sup>+</sup> cells) is enhanced, seeming to promote adipogenesis [148]. Additionally, hypoxia induced by hypertrophy and subsequent enhancement in angiogenesis of pathologic vessels might contribute to capillary permeability [149, 150]. This would explain the fluid increase in the interstitium and therefore the emerging orthostatic edema. All in all, little is known about the composition and properties of adult stem and precursor cells in lipedema.

During the dissertation the isolation and activation process for SVF cells was optimized to generate a highly potent tissue material for clinical use. The usage of physical stimulation was investigated on SVF/ASC cells as well as the liposuction material and the donors harvest site by applying ESWT. Additionally, to the extensively investigated application of ESWT another approach to stimulate cells, the low level light therapy, was examined. In general, physical stimuli might trigger cells to reacting faster or more appropriate when it comes to inflammation or wound healing. Additionally, differences of healthy and lipedema SVF cells were investigated.

Adipose tissue is abundantly available, yielding high amounts of potential cells, which can be isolated to fulfill beneficial regenerative effects but also physically stimulated with different methods to gain high potent material for clinical usage. The clinical usage of this cell material is accompanied with certain drawbacks, which still need to be overcome to provide patients with the best possible treatment.

## 2. Aim of This Study

Adipose tissue, a practicable filler for soft tissue defects has been widely used in cosmetic and plastic surgery because it is abundantly available and easily obtained. Adipose tissue–derived regenerative cells have been proposed in regenerative medicine for a variety of diseases due to their immunomodulatory, anti-inflammatory and pro-regenerative potential.

But the use of adipose tissue as fat graft, CAL and/or cell therapy is accompanied by the following limiting factors:

- Lack of homogeneous material for reproducible fat engraftment
- Time-consuming and expensive cell isolation procedure
- Potential risks (contamination) during isolation (non-closed environment)
- Low functionality and efficacy as well as possible cytotoxicity of the transplanted cells which limits long-term viability and integration of the fat graft
- Tissue resorption due to a lack of vascularization within the transplants

Within this project the limitations as described above in fat grafting and cell-based therapies were addressed using improved isolation procedures and/or physical forces to obtain high quality regenerative cells. To gain a broad spectrum of knowledge different *in vitro* assays were performed and concluded in an *in vivo* evaluation of fat grafting in an established implantation mouse model.

SVF Microtissue was isolated with an improved protocol, using low concentration of collagenase (GMP certified) under sterile and mild conditions. From this, we could obtain a therapeutically relevant cell population by minor manipulation where SVF cells remain in their natural environment providing the maximum possible regenerative potential. Additionally, to improving the isolation process itself different setups to stimulate cells were applied. Extracorporeal shockwave therapy (ESWT), a physical stimulus already used in the clinics, was applied on freshly obtained human liposuction material and on isolated SVF cells (*in vitro*) where we aimed to equalize and enhance stem cell properties and functionality. Based on these beneficial results, ESWT was applied on the adipose tissue harvest site before liposuction (*in situ*) to improve cell properties and functionality. This set-up could reflect a clinical situation of a one-step procedure, avoiding risk factors such as a water bath, tissue processing, collagenase and the expansion of cells. Besides ESWT, the effect of low level light therapy as physical stimulus was applied on SVF cells hypothesizing further beneficial effects. Based on these finding we questioned if the therapeutic relevance of SVF cells derived from diseased adipose tissue has an influence on the cell properties. Hence, we compared SVF cells derived from lipedema patients, a hormone-related women's disease to healthy individuals.

### 3. Methods

In the following sections all applied methods are briefly described in order of the workflow and more details can be found in the manuscripts.

#### 3.1. Cell Isolation

The use of human adipose tissue was approved by the local ethical board with patient's consent. Subcutaneous adipose tissue was obtained during routine outpatient liposuction procedures under local tumescence anesthesia. To guarantee an appropriate amount of cells after isolation, cell isolation was performed directly after liposuction procedure or within the next 24 hours, when stored at 4 degrees. Adipose tissue was mixed with an equal volume of PBS without  $\text{Ca}^{2+}/\text{Mg}^{2+}$ , transferred to a blood bag and the washing solution (PBS) containing blood and tumescent solution was allowed to separate and was afterwards discarded. For the digestion of liposuction material, collagenase was added and incubated. Lysis and washing steps combined with centrifugation steps were performed to finally obtain the SVF.

#### 3.2. Extracorporeal Shockwave Therapy (ESWT)

Different ESWT applications were performed within this project. ESWT was applied on the adipose tissue harvest side (*in situ*), on the obtained liposuction material before the actual SVF isolation or on the isolated SVF cells (*in vitro*).

#### 3.3. Low Level Light Therapy

Low level light therapy is a therapeutically relevant method in wound healing. Thereby the effects of red (635nm), green (516nm) and blue (475nm) LED light with low energy flux densities were applied on the freshly isolated SVF.

#### 3.4. Cell Yield and Viability

After processing human lipoaspirates the cell yield and viability was determined with two different optical methods. The TC-20 CellCounter system is based on a trypan blue exclusion assay whereas the NC-200 system determines the cell yield and viability with DAPI staining

and aggregated cells are processed in a two-step counting procedure. In the first step a cell lysis is performed before the actual counting (all cells are counted), the second counting step is performed without cell lysis (only dead cells are counted). The advanced counting system at the NC-200 was only applied for freshly isolated SVF cells due to their requirement for a more sophisticated counting method because of its heterogeneity.

### 3.5. Surface Marker Profile Analysis

The surface antigen profile of isolated and activated cells was examined by flow cytometry analysis in order to verify isolation of SVF specific cells and to specify the composition of therapeutic relevant subpopulations. In accordance to the statement by IFATS and ISCT, the freshly isolated cells were characterized using antibodies against CD1c, CD13, CD14, CD29, CD31, CD33, CD34, CD44, CD45, CD49d, CD68, CD73, CD90, CD105, CD117, CD133, CD146, CD235a, CD326, CD309, LYVE-1, Podoplanin, SSEA3, Stro-1 and alpha-smooth muscle actin (SMA). For the evaluation of relevant subpopulations a combination of different surface marker antigens were used to identify endothelial progenitor cells (EPC) (CD45<sup>-</sup>/CD31<sup>+</sup>/CD34<sup>+</sup>), pericytes (CD45<sup>-</sup>/CD31<sup>+</sup>/CD146<sup>+</sup>), supra-adventitial ASC (SA-ASC) (CD45<sup>-</sup>/CD31<sup>+</sup>/CD146<sup>-</sup>/CD34<sup>+</sup>), Multilineage differentiation Stress Enduring (Muse) cells (SSEA3<sup>+</sup>/CD105<sup>+</sup>) a pericytic subset (CD90<sup>+</sup>/CD146<sup>+</sup>) and lymphatic endothelial cells (LEC) (Lyve-1<sup>+</sup>/Podoplanin<sup>+</sup>). All surface marker analysis were performed on a FACS Canto.

### 3.6. Cellular Adenosine Tri-Phosphate (ATP)

ATP production is an indicator for energy production and metabolic activity of the cells. Cellular ATP concentration of the isolated cells was determined by using a CellTiter-Glo® Luminescent Cell Viability Assay. The assay is based on a luciferase reaction that produces oxyluciferin and consumes the cellular ATP. Thereby, luciferase-based output signal is direct proportional to the ATP concentration. The output signal was measured with a luminometer.

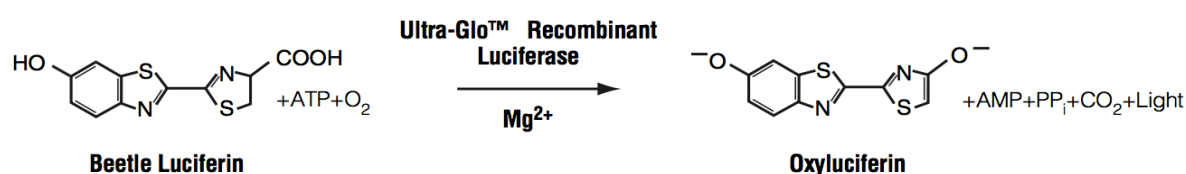


**Figure 6. Luciferase reaction equation [151].**

A luminescent signal is generated through a catalytic process. The reaction is catalyzed by the enzyme luciferase when ATP, Mg<sup>2+</sup> and molecular oxygen are present. Luciferin is metabolized to oxyluciferin.

### 3.7. Cytotoxicity

For the detection of cytotoxicity, a Cytotoxicity Detection Kit was used. This assay is based on the measurement of lactate dehydrogenase (LDH), which is released by damaged cells. Due to the loss of membrane integrity caused by apoptosis or necrosis, LDH is released into the culture medium. To exclude cytotoxicity induced by the ESWT, LLLT or the enzymatic isolation process, LDH release was determined after the treatment or isolation.

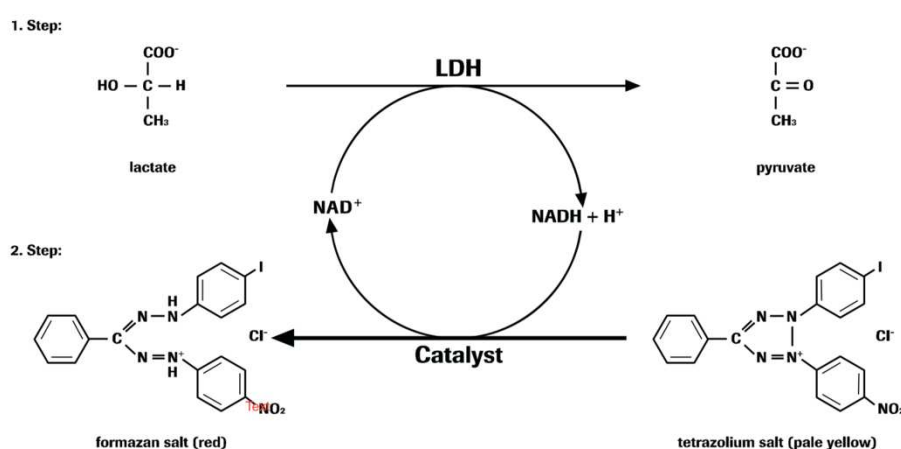


**Figure 7. Reaction equation of the cytotoxicity reaction kit [152].**

First, an oxidation of lactate to pyruvate is done by the released lactate dehydrogenase (LDH) via reduction of  $\text{NAD}^+$  to  $\text{NADH} + \text{H}^+$ . Then a catalyst transfers 2 H from  $\text{NADH} + \text{H}^+$  to the yellow tetrazolium salt INT (2-[4-iodophenyl]-3-[4-nitrophenyl]-5-phenyltetrazolium chloride).

### 3.8. Proliferation, Clonogenic Potential and Morphology

For the proliferation capacity of the isolated cell different methods were use. The population doubling level (PDL) was calculated according to the following formulas for cells cultivated until passage 3. Providing information on how fast a cell population has doubled.

$$k = \frac{\ln N - \ln N_0}{t_1 - t_0} \quad (1)$$

$$t_2 = \frac{\ln 2}{k} \quad (2)$$

$$PDL = \frac{t_{\text{confluent}}}{t_2} \quad (3)$$

k...growth constant  
N0...amount of seeded cells  
N...amount of cells after confluence  
t2...generation time  
t confluent...time when confluence is reached in days

For the determination of the clonogenic potential a colony-forming unit fibroblast (CFU-F) assay was used. This assay is a standard technique to examine the ability of a single cell to grow into a colony.

The observation of cell morphology was performed after seeding the cells until they reached a sub-confluent state, therefore pictures were taken every day. Besides the morphology visual changes concerning the proliferation capacity within the first few days could be observed.

### 3.9. Secretory Profile Analysis

The secretory profile of isolated and activated cells was determined with different methods. As it is a very important for cells to communicate with each other and therefore tissue regeneration could be triggered by secreted proteins and miRNAs, the protein profile was analyzed using membrane-based protein arrays, enzyme-linked immunosorbent assays (ELISA) or with a miRNA screening performed by TAmiRNA GmbH. A broad spectrum of pro- and anti-inflammatory, immunomodulatory, angiogenic and cytoprotective cytokines and miRNAs were analyzed.

### 3.10. Vascularization Potential

Blood vessels are essential for the supply of the cells with oxygen and nutrients. Therefore, neo-vascularization is mandatory for a successful graft integration. For determination of the cells potential to newly form tube-like structures a fibrin clot-culture was performed according to Holnthoner et al. [73, 153]. SVF cells or ASC were mixed with fibrinogen and thrombin for clot formation and cultured on glass coverslips. After the cultivation in EGM-2 supplemented with aprotinin for clot maintenance the clot culture was fix and stained against CD31 coupled with two different fluorescent dyes (Alexa647 and FITC). For identifying living cells a DAPI staining was used. The CD31-Alexa647 antibody was used to take pictures at a greater magnification and to be able to use the direct stochastic optical reconstruction microscopy (dSTORM) technology in cooperation with the FH Linz Medizintechnik for visualizing the 3D clot structure.



### 3.11. Differentiation Potential

For the evaluation of the differentiation potential towards adipogenic, osteogenic and chondrogenic lineage, well established differentiation and quantification protocols were performed. 2D cultures were used for adipogenic and osteogenic differentiation and a 3D pellet culture system for chondrogenic differentiation. After cultivation, cells or pellets were either fixed for histological examination or RNA was extracted for quantification. For determination of the adipogenic differentiation potential an Oil Red O staining, for osteogenesis Alizarin Red and Alkaline Phosphatase staining and for chondrogenesis a Collagen II and Alcian blue staining was performed. Additionally to the histological examination a gen analysis (RT-PCR) for PPAR $\gamma$ , fatty acid binding protein 4 (FABP4) and leptin for adipogenic differentiation; collagen I, secreted phosphoprotein I (SPP1, also known as osteopontin), osteocalcin (bone  $\gamma$ -carboxylglutamic acid-containing protein, BGLAP) and alkaline phosphatase (ALPL) for osteogenic differentiation; and collagen I & II, mitochondrial aspartate-glutamate transporter (AGC1) and versican (chondroitin sulfate proteoglycan, CSPG2) for chondrogenic differentiation was performed.

### 3.12. Immunofluorescence Staining

For the visualization of ASCs present in the isolated microtissue a double staining of the mesenchymal marker CD90 and the (in principle endothelial) marker CD34 was performed. The CD90<sup>+</sup>/CD34<sup>+</sup> subpopulation indicates these regenerative cells. As secondary antibody for visualization a goat anti-mouse Rhodamine Red for CD90 and a donkey anti-rabbit Alexa488 for CD34 was used. Samples were mounted on microscope slides with an antifade kit (Prolong gold) and images were taken using a confocal microscope.

### 3.13. Histological Staining

Samples were fixed in formalin, dehydrated in graded ethanol series and then embedded in paraffin prior to staining. After cutting samples into thin sections, they were deparaffinized for either histochemical or immunohistochemical analysis. As histochemical staining the following was performed: Alcian blue for the visualization of glycosaminoglycan content and hematoxylin and eosin (H&E) for overview of integration. Extracellular matrix (ECM) components (collagen type I, II III) and cell markers (fibroblasts, endothelial cells and pericytes) were immunohistochemically stained. For the visualization of the fat content an osmium tetroxide (OsO<sub>4</sub>) fixation protocol to preserve and visualize lipids was performed. Images were acquired using a light microscope.

### 3.14. *In Vivo* Analysis

NRMI nude mice were used and anesthesia was performed with isoflurane. Test samples were in a randomized fashion injected transcutaneously into the musculus quadriceps femoris hindlimbs. Samples were injected in replicates and were well tolerated, and no adverse effects were observed. After 28 days the animals were euthanized through cervical dislocation under isoflurane inhalation anesthesia. Sample harvesting was performed by resecting the implantation region with the skin and subcutaneous tissue and afterwards samples were fixated and histologically processed. A microCT analysis using Lugol staining for the visualization and different histological stainings to characterize the grafts composition were performed.

## 4. Summary of Publications

Publications are presented in accordance to the workflow, starting with the improved isolation process, followed by biophysical activation approaches and concluding with a description of healthy vs. lipedema cells.

### 4.1. Adipose Tissue-Derived Therapeutic Cells in Their Natural Environment as Novel Autologous Cell Therapy Strategy: The Microtissue-Stromal Vascular Fraction

Nürnberger S<sup>1,2,4</sup>, Lindner C<sup>1,2</sup>, **Maier J**<sup>1,2</sup>, Strohmeier K<sup>1,2,5</sup>, Wurzer C<sup>1,2,3</sup>, Slezak P<sup>1,2</sup>, Suessner S<sup>2,6</sup>, Holnthoner W<sup>1,2</sup>, Redl H<sup>1,2</sup>, Wolbank S<sup>1,2,#</sup>, Priglinger E<sup>1,2,#,\*</sup>.

<sup>1</sup> Ludwig Boltzmann Institute for Experimental and Clinical Traumatology, AUVA Research Centre, Linz/Vienna, Austria

<sup>2</sup> Austrian Cluster for Tissue Regeneration, Vienna, Austria

<sup>3</sup> Liporegena GmbH, Breitenfurt, Austria

<sup>4</sup> Department of Orthopedics and Trauma-Surgery, Division of Trauma-Surgery, Medical University of Vienna, Vienna, Austria

<sup>5</sup> School of Medical Engineering and Applied Social Sciences, University of Applied Sciences Upper Austria, Linz, Austria

<sup>6</sup> Red Cross Blood Transfusion Service of Upper Austria, Linz, Austria

# These authors contribute equally.

\* Corresponding author.

Adipose tissue-derived therapeutic cells in their natural environment as novel autologous cell therapy strategy: The microtissue-stromal vascular fraction.

Acta Biomaterialia (2018).

doi: 10.22203/eCM.v037a08.

The prerequisite for a successful clinical use of autologous adipose-tissue-derived cells is the highest possible regenerative potential of the applied cell population, the stromal vascular fraction (SVF). Current isolation methods depend on high enzyme concentration, lysis buffer, long incubation steps and mechanical stress, resulting in single cell dissociation. The aim of the study was to limit cell manipulation and obtain a derivative comprising therapeutic cells (microtissue-SVF) without dissociation from their natural extracellular matrix, by employing a

gentle good manufacturing practice (GMP)-grade isolation. The microtissue-SVF yielded larger numbers of viable cells as compared to the improved standard-SVF, both with low enzyme concentration and minimal dead cell content. It comprised stromal tissue compounds (collagen, glycosaminoglycans, fibroblasts), capillaries and vessel structures (CD31+, smooth muscle actin+). A broad range of cell types was identified by surface-marker characterisation, including mesenchymal, haematopoietic, pericytic, blood and lymphatic vascular and epithelial cells. Subpopulations such as supra-adventitial adipose-derived stromal/stem cells and endothelial progenitor cells were significantly more abundant in the microtissue-SVF, corroborated by significantly higher potency for angiogenic tube-like structure formation *in vitro*. The microtissue-SVF showed the characteristic phenotype and tri-lineage mesenchymal differentiation potential *in vitro* and an immunomodulatory and pro-angiogenic secretome. *In vivo* implantation of the microtissue-SVF combined with fat demonstrated successful graft integration in nude mice. The present study demonstrated a fast and gentle isolation by minor manipulation of liposuction material, achieving a therapeutically relevant cell population with high vascularisation potential and immunomodulatory properties still embedded in a fraction of its original matrix.

**Keywords:** Stromal vascular fraction, extracellular matrix, adipose-derived stromal/stem cells, endothelial progenitor cells, angiogenesis.

## 4.2. Improvement of Adipose Tissue-Derived Cells by Low-Energy Extracorporeal Shockwave Therapy

Priglinger E<sup>1,2,#,\*</sup>, Schuh C.M.A.P<sup>1,2,#</sup>, Steffenhagen C<sup>1,2</sup>, Wurzer C<sup>1,2</sup>, **Maier J**<sup>1,2</sup>, Nuernberger S<sup>2,3,4</sup>, Holnthoner W<sup>1,2</sup>, Fuchs C<sup>2,5</sup>, Suessner S<sup>2,6</sup>, Ruenzler D<sup>2,5</sup>, Redl H<sup>1,2</sup>, Wolbank S<sup>1,2</sup>.

<sup>1</sup> Ludwig Boltzmann Institute for Experimental and Clinical Traumatology, Austrian Workers' Compensation Board (AUVA) Research Center, Vienna, Austria,

<sup>2</sup> Austrian Cluster for Tissue Regeneration, Vienna, Austria,

<sup>3</sup> Bernhard Gottlieb University Clinic of Dentistry, Universitätsklinik für Zahn-, Mund- und Kieferheilkunde Ges.m.b.H, Vienna, Austria,

<sup>4</sup> Medical University of Vienna, Department of Trauma Surgery, Vienna, Austria,

<sup>5</sup> University of Applied Sciences Technikum Wien, Department of Biochemical Engineering, Vienna, Austria, and

<sup>6</sup> Red Cross Blood Transfusion Service of Upper Austria, Linz, Austria

# These authors contribute equally.

\* Corresponding author.

Improvement of adipose tissue-derived cells by low-energy extracorporeal shockwave therapy.

Cytotherapy (2017).

doi: 10.1016/j.jcyt.2017.05.010.

Cell-based therapies with autologous adipose tissue-derived cells have shown great potential in several clinical studies in the last decades. The majority of these studies have been using the stromal vascular fraction (SVF), a heterogeneous mixture of fibroblasts, lymphocytes, monocytes/macrophages, endothelial cells, endothelial progenitor cells, pericytes and adipose-derived stromal/stem cells (ASC) among others. Although possible clinical applications of autologous adipose tissue-derived cells are manifold, they are limited by insufficient uniformity in cell identity and regenerative potency. In our experimental set-up, low-energy extracorporeal shock wave therapy (ESWT) was performed on freshly obtained human adipose tissue and isolated adipose tissue SVF cells aiming to equalize and enhance stem cell properties and functionality. After ESWT on adipose tissue we could achieve higher cellular adenosine triphosphate (ATP) levels compared with ESWT on the isolated SVF as well as the control. ESWT on adipose tissue resulted in a significantly higher expression of single mesenchymal and vascular marker compared with untreated control. Analysis of SVF protein secretome revealed a significant enhancement in insulin-like growth factor (IGF)-1 and placental growth factor (PLGF) after ESWT on adipose tissue. Summarizing we could show

that ESWT on adipose tissue enhanced the cellular ATP content and modified the expression of single mesenchymal and vascular marker, and thus potentially provides a more regenerative cell population. Because the effectiveness of autologous cell therapy is dependent on the therapeutic potency of the patient's cells, this technology might raise the number of patients eligible for autologous cell transplantation.

**Keywords:** adipose tissue, adipose-derived stromal/stem cells, extracorporeal shockwave therapy, stromal vascular fraction

### 4.3. Extracorporeal Shock Wave Therapy *in situ* – A Novel Approach to Obtain an Activated Fat Graft

Priglinger E<sup>1,2,\*</sup>, Sandhofer M<sup>3</sup>, Peterbauer A<sup>2,4</sup>, Wurzer C<sup>1,2,5</sup>, Steffenhagen C<sup>1,2</sup>, **Maier J**<sup>1,2</sup>, Holnthoner W<sup>1,2</sup>, Nuernberger S<sup>2,6,7</sup>, Redl H<sup>1,2</sup>, Wolbank S<sup>1,2</sup>.

<sup>1</sup> Ludwig Boltzmann Institute for Experimental and Clinical Traumatology, AUVA Research Center, Linz/Vienna, Austria

<sup>2</sup> Austrian Cluster for Tissue Regeneration, Vienna, Austria

<sup>3</sup> Austrian Academy of Cosmetic Surgery and Aesthetic Medicine, Linz, Austria

<sup>4</sup> Red Cross Blood Transfusion Service of Upper Austria, Linz, Austria

<sup>5</sup> Liporegena GmbH, Austria

<sup>6</sup> Bernhard Gottlieb University Clinic of Dentistry, Universitätsklinik für Zahn-, Mund- und Kieferheilkunde Ges.m.b.H, Vienna, Austria

<sup>7</sup> Medical University of Vienna, Department of Trauma Surgery, Vienna, Austria

\* Corresponding author.

Extracorporeal shock wave therapy *in situ* – a novel approach to obtain an activated fat graft. Tissue Engineering and Regenerative Medicine (2017).

doi: 10.1002/term.2467.

One of the mainstays of facial rejuvenation strategies is volume restoration, which can be achieved by autologous fat grafting. In our novel approach, we treated the adipose tissue harvest site with extracorporeal shock wave therapy (ESWT) in order to improve the quality of the regenerative cells *in situ*. The latter was demonstrated by characterizing the cells of the stromal vascular fraction (SVF) in the harvested liposuction material regarding cell yield, adenosine triphosphate (ATP) content, proliferative capacity, surface marker profile, differentiation potential and secretory protein profile. Although the SVF cell yield was only slightly enhanced, viability and ATP concentration of freshly isolated cells as well as proliferation doublings after 3 weeks in culture were significantly increased in the ESWT compared with the untreated group. Likewise, cells expressing mesenchymal and endothelial/pericytic markers were significantly elevated concomitant with an improved differentiation capacity towards the adipogenic lineage and enhancement in specific angiogenic proteins. Hence, *in situ* ESWT might be applied in the future to promote cell fitness, adipogenesis and angiogenesis within the fat graft for successful facial rejuvenation strategies with potential long-term graft survival.

**Keywords:** adipogenesis, adipose tissue, angiogenesis, autologous fat grafting, extracorporeal shock wave therapy (ESWT), stromal vascular fraction (SVF)



#### 4.4. Photobiomodulation of Freshly Isolated Human Adipose Tissue-Derived Stromal Vascular Fraction Cells by Pulsed Light-Emitting Diodes for Direct Clinical Application

Priglinger E<sup>1,2,#,\*</sup>, Maier J<sup>1,2,#</sup>, Caudary S<sup>1,2</sup>, Lindner C<sup>1,2</sup>, Wurzer C<sup>1,2,3</sup>, Rieger S<sup>1,2</sup>, Redl H<sup>1,2</sup>, Wolbank S<sup>1,2</sup>, Dungal P<sup>1,2</sup>.

<sup>1</sup> Ludwig Boltzmann Institute for Experimental and Clinical Traumatology, AUVA Research Center, Linz/Vienna, Austria

<sup>2</sup> Austrian Cluster for Tissue Regeneration, Vienna, Austria

<sup>3</sup> Liporegena GmbH, Breitenfurt, Austria

# These authors contribute equally.

\* Corresponding author.

Photobiomodulation of freshly isolated human adipose tissue-derived stromal vascular fraction cells by pulsed light-emitting diodes for direct clinical application.

Tissue Engineering and Regenerative Medicine (TERM) (2018).

doi: 10.1002/term.2665.

A highly interesting source for adult stem cells is adipose tissue, from which the stromal vascular fraction (SVF) - a heterogeneous cell population including the adipose-derived stromal/stem cells (ASC) - can be obtained. To enhance the regenerative potential of freshly isolated SVF cells low level light therapy (LLLT), was used. The effects of pulsed blue (475 nm), green (516 nm) and red light (635 nm) from light-emitting diodes (LEDs) applied on freshly isolated SVF were analyzed regarding cell phenotype, cell number, viability, adenosine triphosphate content, cytotoxicity and proliferation, but also osteogenic, adipogenic and pro-angiogenic differentiation potential. The colony-forming unit fibroblast assay revealed a significantly increased colony size after LLLT with red light compared to untreated cells, whereas the frequency of colony forming cells was not affected. LLLT with green and red light resulted in a stronger capacity to form vascular tubes by SVF when cultured within 3D fibrin matrices compared to untreated cells, which was corroborated by increased number and length of the single tubes and a significantly higher concentration of vascular endothelial growth factor. Our study showed beneficial effects after LLLT on the vascularization potential and proliferation capacity of SVF cells. Therefore, LLLT using pulsed LED light might represent a new approach for activation of freshly isolated SVF cells for direct clinical application.

**Keywords:** Low Level Light Therapy, LED, Photostimulation, Photobiomodulation, Adipose Tissue, Stromal Vascular Fraction, Vascularization, VEGF

Die approbierte gedruckte Originalversion dieser Dissertation ist an der TU Wien Bibliothek verfügbar.  
The approved original version of this doctoral thesis is available in print at TU Wien Bibliothek.

#### 4.5. The Adipose Tissue-Derived Stromal Vascular Fraction Cells from Lipedema Patients: Are They Different?

Priglinger E<sup>1,2,\*</sup>, Wurzer C<sup>1,2,3</sup>, Steffenhagen C<sup>1,2</sup>, **Maier J**<sup>1,2</sup>, Hofer V<sup>4,5</sup>, Peterbauer A<sup>2,6</sup>, Nuernberger S<sup>2,7,8</sup>, Redl H<sup>1,2</sup>, Wolbank S<sup>1,2,#</sup>, Sandhofer M<sup>5,#</sup>.

<sup>1</sup> AUVA Research Center, Ludwig Boltzmann Institute for Experimental and Clinical Traumatology, Linz, Austria,

<sup>2</sup> Austrian Cluster for Tissue Regeneration, Vienna, Austria,

<sup>3</sup> Liporegena GmbH, Breitenfurt, Austria,

<sup>4</sup> Faculty of Medicine/Dental Medicine, Danube Private University, Krems-Stein, Austria,

<sup>5</sup> Austrian Academy of Cosmetic Surgery and Aesthetic Medicine, Linz, Austria,

<sup>6</sup> Red Cross Blood Transfusion Service of Upper Austria, Linz, Austria,

<sup>7</sup> Bernhard Gottlieb University Clinic of Dentistry, Universitätsklinik für Zahn-, Mund- und Kieferheilkunde Ges.m.b.H, Vienna, Austria, and

<sup>8</sup> Department of Trauma Surgery, Medical University of Vienna, Vienna, Austria

# These authors contribute equally.

\* Corresponding author.

The adipose tissue-derived stromal vascular fraction cells from lipedema patients: Are they different?.

Cytotherapy (2017).

doi: 10.1016/j.jcyt.2017.03.073.

Lipedema is a hormone-related disease of women characterized by enlargement of the extremities caused by subcutaneous deposition of adipose tissue. In healthy patients application of autologous adipose tissue–derived cells has shown great potential in several clinical studies for engrafting of soft tissue reconstruction in recent decades. The majority of these studies have used the stromal vascular fraction (SVF), a heterogeneous cell population containing adipose-derived stromal/ stem cells (ASC), among others. Because cell identity and regenerative properties might be affected by the health condition of patients, we characterized the SVF cells of 30 lipedema patients in comparison to 22 healthy patients. SVF cells were analyzed regarding cell yield, viability, adenosine triphosphate content, colony forming units and proliferative capacity, as well as surface marker profile and differentiation potential in vitro. Our results demonstrated a significantly enhanced SVF cell yield isolated from lipedema compared with healthy patients. In contrast, the adipogenic differentiation potential of SVF cells isolated from lipedema patients was significantly reduced compared with healthy patients. Interestingly, expression of the mesenchymal marker CD90 and the endothelial/pericytic

marker CD146 was significantly enhanced when isolated from lipedema patients. The enhanced number of CD90+ and CD146+ cells could explain the increased cell yield because the other tested surface marker were not reduced in lipedema patients. Because the cellular mechanism and composition in lipedema is largely unknown, our findings might contribute to a better understanding of its etiology.

**Keywords:** adipogenesis, adipose tissue, adult stem cells, CD146, lipedema, stromal vascular fraction

## 4.6. Conference Talks and Poster Presentations

TERMIS EU Chapter Meeting, 28.06. – 01.07.2016, Uppsala, Sweden

Poster and Rapid Fire Oral Presentation: Secretory Activity of the Stromal Vascular Fraction

TERMIS Summer School, 04. – 09.07.2016, Riva del Garda, Italy

Poster and Oral Presentation: Secretory Activity of the Stromal Vascular Fraction

International Conference on Tissue Engineering in conjunction with the International Conference on Regenerative Biomedical Materials, 14. – 19.06.2017, Heraklion, Greece

Oral Presentation: Physical Stimulation of Cells for Tissue Regeneration

ViCEM Inaugural Meeting, 09. – 10.11.2017, Vienna, Austria

Poster: *Ex-vivo* and *in situ* activation of adipose-derived cells

EACTS/PACT Symposium, 30.11. – 01.12.2017, Vienna, Austria

Oral Presentation: Effects of Shockwave on Adipose Derived Stem Cells

TERMIS World, 04. – 07.09.2018, Kyoto, Japan

Poster: *Ex vivo* and *in situ* Activation of Adipose-Derived Cells by Extracorporeal Shockwave Therapy

Austrian Cluster for Tissue Regeneration Meeting, 11. – 13.03.2019, Vienna, Austria

Oral Presentation: Flow Through MSC Activation: Improved Cell Isolation and Activation

## 5. Discussion

The improved Microtissue-SVF isolation process has two big advantages, it provides a highly regenerative cell material within its natural environment and is also performed with GMP grade materials, which makes it applicable in every operating theater. The application of autologous SVF in a homologous transplantation during the same surgical procedure fulfills the requirements of the regulation authorities. There are many ongoing translational studies with SVF and ASC but they showed heterogeneous results regarding efficacy and stem cell potency. The results are depending on different factors, for example tissue processing [55, 154] and the cell isolation process [108, 155, 156] as well as the patient's health condition [157, 158], their body mass index [159, 160] and age [161-163]. There are heterologous applications of SVF cells, which could prove beneficial effects in clinical studies for its bone and cartilage repair. Microtissue-SVF showed an increased immunomodulatory activity and high chondrogenic potential and could therefore provide a potent therapeutic for osteoarthritis (OA) [164-166]. To obtain long-term beneficial effects of the transplanted cell material and an enhanced integration/engraftment, ESWT is used for the treatment of liposuction material before the cell isolation and/or transplantation. A big advantage is that the application of ESWT is already clinically approved. ESWT is used for many years for regeneration purposes in non-union fractures, necrosis, impaired wound healing, ulcers and burn wounds [117-121, 167, 168]. In our study we performed the treatment in a blood bag, which allows direct ESWT treatment and is also compatible with a closed and sterile isolation process. The described setup should be in accordance with GMP settings. Results clearly showed that ESWT on adipose tissue provides cells with a higher ATP content. This may be due to the fact that cells are still in their natural environment and surrounded by tissue. Leaving cells in their natural environment is beneficial for them; we were able to show this with the improved isolation process, providing Microtissue-SVF and also with applying ESWT directly on adipose tissue. The ATP concentration of cells undergoing ESWT prior to isolation was higher compared with the ATP concentration of cells receiving ESWT directly. Based on our *in vitro* application of ESWT on liposuction material and directly on SVF cells, the next step was to apply ESWT directly on the donor before liposuction aiming to enhance the regenerative cell properties before fat engraftment or cell isolation used for CAL. Beneficial effects were already shown in cosmetic and aesthetic medicine, where ESWT was applied for the treatment of cellulite, lipedema and lymphedema patients [124, 169-171]. Besides the cosmetic treatment, ESWT showed an induced VEGF expression in human umbilical vein endothelial cells [172] and enhanced lymphangiogenesis [173]. This is necessary for an early and abundant vascularization for nutrition supply and integration inside the surrounding tissue and functions as perquisite in fat grafting [62, 67]. Within another study, we were able to show an increased VEGF concentration in the supernatants of SVF cells in a fibrin matrix. VEGF functions as potential mediator for vascular tube formation. As already mentioned by Szymanska et al., an increased VEGF and TGF-beta concentration stimulates cell proliferation after light stimulation

[174]. This further suggests the importance of biophysical stimulation triggering cells to increase their VEGF secretion and/or expression, consequently mediating vascular tube formation and therefore increasing vascularization and guaranteeing a sufficient nutrition supply. Park demonstrated an improved functional recovery combined with an enhanced secretion of angiogenic growth factors after LLLT on spheroid ASC in hind limb ischemia mice [111, 112, 175-177]. The induced vascular regeneration further supports the importance of a biophysical stimulation. In our studies a single light or ESWT application was performed, which is preferable as a future application for cell therapies in a one-step procedure. Applying low level light therapy directly on the liposuction material would be of interest in a future study. Another potential application could be a combined ESWT and low level light therapy to further enhance the regenerative properties of the SVF. The question still remaining is, if health conditions do have an impact on therapeutically relevant cells. Concerning lipedema cells, we were able to show an increased cell yield of lipedema cells compared with the cell yield of healthy patients. Interestingly the number of cells positive for the expression of CD90<sup>+</sup> and CD146<sup>+</sup> was elevated, which could explain the increased cell yield in lipedema patients. Additionally, we could confirm the differentiation potential of lipedema SVF cells regarding adipogenic, osteogenic and chondrogenic lineage (as defined by IFATS and ISCT) [78]. However, comparing the adipogenic differentiation capacity of healthy and lipedema SVF cells, the accumulation degree of lipid vesicles was significantly reduced upon adipogenic induction in lipedema patients. Although the reduced adipogenic differentiation potential lipedema cells may nevertheless be a suitable for autologous and/or tissue regeneration strategies as they are fulfilling the requirements defined by IFATS and ISCT [78].

## IV. List of Figures

Figure 1. Self-renewal and differentiation potential of a stem cell [2].....	9
Figure 2. Components and functions of stem cell niches [4]. .....	10
Figure 3. The mesengenic process [18]. .....	12
Figure 4. Different sources of adult stem cells and their differentiation potential towards the meso-, ecto-, and endodermal lineage [35]. .....	13
Figure 5. Composition of adipose tissue and the stromal vascular fraction (SVF) [80].....	15
Figure 6. Luciferase reaction equation [151]. .....	22
Figure 7. Reaction equation of the cytotoxicity reaction kit [152]. .....	23

## V. List of Tables

Table 1. Surface marker profile for SVF and ASC [78, 90]. .....	16
---	----

## VI. Abbreviations

2D/3D	2 dimensional / 3 dimensional
AGC1	aspartate-glutamate transporter
ALPL	alkaline phosphatase
ASC	adipose tissue derived stromal/stem cells
ATMP	advanced therapy medicinal product
ATP	adenosine tri-phosphate
BGBI	Bundesgesetzblatt
BGLAP	bone $\gamma$ -carboxylglutamic acid-containing protein
BM	bone marrow
BM-MSC	bone marrow – mesenchymal stromal/stem cells
BMP-2	bone morphogenetic protein 2
Ca <sup>2+</sup>	calcium
CAL	cell assisted lipotransfer
CD	cluster of differentiation
CFU-F	colony-forming unit fibroblast
CSPG2	chondroitin sulfate proteoglycan
DAPI	4',6-diamidino-2-phenylindole
dSTORM	direct stochastic optical reconstruction microscopy
EACTS	European Association for Cardio- Thoracic Surgery
ECM	extracellular matrix
EGM-2	endothelial growth medium – 2
ELISA	enzyme-linked immunosorbent assay
Erk1/2	extracellular signal-regulated kinase 1/2



ESC	embryonic stem cells
ESWT	extracorporeal shockwave therapy
FABP4	fatty acid binding protein 4
FACS	fluorescence-activated cell sorting
H&E	hematoxylin and eosin
IFATS	International Federation for Adipose Therapeutics and Science
IGF-1	insulin-like growth factor 1
iPS	induced pluripotent stemm cells
ISCT	International Society for Cellular Therapy
IVF	<i>in vitro</i> fertilization
Klf4	kruppel like factor 4
LDH	lactate dehydrogenase
LEDs	light-emitting diodes
LLLT	low level laser therapy
MAPK	mitogen-activated protein kinase
Mg <sup>2+</sup>	Magnesium
miRNA	microRNA / micro ribonucleic acid
MPa	mega pascal
MSC	mesenchymal stromal/stem cells
Myc	proto-oncogene, bHLH transcription factor
OA	osteoarthritis
Oct3/4	octamer-binding transcription factor <sup>3</sup> / <sub>4</sub>
OsO <sub>2</sub>	osmium tetroxide
PACT	platform for advanced cellular therapies Austria
PBS	phosphate buffered saline
PDL	population doubling level
PLGF	placental growth factor
PPAR <sub>γ</sub>	peroxisome proliferator activated receptor gamma
PRP	platelet-rich plasma
Sox2	or SRY-Box 2: sex determining region Y box – 2
SPP1	secreted phosphoprotein I
SVF	stromal vascular fraction
TERM	Tissue Engineering Regenerative Medicine
TERMIS	Tissue Engineering Regenerative Medicine International Society
ViCEM	Vienna Center for Engineering in Medicine
μs	micro seconds

## VII. Literature

1. Ito, K. and T. Suda, *Metabolic requirements for the maintenance of self-renewing stem cells*. Nat Rev Mol Cell Biol, 2014. **15**(4): p. 243-56.
2. Collas, P. and A.M. Hakelien, *Teaching cells new tricks*. Trends Biotechnol, 2003. **21**(8): p. 354-61.
3. Li, L. and R. Bhatia, *Stem cell quiescence*. Clin Cancer Res, 2011. **17**(15): p. 4936-41.
4. Jones, D.L. and A.J. Wagers, *No place like home: anatomy and function of the stem cell niche*. Nat Rev Mol Cell Biol, 2008. **9**(1): p. 11-21.
5. Kolf, C.M., E. Cho and R.S. Tuan, *Mesenchymal stromal cells. Biology of adult mesenchymal stem cells: regulation of niche, self-renewal and differentiation*. Arthritis Res Ther, 2007. **9**(1): p. 204.
6. Lander, A.D., J. Kimble, H. Clevers, E. Fuchs, D. Montarras, M. Buckingham, A.L. Calof, A. Trumpp, and T. Oskarsson, *What does the concept of the stem cell niche really mean today?* BMC Biology, 2012. **10**.
7. Takahashi, K. and S. Yamanaka, *Induction of pluripotent stem cells from mouse embryonic and adult fibroblast cultures by defined factors*. Cell, 2006. **126**(4): p. 663-76.
8. Young, H.E. and A.C. Black, Jr., *Adult stem cells*. Anat Rec A Discov Mol Cell Evol Biol, 2004. **276**(1): p. 75-102.
9. Eridani, S., *Stem Cell Applications: An Overview*. , in *Stem Cells in Aesthetic Procedures*, M. Shiffman, A. Di Giuseppe, and F. Bassetto, Editors. 2014, Springer, Berlin, Heidelberg: Berlin, Heidelberg.
10. P Ramachandran, R. and L.U. Yelledahalli, *Exploring the Recent Advances in Stem Cell Research*. Journal of Stem Cell Research & Therapy, 2011. **01**(03).
11. King, N.M. and J. Perrin, *Ethical issues in stem cell research and therapy*. Stem Cell Res Ther, 2014. **5**(4): p. 85.
12. Sabin, F.R., C.A. Doan and C.E. Forkner, *THE PRODUCTION OF OSTEOGENIC SARCOMATA AND THE EFFECTS ON LYMPH NODES AND BONE MARROW OF INTRAVENOUS INJECTIONS OF RADIUM CHLORIDE AND MESOTHORIUM IN RABBITS*. J Exp Med, 1932. **56**(2): p. 267-89.
13. Thomas, E.D., H.L. Lochte, Jr., W.C. Lu and J.W. Ferrebee, *Intravenous infusion of bone marrow in patients receiving radiation and chemotherapy*. N Engl J Med, 1957. **257**(11): p. 491-6.
14. Friedenstein, A.J., S. Piatetzky, II and K.V. Petrakova, *Osteogenesis in transplants of bone marrow cells*. J Embryol Exp Morphol, 1966. **16**(3): p. 381-90.
15. Caplan, A.I., *Mesenchymal stem cells*. J Orthop Res, 1991. **9**(5): p. 641-50.
16. Pittenger, M.F., A.M. Mackay, S.C. Beck, R.K. Jaiswal, R. Douglas, J.D. Mosca, M.A. Moorman, D.W. Simonetti, S. Craig, and D.R. Marshak, *Multilineage potential of adult human mesenchymal stem cells*. Science, 1999. **284**(5411): p. 143-7.
17. Dominici, M., K. Le Blanc, I. Mueller, I. Slaper-Cortenbach, F. Marini, D. Krause, R. Deans, A. Keating, D. Prockop, and E. Horwitz, *Minimal criteria for defining multipotent mesenchymal stromal cells. The International Society for Cellular Therapy position statement*. Cytotherapy, 2006. **8**(4): p. 315-7.
18. Risbud, M.V. and M. Sitterling, *Tissue engineering: advances in in vitro cartilage generation*. TRENDS in Biotechnology, 2002. **20**(8).
19. Friedenstein, A.J., R.K. Chailakhjan and K.S. Lalykina, *The development of fibroblast colonies in monolayer cultures of guinea-pig bone marrow and spleen cells*. Cell Tissue Kinet, 1970. **3**(4): p. 393-403.
20. Caplan, A.I., *Adult mesenchymal stem cells for tissue engineering versus regenerative medicine*. J Cell Physiol, 2007. **213**(2): p. 341-7.

21. Zuk, P.A., M. Zhu, H. Mizuno, J. Huang, J.W. Futrell, A.J. Katz, P. Benhaim, H.P. Lorenz, and M.H. Hedrick, *Multilineage cells from human adipose tissue: implications for cell-based therapies*. *Tissue Eng*, 2001. **7**(2): p. 211-28.
22. Fukuchi, Y., H. Nakajima, D. Sugiyama, I. Hirose, T. Kitamura and K. Tsuji, *Human placenta-derived cells have mesenchymal stem/progenitor cell potential*. *Stem Cells*, 2004. **22**(5): p. 649-58.
23. De Bari, C., F. Dell'Accio, P. Tylzanowski and F.P. Luyten, *Multipotent mesenchymal stem cells from adult human synovial membrane*. *Arthritis Rheum*, 2001. **44**(8): p. 1928-42.
24. Young, H.E., T.A. Steele, R.A. Bray, J. Hudson, J.A. Floyd, K. Hawkins, K. Thomas, T. Austin, C. Edwards, J. Cuzzourt, M. Duenzl, P.A. Lucas, and A.C. Black, Jr., *Human reserve pluripotent mesenchymal stem cells are present in the connective tissues of skeletal muscle and dermis derived from fetal, adult, and geriatric donors*. *Anat Rec*, 2001. **264**(1): p. 51-62.
25. Zvaifler, N.J., L. Marinova-Mutafchieva, G. Adams, C.J. Edwards, J. Moss, J.A. Burger and R.N. Maini, *Mesenchymal precursor cells in the blood of normal individuals*. *Arthritis Res*, 2000. **2**(6): p. 477-88.
26. Erices, A., P. Conget and J.J. Minguell, *Mesenchymal progenitor cells in human umbilical cord blood*. *Br J Haematol*, 2000. **109**(1): p. 235-42.
27. Wakitani, S., T. Goto, S.J. Pineda, R.G. Young, J.M. Mansour, A.I. Caplan and V.M. Goldberg, *Mesenchymal cell-based repair of large, full-thickness defects of articular cartilage*. *J Bone Joint Surg Am*, 1994. **76**(4): p. 579-92.
28. Puissant, B., C. Barreau, P. Bourin, C. Clavel, J. Corre, C. Bousquet, C. Taureau, B. Cousin, M. Abbal, P. Laharrague, L. Penicaud, L. Casteilla, and A. Blancher, *Immunomodulatory effect of human adipose tissue-derived adult stem cells: comparison with bone marrow mesenchymal stem cells*. *Br J Haematol*, 2005. **129**(1): p. 118-29.
29. Minguell, J.J., A. Erices and P. Conget, *Mesenchymal stem cells*. *Exp Biol Med (Maywood)*, 2001. **226**(6): p. 507-20.
30. Arai, F., O. Ohneda, T. Miyamoto, X.Q. Zhang and T. Suda, *Mesenchymal stem cells in perichondrium express activated leukocyte cell adhesion molecule and participate in bone marrow formation*. *J Exp Med*, 2002. **195**(12): p. 1549-63.
31. Bailo, M., M. Soncini, E. Vertua, P.B. Signoroni, S. Sanzone, G. Lombardi, D. Arienti, F. Calamani, D. Zatti, P. Paul, A. Albertini, F. Zorzi, A. Cavagnini, F. Candotti, G.S. Wengler, and O. Parolini, *Engraftment potential of human amnion and chorion cells derived from term placenta*. *Transplantation*, 2004. **78**(10): p. 1439-48.
32. Tse, W.T., J.D. Pendleton, W.M. Beyer, M.C. Egalka and E.C. Guinan, *Suppression of allogeneic T-cell proliferation by human marrow stromal cells: implications in transplantation*. *Transplantation*, 2003. **75**(3): p. 389-97.
33. Kubo, M., Y. Sonoda, R. Muramatsu and M. Usui, *Immunogenicity of human amniotic membrane in experimental xenotransplantation*. *Invest Ophthalmol Vis Sci*, 2001. **42**(7): p. 1539-46.
34. In 't Anker, P.S., S.A. Scherjon, C. Kleijburg-van der Keur, G.M. de Groot-Swings, F.H. Claas, W.E. Fibbe and H.H. Kanhai, *Isolation of mesenchymal stem cells of fetal or maternal origin from human placenta*. *Stem Cells*, 2004. **22**(7): p. 1338-45.
35. Neirinckx, V., C. Coste, B. Rogister and S. Wislet, *Neural Fate of Mesenchymal Stem Cells and Neural Crest Stem Cells: Which Ways to Get Neurons for Cell Therapy Purpose?*, in *Trends in Cell Signaling Pathways in Neuronal Fate Decision*. 2013.
36. Cinti, S., *The Adipose Organ*, in *Adipose Tissue and Adipokines in Health and Disease*, G. Fantuzzi and T. Mazzone, Editors. 2007, Humana Press. p. 400.
37. Gesta, S., *White Adipose Tissue*, in *Adipose Tissue Biology*, M.E. Symonds, Editor. 2012, Springer-Verlag New York: New York. p. 414.
38. Kiefer, F.W., C. Vernochet, P. O'Brien, S. Spoerl, J.D. Brown, S. Nallamshetty, M. Zeyda, T.M. Stulnig, D.E. Cohen, C.R. Kahn, and J. Plutzky, *Retinaldehyde dehydrogenase 1 regulates a thermogenic program in white adipose tissue*. *Nat Med*, 2012. **18**(6): p. 918-25.

39. Harms, M. and P. Seale, *Brown and beige fat: development, function and therapeutic potential*. Nat Med, 2013. **19**(10): p. 1252-63.
40. Klingenspor, M., *Brown Adipose Tissue*, in *Adipose Tissue Biology*, M.E. Symonds, Editor. 2012, Springer-Verlag New York: New York. p. 414.
41. Kershaw, E.E. and J.S. Flier, *Adipose tissue as an endocrine organ*. J Clin Endocrinol Metab, 2004. **89**(6): p. 2548-56.
42. Frayn, K.N., F. Karpe, B.A. Fielding, I.A. Macdonald and S.W. Coppack, *Integrative physiology of human adipose tissue*. Int J Obes Relat Metab Disord, 2003. **27**(8): p. 875-88.
43. Klein, S.M., L. Prantl and J.H. Dolderer, *Tissue Engineering of Vascularized Adipose Tissue for Soft Tissue Reconstruction*, in *Stem Cells in Aesthetic Procedures*, M. Shiffman, A. Di Giuseppe, and F. Bassetto, Editors. 2014, Springer, Berlin, Heidelberg: Berlin, Heidelberg.
44. Harwood, H.J., Jr., *The adipocyte as an endocrine organ in the regulation of metabolic homeostasis*. Neuropharmacology, 2012. **63**(1): p. 57-75.
45. Coelho, M., T. Oliveira and R. Fernandes, *Biochemistry of adipose tissue: an endocrine organ*. Arch Med Sci, 2013. **9**(2): p. 191-200.
46. Aktan, T.M., S. Duman and C. B., *Cellular and Molecular Aspects of Adipose Tissue*, in *Adipose Stem Cells and Regenerative Medicine*, Y. Illouz and A. Sterodimas, Editors. 2011, Springer, Berlin, Heidelberg: Berlin, Heidelberg.
47. Zuk, P.A., M. Zhu, P. Ashjian, D.A. De Ugarte, J.I. Huang, H. Mizuno, Z.C. Alfonso, J.K. Fraser, P. Benhaim, and M.H. Hedrick, *Human adipose tissue is a source of multipotent stem cells*. Mol Biol Cell, 2002. **13**(12): p. 4279-95.
48. Kern, S., H. Eichler, J. Stoeve, H. Kluter and K. Bieback, *Comparative analysis of mesenchymal stem cells from bone marrow, umbilical cord blood, or adipose tissue*. Stem Cells, 2006. **24**(5): p. 1294-301.
49. Coleman, W.P., 3rd, R.G. Glogau, J.A. Klein, R.L. Moy, R.S. Narins, T.Y. Chuang, E.R. Farmer, C.W. Lewis, and B.J. Lowery, *Guidelines of care for liposuction*. J Am Acad Dermatol, 2001. **45**(3): p. 438-47.
50. Gurney, C.E., *Experimental study of the behavior of free fat transplants*. Surgery, 1938. **3**(5): p. 679-692.
51. Sommer, B. and G. Sattler, *Current concepts of fat graft survival: histology of aspirated adipose tissue and review of the literature*. Dermatol Surg, 2000. **26**(12): p. 1159-66.
52. Yu, N.Z., J.Z. Huang, H. Zhang, Y. Wang, X.J. Wang, R. Zhao, M. Bai, and X. Long, *A systemic review of autologous fat grafting survival rate and related severe complications*. Chin Med J (Engl), 2015. **128**(9): p. 1245-51.
53. von Heimburg, D., K. Hemmrich, S. Haydarlioglu, H. Staiger and N. Pallua, *Comparison of viable cell yield from excised versus aspirated adipose tissue*. Cells Tissues Organs, 2004. **178**(2): p. 87-92.
54. Pu, L.L., S.R. Coleman, X. Cui, R.E. Ferguson, Jr. and H.C. Vasconez, *Autologous fat grafts harvested and refined by the Coleman technique: a comparative study*. Plast Reconstr Surg, 2008. **122**(3): p. 932-7.
55. Tuin, A.J., P.N. Domerchie, R.H. Schepers, J.C. Willemsen, P.U. Dijkstra, F.K. Spijkervet, A. Vissink, and J. Jansma, *What is the current optimal fat grafting processing technique? A systematic review*. J Craniomaxillofac Surg, 2016. **44**(1): p. 45-55.
56. Zhu, M., D.M. Arm and J.K. Fraser, *Adipose-Derived Stem and Regenerative Cells as Filler in Plastic and Reconstructive Surgery*, in *Stem Cells in Aesthetic Procedures*, M. Shiffman, A. Di Giuseppe, and F. Bassetto, Editors. 2014, Springer, Berlin, Heidelberg: Berlin, Heidelberg.
57. Tabit, C.J., G.C. Slack, K. Fan, D.C. Wan and J.P. Bradley, *Fat grafting versus adipose-derived stem cell therapy: distinguishing indications, techniques, and outcomes*. Aesthetic Plast Surg, 2012. **36**(3): p. 704-13.
58. Gentile, P., A. Orlandi, M.G. Scioli, C. Di Pasquali, I. Bocchini, C.B. Curcio, M. Floris, V. Fiaschetti, R. Floris, and V. Cervell, *A comparative translational study: the combined use of enhanced stromal vascular fraction and platelet-rich plasma improves fat*

- grafting maintenance in breast reconstruction*. Stem Cells Transl Med, 2012. **1**(4): p. 341-51.
59. Tremolada, C., G. Palmieri and C. Ricordi, *Adipocyte transplantation and stem cells: plastic surgery meets regenerative medicine*. Cell Transplant, 2010. **19**(10): p. 1217-23.
  60. Jiang, A., M. Li, W. Duan, Y. Dong and Y. Wang, *Improvement of the survival of human autologous fat transplantation by adipose-derived stem-cells-assisted lipotransfer combined with bFGF*. ScientificWorldJournal, 2015. **2015**: p. 968057.
  61. Locke, M., J. Windsor and P.R. Dunbar, *Human adipose-derived stem cells: isolation, characterization and applications in surgery*. ANZ J Surg, 2009. **79**(4): p. 235-44.
  62. Luo, S., L. Hao, X. Li, D. Yu, Z. Diao, L. Ren and H. Xu, *Adipose tissue-derived stem cells treated with estradiol enhance survival of autologous fat transplants*. Tohoku J Exp Med, 2013. **231**(2): p. 101-10.
  63. Rigotti, G., A. Marchi, M. Galie, G. Baroni, D. Benati, M. Krampera, A. Pasini, and A. Sbarbati, *Clinical treatment of radiotherapy tissue damage by lipoaspirate transplant: a healing process mediated by adipose-derived adult stem cells*. Plast Reconstr Surg, 2007. **119**(5): p. 1409-22; discussion 1423-4.
  64. Zhang, Y., J. Cai, T. Zhou, Y. Yao, Z. Dong and F. Lu, *Improved Long-Term Volume Retention of Stromal Vascular Fraction Gel Grafting with Enhanced Angiogenesis and Adipogenesis*. Plast Reconstr Surg, 2018. **141**(5): p. 676e-686e.
  65. Landau, M.J., Z.E. Birnbaum, L.G. Kurtz and J.A. Aronowitz, *Review: Proposed Methods to Improve the Survival of Adipose Tissue in Autologous Fat Grafting*. Plast Reconstr Surg Glob Open, 2018. **6**(8): p. e1870.
  66. Kakagia, D. and N. Pallua, *Autologous fat grafting: in search of the optimal technique*. Surg Innov, 2014. **21**(3): p. 327-36.
  67. Garza, R.M., K.J. Paik, M.T. Chung, D. Duscher, G.C. Gurtner, M.T. Longaker and D.C. Wan, *Studies in fat grafting: Part III. Fat grafting irradiated tissue--improved skin quality and decreased fat graft retention*. Plast Reconstr Surg, 2014. **134**(2): p. 249-57.
  68. Dragoo, J.L., J.Y. Choi, J.R. Lieberman, J. Huang, P.A. Zuk, J. Zhang, M.H. Hedrick, and P. Benhaim, *Bone induction by BMP-2 transduced stem cells derived from human fat*. J Orthop Res, 2003. **21**(4): p. 622-9.
  69. Knippenberg, M., M.N. Helder, B.Z. Doulabi, C.M. Semeins, P.I. Wuisman and J. Klein-Nulend, *Adipose tissue-derived mesenchymal stem cells acquire bone cell-like responsiveness to fluid shear stress on osteogenic stimulation*. Tissue Eng, 2005. **11**(11-12): p. 1780-8.
  70. Lu, Y., F. Qiu, Y. Chen and X. Zhao, *[Cell sheet fabrication of hepatocyte-like cells differentiated from adipose tissue mesenchymal stem cells]*. Sheng Wu Gong Cheng Xue Bao, 2009. **25**(4): p. 599-604.
  71. Yoshimura, K., K. Sato, N. Aoi, M. Kurita, T. Hirohi and K. Harii, *Cell-assisted lipotransfer for cosmetic breast augmentation: supportive use of adipose-derived stem/stromal cells*. Aesthetic Plast Surg, 2008. **32**(1): p. 48-55; discussion 56-7.
  72. Matsumoto, D., K. Sato, K. Gonda, Y. Takaki, T. Shigeura, T. Sato, E. Aiba-Kojima, F. Iizuka, K. Inoue, H. Suga, and K. Yoshimura, *Cell-assisted lipotransfer: supportive use of human adipose-derived cells for soft tissue augmentation with lipoinjection*. Tissue Eng, 2006. **12**(12): p. 3375-82.
  73. Holthoner, W., K. Hohenegger, A.M. Husa, S. Muehleder, A. Meinl, A. Peterbauer-Scherb and H. Redl, *Adipose-derived stem cells induce vascular tube formation of outgrowth endothelial cells in a fibrin matrix*. J Tissue Eng Regen Med, 2015. **9**(2): p. 127-36.
  74. Li, L., S. Pan, B. Ni and Y. Lin, *Improvement in autologous human fat transplant survival with SVF plus VEGF-PLA nano-sustained release microspheres*. Cell Biol Int, 2014. **38**(8): p. 962-70.
  75. Salgarello, M., G. Visconti and E. Farallo, *Autologous fat graft in radiated tissue prior to alloplastic reconstruction of the breast: report of two cases*. Aesthetic Plast Surg, 2010. **34**(1): p. 5-10.

76. Bateman, M.E., A.L. Strong, J.M. Gimble and B.A. Bunnell, *Concise Review: Using Fat to Fight Disease: A Systematic Review of Nonhomologous Adipose-Derived Stromal/Stem Cell Therapies*. *Stem Cells*, 2018. **36**(9): p. 1311-1328.
77. Nguyen, A., J. Guo, D.A. Banyard, D. Fadavi, J.D. Toranto, G.A. Wirth, K.Z. Paydar, G.R. Evans, and A.D. Widgerow, *Stromal vascular fraction: A regenerative reality? Part 1: Current concepts and review of the literature*. *J Plast Reconstr Aesthet Surg*, 2016. **69**(2): p. 170-9.
78. Bourin, P., B.A. Bunnell, L. Casteilla, M. Dominici, A.J. Katz, K.L. March, H. Redl, J.P. Rubin, K. Yoshimura, and J.M. Gimble, *Stromal cells from the adipose tissue-derived stromal vascular fraction and culture expanded adipose tissue-derived stromal/stem cells: a joint statement of the International Federation for Adipose Therapeutics and Science (IFATS) and the International Society for Cellular Therapy (ISCT)*. *Cytotherapy*, 2013. **15**(6): p. 641-8.
79. Ong, W.K. and S. Sugii, *Adipose-derived stem cells: fatty potentials for therapy*. *Int J Biochem Cell Biol*, 2013. **45**(6): p. 1083-6.
80. Shukla, L., W.A. Morrison and R. Shayan, *Adipose-Derived Stem Cells in Radiotherapy Injury: A New Frontier*. *Frontiers in Surgery*, 2015. **2**(1).
81. Sterodimas, A., J. de Faria, B. Nicaretta and F. Boriani, *Autologous fat transplantation versus adipose-derived stem cell-enriched lipografts: a study*. *Aesthet Surg J*, 2011. **31**(6): p. 682-93.
82. Tanikawa, D.Y., M. Aguena, D.F. Bueno, M.R. Passos-Bueno and N. Alonso, *Fat grafts supplemented with adipose-derived stromal cells in the rehabilitation of patients with craniofacial microsomia*. *Plast Reconstr Surg*, 2013. **132**(1): p. 141-52.
83. Ra, J.C., S.K. Kang, I.S. Shin, H.G. Park, S.A. Joo, J.G. Kim, B.C. Kang, Y.S. Lee, K. Nakama, M. Piao, B. Sohl, and A. Kurtz, *Stem cell treatment for patients with autoimmune disease by systemic infusion of culture-expanded autologous adipose tissue derived mesenchymal stem cells*. *J Transl Med*, 2011. **9**: p. 181.
84. Sergeevicheva, V., I. Kruchkova, E. Chernykh, E. Shevela, A. Kulagin, A. Gilevich, I. Lisukov, D. Sergeevichev, and V. Kozlov, *Rapid Recovery from Chronic PRCA by MSC Infusion in Patient after Major ABO-Mismatched alloSCT*. *Case Rep Med*, 2012. **2012**: p. 862721.
85. Cho, Y.B., K.J. Park, S.N. Yoon, K.H. Song, D.S. Kim, S.H. Jung, M. Kim, H.Y. Jeong, and C.S. Yu, *Long-term results of adipose-derived stem cell therapy for the treatment of Crohn's fistula*. *Stem Cells Transl Med*, 2015. **4**(5): p. 532-7.
86. Sandor, G.K., J. Numminen, J. Wolff, T. Thesleff, A. Miettinen, V.J. Tuovinen, B. Mannerstrom, M. Patrikoski, R. Seppanen, S. Miettinen, M. Rautiainen, and J. Ohman, *Adipose stem cells used to reconstruct 13 cases with cranio-maxillofacial hard-tissue defects*. *Stem Cells Transl Med*, 2014. **3**(4): p. 530-40.
87. Thesleff, T., K. Lehtimaki, T. Niskakangas, B. Mannerstrom, S. Miettinen, R. Suuronen and J. Ohman, *Cranioplasty with adipose-derived stem cells and biomaterial: a novel method for cranial reconstruction*. *Neurosurgery*, 2011. **68**(6): p. 1535-40.
88. Riordan, N.H., T.E. Ichim, W.P. Min, H. Wang, F. Solano, F. Lara, M. Alfaro, J.P. Rodriguez, R.J. Harman, A.N. Patel, M.P. Murphy, R.R. Lee, and B. Minev, *Non-expanded adipose stromal vascular fraction cell therapy for multiple sclerosis*. *J Transl Med*, 2009. **7**: p. 29.
89. Bura, A., V. Planat-Benard, P. Bourin, J.S. Silvestre, F. Gross, J.L. Grolleau, B. Saint-Lebese, J.A. Peyrafitte, S. Fleury, M. Gadelorge, M. Taurand, S. Dupuis-Coronas, B. Leobon, and L. Casteilla, *Phase I trial: the use of autologous cultured adipose-derived stroma/stem cells to treat patients with non-revascularizable critical limb ischemia*. *Cytotherapy*, 2014. **16**(2): p. 245-57.
90. Gimble, J.M., *Adipose tissue-derived therapeutics*. *Expert Opinion Biological Therapy*, 2003: p. 705-713.
91. Bacakova, L., J. Zarubova, M. Travnickova, J. Musilkova, J. Pajorova, P. Slepicka, N.S. Kasalkova, V. Svorcik, Z. Kolska, H. Motarjemi, and M. Molitor, *Stem cells: their source, potency and use in regenerative therapies with focus on adipose-derived stem cells - a review*. *Biotechnol Adv*, 2018. **36**(4): p. 1111-1126.

92. Kilroy, G.E., S.J. Foster, X. Wu, J. Ruiz, S. Sherwood, A. Heifetz, J.W. Ludlow, D.M. Stricker, S. Potiny, P. Green, Y.D. Halvorsen, B. Cheatham, R.W. Storms, and J.M. Gimble, *Cytokine profile of human adipose-derived stem cells: expression of angiogenic, hematopoietic, and pro-inflammatory factors*. J Cell Physiol, 2007. **212**(3): p. 702-9.
93. Kronsteiner, B., A. Peterbauer-Scherb, R. Grillari-Voglauer, H. Redl, C. Gabriel, M. van Griensven and S. Wolbank, *Human mesenchymal stem cells and renal tubular epithelial cells differentially influence monocyte-derived dendritic cell differentiation and maturation*. Cell Immunol, 2011. **267**(1): p. 30-8.
94. Kronsteiner, B., S. Wolbank, A. Peterbauer, C. Hackl, H. Redl, M. van Griensven and C. Gabriel, *Human mesenchymal stem cells from adipose tissue and amnion influence T-cells depending on stimulation method and presence of other immune cells*. Stem Cells Dev, 2011. **20**(12): p. 2115-26.
95. Wolbank, S., F. Hildner, H. Redl, M. van Griensven, C. Gabriel and S. Hennerbichler, *Impact of human amniotic membrane preparation on release of angiogenic factors*. J Tissue Eng Regen Med, 2009. **3**(8): p. 651-4.
96. Wolbank, S., A. Peterbauer, M. Fahrner, S. Hennerbichler, M. van Griensven, G. Stadler, H. Redl, and C. Gabriel, *Dose-dependent immunomodulatory effect of human stem cells from amniotic membrane: a comparison with human mesenchymal stem cells from adipose tissue*. Tissue Eng, 2007. **13**(6): p. 1173-83.
97. Gimble, J.M., A.J. Katz and B.A. Bunnell, *Adipose-derived stem cells for regenerative medicine*. Circ Res, 2007. **100**(9): p. 1249-60.
98. Rehman, J., D. Traktuev, J. Li, S. Merfeld-Clauss, C.J. Temm-Grove, J.E. Bovenkerk, C.L. Pell, B.H. Johnstone, R.V. Considine, and K.L. March, *Secretion of angiogenic and antiapoptotic factors by human adipose stromal cells*. Circulation, 2004. **109**(10): p. 1292-8.
99. Yoshimura, K., H. Eto, H. Kato, K. Doi and N. Aoi, *In vivo manipulation of stem cells for adipose tissue repair/reconstruction*. Regen Med, 2011. **6**(6 Suppl): p. 33-41.
100. Miranville, A., C. Heeschen, C. Sengenès, C.A. Curat, R. Busse and A. Bouloumie, *Improvement of postnatal neovascularization by human adipose tissue-derived stem cells*. Circulation, 2004. **110**(3): p. 349-55.
101. Levenstein, M.E., T.E. Ludwig, R.H. Xu, R.A. Llanas, K. VanDenHeuvel-Kramer, D. Manning and J.A. Thomson, *Basic fibroblast growth factor support of human embryonic stem cell self-renewal*. Stem Cells, 2006. **24**(3): p. 568-74.
102. Stivers, K.B., J.E. Beare, P.M. Chilton, S.K. Williams, C.L. Kaufman and J.B. Hoying, *Adipose-derived cellular therapies in solid organ and vascularized-composite allotransplantation*. Curr Opin Organ Transplant, 2017. **22**(5): p. 490-498.
103. Jiang, T., G. Xu, Q. Wang, L. Yang, L. Zheng, J. Zhao and X. Zhang, *In vitro expansion impaired the stemness of early passage mesenchymal stem cells for treatment of cartilage defects*. Cell Death Dis, 2017. **8**(6): p. e2851.
104. McIntosh, K., S. Zvonic, S. Garrett, J.B. Mitchell, Z.E. Floyd, L. Hammill, A. Kloster, Y. Di Halvorsen, J.P. Ting, R.W. Storms, B. Goh, G. Kilroy, X. Wu, and J.M. Gimble, *The immunogenicity of human adipose-derived cells: temporal changes in vitro*. Stem Cells, 2006. **24**(5): p. 1246-53.
105. Pan, Q., S.M. Fouraschen, P.E. de Ruyter, W.N. Dinjens, J. Kwekkeboom, H.W. Tilanus and L.J. van der Laan, *Detection of spontaneous tumorigenic transformation during culture expansion of human mesenchymal stromal cells*. Exp Biol Med (Maywood), 2014. **239**(1): p. 105-15.
106. Safwani, W.K., S. Makpol, S. Sathapan and K.H. Chua, *Alteration of gene expression levels during osteogenic induction of human adipose derived stem cells in long-term culture*. Cell Tissue Bank, 2013. **14**(2): p. 289-301.
107. Agency, E.M., *Scientific recommendation on classification of advanced therapy medicinal products. Article 17 - Regulation (EC) No 1394/2007*, E.M. Agency, Editor. 2012.

108. Oberbauer, E., C. Steffenhagen, C. Wurzer, C. Gabriel, H. Redl and S. Wolbank, *Enzymatic and non-enzymatic isolation systems for adipose tissue-derived cells: current state of the art*. Cell Regen (Lond), 2015. **4**: p. 7.
109. Hamed, S., D. Egozi, D. Kruchevsky, L. Teot, A. Gilhar and Y. Ullmann, *Erythropoietin improves the survival of fat tissue after its transplantation in nude mice*. PLoS One, 2010. **5**(11): p. e13986.
110. Van Pham, P., K.H. Bui, D.Q. Ngo, N.B. Vu, N.H. Truong, N.L. Phan, D.M. Le, T.D. Duong, T.D. Nguyen, V.T. Le, and N.K. Phan, *Activated platelet-rich plasma improves adipose-derived stem cell transplantation efficiency in injured articular cartilage*. Stem Cell Res Ther, 2013. **4**(4): p. 91.
111. Park, I.S., P.S. Chung and J.C. Ahn, *Enhancement of Ischemic Wound Healing by Spheroid Grafting of Human Adipose-Derived Stem Cells Treated with Low-Level Light Irradiation*. PLoS One, 2015. **10**(6): p. e0122776.
112. Park, I.S., A. Mondal, P.S. Chung and J.C. Ahn, *Vascular regeneration effect of adipose-derived stem cells with light-emitting diode phototherapy in ischemic tissue*. Lasers Med Sci, 2015. **30**(2): p. 533-41.
113. Teuschl, A., E.R. Balmayor, H. Redl, M. van Griensven and P. Dungal, *Phototherapy with LED light modulates healing processes in an in vitro scratch-wound model using 3 different cell types*. Dermatol Surg, 2015. **41**(2): p. 261-8.
114. Paspaliaris, B. and J. Thornton, *Methods and apparatuses for isolating and preparing stem cells*. 2014: US.
115. Maioli, M., S. Rinaldi, S. Santaniello, A. Castagna, G. Pigliaru, A. Delitala, F. Bianchi, C. Tremolada, V. Fontani, and C. Ventura, *Radioelectric asymmetric conveyed fields and human adipose-derived stem cells obtained with a nonenzymatic method and device: a novel approach to multipotency*. Cell Transplant, 2014. **23**(12): p. 1489-500.
116. Ogden, J.A., A. Toth-Kischkat and R. Schultheiss, *Principles of shock wave therapy*. Clin Orthop Relat Res, 2001(387): p. 8-17.
117. Elster, E.A., A. Stojadinovic, J. Forsberg, S. Shawen, R.C. Andersen and W. Schaden, *Extracorporeal shock wave therapy for nonunion of the tibia*. J Orthop Trauma, 2010. **24**(3): p. 133-41.
118. Furia, J.P., P.J. Juliano, A.M. Wade, W. Schaden and R. Mittermayr, *Shock wave therapy compared with intramedullary screw fixation for nonunion of proximal fifth metatarsal metaphyseal-diaphyseal fractures*. J Bone Joint Surg Am, 2010. **92**(4): p. 846-54.
119. Mittermayr, R., J. Hartinger, V. Antonic, A. Meinl, S. Pfeifer, A. Stojadinovic, W. Schaden, and H. Redl, *Extracorporeal shock wave therapy (ESWT) minimizes ischemic tissue necrosis irrespective of application time and promotes tissue revascularization by stimulating angiogenesis*. Ann Surg, 2011. **253**(5): p. 1024-32.
120. Schaden, W., R. Thiele, C. Kolpl, M. Pusch, A. Nissan, C.E. Attinger, M.E. Maniscalco-Theberge, G.E. Peoples, E.A. Elster, and A. Stojadinovic, *Shock wave therapy for acute and chronic soft tissue wounds: a feasibility study*. J Surg Res, 2007. **143**(1): p. 1-12.
121. Saggini, R., A. Figus, A. Troccola, V. Cocco, A. Saggini and N. Scuderi, *Extracorporeal shock wave therapy for management of chronic ulcers in the lower extremities*. Ultrasound Med Biol, 2008. **34**(8): p. 1261-71.
122. Weihs, A.M., C. Fuchs, A.H. Teuschl, J. Hartinger, P. Slezak, R. Mittermayr, H. Redl, W.G. Junger, H.H. Sitte, and D. Runzler, *Shock wave treatment enhances cell proliferation and improves wound healing by ATP release-coupled extracellular signal-regulated kinase (ERK) activation*. J Biol Chem, 2014. **289**(39): p. 27090-104.
123. Chen, Y.J., Y.R. Kuo, K.D. Yang, C.J. Wang, S.M. Sheen Chen, H.C. Huang, Y.J. Yang, S. Yi-Chih, and F.S. Wang, *Activation of extracellular signal-regulated kinase (ERK) and p38 kinase in shock wave-promoted bone formation of segmental defect in rats*. Bone, 2004. **34**(3): p. 466-77.
124. Siems, W., T. Grune, P. Voss and R. Brenke, *Anti-fibrosclerotic effects of shock wave therapy in lipedema and cellulite*. Biofactors, 2005. **24**(1-4): p. 275-82.



125. Schlaudraff, K.U., M.C. Kiessling, N.B. Csaszar and C. Schmitz, *Predictability of the individual clinical outcome of extracorporeal shock wave therapy for cellulite*. Clin Cosmet Investig Dermatol, 2014. **7**: p. 171-83.
126. Knobloch, K. and R. Kraemer, *Extracorporeal shock wave therapy (ESWT) for the treatment of cellulite--A current metaanalysis*. Int J Surg, 2015. **24**(Pt B): p. 210-7.
127. Sandhofer, M., *Radial shockwave therapy after cryolipolysis™ in cellulite and lymphedema - A field report*, in *Cosmetic Medicine*. 2015. p. 12-13.
128. Christ, C., R. Brenke, G. Sattler, W. Siems, P. Novak and A. Daser, *Improvement in skin elasticity in the treatment of cellulite and connective tissue weakness by means of extracorporeal pulse activation therapy*. Aesthet Surg J, 2008. **28**(5): p. 538-44.
129. Angehrn, F., C. Kuhn and A. Voss, *Can cellulite be treated with low-energy extracorporeal shock wave therapy?* Clin Interv Aging, 2007. **2**(4): p. 623-30.
130. Kraemer, R., H. Sorg, V. Forstmeier, K. Knobloch, E. Liodaki, F.H. Stang, P. Mailaender, and T. Kisch, *Immediate Dose-Response Effect of High-Energy Versus Low-Energy Extracorporeal Shock Wave Therapy on Cutaneous Microcirculation*. Ultrasound Med Biol, 2016. **42**(12): p. 2975-2982.
131. Huang, Y.-Y., *Low-level laser therapy: an emerging clinical paradigm*. SPIE Newsroom 9, 2009: p. 1-3.
132. Chung, H., T. Dai, S.K. Sharma, Y.Y. Huang, J.D. Carroll and M.R. Hamblin, *The nuts and bolts of low-level laser (light) therapy*. Ann Biomed Eng, 2012. **40**(2): p. 516-33.
133. Kim, H., K. Choi, O.K. Kweon and W.H. Kim, *Enhanced wound healing effect of canine adipose-derived mesenchymal stem cells with low-level laser therapy in athymic mice*. J Dermatol Sci, 2012. **68**(3): p. 149-56.
134. Mvula, B., T.J. Moore and H. Abrahamse, *Effect of low-level laser irradiation and epidermal growth factor on adult human adipose-derived stem cells*. Lasers Med Sci, 2010. **25**(1): p. 33-9.
135. Tuby, H., L. Maltz and U. Oron, *Low-level laser irradiation (LLLI) promotes proliferation of mesenchymal and cardiac stem cells in culture*. Lasers Surg Med, 2007. **39**(4): p. 373-8.
136. Klebanov, G.I., N. Shuraeva, T.V. Chichuk, A.N. Osipov, T.G. Rudenko, A.B. Shekhter and A. Vladimirov Iu, *[A comparative study of the effects of laser and light-emitting diode irradiation on the wound healing and functional activity of wound exudate leukocytes]*. Biofizika, 2005. **50**(6): p. 1137-44.
137. Corazza, A.V., J. Jorge, C. Kurachi and V.S. Bagnato, *Photobiomodulation on the angiogenesis of skin wounds in rats using different light sources*. Photomed Laser Surg, 2007. **25**(2): p. 102-6.
138. de Vasconcelos Catao, M.H., C.F. Nonaka, R.L. de Albuquerque, Jr., P.M. Bento and R. de Oliveira Costa, *Effects of red laser, infrared, photodynamic therapy, and green LED on the healing process of third-degree burns: clinical and histological study in rats*. Lasers Med Sci, 2015. **30**(1): p. 421-8.
139. Allen, E.V. and E.A. Hines, *Lipedema of the legs: a syndrome characterized by fat legs and orthostatic edema*. Proc Staff Mayo Clinic, 1940. **15**: p. 184-187.
140. Wold, L.E., E.A. Hines, Jr. and E.V. Allen, *Lipedema of the legs; a syndrome characterized by fat legs and edema*. Ann Intern Med, 1951. **34**(5): p. 1243-50.
141. Fife, C.E., E.A. Maus and M.J. Carter, *Lipedema: a frequently misdiagnosed and misunderstood fatty deposition syndrome*. Adv Skin Wound Care, 2010. **23**(2): p. 81-92; quiz 93-4.
142. Kaiserling, E., *Morphologische Befunde bei Lymphödem, Lipödem, Lipolymphödem*, in *Lehrbuch der Lymphologie*, M. Földi, E. Földi, and S. Kubik, Editors. 2005, Gustav Fischer: Stuttgart, New York. p. 374-378.
143. Brenner, E., *Plasma - interstitielle Flüssigkeit - Lymphe*. Lymphforschung, 2009. **13**: p. 25-27.
144. Harwood, C.A., R.H. Bull, J. Evans and P.S. Mortimer, *Lymphatic and venous function in lipoeidema*. Br J Dermatol, 1996. **134**(1): p. 1-6.

145. Child, A.H., K.D. Gordon, P. Sharpe, G. Brice, P. Ostergaard, S. Jeffery and P.S. Mortimer, *Lipedema: an inherited condition*. Am J Med Genet A, 2010. **152a**(4): p. 970-6.
146. Gavin, K.M., E.E. Cooper and R.C. Hickner, *Estrogen receptor protein content is different in abdominal than gluteal subcutaneous adipose tissue of overweight-to-obese premenopausal women*. Metabolism, 2013. **62**(8): p. 1180-8.
147. Kang, Q., W.X. Song, Q. Luo, N. Tang, J. Luo, X. Luo, J. Chen, Y. Bi, B.C. He, J.K. Park, W. Jiang, Y. Tang, J. Huang, Y. Su, G.H. Zhu, Y. He, H. Yin, Z. Hu, Y. Wang, L. Chen, G.W. Zuo, X. Pan, J. Shen, T. Vokes, R.R. Reid, R.C. Haydon, H.H. Luu, and T.C. He, *A comprehensive analysis of the dual roles of BMPs in regulating adipogenic and osteogenic differentiation of mesenchymal progenitor cells*. Stem Cells Dev, 2009. **18**(4): p. 545-59.
148. Suga, H., J. Araki, N. Aoi, H. Kato, T. Higashino and K. Yoshimura, *Adipose tissue remodeling in lipedema: adipocyte death and concurrent regeneration*. J Cutan Pathol, 2009. **36**(12): p. 1293-8.
149. Szolnok, G., A. Nemes, H. Gavalier, T. Forster and L. Kemeny, *Lipedema is associated with increased aortic stiffness*. Lymphology, 2012. **45**(2): p. 71-9.
150. *Morphologische Befunde bei Lymphödem, Lipödem, Lipolymphödem*, in *Lehrbuch der Lymphologie*, M. Földi, E. Földi, and S. Kubik, Editors. 2005, Gustav Fischer: Stuttgart, New York. p. 374-378.
151. Corporation, P. *CellTiter-Glo Luminescent Cell Viability Assay*. [cited 2019 20.08.2019]; Protocol]. Available from: <https://at.promega.com/resources/protocols/technical-bulletins/0/celltiter-glo-luminescent-cell-viability-assay-protocol/>.
152. Roche. *Cytotoxicity Detection Kit (LDH)*. [cited 2019 20.08.2019]; Protocol]. Available from: <https://www.sigmaaldrich.com/content/dam/sigmaaldrich/docs/Roche/Bulletin/1/11644793001bul.pdf>.
153. Rohringer, S., P. Hofbauer, K.H. Schneider, A.M. Husa, G. Feichtinger, A. Peterbauer-Scherb, H. Redl, and W. Holthöner, *Mechanisms of vasculogenesis in 3D fibrin matrices mediated by the interaction of adipose-derived stem cells and endothelial cells*. Angiogenesis, 2014. **17**(4): p. 921-33.
154. Fisher, C., T.L. Grahovac, M.E. Schafer, R.D. Shippert, K.G. Marra and J.P. Rubin, *Comparison of harvest and processing techniques for fat grafting and adipose stem cell isolation*. Plast Reconstr Surg, 2013. **132**(2): p. 351-61.
155. Aronowitz, J.A., R.A. Lockhart and C.S. Hakakian, *Mechanical versus enzymatic isolation of stromal vascular fraction cells from adipose tissue*. Springerplus, 2015. **4**: p. 713.
156. Faustini, M., M. Bucco, T. Chlapanidas, G. Lucconi, M. Marazzi, M.C. Tosca, P. Gaetani, M. Klinger, S. Villani, V.V. Ferretti, D. Vigo, and M.L. Torre, *Nonexpanded mesenchymal stem cells for regenerative medicine: yield in stromal vascular fraction from adipose tissues*. Tissue Eng Part C Methods, 2010. **16**(6): p. 1515-21.
157. Yamanaka, S., S. Yokote, A. Yamada, Y. Katsuoka, L. Izuhara, Y. Shimada, N. Omura, H.J. Okano, T. Ohki, and T. Yokoo, *Adipose tissue-derived mesenchymal stem cells in long-term dialysis patients display downregulation of PCAF expression and poor angiogenesis activation*. PLoS One, 2014. **9**(7): p. e102311.
158. Fortini, C., D. Cesselli, A.P. Beltrami, N. Bergamin, A. Caragnano, L. Moretti, F. Cecaro, G. Aquila, P. Rizzo, C. Riberti, L. Tavazzi, A. Fucili, C.A. Beltrami, and R. Ferrari, *Alteration of Notch signaling and functionality of adipose tissue derived mesenchymal stem cells in heart failure*. Int J Cardiol, 2014. **174**(1): p. 119-26.
159. Frazier, T.P., J.M. Gimble, J.W. Devay, H.A. Tucker, E.S. Chiu and B.G. Rowan, *Body mass index affects proliferation and osteogenic differentiation of human subcutaneous adipose tissue-derived stem cells*. BMC Cell Biol, 2013. **14**: p. 34.
160. Yang, H.J., K.J. Kim, M.K. Kim, S.J. Lee, Y.H. Ryu, B.F. Seo, D.Y. Oh, S.T. Ahn, H.Y. Lee, and J.W. Rhie, *The stem cell potential and multipotency of human adipose tissue-derived stem cells vary by cell donor and are different from those of other types of stem cells*. Cells Tissues Organs, 2014. **199**(5-6): p. 373-83.

161. Choudhery, M.S., M. Badowski, A. Muise, J. Pierce and D.T. Harris, *Donor age negatively impacts adipose tissue-derived mesenchymal stem cell expansion and differentiation*. J Transl Med, 2014. **12**: p. 8.
162. Dos-Anjos Vilaboa, S., M. Navarro-Palou and R. Llull, *Age influence on stromal vascular fraction cell yield obtained from human lipoaspirates*. Cytotherapy, 2014. **16**(8): p. 1092-7.
163. Madonna, R., F.V. Renna, C. Cellini, R. Cotellese, N. Picardi, F. Francomano, P. Innocenti, and R. De Caterina, *Age-dependent impairment of number and angiogenic potential of adipose tissue-derived progenitor cells*. Eur J Clin Invest, 2011. **41**(2): p. 126-33.
164. Jo, C.H., Y.G. Lee, W.H. Shin, H. Kim, J.W. Chai, E.C. Jeong, J.E. Kim, H. Shim, J.S. Shin, I.S. Shin, J.C. Ra, S. Oh, and K.S. Yoon, *Intra-articular injection of mesenchymal stem cells for the treatment of osteoarthritis of the knee: a proof-of-concept clinical trial*. Stem Cells, 2014. **32**(5): p. 1254-66.
165. Pak, J., J.H. Lee, K.S. Park, B.C. Jeong and S.H. Lee, *Regeneration of Cartilage in Human Knee Osteoarthritis with Autologous Adipose Tissue-Derived Stem Cells and Autologous Extracellular Matrix*. Biores Open Access, 2016. **5**(1): p. 192-200.
166. Spasovski, D., V. Spasovski, Z. Bascarevic, M. Stojiljkovic, M. Vreca, M. Anđelković and S. Pavlović, *Intra-articular injection of autologous adipose-derived mesenchymal stem cells in the treatment of knee osteoarthritis*. J Gene Med, 2018. **20**(1).
167. Schaden, W., A. Fischer and A. Sailler, *Extracorporeal shock wave therapy of nonunion or delayed osseous union*. Clin Orthop Relat Res, 2001(387): p. 90-4.
168. Mittermayr, R., V. Antonic, J. Hartinger, H. Kaufmann, H. Redl, L. Teot, A. Stojadinovic, and W. Schaden, *Extracorporeal shock wave therapy (ESWT) for wound healing: technology, mechanisms, and clinical efficacy*. Wound Repair Regen, 2012. **20**(4): p. 456-65.
169. Cebicci, M.A., S.T. Sutbeyaz, S.S. Goksu, S. Hocaoglu, A. Oguz and A. Atilabey, *Extracorporeal Shock Wave Therapy for Breast Cancer-Related Lymphedema: A Pilot Study*. Arch Phys Med Rehabil, 2016. **97**(9): p. 1520-1525.
170. Sandhofer, M., *Radial shockwave therapy after cryolipolysis in cellulite and lymphedema - A filed report*. Cosmetic Medicine, 2015. **36**.
171. Bae, H. and H.J. Kim, *Clinical outcomes of extracorporeal shock wave therapy in patients with secondary lymphedema: a pilot study*. Ann Rehabil Med, 2013. **37**(2): p. 229-34.
172. Holfeld, J., C. Tepekoylu, S. Blunder, D. Lobenwein, E. Kirchmair, M. Dietl, R. Kozaryn, D. Lener, M. Theurl, P. Paulus, R. Kirchmair, and M. Grimm, *Low energy shock wave therapy induces angiogenesis in acute hind-limb ischemia via VEGF receptor 2 phosphorylation*. PLoS One, 2014. **9**(8): p. e103982.
173. Rohringer, S., W. Holnthoner, M. Hackl, A.M. Weihs, D. Rünzler, S. Skalicky, M. Karbiener, M. Scheideler, J. Pröll, C. Gabriel, B. Schweighofer, M. Gröger, A. Spittler, J. Grillari, and H. Redl, *Molecular and cellular effects of in vitro shockwave treatment on lymphatic endothelial cells*. PLoS One, 2014. **9**(12): p. e114806.
174. Szymanska, J., K. Goralczyk, J.J. Klawe, M. Lukowicz, M. Michalska, B. Goralczyk, P. Zalewski, J.L. Newton, L. Gryko, A. Zajac, and D. Rosc, *Phototherapy with low-level laser influences the proliferation of endothelial cells and vascular endothelial growth factor and transforming growth factor-beta secretion*. J Physiol Pharmacol, 2013. **64**(3): p. 387-91.
175. Park, I.S., P.S. Chung and J.C. Ahn, *Adipose-derived stem cell spheroid treated with low-level light irradiation accelerates spontaneous angiogenesis in mouse model of hindlimb ischemia*. Cytotherapy, 2017. **19**(9): p. 1070-1078.
176. Park, I.S., P.S. Chung and J.C. Ahn, *Enhanced angiogenic effect of adipose-derived stromal cell spheroid with low-level light therapy in hind limb ischemia mice*. Biomaterials, 2014. **35**(34): p. 9280-9.
177. Park, I.S., P.S. Chung, J.C. Ahn and A. Leproux, *Human adipose-derived stem cell spheroid treated with photobiomodulation irradiation accelerates tissue regeneration in mouse model of skin flap ischemia*. Lasers Med Sci, 2017. **32**(8): p. 1737-1746.

## VIII. Appendix

All publications presented in this thesis are attached.

## ADIPOSE-TISSUE-DERIVED THERAPEUTIC CELLS IN THEIR NATURAL ENVIRONMENT AS AN AUTOLOGOUS CELL THERAPY STRATEGY: THE MICROTISSUE-STROMAL VASCULAR FRACTION

S. Nürnberger<sup>1,2,4</sup>, C. Lindner<sup>1,2</sup>, J. Maier<sup>1,2</sup>, K. Strohmeier<sup>1,2,5</sup>, C. Wurzer<sup>1,2,3</sup>, P. Slezak<sup>1,2</sup>, S. Suessner<sup>2,6</sup>, W. Holnthoner<sup>1,2</sup>, H. Redl<sup>1,2</sup>, S. Wolbank<sup>1,2,§</sup> and E. Priglinger<sup>1,2,§\*</sup>

<sup>1</sup>Ludwig Boltzmann Institute for Experimental and Clinical Traumatology, AUVA Research Centre, Linz/Vienna, Austria

<sup>2</sup>Austrian Cluster for Tissue Regeneration, Vienna, Austria

<sup>3</sup>Liporegena GmbH, Breitenfurt, Austria

<sup>4</sup>Department of Orthopedics and Trauma-Surgery, Division of Trauma-Surgery, Medical University of Vienna, Vienna, Austria

<sup>5</sup>School of Medical Engineering and Applied Social Sciences, University of Applied Sciences Upper Austria, Linz, Austria

<sup>6</sup>Red Cross Blood Transfusion Service of Upper Austria, Linz, Austria

<sup>§</sup>These authors contributed equally

### Abstract

The prerequisite for a successful clinical use of autologous adipose-tissue-derived cells is the highest possible regenerative potential of the applied cell population, the stromal vascular fraction (SVF). Current isolation methods depend on high enzyme concentration, lysis buffer, long incubation steps and mechanical stress, resulting in single cell dissociation. The aim of the study was to limit cell manipulation and obtain a derivative comprising therapeutic cells (microtissue-SVF) without dissociation from their natural extracellular matrix, by employing a gentle good manufacturing practice (GMP)-grade isolation. The microtissue-SVF yielded larger numbers of viable cells as compared to the improved standard-SVF, both with low enzyme concentration and minimal dead cell content. It comprised stromal tissue compounds (collagen, glycosaminoglycans, fibroblasts), capillaries and vessel structures (CD31<sup>+</sup>, smooth muscle actin<sup>+</sup>). A broad range of cell types was identified by surface-marker characterisation, including mesenchymal, haematopoietic, pericytic, blood and lymphatic vascular and epithelial cells. Subpopulations such as supra-adventitial adipose-derived stromal/stem cells and endothelial progenitor cells were significantly more abundant in the microtissue-SVF, corroborated by significantly higher potency for angiogenic tube-like structure formation *in vitro*. The microtissue-SVF showed the characteristic phenotype and tri-lineage mesenchymal differentiation potential *in vitro* and an immunomodulatory and pro-angiogenic secretome. *In vivo* implantation of the microtissue-SVF combined with fat demonstrated successful graft integration in nude mice. The present study demonstrated a fast and gentle isolation by minor manipulation of liposuction material, achieving a therapeutically relevant cell population with high vascularisation potential and immunomodulatory properties still embedded in a fraction of its original matrix.

**Keywords:** Stromal vascular fraction, extracellular matrix, adipose-derived stromal/stem cells, endothelial progenitor cells, angiogenesis.

**\*Address for correspondence:** Dr Eleni Priglinger, Ludwig Boltzmann Institute for Experimental and Clinical Traumatology, Krankenhausstraße 7, A-4010 Linz, Austria.

Telephone number: +43 6648234342 Email: Eleni.Priglinger@trauma.lbg.ac.at

**Copyright policy:** This article is distributed in accordance with Creative Commons Attribution Licence (<http://creativecommons.org/licenses/by-sa/4.0/>).

### Introduction

Adipose-tissue-derived cells are successfully applied for the reconstruction and regeneration of damaged

or diseased tissues where common therapies fail (Pak *et al.*, 2018). Their high regenerative potential is underlined by several clinical trials. More pre-clinical studies have progressed into clinical trials,

with mesenchymal stromal/stem cells (MSCs) derived from adipose tissue, than from other sources, e.g. the bone marrow (Macrin *et al.*, 2017). The adipose tissue is abundantly available as an autologous cell source in most patients and provides easily obtainable regenerative cells in large amounts (Bacakova *et al.*, 2018). The isolated cell population, the stromal vascular fraction (SVF), contains a variety of stem, progenitor and mature cell types from haematopoietic, vascular and mesenchymal origin, such as lymphocytes, monocytes/macrophages, endothelial cells, pericytes, smooth muscle cells, fibroblasts and adipose-derived stromal/stem cells (ASCs) among others (Bourin *et al.*, 2013; Zimmerlin *et al.*, 2010).

ASCs can be selected as one of the adherent cell fractions, by cultivating the SVF on tissue culture plastic (Bourin *et al.*, 2013). They are characterised by their self-renewal potency and ability to give rise to at least adipocytic, osteocytic, chondrocytic and myocytic lineages (De Francesco *et al.*, 2015; Gimble and Guilak, 2003a; Gimble and Guilak, 2003b; Zuk *et al.*, 2002; Zuk *et al.*, 2001). ASCs in culture express some common mesenchymal stromal/stem cell markers including CD90, CD73, CD105 and CD44 and remain negative for CD45 and CD31 (Bourin *et al.*, 2013). During regeneration, they act as immunomodulators and can migrate to damaged areas of the body, where they secrete factors facilitating tissue repair (Bateman *et al.*, 2018). ASCs have regenerative potential *in vitro*, in animal models and in clinical studies for soft tissue reconstruction, bone and cartilage regeneration, treatment of immune diseases, cardiovascular diseases, gastrointestinal diseases, neurological diseases and diabetes, with variable success (Bateman *et al.*, 2018; Nguyen *et al.*, 2015).

In recent years, there has been a shift towards using the total SVF cell population, following the concept of an intraoperative procedure bringing autologous cells back into the patient without further processing. In terms of cell-assisted lipotransfer (CAL), the addition of the SVF is successfully established in fat grafting, enhancing long-term graft stability (Gentile *et al.*, 2012; Jiang *et al.*, 2015). With its potential for immunomodulation and angiogenesis, the SVF recruits vessels and induces a local regulatory, pro-regenerative immune cell phenotype (reviewed by Stivers *et al.*, 2017). Providing a clinical grade product is a critical requirement for ASC or SVF application. In contrast to the SVF, ASCs depend on *in vitro* expansion, which is associated with challenges such as possible cell transformation risks or stemness loss (Jiang *et al.*, 2017; McIntosh K., 2006; Pan *et al.*, 2014; Safwani *et al.*, 2013). Moreover, using the SVF during a surgical procedure in an autologous and homologous way is not considered an advanced therapy medicinal product (ATMP) (European Medicines Agency, 2012). Still, the multiple steps of collagenase and erythrocyte lysis buffer incubation, as well as centrifugation and filtration can negatively

impact on cell efficacy (Hagman *et al.*, 2012). Hence, there is an unmet need for a gentle isolation method providing regenerative cell populations protected by their natural environment and fulfilling all the regulatory requirements of a minimally manipulated cellular product.

The present study described a fast and particularly gentle method of SVF isolation by minor manipulation of liposuction material, achieving an SVF cell population, still embedded in a fraction of its original matrix. The microtissue-SVF was isolated from the adipose tissue with a good manufacturing practice (GMP)-certified collagenase under sterile and mild conditions and compared to the standard-SVF, both isolated with low collagenase concentration. The freshly isolated microtissue-SVF was thoroughly characterised with regards to vitality, matrix composition, cell identity and functionality. This was achieved by analysing tissue morphology, cellular composition, surface marker profile, adipogenic, osteogenic, chondrogenic and vasculogenic potential, regenerative secretome protein profile and support of graft integration after intramuscular injection in nude mice. Since adipose tissue consists of various extracellular matrix (ECM) components, together with a variety of therapeutic cells (Liu *et al.*, 2011), the working hypothesis was that adipose-derived microtissue-SVF, comprising therapeutic cells without dissociation from the adipose tissue ECM, might represent an optimised product for tissue repair.

## Materials and Methods

### Liposuction

The collection of human adipose tissue was approved by the local ethical board (application/approval number 200, 12.05.2005 and 19.05.2014) and written patient's consent. Subcutaneous adipose tissue was obtained from 25 patients [age:  $39 \pm 10$  years; body mass index (BMI):  $33.6 \pm 6.7$  kg/m<sup>2</sup>] during routine outpatient liposuction procedures under local tumescence anaesthesia.

### Standard-SVF isolation

Standard-SVF isolation was optimised to obtain the highest yield of a highly viable single-cell suspension under mild proteolytic conditions. Liposuction material was collected in a fully closed container and 100 mL liposuction material was transferred into a blood bag (Macopharma, Langen, Germany) and washed with an equal volume of phosphate buffered saline (PBS), to remove blood and tumescence solution (Table 1). Next, for tissue digestion, PBS was replaced with 0.2 U/mL collagenase NB4 (Serva, Vienna, Austria) dissolved in 100 mL PBS containing Ca<sup>2+</sup>/Mg<sup>2+</sup> and 25 mM N-(2-hydroxyethyl)piperazine-N'-(2-ethanesulfonic acid) (HEPES; Sigma-Aldrich), resulting in a final collagenase concentration of 0.1 U/mL. The blood bag was incubated at 37 °C under

**Table 1. Overview of standard-SVF and microtissue-SVF isolation.** The optimised standard-SVF isolation protocol was adapted for microtissue-SVF isolation using GMP-compliant reagents, avoiding erythrocyte lysis buffer, one extra centrifugation step and filtration.

	Standard-SVF isolation	Microtissue-SVF isolation
Washing I	1× with PBS	1× with PBS
Collagenase	NB4, 0.1 U/mL, 37 °C, 180 rpm, 1 h	NB6, 0.1 U/mL, 37 °C, 180 rpm, 1 h
Centrifugation I	1200 ×g, 7 min	1200 ×g, 7 min
Erythrocyte lysis	Erythrocyte lysis buffer, 5 min, 37 °C	-
Centrifugation II	500 ×g, 5 min	-
Washing II	1× with PBS	1× with PBS
Filtration	100 µm	-
Centrifugation III	500 ×g, 5 min	300 ×g, 5 min

moderate shaking (180 rpm) for 1 h. The digested tissue was transferred into 50 mL tubes. After centrifugation at 1200 ×g for 7 min, the cell pellet was incubated with 100 mL erythrocyte lysis buffer for 5 min at 37 °C, to eliminate red blood cells. The supernatant was aspirated after centrifugation for 5 min at 500 ×g. The pellet was washed with PBS and filtered through a 100 µm cell strainer (Greiner). After another centrifugation step at 500 ×g for 5 min, the supernatant was removed. The isolated standard-SVF was resuspended in endothelial growth medium 2 (EGM-2; Lonza) and used for further analyses.

#### Microtissue-SVF isolation

For microtissue-SVF isolation, liposuction material was collected in a fully closed container and 100 mL were transferred into a blood bag and washed with an equal volume of PBS to remove blood and tumescence solution (Table 1). Next, for tissue digestion, PBS was replaced with 0.2 U/mL collagenase NB6 (Serva) dissolved in 100 mL PBS containing Ca<sup>2+</sup>/Mg<sup>2+</sup> and 25 mM HEPES, resulting in a final collagenase concentration of 0.1 U/mL. The blood bag was incubated at 37 °C under moderate shaking (180 rpm) for 1 h. The digested tissue was transferred into 50 mL tubes. After centrifugation at 1200 ×g for 7 min, the cell pellet was washed with PBS. After another centrifugation step at 300 ×g for 5 min, the microtissue-SVF was resuspended in EGM-2 and used for further analyses.

#### Standard-SVF and microtissue-SVF cultivation

To analyse the differentiation potential, the isolated standard-SVF and microtissue-SVF were cultured for 1 week in EGM-2 at 37 °C, 5 % CO<sub>2</sub> and 95 % air humidity, allowing the adherent cell fraction, including ASCs, to outgrow as an adherent monolayer on tissue culture plastic. The cells were cultured to a sub-confluent state and detached with 1× trypsin/ethylenediaminetetraacetic acid (EDTA, Lonza) at 37 °C. Medium was changed every 3-4 d.

#### Cell yield and viability quantification

To visualise cell vitality in pure fat (liposuction material), isolated microtissue-SVF and standard-SVF, calcein AM (ThermoFisher Scientific) and ethidium homodimer 1 (EthD-1; Sigma-Aldrich) were used. Pure fat and the isolated microtissue-SVF were placed into a 6-well plate, while the standard-SVF was pipetted into 15 mL tubes for centrifugation after each step. All 3 conditions were washed with PBS + 10 % foetal calf serum (FCS; PAA Laboratories GmbH, Pasching, Austria) and incubated at room temperature for 10 min in the dark with the staining solution containing calcein AM (2 µg/mL) and EthD-1 (1.4 µg/mL) dissolved in PBS + 10 % FCS. Next, all three conditions were washed with PBS + 10 % FCS, transferred on to microscope slides and covered with cover slips. Fluorescence and brightfield/phase lens 1 (Ph1) images were acquired using a fluorescence microscope (Axiovert 200; Zeiss). For quantification of cell yield and viability after standard-SVF and microtissue-SVF isolation, cells were stained with 4',6-diamidino-2-phenylindole (DAPI) and analysed using a cell counter (NucleoCounter<sup>®</sup> NC-200<sup>™</sup>; ChemoMetec, Allerød, Denmark) with integrated fluorescence microscope following the "Viability and Cell Count – Aggregated Cells Assay" protocol. Each sample was transferred into a Via1-Cassette<sup>™</sup> (ChemoMetec) coated with DAPI and two measurements were performed: one with cell lysis solution, to stain all cell nuclei in the sample, and one without lysis solution, to stain only non-viable cells.

#### Cellular adenosine triphosphate (ATP)

To determine cell vitality, the cellular ATP concentration, was measured using the CellTiter-Glo<sup>®</sup> Luminescent Cell Viability Assay (Promega) according to the manufacturer's instructions. The luminescent signal was detected with an Infinite<sup>®</sup> M200 Multimode Microplate Reader (Tecan, Grödig, Austria) at an exposure time of 2 s and analysed using an ATP standard curve.

### Flow cytometry analysis

Freshly isolated SVF after standard-SVF or microtissue-SVF isolation were characterised using antibodies against a number of antigens (Table 2a). Specific subpopulations were analysed through combination of the antibodies CD31, CD34, CD45-V500 Horizon (BD Biosciences), CD90, CD146, SSEA3, CD105, LYVE-1 and podoplanin (Table 2b). For staining,  $5 \times 10^5$  cells in 50  $\mu$ L PBS with 1 % FCS were incubated with 5  $\mu$ L primary labelled antibodies at room temperature for 15 min in the dark. Cells were washed with 1.5 mL Cell Wash™ (BD Biosciences, Schwechat, Austria) and centrifuged for 5 min at 400  $\times$ g. The supernatant was discarded and the cell pellet resuspended in 300  $\mu$ L 1 $\times$  Cell Fix™ (BD Biosciences; diluted 1 : 10 with Aqua Dest, Fresenius Kabi, Linz, Austria). For staining with the intracellular marker  $\alpha$ -SMA, cells were first resuspended in 1 $\times$  Cell Fix™ and Cell Wash™ containing 0.1 % Triton X-100 was used for all washing steps. 3  $\mu$ L of  $\alpha$ -SMA were added, cells were incubated at room temperature for 30 min in the dark and, after centrifugation for 5 min at 400  $\times$ g, resuspended in PBS. All samples were analysed using a flow cytometer (FACSCanto; BD Biosciences).

### Histological staining

*In vitro* and *in vivo* standard histological samples were fixed with 4 % neutral buffered formalin for 24 h and rinsed in PBS. Then, samples were dehydrated in graded series of ethanol, followed by xylol and embedding in paraffin. 3–4  $\mu$ m-thick sections were cut using a rotary microtome (HM355S Microm; ThermoFisher Scientific) and deparaffinised for either histochemical or immunohistochemical analysis. Microtissue-SVF and pellets were histochemically stained with alcian blue to display the glycosaminoglycan content. Subcutaneously implanted fat and microtissue-SVF-samples were stained with haematoxylin and eosin (H&E) for overview of integration into the surrounding skin and muscles. Microtissue-SVF and pellets were immunohistochemically stained for ECM components (collagen type I, type II and type III) and cell markers [fibroblast (clone TE-7), endothelial cells (CD31) and pericytes (SMA)]. Deparaffinised sections were prepared by blocking the endogenous peroxidases and alkaline phosphatase with BIOXALL® (Vector Labs); antibody retrieval was performed with steaming at pH 9.0 (Tris-EDTA buffer) for SMA and pH 6 (citrate buffer) for collagen type I and CD31, pepsin for collagen type II, proteinase K for collagen type III, fibroblasts and CD31. Then, antibodies were incubated for 1 h: collagen type I (Abcam) 2  $\mu$ g/mL, collagen type II (ThermoFisher Scientific) 2  $\mu$ g/mL, collagen type III (Abcam) 5  $\mu$ g/mL, fibroblasts (Millipore) 0.125  $\mu$ g/mL, CD31 (DAKO) 10.25  $\mu$ g/mL, SMA (Sigma-Aldrich) 0.4–1.2  $\mu$ g/mL. The polymer-labelled system Bright vision poly HRP (Immunologic, Duiven, the Netherlands) was used as secondary antibody and incubated for

30 min. Visualisation was done with the peroxidase substrate NovaRED™ (Vector Laboratories) and counterstaining with haematoxylin. A special fixation protocol was further used to display the fat content in pure fat samples, microtissue-SVF and standard-SVF. After primary fixation with formalin and rinsing, the samples were fixed for 4 h with 2 % osmium tetroxide (OsO<sub>4</sub>) to preserve and visualise lipids. After subsequent rinsing, the samples were processed as the standard histological sections and stained with H&E. Images were acquired with a light microscope (Nikon E800; Nikon).

### Immunofluorescence staining

To visualise CD34<sup>+</sup>/CD90<sup>+</sup> cells as indicator for ASCs presence (De Francesco *et al.*, 2009), pure fat and isolated microtissue-SVF were placed into a 12-well plate. Both were washed with PBS, then blocked at room temperature for 2 h with a solution containing PBS, 0.2 % bovine serum albumin (BSA; BD Biosciences) and 0.1 % gelatine from cold-water-fish skin (Sigma-Aldrich). The same solution was used during the incubation with the antibody and for the washing steps, if not indicated differently. The primary antibodies CD34 and CD90 (both 1  $\mu$ g/mL; Novus/Bio-Techne Ltd., Abingdon, UK) were applied overnight at 4 °C. On the next day, both conditions were washed and incubated for 4 h at room temperature in the dark with the secondary antibodies goat anti-mouse Rhodamine Red™-X and donkey anti-rabbit Alexa Fluor 488 (both 1  $\mu$ g/mL; Invitrogen). Nuclear counterstaining was performed with DAPI (0.38 ng/mL; Invitrogen) at room temperature for 10 min in the dark. The samples were washed with PBS and mounted on microscope slides using the Prolong Antifade kit (Molecular Probes). Images were acquired using a confocal microscope (Nikon C2, Nikon).

### Enzyme-linked immunosorbent assay (ELISA)

To analyse the secretion of human indoleamine 2,3-dioxygenase (IDO) and prostaglandin E2 (PGE2), the supernatant of freshly isolated standard-SVF and microtissue-SVF was cultivated for 24 h in sterile-filtered Dulbecco's modified Eagle's medium (DMEM)-low glucose (Lonza) containing 10 % FCS and 2 mM L-glutamine (PAA Laboratories GmbH). The supernatant was collected and stored at – 80 °C until analysis. An IDO DuoSet ELISA Development System kit (R&D Systems) and a Prostaglandin E2 ELISA Kit (Abcam) were used according to the manufacturer's instructions. Absorbance was measured using an Infinite® M200 Multimode Microplate Reader (Tecan) and correlated to a standard curve.

### Trophic factor release

For trophic factor release analysis of freshly isolated standard-SVF and microtissue-SVF,  $5 \times 10^5$  cells were seeded in a T-25 flask in 2.5 mL EGM-2 medium. Cells were allowed to adhere for 2 h and, subsequently,



**Table 2a. List of antibodies against which antigens were obtained.** Freshly isolated SVF after standard-SVF or microtissue-SVF isolation were characterised using antibodies against these antigens. Details of suppliers are included.  $\alpha$ -SMA: alpha-smooth muscle actin; APC: allophycocyanin; CD: cluster of differentiation; PerCP: peridinin chlorophyll protein complex; FITC: fluorescein-isothiocyanate; PE: phycoerythrin; LYVE-1: lymphatic vessel endothelial receptor 1; SSEA3: stage-specific embryonic antigen 3.

Antibody against	Supplier
$\alpha$ -SMA-APC	R&D, Wiesbaden-Nordenstadt, Germany
CD1c-PerCP	BioLegend, San Diego, CA, USA
CD13-FITC	eBioscience, Vienna, Austria
CD14-FITC	BD Biosciences, Schwechat, Austria
CD29-PerCP	ProtTech, Phoenixville, PA, USA
CD31-FITC	BD Biosciences, Schwechat, Austria
CD33-PE	eBioscience, Vienna, Austria
CD34-APC	BD Biosciences, Schwechat, Austria
CD44-APC	BioLegend, San Diego, CA, USA
CD45-PerCP	BioLegend, San Diego, CA, USA
CD45-V500 Horizon	BD Biosciences, Schwechat, Austria
CD49d-PE	BD Biosciences, Schwechat, Austria
CD68-APC	BioLegend, San Diego, CA, USA
CD73-FITC	BD Biosciences, Schwechat, Austria
CD90-PE	eBioscience, Vienna, Austria
CD105-APC	BD Biosciences, Schwechat, Austria
CD117-APC	eBioscience, Vienna, Austria
CD133-PE	Milteny Biotec, Bergisch Gladbach, Germany
CD146-PerCP	R&D, Wiesbaden-Nordenstadt, Germany
CD235a-FITC	eBioscience, Vienna, Austria
CD326-PE	eBioscience, Vienna, Austria
CD309-APC	Milteny Biotec, Bergisch Gladbach, Germany
LYVE-1-APC	R&D, Wiesbaden-Nordenstadt, Germany
Podoplanin-PE	BioLegend, San Diego, CA, USA
SSEA3-FITC	BD Biosciences, Schwechat, Austria
Stro-1-PerCP	Novus/Bio-Techne Ltd., Abingdon, UK

**Table 2b. Combinations of antibodies used.** Specific subpopulations were analysed through the following combination of the antibodies against CD31, CD34, CD45, CD90, CD146, SSEA3, CD105, LYVE-1 and podoplanin.

Cell subpopulation	Antibody combination
Endothelial progenitor cells (EPCs)	CD45 <sup>-</sup> /CD31 <sup>+</sup> /CD34 <sup>+</sup>
Pericyte-like cells	CD45 <sup>-</sup> /CD31 <sup>-</sup> /CD146 <sup>+</sup>
Supra-adventitial ASCs (SA-ASCs)	CD45 <sup>-</sup> /CD31 <sup>-</sup> /CD146 <sup>-</sup> /CD34 <sup>+</sup>
A mesenchymal subset	CD34 <sup>+</sup> /CD90 <sup>+</sup> A
A pericytic subset	CD90 <sup>+</sup> /CD146 <sup>+</sup>
Lymphatic endothelial cells (LECs)	LYVE-1 <sup>+</sup> /podoplanin <sup>+</sup>
Multilineage differentiating stress enduring (Muse) cells	SSEA3 <sup>+</sup> /CD105 <sup>+</sup>

EGM-2 media was changed to serum-free media (DMEM-low glucose with 2 mM L-glutamine). To include also non-adherent suspension cells, cells were collected, centrifuged and returned to the flask. 24 h after seeding, the supernatant was collected and stored at  $-80^{\circ}\text{C}$  until analysis. A customised array (RayBio, Norcross, GA, USA) was used for the trophic factor release analysis and performed according to the manufacturer's instructions. Signals were detected by enhanced chemiluminescence and recorded on an X-ray film. Signals were densitometrically quantified using ImageJ (NIH).

### Vascularisation induction and detection

For determination of the vascularisation potential of standard-SVF and microtissue-SVF, a fibrin clot culture was performed (Holnthoner *et al.*, 2015).  $4 \times 10^5$  SVF cells after standard-SVF and microtissue-SVF isolation were mixed with fibrinogen (2.5 mg/mL; Baxter) and thrombin (0.2 U/mL; Baxter) for clot formation and pipetted on coverslips in 12-well plates. Clots were polymerised at  $37^{\circ}\text{C}$  for 30 min and cultured for 2 weeks in EGM-2 containing aprotinin (100 KIU/mL; Baxter). Medium was changed every 3-4 d. After cultivation, clots were fixed with 4 % paraformaldehyde (PFA), washed with PBS and incubated for 12 h in the dark with a FITC-conjugated monoclonal mouse anti-human CD31 antibody (1 : 50 dilution in PBS/1 % BSA). Clots were again washed with PBS, then nuclear counterstaining was performed with DAPI (0.38 ng/mL in PBS/1 % BSA) for 10 min at room temperature in the dark. For images in higher magnification, clots were incubated for 12 h in the dark with an Alexa-Fluor<sup>®</sup>-647-conjugated monoclonal mouse anti-human CD31 antibody (BD Biosciences; 1 : 100 dilution in PBS/1 % BSA). Images were acquired using a fluorescence microscope (Axiovert 200 or Observer Z.1 for higher magnification). Number of vascular tubes per picture was counted.

### In vivo experiments

An animal experiment permit was issued by the municipal government of Vienna and all experimental methods were consistent with the Guide for the Care and Use of Laboratory Animals of the US National Research Council (2011). For analysis of graft integration, pure fat and fat enriched with microtissue-SVF ( $2.5 \times 10^5$  cells/50  $\mu\text{L}$  fat) in a 9 : 1 ratio were injected intramuscularly into nude mice. A total of 16 NMRI nude mice (Charles River) weighting 22-27 g underwent surgery. After induction of anaesthesia by isoflurane (AbbVie), 50  $\mu\text{L}$  test samples were injected transcutaneously into the musculus quadriceps femoris hindlimbs in a randomised fashion. Either microtissue-SVF or a combination of fat and microtissue-SVF were applied in 6 replicates, while the remaining untreated hindlimbs served as an empty control. The implants were well tolerated and no adverse effects were observed. Analgesia was provided orally by 1 mg/kg

meloxicam (Boehringer Ingelheim) prior to surgery and for up to 3 d post-surgery. After 28 d, the animals were euthanised through cervical dislocation under isoflurane inhalation anaesthesia and samples were harvested by resecting the implantation region with the skin and subcutaneous tissue. The samples were fixated and histologically processed as described above in the histological staining section.

### Adipogenic differentiation and detection

For adipogenic differentiation, cells derived from microtissue-SVF after 1 week in culture were seeded at a density of  $7.4 \times 10^3/\text{cm}^2$  in EGM-2 and incubated overnight. On the next day, medium was changed to adipogenic differentiation medium (DMEM)-high glucose (Lonza) containing 10 % FCS, 2 mM L-glutamine, 100 U/mL penicillin/streptomycin (P/S; Lonza), 1  $\mu\text{M}$  dexamethasone (Sigma-Aldrich), 0.5 mM 3-isobutyl-1-methylxanthine (IBMX; Sigma-Aldrich), 10  $\mu\text{g}/\text{mL}$  insulin (Sigma-Aldrich) and 100  $\mu\text{M}$  indomethacin (Sigma-Aldrich) or control medium consisting of DMEM : F12/L-glutamine (Lonza) with 10 % FCS and 100 U/mL P/S. Medium was changed every 3-4 d. After 1, 2, 3 and 7 d, adipogenic differentiation was analysed with oil red O staining and quantification through RT-PCR of the specific markers, peroxisome proliferator-activated receptor gamma (PPAR $\gamma$ ), fatty acid-binding protein 4 (FABP4) and leptin (LEP). For oil red O staining of lipid droplets, cells were fixed for 1 h with 4 % formaldehyde. After washing with Aqua Dest, the cells were rinsed with 70 % ethanol for 2 min and stained for 5-15 min with oil red O solution (Sigma-Aldrich). Then, the cells were washed with Aqua Dest, counterstained for 1-3 min with haematoxylin solution and washed with tap water. Images were acquired using a light microscope (Axiovert 200).

### Osteogenic differentiation and detection

For osteogenic differentiation, cells derived from microtissue-SVF after 1 week in culture were seeded at a density of  $1.1 \times 10^3/\text{cm}^2$  in EGM-2 and incubated overnight. On the next day, medium was changed to osteogenic differentiation medium DMEM-low glucose containing 10 % FCS, 2 mM L-glutamine, 100 U/mL P/S, 10 nM dexamethasone, 150  $\mu\text{M}$  ascorbat-2-phosphate (Sigma-Aldrich), 10 mM  $\beta$ -glycerophosphate (StemCell Technologies, Cologne, Germany) and 10 nM dihydroxy-vitamin D3 (Sigma-Aldrich) or control medium consisting of DMEM : F12/L-glutamine with 10 % FCS and 100 U/mL P/S. Medium was changed every 3-4 d. After 21 d, osteogenic differentiation was analysed with alizarin red staining and quantification through RT-PCR of the specific markers alkaline phosphatase (ALPL), osteocalcin (BGLAP) and osteopontin (SPP1). For alizarin red staining of calcified structures, cells were fixed for 1 h with 70 % ethanol at  $-20^{\circ}\text{C}$  and stained with alizarin red solution (Merck) for 15 min. Images were acquired using a light microscope (Axiovert 200).

### Chondrogenic differentiation and detection

For chondrogenic differentiation in 3D micromass pellet cultures,  $3 \times 10^5$  cells derived from microtissue-SVF after 1 week in culture were centrifuged in chondrogenic differentiation medium [hMSC Chondro BulletKit (Lonza), 10 ng/mL BMP-6 (R&D) and 10 ng/mL TGF- $\beta$ 3 (Lonza)] in screw-cap micro tubes. The tubes were placed in an incubator at 37 °C, 5 % CO<sub>2</sub> and 95 % humidity with slightly open cap to allow for gas exchange. After 2 d, the pellets were transferred to 96-well U-bottom plates (Greiner) with fresh medium. Medium was changed every 2-3 d. After 35 d of differentiation, chondrogenic differentiation was analysed with alcian blue and collagen type II staining as well as quantification through RT-PCR for the specific markers collagen type II alpha 1 (COL2A1) and aggrecan (AGC1) *versus* collagen type I alpha 1 (COL1A1) and versican (CSPG2). Histological samples were processed as described above in the histological staining section.

### Quantitative RT-PCR

Samples for qRT-PCR were collected at distinct time points as indicated in the differentiation paragraphs and lysed or homogenised in TriReagent (Sigma-Aldrich). Extraction was facilitated by repeated pipetting of the cells or pellets. For total RNA isolation, the samples were centrifuged for 10 min at 4 °C and the supernatant was transferred into a fresh tube. For phase separation, 0.1 mL of 1-bromo-3-chloropropane (BCP; Sigma-Aldrich) was added and samples shaken vigorously, incubated for 10 min and centrifuged for 10 min at 4 °C. The aqueous phase was transferred into a fresh tube and precipitated with isopropanol for 30 min at -20 °C. After centrifugation for 30 min at 4 °C, the RNA pellet was washed with 75 % ethanol, vortexed and centrifuged for 5 min at 4 °C. Finally, RNA pellets were air-dried before dissolving them in nuclease-free water (Promega). Samples were stored at -80 °C until use. RNA content and integrity were assessed using an Agilent 2100 Bioanalyzer with the RNA 6000 Nano Chips Kit (no. 5065-4476, Agilent Technologies). Isolated RNA was retrotranscribed to cDNA according to the High Capacity cDNA Archive Kit protocol (Applied Biosystems). Quantification of specific cDNAs was conducted in triplicate, using a LightCycler W 480 (Roche) and TaqMan™ gene expression assay (Applied Biosystems) for PPAR $\gamma$  (Hs00234592\_m1), FABP4 (Hs00609791\_m1), LEP (Cf02692890\_m1), ALPL (Hs00758162\_m1), BGLAP (Hs01587813\_g1), SPP1 (Hs00167093\_m1), CSPG2 (Hs00171642\_m1), COL1A1 (Hs00164004\_m1), COL2A1 (Hs00264051\_m1) and AGC1 (Hs0015936\_m1). The PCR was programmed as follows: initial denaturation at 95 °C for 10 min, followed by 95 °C for 10 s, 60 °C for 45 s, cycled 50 times. Cooling to 40 °C was held for 30 s. Slope speed was 20 °C/s. Standard curves were prepared for quantification and expression values were normalised to the housekeeping gene, hypoxanthine-guanine phosphoribosyl transferase

(HPRT). The efficiency-corrected quantification was performed automatically, using the LightCycler 480 Relative Quantification Software (Roche).

### Statistical analysis

Data are presented as mean  $\pm$  standard deviation (SD). Statistical analysis was performed using PRISM6 (GraphPad), parametric two-tailed *t*-test or two-way ANOVA Tukey's *post-hoc* for trophic factor release analysis.  $p < 0.05$  was considered statistically significant.

## Results

The optimised standard-SVF isolation protocol with low collagenase concentration was adapted resulting in SVF cells being protected within their natural environment, hence providing a microtissue devoid of fat components and highly enriched in SVF cells.

### Microtissue-SVF isolation increased cell yield and viability

The macroscopic and microscopic appearance of the microtissue-SVF was characterised by a heterogeneous and partially fibrous matrix with individually distributed cells and cell aggregates. In contrast, pure fat contained few individual cells and was dominated by lipid droplets, while the standard-SVF consisted of single cells and small cell aggregates (Fig. 1a; phase contrast, live/dead staining, OsO<sub>4</sub> fixation). Staining of live (calcein AM) *versus* dead (EthD-1) cells revealed a small and moderate number of dead cells in pure fat and standard-SVF, respectively, but almost none in the microtissue-SVF. The appearance of the native fat tissue was dominated by living cells with adipocyte morphology. In the microtissue-SVF, the living cells mainly resided within the ECM areas, which suggested a protective role of the microtissue. Automated quantification of the viable *versus* dead cells in microtissue-SVF *versus* standard-SVF isolation supported the morphological data. Microtissue-SVF had a 10 % increased viability as compared to standard-SVF isolation (Fig. 1b). Not only the viability was increased in the microtissue-SVF but also the total cell yield, which was significantly higher (1.8-fold) as compared to standard-SVF isolation (Fig. 1b). ATP concentration as an indicator for cellular fitness and energy production was at similarly high levels in both SVF isolates.

### The microtissue-SVF maintained the heterogeneous SVF character

According to the guidelines of the International Federation for Adipose Therapeutics and Science (IFATS) and the International Society for Cellular Therapy (ISCT) (Bourin *et al.*, 2013), the isolated standard-SVF and microtissue-SVF were characterised for the distinct surface marker profile by flow cytometric analysis. The percentage of cells positive for the mesenchymal markers CD73 (>45 %) and CD90

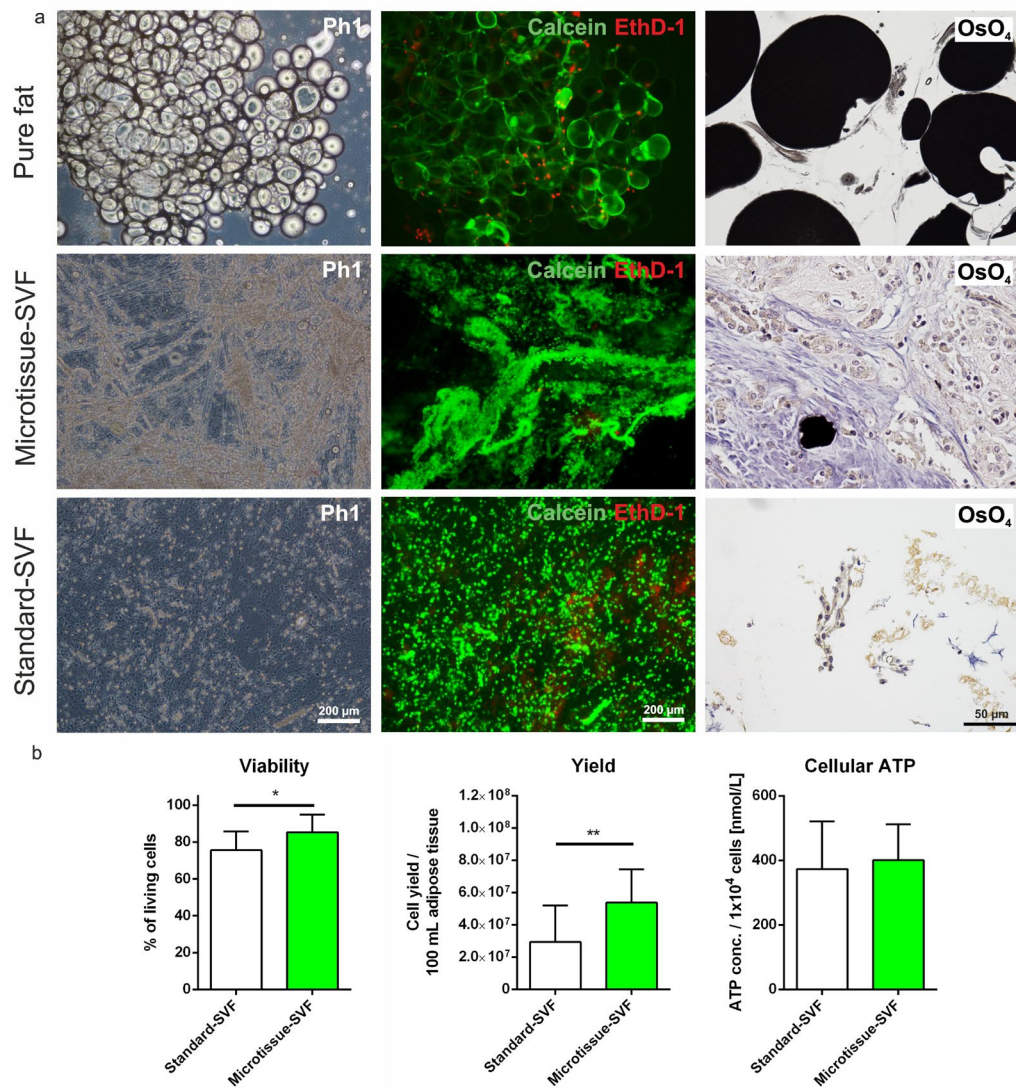


**Fig. 1. Morphology and vitality of pure fat, microtissue-SVF and standard-SVF.** (a) Structure and vitality of fresh pure fat (liposuction material), microtissue-SVF and standard-SVF. Phase contrast images reveal that pure fat mainly contained lipid droplets, while the microtissue-SVF had a fibrous appearance and the standard-SVF was mainly cellular. Live/dead staining showed mainly vital cells (green) in all three groups, with the lowest number of dead cells (red-stained nuclei) in the microtissue-SVF ( $n = 3$ ). OsO<sub>4</sub>-fixed and sectioned samples displaying lipid droplets in black revealed that, in contrary to the large droplets in pure fat, the microtissue-SVF contained only individual small droplets enclosed inside the matrix. The standard-SVF showed no signs of residual lipid material. Representative images showing different locations of each sample (Ph1, calcein, EthD-1 and OsO<sub>4</sub>). Scale bars = 200 μm and 50 μm. (b) Viability, cell yield and ATP concentration of the microtissue-SVF ( $n = 8$  for viability and cell yield;  $n = 4$  for ATP) versus standard-SVF ( $n = 15$  for viability and cell yield;  $n = 13$  for ATP) showed a higher viability and larger cell percentage in the microtissue-SVF, but a similar cellular ATP level. Data are presented as mean ± SD. \*  $p < 0.05$ ; \*\*  $p < 0.01$ .

(> 65 %), the progenitor marker CD34 ( $\geq 60$  %) and the haematopoietic marker CD45 (< 35 %) complied with the guidelines of the IFATS and ISCT. The percentage of cells positive for the vascular marker CD31 was approximately 45 % and 55 %, larger as compared to < 20 % defined by Bourin *et al.* (2013) (Table 3). Due to the heterogeneous character of the SVF, the isolated standard-SVF and microtissue-SVF were further screened for a panel of various immunophenotypic markers and markers represented on MSCs, preadipocytes, fibroblasts, vascular smooth muscle cells, endothelial cells, endothelial progenitor cells,

pericyte-like cells, macrophages, lymphocytes and lymphatic endothelial cells were identified, among others (Table 3). The percentages of all tested markers were enhanced in the microtissue-SVF as compared to the standard-SVF (apart from CD33, CD146), but only  $\alpha$ -SMA reached significance. Additionally to these, specific subpopulations of a mesenchymal subset (CD34<sup>+</sup>/CD90<sup>+</sup>), a pericytic subset (CD90<sup>+</sup>/CD146<sup>+</sup>), LECs (podoplanin<sup>+</sup>/LYVE-1) and Muse cells (SSEA3<sup>+</sup>/CD105<sup>+</sup>) were identified in the isolated standard-SVF and microtissue-SVF in similar percentages (Table 4).

**Table 3. Identification and quantification of surface marker in standard-SVF and microtissue-SVF with flow cytometry analysis.** The standard-SVF and microtissue-SVF revealed all SVF-specific immunophenotype marker analysed by flow cytometry according to the guidelines of the IFATS and ISCT. Additionally, further marker for distinct stem and progenitor cell types could be detected ( $n = 4$  for microtissue-SVF and  $n = 3$  for standard-SVF). Data are presented as mean  $\pm$  SD.

Marker		Positive cells (%)	
		Standard-SVF	Microtissue-SVF
CD29	Mesenchymal stromal	76 $\pm$ 25	89 $\pm$ 3
CD90	Mesenchymal stromal	68 $\pm$ 20	76 $\pm$ 6
CD44	Mesenchymal stromal	60 $\pm$ 19	68 $\pm$ 8
CD34	Progenitor	60 $\pm$ 15	67 $\pm$ 6
CD73	Mesenchymal stromal	48 $\pm$ 22	59 $\pm$ 7
$\alpha$ -SMA	Vascular smooth muscle	30 $\pm$ 9	58 $\pm$ 25
CD31	Endothelial	45 $\pm$ 11	55 $\pm$ 6
CD13	Monocyte, granulocyte, fibroblast	33 $\pm$ 14	48 $\pm$ 11
CD146	Pericyte-like, endothelial	34 $\pm$ 11	34 $\pm$ 4
Podoplanin	Lymphatic endothelial	25 $\pm$ 11	33 $\pm$ 11
CD45	Haematopoietic	23 $\pm$ 7	31 $\pm$ 10
CD68	Monocyte, macrophage	8 $\pm$ 3	31 $\pm$ 6
CD235a	Erythrocyte	23 $\pm$ 22	29 $\pm$ 23
CD49d	Lymphocyte	7 $\pm$ 1	26 $\pm$ 17
CD117	Haematopoietic	14 $\pm$ 7	25 $\pm$ 8
LYVE-1	Lymphatic endothelial	18 $\pm$ 6	24 $\pm$ 6
CD14	Macrophage, monocyte, lymphocyte, haematopoietic	7 $\pm$ 3	16 $\pm$ 5
CD133	Endothelial progenitor	5 $\pm$ 2	15 $\pm$ 7
SSEA3	Embryonic stem cell, Muse cell	12 $\pm$ 8	14 $\pm$ 6
CD105	Mesenchymal stromal	12 $\pm$ 4	14 $\pm$ 3
CD326	Epithelial	7 $\pm$ 3	12 $\pm$ 6
CD33	Leukocyte, natural killer, T-cell	12 $\pm$ 7	9 $\pm$ 2
CD309	Vascular endothelial	5 $\pm$ 2	8 $\pm$ 4
Stro-1	Mesenchymal stromal	6 $\pm$ 1	8 $\pm$ 5

### Microtissue-SVF structure

Comparison between microtissue-SVF, standard-SVF and pure fat revealed that the most obvious feature of the microtissue-SVF was the large amount of ECM with a simultaneous lack of lipid, represented by few residual droplets only (Fig. 1). Also, macroscopically, the appearance of the microtissue-SVF was dominated by its matrix that gave the material a translucent to opaque mucous appearance containing fibrous elements (Fig. 2a). To characterise this matrix and its structural relation with the cells, detailed morphological analyses were performed. Matrix-specific histochemical and immunohistochemical stainings identified mucopolysaccharides (alcian blue) and collagen type I (antibody labelling) as the main ECM

components (Fig. 2b,c). Mucopolysaccharides appeared as homogenous areas with few cells that were mainly individually distributed. Collagen type I formed fibrous strands within the mucous matrix or areas of fine fibrillary networks. The latter were co-localised with collagen type III and areas of high cellularity (Fig. 2d). Cells forming lumina and tube-like structures were identified as endothelial cells (CD31<sup>+</sup>), either appearing alone as capillaries or surrounded by pericytes (SMA<sup>+</sup>) (Fig. 2f). Within these vessel and cell aggregates, also fibroblasts (clone TE-7<sup>+</sup>) were identified (Fig. 2e). The areas with high cellularity, rich in collagen matrix, and the areas with low cellularity, rich in mucopolysaccharides, had an extension of few hundreds  $\mu$ m and were spread-out evenly throughout the microtissue-SVF (Fig. 2b-f).

**Table 4. Double staining of distinct surface markers in standard-SVF and microtissue-SVF by flow cytometry analysis.** Standard-SVF and microtissue-SVF revealed a mesenchymal subset (CD34<sup>+</sup>/CD90<sup>+</sup>), a pericytic subset (CD90<sup>+</sup>/CD146<sup>+</sup>), lymphatic endothelial cells (podoplanin<sup>+</sup>/LYVE-1) and multilineage differentiating stress enduring cells (SSEA3<sup>+</sup>/CD105<sup>+</sup>) ( $n = 4$  for microtissue-SVF and  $n = 3$  for standard-SVF). Data are presented as mean  $\pm$  SD.

Marker		Positive cells (%)	
		Standard-SVF	Microtissue-SVF
CD34 <sup>+</sup> /CD90 <sup>+</sup>	Mesenchymal subset	62 $\pm$ 17	67 $\pm$ 4
CD90 <sup>+</sup> /CD146 <sup>+</sup>	Pericytic subset	39 $\pm$ 13	36 $\pm$ 6
Podoplanin <sup>+</sup> /Lyve-1 <sup>+</sup>	Lymphatic endothelial cell	14 $\pm$ 2	17 $\pm$ 7
SSEA3 <sup>+</sup> /CD105 <sup>+</sup>	Muse cell	7 $\pm$ 3	7 $\pm$ 1

### The microtissue-SVF provided regenerative cells

Viable, regenerative cells are required for successful therapeutic applications (Dykstra *et al.*, 2017). Pure fat and microtissue-SVF were stained for the mesenchymal marker CD90 and CD34, a marker associated with cells of a progenitor status (Sidney *et al.*, 2014). In pure fat, there were elongated CD34<sup>+</sup> cells and few CD90<sup>+</sup> cells visible (Fig. 3). Some CD90<sup>+</sup>/CD34<sup>+</sup> cells were visible. In contrast, the isolated microtissue-SVF was rich in CD90<sup>+</sup> and CD34<sup>+</sup> cells and contained CD90<sup>+</sup>/CD34<sup>+</sup> cells, confirming the presence of regenerative cells within the microtissue-SVF. These results confirmed that the isolated microtissue-SVF contained viable and regenerative cells, highly enriched in its ECM.

### Microtissue-SVF isolation increased the percentage of specific subpopulations

As the cell yield was increased after microtissue-SVF isolation, whether this increase might correlate with the enrichment of specific subpopulations within the heterogeneous SVF was examined. Interestingly, EPCs (1.8-fold) and SA-ASCs (1.7-fold) were significantly increased by microtissue-SVF isolation as compared to standard-SVF isolation (Fig. 4). The relative number of pericyte-like cells was similar after standard-SVF and microtissue-SVF isolation.

### The microtissue-SVF showed enhanced release of PGE2

As trophic factors are highly relevant for tissue repair (Fu *et al.*, 2017), the secretion of pro-regenerative factors (*e.g.* angiogenic and immunomodulatory) was explored in supernatants conditioned for 24 h with freshly isolated standard-SVF and microtissue-SVF. Substantial levels of IDO and PGE2, two mediators of immunomodulation, were detected in both SVF variants. IDO concentration was increased in microtissue-SVF (2.4-fold) as compared to standard-SVF supernatant, although not reaching significance (Fig. 5). However, there was a highly significant increase in PGE2 (15-fold) in microtissue-SVF as compared to standard-SVF supernatant. All analysed factors were expressed in the supernatant of both SVFs (Fig. 5) at similar protein levels in the standard-SVF and microtissue-SVF, as measured by a customised

array microarray (RayBio). There was a slight but not significantly enhanced release of interleukin-8 (IL-8), monocyte chemoattractant protein-1 (MCP-1), tissue inhibitor of metalloproteinase (TIMP)-1, TIMP-2 and epidermal growth factor (EGF) after microtissue-SVF isolation.

### The microtissue-SVF displayed a high vascularisation potential

Efficient vascularisation is a key element in regeneration and for successful graft integration and survival in tissue engineering (Eto *et al.*, 2012). Therefore, standard-SVF and microtissue-SVF were characterised in 3D fibrin matrices for their potential to form tube-like structures, an *in vitro* indicator for angiogenesis (Rohringer *et al.*, 2014). After 2 weeks, microtissue-SVF isolation showed a more pronounced vascular network formation of CD31<sup>+</sup> cells as compared to standard-SVF isolation (Fig. 6a). A higher magnification demonstrated a branching point in the microtissue-SVF. Quantitative analysis revealed a significantly larger number of tubes in the microtissue-SVF group (2.9-fold) (Fig. 6b), suggesting an improved vascularisation potential.

### The microtissue-SVF was successfully integrated into the surrounding tissue after intramuscular injection

One typical clinical application is the use of SVF together with fat grafting material to prolong graft survival, improve vascularisation and integration of transplanted grafts in the surrounding tissue (Yoshimura *et al.*, 2008). Therefore, pure fat and fat enriched with microtissue-SVF were injected intramuscularly into nude mice. Both grafts integrated after 14 d, whereas microtissue-SVF co-transplantation resulted in high cellularity in the adipose tissue and a high degree of vascularisation (Fig. 7).

### The microtissue-SVF showed a trilineage differentiation potential

The microtissue-SVF was analysed for its *in vitro* differentiation potential using standard differentiation cultures, analysed by quantitative RT-PCR and histological staining. Upon adipogenic

induction, the adipogenic markers PPAR $\gamma$ , FABP4 and LEP were significantly upregulated after only 1 d (Fig. 8a). The staining with oil red O demonstrated that lipid droplet formation started after only 2 d and was pronounced after 7 d of differentiation (Fig. 8b). These results indicated the excellent adipogenic differentiation potential of the microtissue-SVF, as adipogenic differentiation is detected after 14-21 d of induction in previous studies (Priglinger *et al.*, 2018; Priglinger *et al.*, 2017). Upon osteogenic induction, expression of the specific osteogenic markers ALPL, BGLAP and SPP1 was increased after 21 d, being significant for BGLAP and SPP1 (Fig. 8c). Mineral deposition staining with alizarin red at the same time point confirmed the osteogenic differentiation

of the microtissue-SVF (Fig. 8d). Chondrogenic differentiation was analysed using 3D micromass pellet cultures. After 35 d, the general expression of matrix proteins was significantly enhanced as compared to standard-SVF (COL1A1, COL2A1 and AGC1; Fig. 8e). The differentiation index of COL2A1/COL1A1 and AGC1/CSPG2 revealed a higher activation of cartilage specific components (Fig. 8f). Also, the histological analysis showed a strong staining with alcian blue and collagen type II, which demonstrated the potential for chondrogenic differentiation and cartilage-like tissue formation (Fig. 8g). These results confirmed the trilineage differentiation potential of the microtissue-SVF.

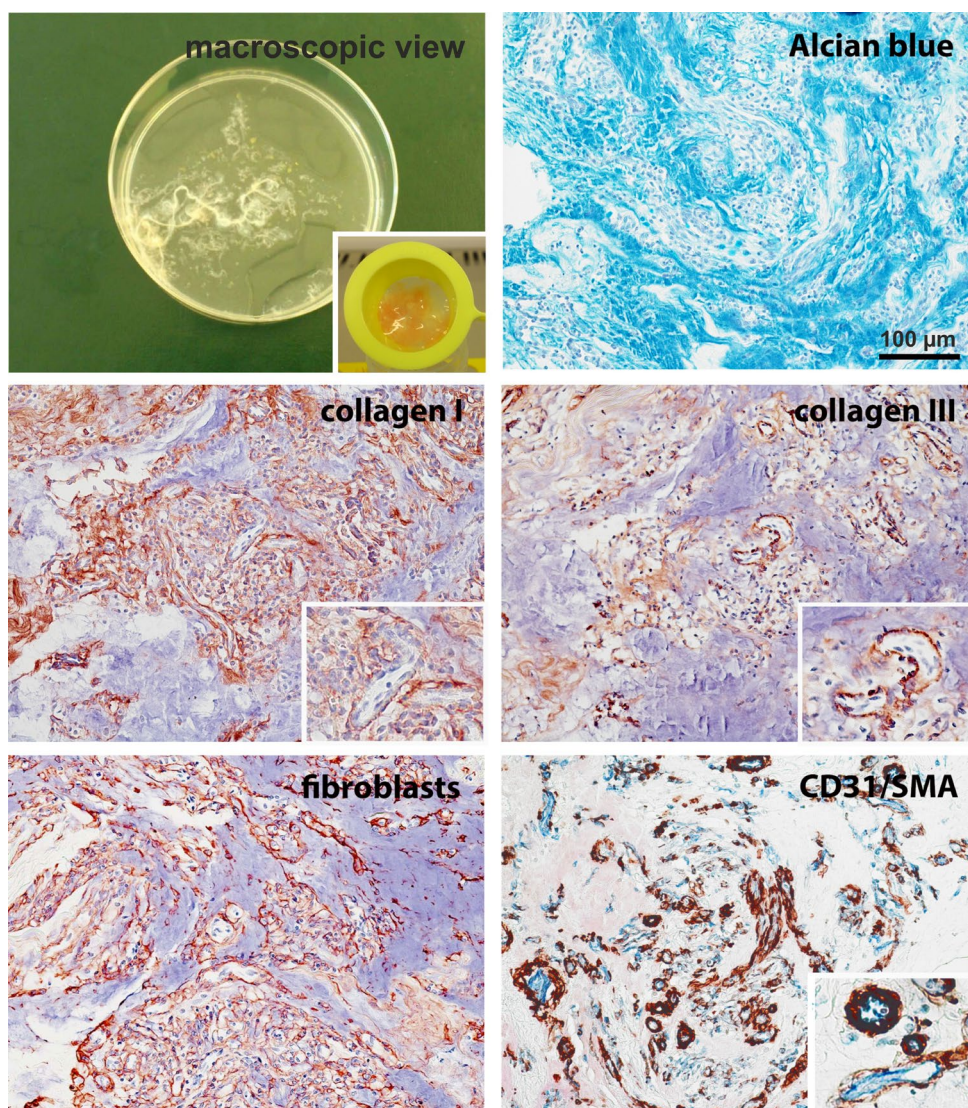


**Fig. 2. Characterisation of the matrix and cellular components of the microtissue-SVF.** (a) Macroscopically, the microtissue-SVF appeared as a translucent to opaque mucous material with fibrous elements. In histological sections, the matrix stained with (b) alcian blue for mucopolysaccharides in some regions, while other areas were positive for (c) collagen type I and (d) III, which were co-localised. Collagen-rich areas were highly cellular and vessels were discernible (inserts). (e) The inner wall of the vessels was positive for the endothelial marker CD31 and, in some cases, the surrounding cells were SMA<sup>+</sup>, indicating pericytes. Apart from vessels, also fibroblasts (e) were identified in the highly cellular, collagen-rich areas ( $n = 3$ ). Representative images. Scale bar = 100  $\mu\text{m}$ .

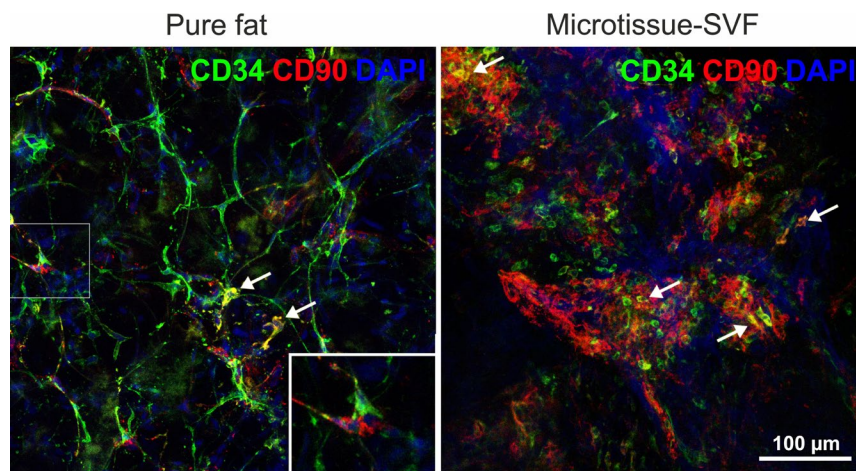


**Fig. 3. Fluorescence microscopic images of pure fat and microtissue-SVF labelled against the marker for regenerative cells (CD34, CD90).** In pure fat (left), CD34<sup>+</sup> cells (green) located between the lipid droplets and few CD90<sup>+</sup> cells (red) were visible (nuclei stained blue). The insert showed a higher magnification of a pair of CD34<sup>+</sup> and CD90<sup>+</sup> cells. Some cells were double stained and appeared in yellow (arrows). In the microtissue-SVF (right), cells were aggregated on/in the matrix. Apart from the green CD34<sup>+</sup> cells, a large proportion of cells were CD90<sup>+</sup> (red) and some were double stained (arrow). Representative confocal images, overlay. Scale bar = 100  $\mu$ m.

## Discussion

The regenerative characteristics of an intraoperative GMP-compliant fat derivative with minimally manipulated cells termed microtissue-SVF was described. Until now, there were two ways for SVF isolation, diverse non-enzymatic methods using physical forces and enzymatic methods *e.g.* using collagenase, both followed by a cell selection step, mostly performed by centrifugation (Oberbauer *et al.*, 2015). Mechanical emulsification alone leads to partial disruption of mature adipocytes and ECM components – generating homogenised adipose tissue fragments which are optimal for fat grafting – but does not generate single SVF cells (Oberbauer *et al.*, 2015). Differently, the enzymatic dissociation of cell-cell and cell-tissue/matrix contacts provides a single-cell suspension defined by the IFATS and ISCT as SVF (Bourin *et al.*, 2013).

Several isolation protocols aim to optimise and standardise the SVF isolation procedure (Aronowitz *et al.*, 2018; Rapisio *et al.*, 2017). SVF cells dissociated from their natural microenvironment lack ECM protection from possible negative enzymatic impact (Busser *et al.*, 2014; Seaman *et al.* 2015). A rough enzymatic treatment, modifying substantially cell-matrix compounds, may affect the expression of surface antigens and immune cell function (Autengruber *et al.*, 2012; Hagman *et al.*, 2012). Substantial cell manipulation may impact cell therapeutic classification according to the local regulatory requirements. Since both, the current physical force and enzymatic isolation strategies, have drawbacks, there is a demand for an advanced SVF generation strategy. The described SVF-derivative delivered minimally manipulated therapeutic cells incorporated within their ECM,

which served as a protective scaffold and provided the most natural environment for the cells. To demonstrate the highest possible cell quality for transplantation, the microtissue-SVF was analysed immediately after isolation. In comparison with the standard-SVF, which is a protocol already optimised by the authors with low enzyme concentration, the microtissue-SVF revealed a substantially higher cell yield, combined with high vitality and metabolic activity of the enriched cells. The percentage of dead cells was very low, suggesting that the procedure was well suited to actively remove adipocytes, while maintaining SVF cells highly viable.

Microtissue-SVF cells were supported by a gel-like carrier (ECM residuals) and represented the

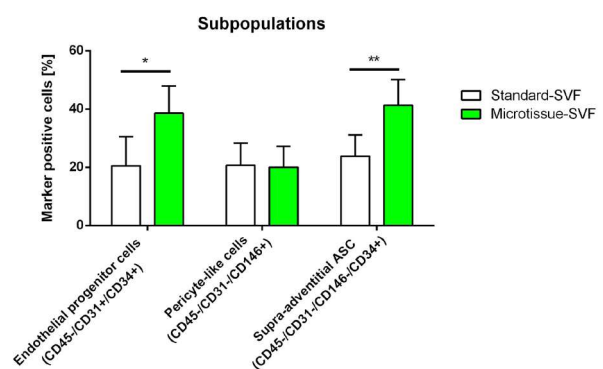


**Fig. 4. Flow cytometry analysis of SVF subpopulations.** In the microtissue-SVF, endothelial progenitor cells and supra-adventitial adipose-derived stromal/stem cells were significantly enriched as compared to the standard-SVF. Pericyte-like cells had similar abundance in both types ( $n = 4$ ). Data are presented as mean  $\pm$  SD; \*  $p < 0.05$ ; \*\*  $p < 0.01$ .



stromal and the vascular fraction of the adipose tissue. It comprised fragmented connective tissue matrix and vascular structures composed of endothelial cells and pericytes and other regenerative cells, such as the ASCs. ECM components directly influence cell behaviour, including adhesion, spreading, proliferation and migration (Geutjes *et al.*, 2010; Kim *et al.*, 2012; Prockop, 2007; Wang *et al.*, 2013a), suggesting a positive effect on the cells embedded in the microtissue-SVF. Qiu *et al.* (2018) employ decellularised fat tissue ECM as a scaffold for reseeding MSCs, resulting in improved regenerative efficacy in muscle tissue injury. Beside the typical IFATS-defined SVF-cell surface markers for mesenchymal, endothelial and haematopoietic cells (Bourin *et al.*, 2013), the microtissue-SVF contained a broad range of cell types including

pericytic, blood and lymphatic vascular and epithelial cells. Almost all markers tended to be enhanced in the microtissue-SVF as compared to the standard-SVF. Considering the morphological appearance of the microtissue-SVF, the additional cells might derive from densely organised, collagen- and vessel-rich areas of the derivative that were partially lost during the additional processing of the standard-SVF isolation. Beside surface markers, a functional criterion to define the ASCs is their trilineage differentiation potential into the mesodermal lineages (Bourin *et al.*, 2013). The microtissue-SVF revealed a high differentiation potential towards the adipo-, osteo- and chondrogenic lineage, which confirmed the large number of ASCs, as indicated by the phenotypic MSC marker profile. Especially, adipogenesis was surprisingly rapid and could be

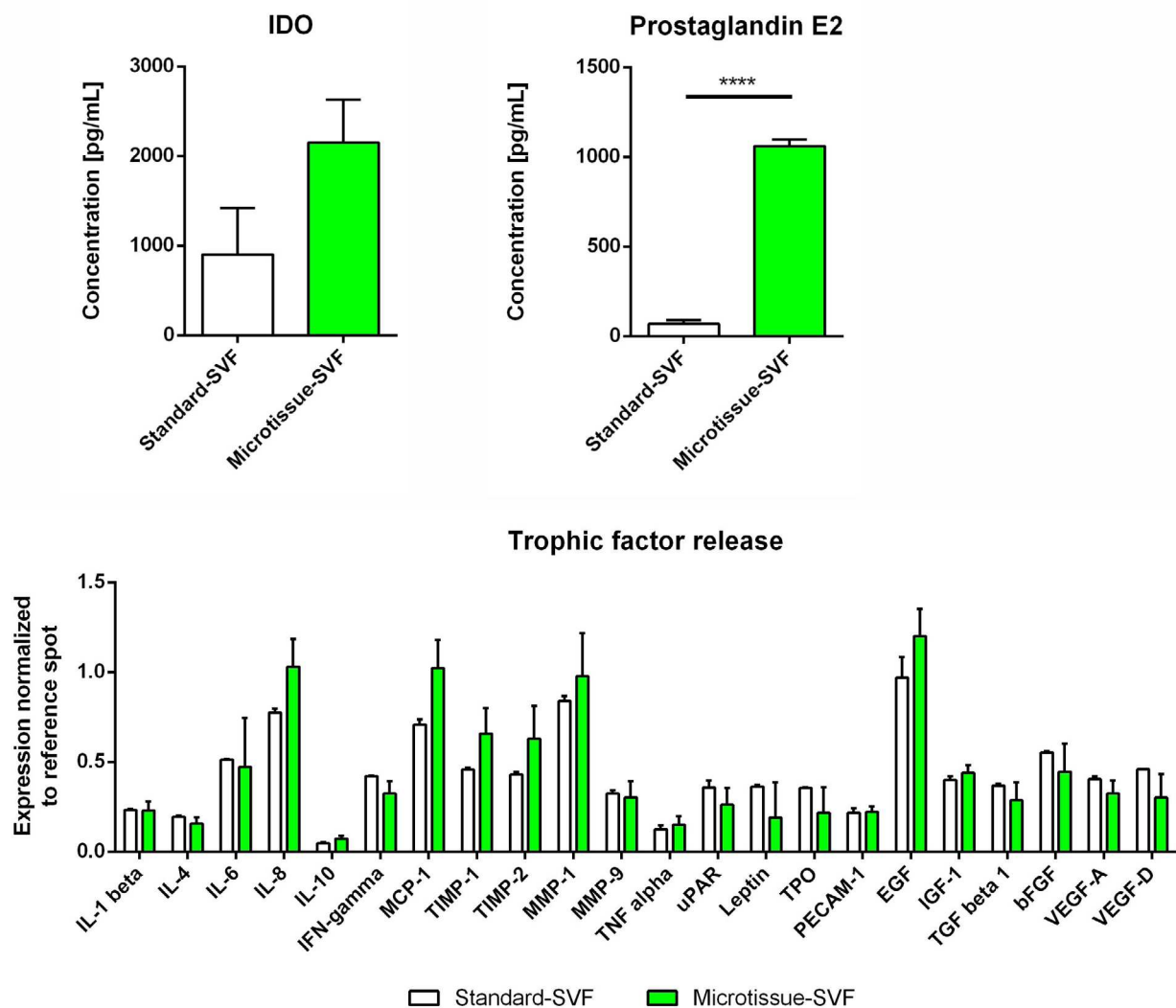


**Fig. 5. Trophic factor release by the standard-SVF and microtissue-SVF.** Both SVF types showed a typical immunomodulatory and pro-angiogenic protein profile. Notably, the microtissue-SVFs ( $n = 1-2$ , 2-4 biological replicates) secreted more IDO as compared to the standard-SVFs ( $n = 1$ , 2-4 biological replicates) and significantly more PGE<sub>2</sub>, both anti-inflammatory factors. In general, inflammatory and anti-inflammatory factors of both SVF types showed a similar tendency, with individual marker slightly up or down regulated. Data are presented as mean  $\pm$  SD; \*\*\*\*  $p < 0.0001$ .

observed already after 2-3 d of differentiation by FABP4 and LEP RT-PCR.

For a potential cell therapeutic, it is important to deliver highly regenerative cell types (Corselli *et al.*, 2013), which were found in the microtissue-SVF by subpopulation screening. Distinct regenerative SVF populations, such as Muse cells [a stress resistant stem cell population (Kuroda and Dezawa, 2014)], a pericytic subset CD90<sup>+</sup>/CD146<sup>+</sup> (Priglinger *et al.*, 2017) and lymphatic endothelial cells, were present in the microtissue-SVF. Kuroda *et al.* (2010) show that Muse cells can be obtained as a minor subset from MSCs and are able to differentiate into ectodermal, endodermal and mesodermal lineage *in vivo* and have the capacity to replace damaged tissue, as demonstrated for liver regeneration (Katagiri *et al.*, 2016). Other regenerative subpopulations identified in the microtissue-SVF were luminal EPCs (CD45<sup>-</sup>/CD31<sup>+</sup>/CD34<sup>+</sup>), SA-ASCs (CD45<sup>-</sup>/CD31<sup>-</sup>/CD146<sup>-</sup>/CD34<sup>+</sup>) and adventitial pericytes (CD45<sup>-</sup>/CD31<sup>-</sup>/CD146<sup>+</sup>), the two former of which were more abundant than in the standard-SVF. Those three populations are located on the outer adventitial stromal ring in the SVF (Zimmerlin *et al.*, 2010). Bianchi *et al.* (2013) obtain an increased number of pericytes and MSCs after mechanical cell isolation and enzymatic treatment as compared

to lipoaspirate. A very abundant CD90<sup>+</sup>/CD34<sup>+</sup> mesenchymal subset (De Francesco *et al.*, 2009) was detected in the microtissue-SVF, which was also apparent in the fluorescence staining. Zwiernina *et al.* (2015) define ASCs as DLK1<sup>-</sup>/cs-CD34<sup>+</sup>/CD90<sup>+</sup>/CD105<sup>+</sup>dim/ $\alpha$ -SMA<sup>+</sup>/CD45<sup>-</sup>/CD31<sup>-</sup> cells with spindle-shaped morphology and adipogenic potential, located on the adventitial stromal ring of vessels. In terms of regenerative action, CD34 is an important marker in SVF-derived cells (Guo *et al.*, 2016). CD34 is expressed on various subpopulations of progenitor cells (Scherberich *et al.*, 2013) and tissue-resident MSCs (Lin *et al.*, 2012); however, its expression is lost during cell expansion (Mitchell *et al.*, 2006). In the microtissue-SVF, flow cytometry double staining revealed that all CD34<sup>+</sup> cells were also CD90<sup>+</sup>, which was in accordance with a recent publication by Lutfi *et al.* (2018).

The MSC regenerative potential does not only derive from the cells with the potential to integrate and form new tissues but also from the factors they release to impact the local cells at the defect site (Kober *et al.*, 2016; Salgado *et al.*, 2010). These include immunomodulatory, angiogenic and anti-apoptotic factors (Kapur and Katz, 2013). Both, the microtissue-SVF and standard-SVF showed a typical

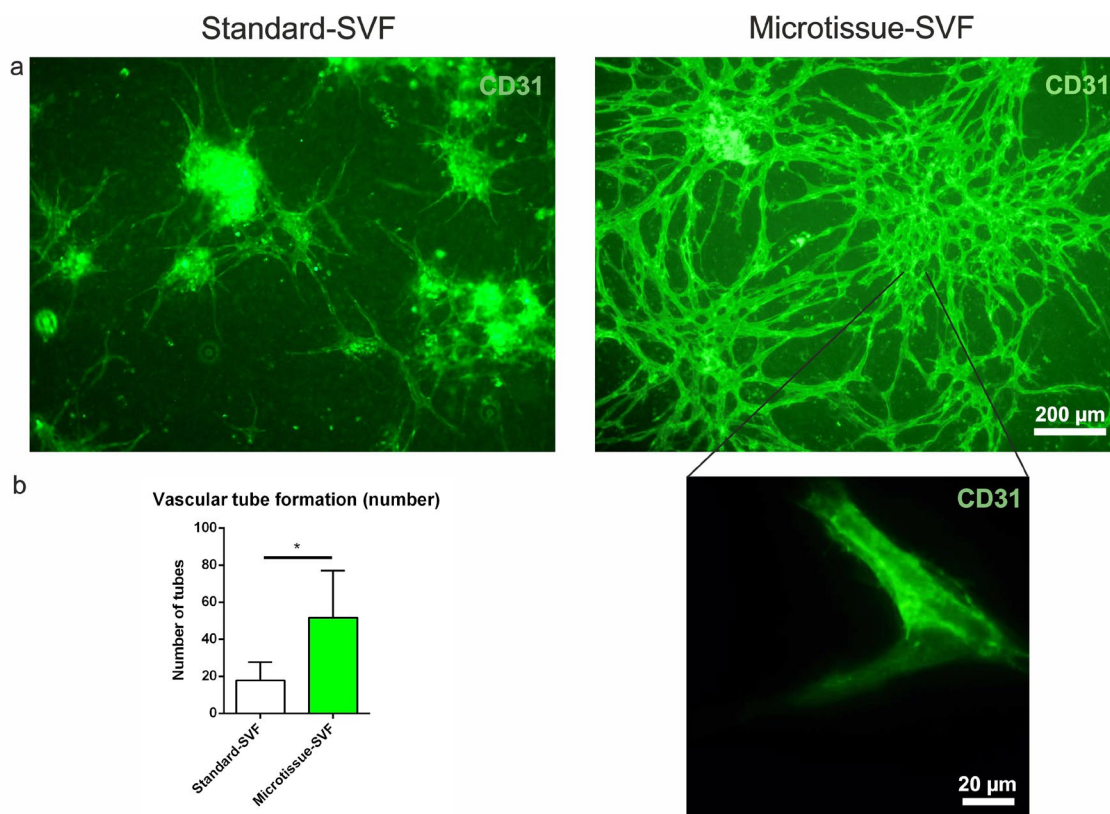


**Fig. 6. Vascularisation potential of the microtissue-SVF *in vitro*.** (a) The standard-SVF and microtissue-SVF cultured in a 3D fibrin matrix and labelled with the endothelial marker CD31 showed more tube-like structures in the microtissue-SVF group. The higher magnification image showed the tube-like arrangement of two cells in more details. Representative images. Scale bar = 200 µm and 20 µm. (b) Quantitative analysis of tube number confirmed the morphological impression with a significant increased number of tubes in the microtissue-SVF group ( $n = 3$ ; 5 biological replicates) as compared to the standard-SVF group ( $n = 4$ ; 6 biological replicates). Data are presented as mean  $\pm$  SD; \*  $p < 0.05$ .

immunomodulatory and pro-angiogenic protein profile, reflecting MSC properties (Ward *et al.*, 2018). Notably, the microtissue-SVF secreted substantially higher PGE2 levels, which is a major mediator of MSC immunomodulation (Gao *et al.*, 2016; Kota *et al.*, 2017). Successful adipose tissue formation can be observed with decellularised adipose tissue ECM combined with ASCs after 8 weeks in rats (Wang *et al.*, 2013b). The regenerative macrophage-regulating interplay between MSCs and heart-tissue ECM can also be observed after decellularisation and reseeded of ECM scaffold in muscle regeneration (Qiu *et al.*, 2018). In contrast, the gentle isolation procedure described resulted in therapeutic cells without dissociation and denaturation from the surrounding ECM, thereby making the procedure of decellularisation and reseeded redundant and providing a gently treated microtissue, which might positively influence a balanced M1/M2 macrophage response.

In fat grafting for cosmetic or reconstructive reasons, multiple strategies aim at generating a micronised homogenous tissue, which allows transplantation of an adipose matrix depleted of mature adipocytes. These strategies lead to improved volume retention lacking cysts and necrotic tissue (Li *et al.*, 2017). Similar to the described approach, the enrichment of the SVF together with matrix and microvasculature may contribute substantially to the superior quality of these grafting materials (Feng *et al.*, 2015; van Dongen *et al.*, 2016). In comparison to the standard-SVF, the microtissue-SVF demonstrated a highly elevated potential to form tube-like structures *in vitro*, indicative of its angiogenic potential *in vivo*. The reason for the remarkable angiogenic potential may relate to the components of the micro vessels and capillaries (found in histology) that were preserved by the gentle isolation protocol. The interplay of vascular cells with ASCs and their secreted angiogenic factors

(Rohringer *et al.*, 2014) give rise to a faster and more efficient angiogenic process (Pill *et al.*, 2015). A high angiogenic potential is obligatory for successful graft integration and survival (Kakagia and Pallua, 2014; Luo *et al.*, 2013). Luo *et al.* (2015) co-implant sorted endothelial cells from SVF with a fat graft in mouse leading to a high degree of vascularisation in a dose-dependent manner. This is in concordance with the presented *in vivo* implantation experiment, showing that co-transplantation of the microtissue-SVF with fat resulted in vascularisation of the integrated graft.

Enhanced wound healing properties are demonstrated with a fat graft termed ECM/SVF-gel, secreting high MCP-1 and angiogenic factors (Liu *et al.*, 2011; Sun *et al.*, 2017), suggesting wound healing as another field of application for the microtissue-SVF. A high angiogenic potential particularly predestines the material for regeneration of large areas of vascularised tissues, such as large skin defects and bone replacement (Jacobsen *et al.*, 2008). SVF enhances bone formation due to its pro-angiogenic properties, as shown in a clinical study with natural scaffolds (Farre-Guasch *et al.*, 2018). The microtissue-SVF as cell-loaded, pre-vascularised matrix could serve as graft or additive to vascularise newly developing tissue and reconnect vessels to host tissue. In myocardial regeneration, apart from vascularisation, also the mode of application of therapeutic cells and factors to the site of damage has raised problems. Intracoronary and intramyocardial injection of stem cells of different sources does not lead to the expected clinical outcome (Choudhury *et al.*, 2017; Comella *et al.*, 2016; Gyongyosi *et al.*, 2015; Povsic *et al.*, 2016) and application with biomaterials has limited success in clinical trials (Frey *et al.*, 2014; Rao *et al.*, 2015). As the microtissue-SVF is a cell-loaded hydrogel-like material, it might be a feasible material for application to the site of injury

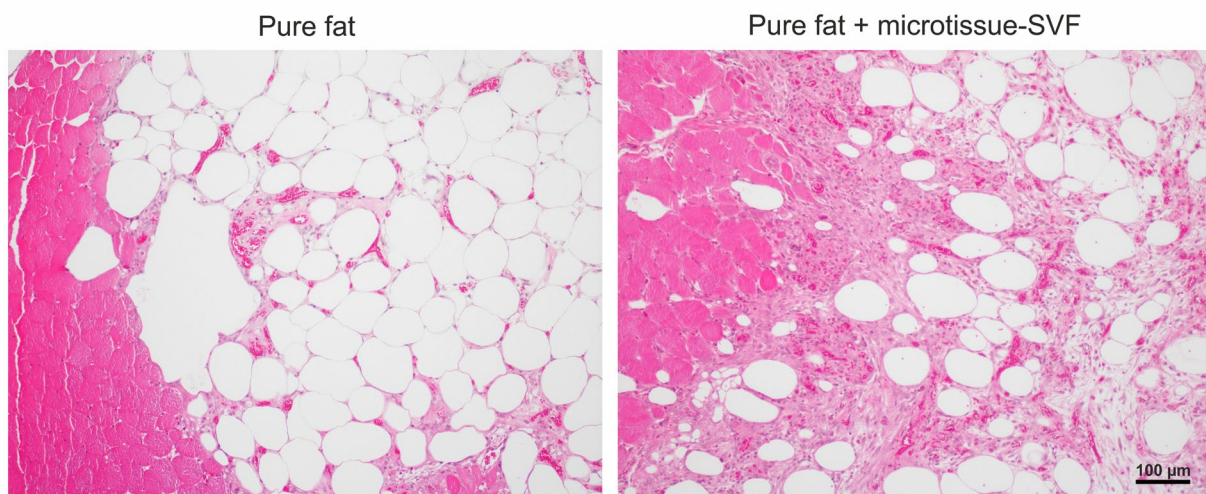


**Fig. 7.** *In vivo* implantation of pure-fat- and microtissue-SVF-supported fat graft. Pure fat either alone or in combination with the microtissue-SVF were intramuscularly injected into nude mice ( $n = 16$ ) and showed better integration (connective tissue formation) and higher vascularisation in the presence of the microtissue-SVF. H&E staining. Representative images. Scale bar = 100  $\mu\text{m}$ .

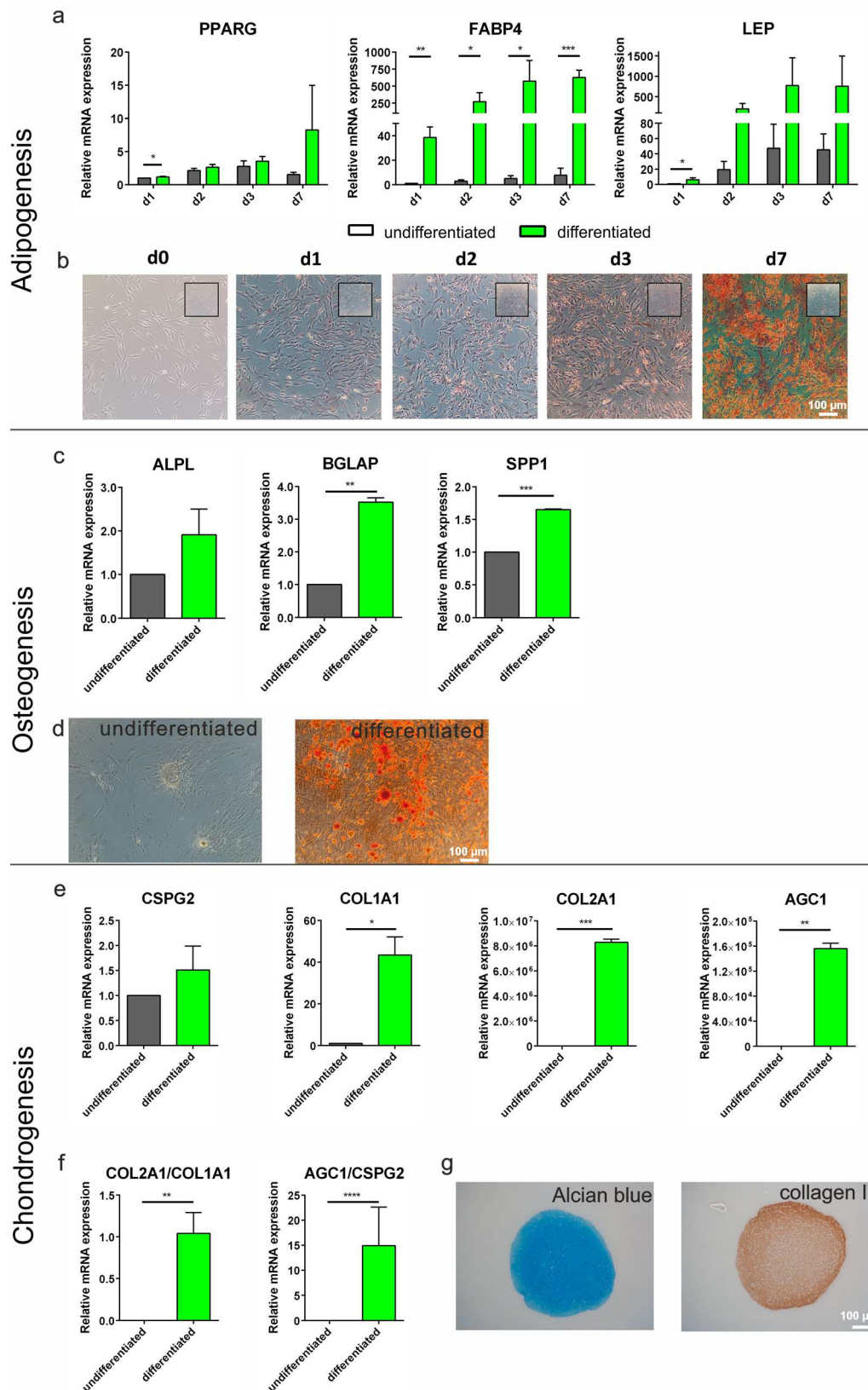


**Fig. 8. Trilineage differentiation potential of the microtissue-SVF tested *in vitro*.** Adipogenic ( $n = 3$ ), osteogenic ( $n = 3$ ) and chondrogenic ( $n = 2$ ) differentiation potential of the microtissue-SVF adherent cells was compared to undifferentiated control cells. (a) qRT-PCR of the adipogenic markers, PPAR $\gamma$ , FABP4 and LEP and (b) oil red O staining revealed the strong differentiation capacity of the microtissue-SVF-derived cells within days. (c) Expression of osteogenic marker genes, ALP, BGLAP and SPP1 and (d) alizarin red staining showed differentiation after 21 d. (e) Chondrogenic differentiation after 35 d was demonstrated by qRT-PCR of CSPG2, COL1A1, COL2A1 and AGC1, (f) the differentiation index of COL2A1/ COL1A1 and AGC1/ CSPG2, as well as (g) alcian blue and collagen type II matrix staining. Data are shown as mean  $\pm$  SD. \*  $p < 0.05$ ; \*\*  $p < 0.01$ ; \*\*\*  $p < 0.001$ ; \*\*\*\*  $p < 0.0001$ . Representative images. Scale bar = 100  $\mu$ m.

and likewise delivering therapeutic cells and their secretome to the myocardium.

The increased immunomodulatory activity of the microtissue-SVF and the presence of regenerative cells predestine it for application in inflammatory disease with associated tissue damage. Since the microtissue-SVF further revealed a high chondrogenic differentiation potential (collagen type II and aggrecan expression and matrix deposition), it fulfils the requirements for application in osteoarthritis (OA). Previous approaches already show a therapeutic effect of either ASCs or SVF after intraarticular injection into the osteoarthritic joints (Jo *et al.*, 2014; Pak *et al.*, 2016a; Spasovski *et al.*, 2017). The microtissue-SVF could be suitable to further improve the regenerative efficiency of SVF-based methods by direct application of the matrix-entrapped cells to smoothen the rough surface and provide a temporal scaffold. The ECM protects the cells from direct impact by the surrounding tissues, which might increase the chance for survival and tissue regeneration. In contrast to similar approaches with current mechanical breakdown of the ECM (Pak *et al.*, 2016b), the microtissue-SVF was minimally manipulated to reduce the stress on the cells (compression, shear force from preparation, pipetting and centrifugation) and to retain most possible bioactive composites. The ECM with its partially large collagen bundles provides a scaffolding effect and is especially predestined for applications such as strongly affected joints with large cartilage tissue loss.

In summary, a microtissue-SVF was developed from adipose tissue for intraoperative use by optimising an isolation protocol using GMP-grade reagents and procedures. The microtissue-SVF was rich in regenerative cells surrounded by intact vessels and endogenous ECM, creating a unique natural transplantable niche. This complex environment of ECM, SVF cells and their secretome potentially facilitates neovascularisation, immunomodulation and differentiation. The microtissue-SVF could provide a potent transplant for structural restoration of tissue defects for autologous clinical applications in regenerative medicine.

### Acknowledgements

We would like to acknowledge Dr Hajnal Kiprof and Dr Matthias Sandhofer for providing liposuction material and valuable discussion. This work was funded by a grant from the Austrian Research Promotion Agency (FFG) (Bridge1 programme, grant number 846062).

Heinz Redl is cofounder of Liporegena. The other authors declare that they have no competing interests. The authors alone are responsible for the content and writing of the manuscript.

### References

- Aronowitz JA, Lockhart RA, Hakakian CS (2018) A method for isolation of stromal vascular fraction cells in a clinically relevant time frame. *Methods Mol Biol* **1773**: 11-19.
- Autengruber A, Gereke M, Hansen G, Hennig C, Bruder D (2012) Impact of enzymatic tissue disintegration on the level of surface molecule expression and immune cell function. *Eur J Microbiol Immunol (Bp)* **2**: 112-120.
- Bacakova L, Zarubova J, Travnickova M, Musilkova J, Pajorova J, Slepicka P, Kasalkova NS, Svorcik V, Kolska Z, Motarjemi H, Molitor M (2018) Stem cells: their source, potency and use in regenerative therapies with focus on adipose-derived stem cells – a review. *Biotechnol Adv* **36**: 1111-1126.
- Bateman ME, Strong AL, Gimble JM, Bunnell BA (2018) Using fat to fight disease: a systematic review of non-homologous adipose-derived stromal/stem cell therapies. *Stem Cells* **36**: 1311-1328.
- Bianchi F, Maioli M, Leonardi E, Olivi E, Pasquinelli G, Valente S, Mendez AJ, Ricordi C, Raffaini M, Tremolada C, Ventura C (2013) A new nonenzymatic method and device to obtain a fat tissue derivative highly enriched in pericyte-like elements by mild mechanical forces from human lipoaspirates. *Cell Transplant* **22**: 2063-2077.
- Bourin P, Bunnell BA, Casteilla L, Dominici M, Katz AJ, March KL, Redl H, Rubin JP, Yoshimura K, Gimble JM (2013) Stromal cells from the adipose tissue-derived stromal vascular fraction and culture expanded adipose tissue-derived stromal/stem cells: a joint statement of the International Federation for Adipose Therapeutics and Science (IFATS) and the International Society for Cellular Therapy (ISCT). *Cytotherapy* **15**: 641-648.
- Busser H, De Bruyn C, Urbain F, Najar M, Pieters K, Raicevic G, Meuleman N, Bron D, Lagneaux L (2014) Isolation of adipose-derived stromal cells without enzymatic treatment: expansion, phenotypical, and functional characterization. *Stem Cells Dev* **23**: 2390-2400.
- Choudhury T, Mozid A, Hamshere S, Yeo C, Pellaton C, Arnous S, Saunders N, Brookman P, Jain A, Locca D, Archbold A, Knight C, Wragg A, Davies C, Mills P, Parmar M, Rothman M, Choudry F, Jones DA, Agrawal S, Martin J, Mathur A (2017) An exploratory randomized control study of combination cytokine and adult autologous bone marrow progenitor cell administration in patients with ischaemic cardiomyopathy: the REGENERATE-IHD clinical trial. *Eur J Heart Fail* **19**: 138-147.
- Comella K, Parcerro J, Bansal H, Perez J, Lopez J, Agrawal A, Ichim T (2016) Effects of the intramyocardial implantation of stromal vascular fraction in patients with chronic ischemic cardiomyopathy. *J Transl Med* **14**: 158. DOI: 10.1186/s12967-016-0918-5.

Corselli M, Crisan M, Murray IR, West CC, Scholes J, Codrea F, Khan N, Peault B (2013) Identification of perivascular mesenchymal stromal/stem cells by flow cytometry. *Cytometry A* **83**: 714-720.

De Francesco F, Ricci G, D'Andrea F, Nicoletti GF, Ferraro GA (2015) Human adipose stem cells: from bench to bedside. *Tissue Eng Part B Rev* **21**: 572-584.

De Francesco F, Tirino V, Desiderio V, Ferraro G, D'Andrea F, Giuliano M, Libondi G, Pirozzi G, De Rosa A, Papaccio G (2009) Human CD34/CD90 ASCs are capable of growing as sphere clusters, producing high levels of VEGF and forming capillaries. *PLoS One* **4**: e6537. DOI: 10.1371/journal.pone.0006537.

Dykstra JA, Facile T, Patrick RJ, Francis KR, Milanovich S, Weimer JM, Kota DJ (2017) Concise review: fat and furious: harnessing the full potential of adipose-derived stromal vascular fraction. *Stem Cells Transl Med* **6**: 1096-1108.

Eto H, Kato H, Suga H, Aoi N, Doi K, Kuno S, Yoshimura K (2012) The fate of adipocytes after nonvascularized fat grafting: evidence of early death and replacement of adipocytes. *Plast Reconstr Surg* **129**: 1081-1092.

European Medicines Agency (2012) Scientific recommendation on classification of advanced therapy medicinal products. Article 17 – Regulation (EC) No 1394/2007.

Farre-Guasch E, Bravenboer N, Helder MN, Schulten E, Ten Bruggenkate CM, Klein-Nulend J (2018) Blood vessel formation and bone regeneration potential of the stromal vascular fraction seeded on a calcium phosphate scaffold in the human maxillary sinus floor elevation model. *Materials (Basel)* **11**: pii: E161. DOI: 10.3390/ma11010161.

Feng J, Doi K, Kuno S, Mineda K, Kato H, Kinoshita K, Kanayama K, Mashiko T, Yoshimura K (2015) Micronized cellular adipose matrix as a therapeutic injectable for diabetic ulcer. *Regen Med* **10**: 699-708.

Frey N, Linke A, Suselbeck T, Muller-Ehmsen J, Vermeersch P, Schoors D, Rosenberg M, Bea F, Tuvia S, Leor J (2014) Intracoronary delivery of injectable bioabsorbable scaffold (IK-5001) to treat left ventricular remodeling after ST-elevation myocardial infarction: a first-in-man study. *Circ Cardiovasc Interv* **7**: 806-812.

Fu Y, Karbaat L, Wu L, Leijten J, Both SK, Karperien M (2017) Trophic effects of mesenchymal stem cells in tissue regeneration. *Tissue Eng Part B Rev* **23**: 515-528.

Gao F, Chiu SM, Motan DA, Zhang Z, Chen L, Ji HL, Tse HF, Fu QL, Lian Q (2016) Mesenchymal stem cells and immunomodulation: current status and future prospects. *Cell Death Dis* **7**: e2062. DOI: 10.1038/cddis.2015.327.

Gentile P, Orlandi A, Scioli MG, Di Pasquali C, Bocchini I, Cervelli V (2012) Concise review: adipose-derived stromal vascular fraction cells and platelet-rich plasma: basic and clinical implications for tissue engineering therapies in regenerative surgery. *Stem Cells Transl Med* **1**: 230-236.

Geutjes PJ, van der Vliet JA, Faraj KA, de Vries N, van Moerkerk HT, Wismans RG, Hendriks T, Daamen WF, van Kuppevelt TH (2010) Preparation and characterization of injectable fibrillar type I collagen and evaluation for pseudoaneurysm treatment in a pig model. *J Vasc Surg* **52**: 1330-1338.

Gimble J, Guilak F (2003a) Adipose-derived adult stem cells: isolation, characterization, and differentiation potential. *Cytotherapy* **5**: 362-369.

Gimble JM, Guilak F (2003b) Differentiation potential of adipose derived adult stem (ADAS) cells. *Curr Top Dev Biol* **58**: 137-160.

Guo J, Nguyen A, Banyard DA, Fadavi D, Toranto JD, Wirth GA, Paydar KZ, Evans GR, Widgerow AD (2016) Stromal vascular fraction: a regenerative reality? Part 2: mechanisms of regenerative action. *J Plast Reconstr Aesthet Surg* **69**: 180-188.

Gyongyosi M, Wojakowski W, Lemarchand P, Lunde K, Tendera M, Bartunek J, Marban E, Assmus B, Henry TD, Traverse JH, Moye LA, Surder D, Corti R, Huikuri H, Miettinen J, Wohrle J, Obradovic S, Roncalli J, Malliaras K, Pokushalov E, Romanov A, Kastrup J, Bergmann MW, Atsma DE, Diederichsen A, Edes I, Benedek I, Benedek T, Pejkov H, Nyolczas N, Pavo N, Bergler-Klein J, Pavo IJ, Sylven C, Berti S, Navarese EP, Maurer G, Investigators A (2015) Meta-Analysis of Cell-based CaRdiac stUdiEs (ACCRUE) in patients with acute myocardial infarction based on individual patient data. *Circ Res* **116**: 1346-1360.

Hagman DK, Kuzma JN, Larson I, Foster-Schubert KE, Kuan LY, Cignarella A, Geamanu E, Makar KW, Gottlieb JR, Kratz M (2012) Characterizing and quantifying leukocyte populations in human adipose tissue: impact of enzymatic tissue processing. *J Immunol Methods* **386**: 50-59.

Holnthoner W, Hohenegger K, Husa AM, Muehleider S, Meinel A, Peterbauer-Scherb A, Redl H (2015) Adipose-derived stem cells induce vascular tube formation of outgrowth endothelial cells in a fibrin matrix. *J Tissue Eng Regen Med* **9**: 127-136.

Jacobsen KA, Al-Aql ZS, Wan C, Fitch JL, Stapleton SN, Mason ZD, Cole RM, Gilbert SR, Clemens TL, Morgan EF, Einhorn TA, Gerstenfeld LC (2008) Bone formation during distraction osteogenesis is dependent on both VEGFR1 and VEGFR2 signaling. *J Bone Miner Res* **23**: 596-609.

Jiang A, Li M, Duan W, Dong Y, Wang Y (2015) Improvement of the survival of human autologous fat transplantation by adipose-derived stem-cells-assisted lipotransfer combined with bFGF. *ScientificWorldJournal* **2015**: 968057. DOI: 10.1155/2015/968057.

Jiang T, Xu G, Wang Q, Yang L, Zheng L, Zhao J, Zhang X (2017) *In vitro* expansion impaired the stemness of early passage mesenchymal stem cells for treatment of cartilage defects. *Cell Death Dis* **8**: e2851. DOI: 10.1038/cddis.2017.215.

Jo CH, Lee YG, Shin WH, Kim H, Chai JW, Jeong EC, Kim JE, Shim H, Shin JS, Shin IS, Ra JC, Oh S, Yoon KS (2014) Intra-articular injection of mesenchymal stem cells for the treatment of osteoarthritis of the

knee: a proof-of-concept clinical trial. *Stem Cells* **32**: 1254-1266.

Kakagia D, Pallua N (2014) Autologous fat grafting: in search of the optimal technique. *Surg Innov* **21**: 327-336.

Kapur SK, Katz AJ (2013) Review of the adipose derived stem cell secretome. *Biochimie* **95**: 2222-2228.

Katagiri H, Kushida Y, Nojima M, Kuroda Y, Wakao S, Ishida K, Endo F, Kume K, Takahara T, Nitta H, Tsuda H, Dezawa M, Nishizuka SS (2016) A distinct subpopulation of bone marrow mesenchymal stem cells, muse cells, directly commit to the replacement of liver components. *Am J Transplant* **16**: 468-483.

Kim BS, Choi JS, Kim JD, Choi YC, Cho YW (2012) Recellularization of decellularized human adipose-tissue-derived extracellular matrix sheets with other human cell types. *Cell Tissue Res* **348**: 559-567.

Kober J, Gugerell A, Schmid M, Zeyda M, Buchberger E, Nickl S, Hacker S, Ankersmit HJ, Keck M (2016) Wound healing effect of conditioned media obtained from adipose tissue on human skin cells: a comparative *in vitro* study. *Ann Plast Surg* **77**: 156-163.

Kota DJ, Prabhakara KS, Toledano-Furman N, Bhattarai D, Chen Q, DiCarlo B, Smith P, Triolo F, Wenzel PL, Cox CS, Jr., Olson SD (2017) Prostaglandin E2 indicates therapeutic efficacy of mesenchymal stem cells in experimental traumatic brain injury. *Stem Cells* **35**: 1416-1430.

Kuroda Y, Dezawa M (2014) Mesenchymal stem cells and their subpopulation, pluripotent muse cells, in basic research and regenerative medicine. *Anat Rec (Hoboken)* **297**: 98-110.

Kuroda Y, Kitada M, Wakao S, Nishikawa K, Tanimura Y, Makinoshima H, Goda M, Akashi H, Inutsuka A, Niwa A, Shigemoto T, Nabeshima Y, Nakahata T, Nabeshima Y, Fujiiyoshi Y, Dezawa M (2010) Unique multipotent cells in adult human mesenchymal cell populations. *Proc Natl Acad Sci U S A* **107**: 8639-8643.

Li K, Li F, Li J, Wang H, Zheng X, Long J, Guo W, Tian W (2017) Increased survival of human free fat grafts with varying densities of human adipose-derived stem cells and platelet-rich plasma. *J Tissue Eng Regen Med* **11**: 209-219.

Lin CS, Ning H, Lin G, Lue TF (2012) Is CD34 truly a negative marker for mesenchymal stromal cells? *Cytotherapy* **14**: 1159-1163.

Liu S, Zhang H, Zhang X, Lu W, Huang X, Xie H, Zhou J, Wang W, Zhang Y, Liu Y, Deng Z, Jin Y (2011) Synergistic angiogenesis promoting effects of extracellular matrix scaffolds and adipose-derived stem cells during wound repair. *Tissue Eng Part A* **17**: 725-739.

Luo S, Hao L, Li X, Yu D, Diao Z, Ren L, Xu H (2013) Adipose tissue-derived stem cells treated with estradiol enhance survival of autologous fat transplants. *Tohoku J Exp Med* **231**: 101-110.

Luo X, Cao W, Xu H, Wang L, Zhang Z, Lu Y, Jin X, Ren X, He J, Fu M, Huang Y, Pi Q, Fan Z (2015) Coimplanted endothelial cells improve adipose

tissue grafts' survival by increasing vascularization. *J Craniofac Surg* **26**: 358-364.

Lutfi D LL, Zeyda M, Stulnig T, Singer CF, Turkof E (2018) Centrifugation of adipose tissue aspirate causes endothelial cell enrichment. *J Stem Cell Res Med* **3**. DOI: 10.15761/JSCRM.1000126.

Macrin D, Joseph JP, Pillai AA, Devi A (2017) Eminent sources of adult mesenchymal stem cells and their therapeutic imminence. *Stem Cell Rev* **13**: 741-756.

McIntosh K1, Zvonic S, Garrett S, Mitchell JB, Floyd ZE, Hammill L, Kloster A, Di Halvorsen Y, Ting JP, Storms RW, Goh B, Kilroy G, Wu X, Gimble JM (2006) The immunogenicity of human adipose-derived cells: temporal changes *in vitro*. *Stem Cells* **24**: 1246-1253.

Mitchell JB, McIntosh K, Zvonic S, Garrett S, Floyd ZE, Kloster A, Di Halvorsen Y, Storms RW, Goh B, Kilroy G, Wu X, Gimble JM (2006) Immunophenotype of human adipose-derived cells: temporal changes in stromal-associated and stem cell-associated markers. *Stem Cells* **24**: 376-385.

National Research Council (US) Committee for the Update of the Guide for the Care and Use of Laboratory Animals (2011) *Guide for the care and use of laboratory animals*, 8<sup>th</sup> edition. National Academies Press, Washington, DC, USA.

Nguyen A, Guo J, Banyard DA, Fadavi D, Toranto JD, Wirth GA, Paydar KZ, Evans GR, Widgerow AD (2015) Stromal vascular fraction: a regenerative reality? Part 1: current concepts and review of the literature. *J Plast Reconstr Aesthet Surg* **69**: 170-179.

Oberbauer E, Steffenhagen C, Wurzer C, Gabriel C, Redl H, Wolbank S (2015) Enzymatic and non-enzymatic isolation systems for adipose tissue-derived cells: current state of the art. *Cell Regen (Lond)* **4**: 7. DOI: 10.1186/s13619-015-0020-0.

Pak J, Lee JH, Kartolo WA, Lee SH (2016a) Cartilage regeneration in human with adipose tissue-derived stem cells: current status in clinical implications. *Biomed Res Int* **2016**: 4702674. DOI: 10.1155/2016/4702674.

Pak J, Lee JH, Park KS, Jeong BC, Lee SH (2016b) Regeneration of cartilage in human knee osteoarthritis with autologous adipose tissue-derived stem cells and autologous extracellular matrix. *Biores Open Access* **5**: 192-200.

Pak J, Lee JH, Pak N, Pak Y, Park KS, Jeon JH, Jeong BC, Lee SH (2018) Cartilage regeneration in humans with adipose tissue-derived stem cells and adipose stromal vascular fraction cells: updated status. *Int J Mol Sci* **19**. DOI: 10.3390/ijms19072146.

Pan Q, Fouraschen SM, de Ruiter PE, Dinjens WN, Kwekkeboom J, Tilanus HW, van der Laan LJ (2014) Detection of spontaneous tumorigenic transformation during culture expansion of human mesenchymal stromal cells. *Exp Biol Med (Maywood)* **239**: 105-115.

Pill K, Hofmann S, Redl H, Holnthoner W (2015) Vascularization mediated by mesenchymal stem cells from bone marrow and adipose tissue: a comparison. *Cell Regen (Lond)* **4**: 8. DOI: 10.1186/s13619-015-0025-8.

Povsic TJ, Henry TD, Traverse JH, Fortuin FD, Schaer GL, Kereiakes DJ, Schatz RA, Zeiher AM, White CJ, Stewart DJ, Jolicoeur EM, Bass T, Henderson DA, Dignacco P, Gu Z, Al-Khalidi HR, Junge C, Nada A, Hunt AS, Losordo DW, Investigators R (2016) The RENEW Trial: efficacy and safety of intramyocardial autologous CD34(+) cell administration in patients with refractory angina. *JACC Cardiovasc Interv* **9**: 1576-1585.

Priglinger E, Maier J, Chaudary S, Lindner C, Wurzer C, Rieger S, Redl H, Wolbank S, Dungal P (2018) Photobiomodulation of freshly isolated human adipose tissue-derived stromal vascular fraction cells by pulsed light-emitting diodes for direct clinical application. *J Tissue Eng Regen Med* **12**: 1352-1362.

Priglinger E, Schuh C, Steffenhagen C, Wurzer C, Maier J, Nuernberger S, Holnthoner W, Fuchs C, Suessner S, Runzler D, Redl H, Wolbank S (2017) Improvement of adipose tissue-derived cells by low-energy extracorporeal shock wave therapy. *Cytotherapy* **19**: 1079-1095.

Prockop DJ (2007) "Stemness" does not explain the repair of many tissues by mesenchymal stem/multipotent stromal cells (MSCs). *Clin Pharmacol Ther* **82**: 241-243.

Qiu X, Liu S, Zhang H, Zhu B, Su Y, Zheng C, Tian R, Wang M, Kuang H, Zhao X, Jin Y (2018) Mesenchymal stem cells and extracellular matrix scaffold promote muscle regeneration by synergistically regulating macrophage polarization toward the M2 phenotype. *Stem Cell Res Ther* **9**: 88. DOI: 10.1186/s13287-018-0821-5.

Rao SV, Zeymer U, Douglas PS, Al-Khalidi H, Liu J, Gibson CM, Harrison RW, Joseph DS, Heyrman R, Krucoff MW (2015) A randomized, double-blind, placebo-controlled trial to evaluate the safety and effectiveness of intracoronary application of a novel bioabsorbable cardiac matrix for the prevention of ventricular remodeling after large ST-segment elevation myocardial infarction: rationale and design of the PRESERVATION I trial. *Am Heart J* **170**: 929-937.

Raposo E, Simonacci F, Perrotta RE (2017) Adipose-derived stem cells: comparison between two methods of isolation for clinical applications. *Ann Med Surg (Lond)* **20**: 87-91.

Rohringer S, Hofbauer P, Schneider KH, Husa AM, Feichtinger G, Peterbauer-Scherb A, Redl H, Holnthoner W (2014) Mechanisms of vasculogenesis in 3D fibrin matrices mediated by the interaction of adipose-derived stem cells and endothelial cells. *Angiogenesis* **17**: 921-933.

Safwani WK, Makpol S, Sathapan S, Chua KH (2013) Alteration of gene expression levels during osteogenic induction of human adipose derived stem cells in long-term culture. *Cell Tissue Bank* **14**: 289-301.

Salgado AJ, Reis RL, Sousa NJ, Gimble JM (2010) Adipose tissue derived stem cells secretome: soluble factors and their roles in regenerative medicine. *Curr Stem Cell Res Ther* **5**: 103-110.

Scherberich A, Di Maggio ND, McNagny KM (2013) A familiar stranger: CD34 expression and putative functions in SVF cells of adipose tissue. *World J Stem Cells* **5**: 1-8.

Seaman SA, Tannan SC, Cao Y, Peirce SM, Lin KY (2015) Differential effects of processing time and duration of collagenase digestion on human and murine fat grafts. *Plast Reconstr Surg* **136**: 189e-199e.

Sidney LE, Branch MJ, Dunphy SE, Dua HS, Hopkinson A (2014) Concise review: evidence for CD34 as a common marker for diverse progenitors. *Stem Cells* **32**: 1380-1389.

Spasovski D, Spasovski V, Bascarevic Z, Stojiljkovic M, Vreca M, Anđelković M, Pavlović S (2017) Intra-articular injection of autologous adipose-derived mesenchymal stem cells in the treatment of knee osteoarthritis. *J Gene Med* **20**. DOI: 10.1002/jgm.3002.

Stivers KB, Beare JE, Chilton PM, Williams SK, Kaufman CL, Hoying JB (2017) Adipose-derived cellular therapies in solid organ and vascularized-composite allotransplantation. *Curr Opin Organ Transplant* **22**: 490-498.

Sun M, He Y, Zhou T, Zhang P, Gao J, Lu F (2017) Adipose extracellular matrix/stromal vascular fraction gel secretes angiogenic factors and enhances skin wound healing in a murine model. *Biomed Res Int* **2017**: 3105780. DOI: 10.1155/2017/3105780.

van Dongen JA, Stevens HP, Parvizi M, van der Lei B, Harmsen MC (2016) The fractionation of adipose tissue procedure to obtain stromal vascular fractions for regenerative purposes. *Wound Repair Regen* **24**: 994-1003.

Wang L, Johnson JA, Zhang Q, Beahm EK (2013a) Combining decellularized human adipose tissue extracellular matrix and adipose-derived stem cells for adipose tissue engineering. *Acta Biomater* **9**: 8921-8931.

Wang X, Wang Y, Gou W, Lu Q, Peng J, Lu S (2013b) Role of mesenchymal stem cells in bone regeneration and fracture repair: a review. *Int Orthop* **37**: 2491-2498.

Ward MR, Abadeh A, Connelly KA (2018) Concise review: rational use of mesenchymal stem cells in the treatment of ischemic heart disease. *Stem Cells Transl Med* **7**: 543-550.

Yoshimura K, Sato K, Aoi N, Kurita M, Hirohi T, Harii K (2008) Cell-assisted lipotransfer for cosmetic breast augmentation: supportive use of adipose-derived stem/stromal cells. *Aesthetic Plast Surg* **32**: 48-57.

Zimmerlin L, Donnenberg VS, Pfeifer ME, Meyer EM, Peault B, Rubin JP, Donnenberg AD (2010) Stromal vascular progenitors in adult human adipose tissue. *Cytometry A* **77**: 22-30.

Zuk PA, Zhu M, Ashjian P, De Ugarte DA, Huang JI, Mizuno H, Alfonso ZC, Fraser JK, Benhaim P, Hedrick MH (2002) Human adipose tissue is a source of multipotent stem cells. *Mol Biol Cell* **13**: 4279-4295.

Zuk PA, Zhu M, Mizuno H, Huang J, Futrell JW, Katz AJ, Benhaim P, Lorenz HP, Hedrick MH (2001) Multilineage cells from human adipose tissue:



implications for cell-based therapies. *Tissue Eng* 7: 211-228.

Zwierzina ME, Ejaz A, Bitsche M, Blumer MJ, Mitterberger MC, Mattesich M, Amann A, Kaiser A, Pechriggl EJ, Horl S, Rostek U, Pierer G, Fritsch H, Zwerschke W (2015) Characterization of DLK1(PREF1)+/CD34+ cells in vascular stroma of human white adipose tissue. *Stem Cell Res* 15: 403-418.

### Discussion with Reviewer

**Giovanna Desando:** What was the biological mechanism of action of the microtissue-SVF to foster tissue regeneration?

**Authors:** The microtissue-SVF was a fat derivative, a SVF without dissociation from its natural extracellular matrix. According to the *in vitro* findings, it was especially rich in regenerative, viable cells with a high differentiation and vascularisation potential and protected by endogenous matrix. The cells displayed parameters associated with immunomodulatory, pro-angiogenic and anti-inflammatory behaviour. All of which might contribute to its regenerative potential in tissue regeneration. The association with their extracellular matrix might further contribute to a better integration and survival after transplantation. These beneficial properties might allow the therapeutic cells to fulfil the desired purpose at each respective location.

**Giovanna Desando:** What could be the main clinical application in using the microtissue-SVF fraction?

**Authors:** Any clinical application that requires local application of SVF would be recommended, especially interesting are soft tissue regeneration, wound healing and OA. Previous approaches reveal that MSCs or SVFs have a beneficial effect in OA scores when injected intraarticularly into the osteoarthritic joints (Jo *et al.*, 2014, additional reference; Pak *et al.*, 2016; Spasovski *et al.*, 2018, additional reference). This effect is attributed to

their immunomodulatory and anti-inflammatory properties. The microtissue-SVF contained highly viable matrix-protected cells, which might protect the cells in the local joint environment. The *in vitro* data further suggested a high immunomodulatory, anti-inflammatory and chondrogenic potential. Due to these *in vitro* pro-regenerative properties, the microtissue-SVF has the potential to act as improved cell therapy in OA.

**Giovanna Desando:** Do the authors think that the use of only secretome from the microtissue-SVF could represent a good therapeutic strategy?

**Authors:** The microtissue-SVF appeared to be rich in regenerative cells and could be a potent source for secretome of immunomodulatory, pro-angiogenic and anti-inflammatory factors or extracellular vesicles. However, the specific concept of the microtissue-SVF was that the preserved extracellular matrix not only limited manipulation during isolation but also protected the cellular components after delivering to regenerative sites and should, hence, be especially useful as cell therapeutic.

### Additional References

Jo CH, Lee YG, Shin WH, Kim H, Chai JW, Jeong EC, Kim JE, Shim H, Shin JS, Shin IS, Ra JC, Oh S, Yoon KS. Intra-articular injection of mesenchymal stem cells for the treatment of osteoarthritis of the knee: a proof-of-concept clinical trial. *Stem Cells* 32: 1254-1266.

Spasovski D, Spasovski V, Bašćarević Z, Stojiljković M, Vreća M, Anđelković M, Pavlović S (2018) Intra-articular injection of autologous adipose-derived mesenchymal stem cells in the treatment of knee osteoarthritis. *J Gene Med* 20. DOI: 10.1002/jgm.3002.

**Editor's note:** The Scientific Editor responsible for this paper was Chris Evans.

## Improvement of adipose tissue-derived cells by low-energy extracorporeal shock wave therapy

ELENI PRIGLINGER<sup>1,2,★★</sup>, CHRISTINA M.A.P. SCHUH<sup>1,2,★★</sup>, CAROLIN STEFFENHAGEN<sup>1,2</sup>, CHRISTOPH WURZER<sup>1,2</sup>, JULIA MAIER<sup>1,2</sup>, SYLVIA NUERNBERGER<sup>2,3,4</sup>, WOLFGANG HOLNTHONER<sup>1,2</sup>, CHRISTIANE FUCHS<sup>2,5</sup>, SUSANNE SUESSNER<sup>2,6</sup>, DOMINIK RÜNZLER<sup>2,5</sup>, HEINZ REDL<sup>1,2</sup> & SUSANNE WOLBANK<sup>1,2</sup>

<sup>1</sup>Ludwig Boltzmann Institute for Experimental and Clinical Traumatology, Austrian Workers' Compensation Board (AUVA) Research Center, Vienna, Austria, <sup>2</sup>Austrian Cluster for Tissue Regeneration, Vienna, Austria, <sup>3</sup>Bernhard Gottlieb University Clinic of Dentistry, Universitätsklinik für Zahn-, Mund- und Kieferheilkunde Ges.m.b.H, Vienna, Austria, <sup>4</sup>Medical University of Vienna, Department of Trauma Surgery, Vienna, Austria, <sup>5</sup>University of Applied Sciences Technikum Wien, Department of Biochemical Engineering, Vienna, Austria, and <sup>6</sup>Red Cross Blood Transfusion Service of Upper Austria, Linz, Austria

### Abstract

**Background.** Cell-based therapies with autologous adipose tissue-derived cells have shown great potential in several clinical studies in the last decades. The majority of these studies have been using the stromal vascular fraction (SVF), a heterogeneous mixture of fibroblasts, lymphocytes, monocytes/macrophages, endothelial cells, endothelial progenitor cells, pericytes and adipose-derived stromal/stem cells (ASC) among others. Although possible clinical applications of autologous adipose tissue-derived cells are manifold, they are limited by insufficient uniformity in cell identity and regenerative potency. **Methods.** In our experimental set-up, low-energy extracorporeal shock wave therapy (ESWT) was performed on freshly obtained human adipose tissue and isolated adipose tissue SVF cells aiming to equalize and enhance stem cell properties and functionality. **Results.** After ESWT on adipose tissue we could achieve higher cellular adenosine triphosphate (ATP) levels compared with ESWT on the isolated SVF as well as the control. ESWT on adipose tissue resulted in a significantly higher expression of single mesenchymal and vascular marker compared with untreated control. Analysis of SVF protein secretome revealed a significant enhancement in insulin-like growth factor (IGF)-1 and placental growth factor (PLGF) after ESWT on adipose tissue. **Discussion.** Summarizing we could show that ESWT on adipose tissue enhanced the cellular ATP content and modified the expression of single mesenchymal and vascular marker, and thus potentially provides a more regenerative cell population. Because the effectiveness of autologous cell therapy is dependent on the therapeutic potency of the patient's cells, this technology might raise the number of patients eligible for autologous cell transplantation.

**Key Words:** adipose tissue, adipose-derived stromal/stem cells, extracorporeal shock wave therapy, stromal vascular fraction

### Introduction

Cell-based therapies with autologous adipose tissue-derived cells have shown great potential in several clinical studies in the last decades. In the field of aesthetic and reconstructive medicine an abundance of knowledge was accumulated in the last century [1] and later was extended through clinical studies in regenerative medicine and tissue engineering [2–4]. The majority of studies have been using the stromal vascular fraction (SVF), a heterogeneous mixture of fibroblasts, lymphocytes, monocytes/macrophages, endothelial cells, endothelial progenitor cells, pericytes

and adipose-derived stromal/stem cells (ASC) among others [5–10]. In clinical case studies and trials treating soft tissue defects [4,11–14], bone and cartilage defects [15–19], gastrointestinal lesions [20], immune disorders [21,22], neurological injuries [23] and cardiovascular diseases [24], SVF and ASC have already proven their regenerative potential. Although possible clinical applications of autologous adipose tissue-derived cells are manifold, they are limited by drawbacks concerning stem cell identity and potency of the isolated cell population. Different cell isolation protocols and methods but also closed automated isolation devices bring up cell populations with

★★These authors contributed equally.

Correspondence: Eleni Priglinger, PhD, Ludwig Boltzmann Institute for Experimental and Clinical Traumatology, Donaueschingenstraße 13, Vienna A-1200, Austria. E-mail: eleni.priglinger@trauma.lbg.ac.at

(Received 25 May 2016; accepted 23 May 2017)

ISSN 1465-3249 Copyright © 2017 International Society for Cellular Therapy. Published by Elsevier Inc. All rights reserved.  
<http://dx.doi.org/10.1016/j.jcyt.2017.05.010>

variable content of potentially therapeutic cells within the fat graft or the SVF [25]. In addition, donor variability results in a highly heterogeneous cell composition and functionality, which may reduce reproducibility and efficacy, and increase the risk for transplantation of low-potent cells into the patient. SVF cells and ASC can be characterized with a distinct surface marker profile and have the ability to differentiate at least into the mesodermal lineages. This is defined in a joint statement of the International Federation for Adipose Therapeutics and Science (IFATS) together with the International Society for Cellular Therapy (ISCT) to provide guidance for standardization between different research groups [26]. Cultivation, purification and differentiation of ASC are standard procedures for clinical trials, but it remains difficult to meet the requirements of regulatory agencies for stem cell translation into clinics. To increase therapeutic cell potency, numerous strategies have been evaluated for activation of cells or cell material such as physical stimulation using low level light therapy (LLLT) [27–29], photobiostimulation [30,31] or radio electric asymmetric conveyer [32]. Moreover, the efficiency of ASC transplants was improved by the addition of activated platelet-rich plasma (PRP) [33,34] or growth factors [35].

In this study we aimed to improve stem cell properties and reduce donor variability by mild mechanical stimulation using extracorporeal shock wave therapy (ESWT).

Extracorporeal shock waves are sonic pulses, characterized by an initial increase, reaching a positive peak of up to 100 MPa within 10 ns, followed by a negative amplitude of up to -10 MPa and a total life cycle of less than 10  $\mu$ s [36]. Biological responses are thought to be triggered by the high initial pressure, followed by a tensile force and the resulting mechanical stimulation [36]. ESWT has been applied for several decades in the clinics and has demonstrated beneficial effects on tissue regeneration in non-union fractures [37–39], ischemia-induced tissue necrosis [40] or post-traumatic necrosis, disturbed healing wounds, ulcers and burn wounds [41,42]. We have previously shown that low-energy ESWT enhances proliferation and differentiation of ASC lines *in vitro* [43,44]. These *in vitro* studies corroborate the clinical success of ESWT in wound healing, nerve regeneration and vascularization [45,46].

In our experimental set-up, low-energy ESWT was applied to freshly isolated SVF cells from human adipose tissue aiming to equalize and enhance cell properties and functionality. To limit the degree of manipulation of the cells during the SVF isolation process we applied in a second approach ESWT directly on the freshly obtained human adipose tissue and compared it with ESWT on isolated SVF cells.

Based on this, we studied cellular adenosine triphosphate (ATP) content, immunophenotype, cell yield, viability, colony-forming unit fibroblast (CFU-F) assay and protein secretome of the SVF. Furthermore, we cultured ASC from these SVF and investigated proliferation and differentiation potential toward the adipo-, osteo- and chondrogenic lineage.

## Methods

### SVF/ASC isolation

The use of human adipose tissue was approved by the local ethical board with patient's consent. Subcutaneous adipose tissue was obtained during routine outpatient liposuction procedures under local tumescence anesthesia. SVF isolation was performed as modified from Wolbank *et al.* [47] as follows. Briefly, 100 mL liposuction material was transferred to a blood bag (400 mL Macopharma) and washed with an equal volume of phosphate-buffered saline (PBS) to remove blood and tumescence solution. Afterward, for tissue digestion PBS was replaced with 0.2 U/mL collagenase NB4 (Serva) dissolved in 100 mL PBS containing  $\text{Ca}^{2+}/\text{Mg}^{2+}$  and 25 mmol/L N-2-hydroxyethylpiperazine-N0-2-ethanesulfonic acid (HEPES; Sigma) and the blood bag was incubated at 37°C under moderate shaking (180 rpm) for 1 h. The digested tissue was transferred into four 50-mL tubes (Greiner). After centrifugation at 1200g for 7 min, the cell pellets were incubated with 100 mL erythrocyte lysis buffer (154 mmol/L ammonium chloride [Sigma], 10 mmol/L potassium bicarbonate [Sigma], 0.1 mmol/L ethylenediamine-tetraacetic acid [EDTA; Biochrom] in aqua dest) for 3 min at 37°C to eliminate red blood cells. The supernatant was aspirated after centrifugation for 5 min at 500g. The pellets were pooled, washed with PBS and filtered through a 100- $\mu$ m cell strainer (Greiner). After another centrifugation step at 500g for 5 min, the supernatant was removed and the isolated SVF cells were cultured in endothelial growth medium (EGM-2; Lonza) at 37°C, 5% CO<sub>2</sub> and 95% air humidity or resuspended in EGM-2 for further analyses. To obtain the adherent cell fraction including ASC, SVF were seeded on a plastic surface in expansion media (EGM-2), and cultured to a subconfluent state. Media was changed every 3 to 4 days. Cells were detached with Accutase (PAA) for 5 min at 37°C and collected in a tube. After centrifugation the pellet was resuspended in EGM-2 and cells were quantified with trypan blue exclusion in a cell counter (TC-20; Biorad).

### In vitro ESWT

For *in vitro* shock wave treatment, an unfocused electrohydraulic device was used (DermaGold 100; MTS

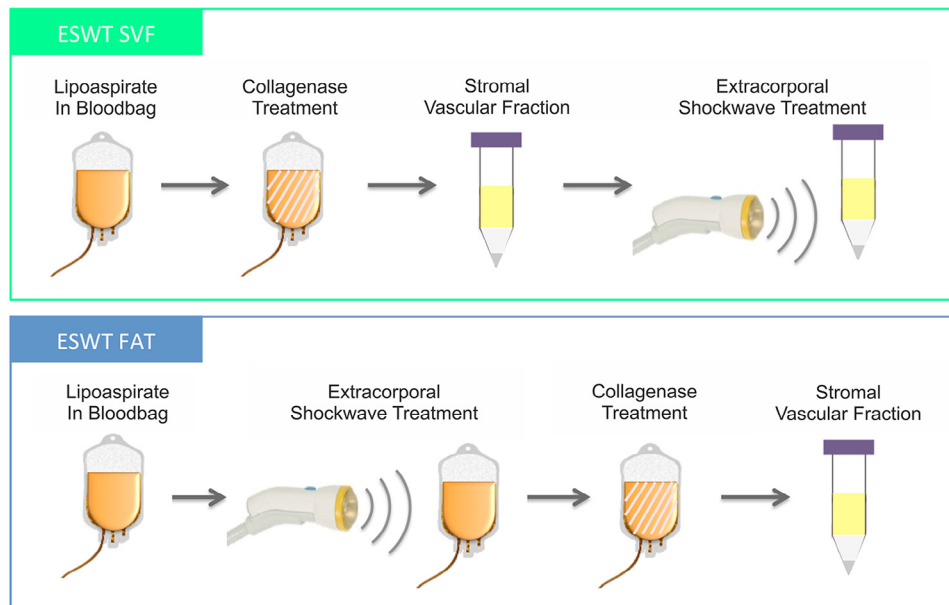


Figure 1. Set-up of ESWT. For shock wave treatment of freshly isolated SVF cells, cells were transferred into conical 15-mL polypropylene centrifuge tubes and placed in front of the applicator inside a water bath (referred to as “ESWT SVF”). For shock wave treatment of adipose tissue, unfocused shock waves were applied after the first washing step of the lipoaspirate on both sides of the blood bag (referred to as “ESWT FAT”). Afterward, isolation of SVF was continued with the enzymatic digestion.

Medical) alone or in combination with a water bath to allow reproducible physical propagation and application of shock waves, as described by Holfeld *et al.* [48]. For shock wave treatment of adipose tissue, unfocused shock waves were applied after the first washing step of the lipoaspirate with the following parameters: 200 pulses at an energy level of  $0.09 \text{ mJ/mm}^2$  with a frequency of 3 Hz on both sides of the blood bag (further referred to as “ESWT FAT”). Afterward, isolation of SVF was continued using enzymatic digestion as described above. For shock wave treatment of freshly isolated SVF cells,  $1\text{--}3 \times 10^7$  cells/mL suspended in a total volume of 1 mL were transferred into conical 15-mL polypropylene centrifuge tubes (PAA) and placed in front of the applicator inside the water bath. Unfocused shock waves were applied to SVF cells with the same parameters like for shock wave treatment of adipose tissue (further referred to as “ESWT SVF”). The principle of the experimental set-up is shown in Figure 1. Shock wave parameters were chosen according to previous studies [43] and preliminary experiments to maximize the effect of the ESWT while concurrently minimizing possible negative effects.

#### Cell yield and viability

Cell number and viability were determined using trypan blue exclusion and quantification in a cell counter (TC-20; Bio-Rad). For quantification of cell viability, the

percentage of living cells compared with total cell count was analyzed with the cell counter.

#### Intra/extracellular ATP

The amount of intra/extracellular ATP is an indicator for the viability of the cells. To determine the intra/extracellular ATP concentration CellTiter-Glo Luminescent Cell Viability Assay (Promega) was used and performed according to the manufacturer’s instructions. Freshly isolated SVF cells were seeded at a density of  $1 \times 10^4$  cells per well in a black 96-well plate (Greiner) in  $100 \mu\text{L}$  EGM-2. After 2 h,  $100 \mu\text{L}$  CellTiter-Glo Reagent were added to each well and the plate was gently agitated on a shaker for 2 min. Afterward the plate was incubated for 10 min in the dark. The combination of intracellular and extracellular ATP can be measured as CellTiter-Glo Reagent includes a cell lysis buffer. The luminescent signal was detected with a luminometer (GloMax; Promega) at an exposure time of 2000 ms and correlated to an ATP standard curve.

#### Proliferation

Proliferation potential was analyzed by determining the population doubling level (PDL). Freshly isolated SVF cells were seeded at a density of  $5 \times 10^5$  cells per T-25 culture flask and cultured in EGM-2. Media was changed every 3 to 4 days. When cells had reached a subconfluent state they were passaged and cell

number was determined as described above. For further analysis of PDL, ASC were seeded at a density of  $5 \times 10^4$  in T-25 culture flasks and cultured until passage 3. Cell number was determined after each passage.

#### CFU-F assay

A defined number of SVF cells (4, 20, 100, 500, 2500 and 12500) was seeded in each well of a 6-well plate (Sarstedt) and cells were cultured in EGM-2 for 14 days. Medium was changed on day 7 after cell seeding. After 14 days of culture, cells were fixed with 4% formaldehyde and stained with hematoxylin. Afterward, the cells were washed with tap water and stained with eosin solution (Roth/Lactan). The percentage of cells that formed visible colonies was calculated and compared with the total number of seeded cells.

#### Flow cytometry analysis of cell surface marker

Freshly isolated SVF cells were characterized using flow cytometry for cell surface marker characteristic for SVF. Cells were incubated with the following antibodies on ice and in the dark for 25 min: 2  $\mu$ L anti-CD14 fluorescein isothiocyanate (FITC), 1.5  $\mu$ L anti-CD34 FITC, 1.5  $\mu$ L anti-CD45 phycoerythrin (PE), 1  $\mu$ L anti-CD73 PE, 1  $\mu$ L anti-CD90 PE (all mouse monoclonal; BD Bioscience), 1.2  $\mu$ L anti-CD105 FITC (mouse monoclonal; Abcam), 2  $\mu$ L anti-CD31 FITC (eBiosciences) and 2  $\mu$ L CD146-PerCP (R&D). Cells were washed twice with 1.5 mL Cell Wash (BD) and centrifuged for 5 min at 250g. The supernatant was discarded and the cell pellet resuspended in 200  $\mu$ L Cell Wash. Samples were analyzed on a BD FACS Canto II (BD Bioscience): 10,000 events were detected and flow cytometry data were evaluated with the use of FlowJo Version 8.8 (Tree Star Inc.). Specific subpopulations were analyzed from thawed SVF cells through the combination of antibodies against CD45, CD31, CD34 and CD146 as well as CD90 and CD146: endothelial progenitor cells (EPC; CD45-/CD31+/CD34+), pericyte-like cells (CD45-/CD31-/CD146+), supra-adventitial ASC (SA-ASC; CD45-/CD31-/CD146-/CD34+) and mesenchymal/pericytic subset (CD90+/CD146+). For staining,  $5 \times 10^5$  cells in 50  $\mu$ L PBS with 1% fetal calf serum (FCS) were incubated with 5  $\mu$ L primary labeled antibodies at room temperature for 15 min in the dark. Cells were washed with 1.5 mL Cell Wash and centrifuged for 5 min at 400g. The supernatant was discarded and the cell pellet resuspended in 300  $\mu$ L  $1 \times$  Cell Fix (BD; diluted 1:10 with aqua dest). Samples were stored at 4°C in the dark until analysis on a FACSaria II (BD).

#### Osteogenic differentiation and detection

For osteogenic differentiation, cells were seeded at a density of  $2 \times 10^3$  cells per well in a 24-well plate in EGM-2 and incubated overnight. On the next day, media was changed to osteogenic differentiation media Dulbecco's Modified Eagle's Medium (DMEM)-low glucose (Lonza) containing 10% FCS, 2 mmol/L L-glutamine (PAA), 100 U/mL penicillin/streptomycin (Pen/Strep) (Lonza), 10 nmol/L dexamethasone (Sigma), 150  $\mu$ mol/L ascorbat-2-phosphate (Sigma), 10 mmol/L  $\beta$ -glycerophosphate (StemCell Technologies) and 10 nmol/L dihydroxy-vitamin D3 (Sigma) or control media consisting of DMEM:F12/L-glutamine (Lonza) with 10% FCS and 100 U/mL Pen/Strep. Media was changed every 3 to 4 days. After 21 days, osteogenic differentiation was analyzed with alizarin red staining and quantification, as well as determination of intracellular alkaline phosphatase (ALP) activity. For alizarin red staining of calcified structures, cells were fixed for 1 h with 70% ethanol at  $-20^\circ\text{C}$  and stained with alizarin red solution (Merck) for 15 min. For quantitative analysis of alizarin red staining, the supernatant was discarded and the cells were incubated with 500  $\mu$ L 20% methanol and 10% acidic acid (diluted in aqua dest) for 15 min. After resuspension, the mixture of cells and methanol/acidic acid was transferred to a transparent 96-well plate (100  $\mu$ L per well). The absorbance was measured at 450 nm with an Infinite M200 Multimode Microplate Reader (Tecan). The second method to analyze osteogenic differentiation is the detection of the activity of intracellular ALP, which is located on the surface of osteoblast cells and has been shown to be a biochemical indicator of bone maturation, mineralization and bone turnover. Cells were incubated with 100  $\mu$ L PBS for 1 h at  $-20^\circ\text{C}$ . Afterward, the cells were lysed for 1 h by addition of 100  $\mu$ L PBS containing 0.5% TritonX-100 (Sigma). For quantitative detection of ALP activity, 100  $\mu$ L substrate solution (4-nitrophenylphosphate; Sigma) were added in each well and incubated for 1 h in the dark. Finally, the solution was transferred to a transparent 96-well plate (100  $\mu$ L per well) and absorbance was measured at 405 nm together with a reference wavelength of 620 nm in an Infinite M200 Multimode Microplate Reader (Tecan). By creating a standard curve with known p-nitrophenol concentrations diluted in stop solution (0.5% TritonX-100 diluted in PBS 1:2) and measuring the corresponding absorption, the ALP activity of the samples was calculated.

#### Adipogenic differentiation and detection

For adipogenic differentiation, cells were seeded at a density of  $1.4 \times 10^4$  cells per well in a 24-well plate in EGM-2 and incubated overnight. On the next day,

media was changed to adipogenic differentiation media DMEM-high glucose (Lonza) containing 10% FCS, 2 mmol/L L-glutamine, 100 U/mL Pen/Strep, 1  $\mu$ mol/L dexamethasone, 0.5 mmol/L 3-isobutyl-1-methylxanthine (IBMX; Sigma), 10  $\mu$ g/mL insulin (Sigma) and 100  $\mu$ mol/L indomethacin (Sigma) or control media consisting of DMEM:F12/L-glutamine with 10% FCS and 100 U/mL Pen/Strep. Media was changed every 3 to 4 days. After 21 days, adipogenic differentiation was analyzed with oil red O staining and quantification. Cells were fixed with 4% formaldehyde for 1 h. After washing with aqua dest, the cells were rinsed with 70% ethanol for 2 min and stained for 5–15 min with oil red O solution (Sigma). Then the cells were washed with aqua dest, counterstained for 1–3 min with Mayer's hematoxylin solution and blued with tap water. For quantitative detection of oil red O staining, the supernatant was discarded and 500  $\mu$ L isopropanol were added in each well. After resuspension, the mixture of cells and isopropanol was transferred to a transparent 96-well plate (100  $\mu$ L per well). The absorbance was measured at 510 nm with an Infinite M200 Multimode Microplate Reader (Tecan).

#### *Chondrogenic differentiation and detection*

For chondrogenic differentiation in 3-D micromass pellet cultures,  $3 \times 10^5$  cells were centrifuged in chondrogenic differentiation media (hMSC Chondro BulletKit; Lonza) containing 10 ng/mL bone morphogenetic protein (BMP)-6 (R&D) and 10 ng/mL transforming growth factor (TGF)- $\beta$ 3 (Lonza) in screw cap microtubes. The tubes were placed in an incubator at 37°C, 5% CO<sub>2</sub> and 95% humidity with slightly open cap for gas exchange. After 2 days the pellets were transferred to 96-well U-bottom plates (Greiner) with fresh media. Media was changed every 2 to 3 days. After 35 days of differentiation, micromass pellets were fixed in 4% phosphate-buffered formalin overnight for histological analysis. The next day the pellets were washed in 1x PBS and dehydrated in increasing concentrations of ethanol. After rinsing the pellets in xylol and infiltration with paraffin, deparaffinized sections were stained with alcian blue for 30 min and counterstained for 2 min with Mayer's hematoxylin. For collagen type II staining, sections were treated with pepsin for 10 min at 37°C (AP-9007 RTU, Thermo Scientific). Endogenous peroxidase was quenched with freshly prepared 3% H<sub>2</sub>O<sub>2</sub> for 10 min at room temperature, followed by normal horse serum 2.5% (Vector RTU) to block unspecific binding. Sections were incubated 1 h with monoclonal anti-collagen type II (MS-306 P0; Thermo Scientific) at 1:100. After washing with Tris-buffered saline (TBS), sections were incubated with the secondary antibody (anti mouse DAKO

EnVision+ System HRP labelled Polymer; Dako) for 30 min and rinsed in TBS again. Bindings were visualized using Nova Red (SK4800 Vector Labs) for 6 min. Counterstaining was performed with Mayer's hematoxylin for 2 min.

#### *Secretory protein profile*

For protein secretome analysis of freshly isolated cells,  $5 \times 10^5$  cells were seeded in a T-25 flask in 2.5 mL EGM-2. Cells were allowed to adhere for 2 h and subsequently, EGM-2 was changed to serum-free media (DMEM-low glucose with 2 mmol/L L-glutamine). To include also non-adherent suspension cells, cells were collected, centrifuged and returned to the flask. Then, 24 h after seeding the supernatant was collected and stored at -80°C until analysis.

For the analysis of the secretory profile a Human Growth Factor Array (RayBio) was used according to the manufacturer's instructions. Briefly, the membrane was blocked with a blocking buffer for 30 min prior to sample incubation for 5 h at room temperature. Every incubation and washing step, excluding the incubation of detection buffer, was performed under gentle rotation (0.8 cycles/sec). Subsequently, the biotinylated antibody was incubated overnight at 4°C, followed by another washing step. The membrane was incubated with horseradish peroxidase (HRP)-conjugated streptavidin for 2 h. Prior to detection, the membrane was washed with washing buffer. Signals were detected using enhanced chemiluminescence and recorded on an X-ray film. Signals were densitometrically quantified using ImageJ (National Institutes of Health).

#### *Statistical analysis*

All data in this study represent single values for each donor or mean  $\pm$  standard deviation. Statistical analysis was performed using Prism6 (GraphPad Software, Inc.), paired *t* test (ATP analysis, flow cytometry of single marker), unpaired *t* test (cell yield, viability, CFU), two-way analysis of variance (ANOVA)-Tukey post hoc (flow cytometry of subpopulations, PDL, quantitative analyses of ALP, alizarin red, oil red O) or one-way ANOVA-Fisher's least significant difference (LSD) post hoc (secretory profile). Statistical significance was considered for  $P < 0.05$ .

## **Results**

### *Comparison of ESWT on human adipose tissue to ESWT on SVF cells*

To identify the most beneficial set-up, ESWT was applied either directly on adipose tissue isolated via liposuction from five different donors or on freshly processed SVF cells derived from the same donors.

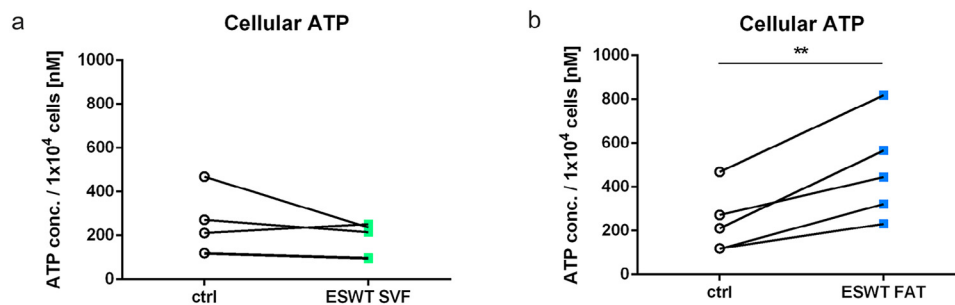


Figure 2. ESWT of adipose tissue leads to increased cellular ATP. Freshly isolated ESWT-treated SVF cells and SVF cells derived from ESWT-treated adipose tissue were examined for cellular ATP concentration and compared with untreated control. After ESWT on SVF cells, ATP concentration decreased apart from one donor (a), whereas cells from ESWT-treated adipose tissue showed significantly higher cellular ATP concentration for all donors (b) compared with control. Data are shown as single values for each donor  $\pm$  ESWT. Asterisks indicate significant difference between the groups of  $n = 5$ .  $**P < 0.01$ .

Figure 2 and Figures 3–5 show the data of each single donor before (control condition, identical for both groups) and after the respective ESWT.

#### ESWT on adipose tissue enhances cellular ATP

Cellular ATP levels were assessed 2 h after cell seeding, comparing the untreated control group with ESWT-treated SVF and ESWT-treated adipose tissue. Cellular ATP concentration tended to decrease after ESWT on SVF cells (Figure 2a) to a mean of  $181 \pm 91$  nmol/L compared with untreated cells ( $225 \pm 119$  nmol/L). Only one donor showed a slightly elevated ATP concentration after ESWT on SVF cells. In contrast, after ESWT on adipose tissue all donors showed a significantly ( $P = 0.0081$ ) increased ATP concentration (Figure 2b) with a mean of  $475 \pm 204$  nmol/L.

#### ESWT on SVF and adipose tissue positively affects cell surface marker expression

To determine the impact of ESWT on the cellular phenotype in the SVF, we investigated the surface marker expression of freshly isolated SVF cells. Treatment of ESWT on SVF cells led to an increased expression of mesenchymal stromal cell markers CD73, CD90 and CD105 in all donors compared with control (Figure 3; MSC marker) resulting in  $40.4 \pm 5.4\%$  CD73-positive cells (versus  $29.1 \pm 5.4\%$  for control),  $67.3 \pm 7.4\%$  CD90-positive cells (versus  $57.3 \pm 9.0\%$  for control) and  $22.3 \pm 3.8\%$  CD105-positive cells (versus  $12.2 \pm 3.3\%$  for control). Similarly, ESWT on adipose tissue also enhanced the percentage of MSC marker of all donors significantly (Figure 3; MSC marker). This increase was stronger compared with the effect of ESWT on SVF cells and resulted in  $49.5 \pm 4.7\%$  CD73-positive cells,  $76.0 \pm 3.2\%$  CD90-positive cells and  $27.8 \pm 6.9\%$  CD105-positive cells. Furthermore, other marker profiles within the SVF were enhanced after ESWT. All donors showed an increase of the endothelial/pericytic marker CD146 after

ESWT on SVF cells, which was significant after ESWT on adipose tissue (Figure 4; vascular marker). While in untreated SVF cells a mean of  $16.7 \pm 3.6\%$  were CD146-positive,  $21.4 \pm 5.7\%$  of ESWT-treated SVF and  $28.2 \pm 6.8\%$  of cells derived from ESWT-treated adipose tissue were CD146-positive. Both forms of ESWT application increased the proportion of CD31 (endothelial marker) positive cells in all donors, which was more pronounced in cells derived from ESWT-treated adipose tissue (Figure 4; vascular marker). The mean CD31 expression of untreated cells was  $25.8 \pm 5.0\%$ , whereas ESWT enhanced the expression to  $32.2 \pm 6.6\%$  and  $35.9 \pm 4.5\%$ . In contrast, expression of the hematopoietic progenitor/vascular endothelial marker CD34 was not enhanced in any donor after ESWT on SVF cells and in only 2 of 5 donors after ESWT on adipose tissue (Figure 4; vascular marker). Therefore, mean expression levels of CD34 were similar in all three conditions ( $45.5 \pm 2.4\%$  untreated,  $43.4 \pm 3.0\%$  ESWT-treated SVF and  $44.3 \pm 3.1\%$  ESWT-treated adipose tissue). There was a minimal percentage of the monocyte/macrophage marker CD14 present in all three conditions and no difference between the groups untreated, ESWT-treated SVF or ESWT-treated adipose tissue (Figure 5; hematopoietic marker; mean for control  $6.3 \pm 2.5\%$ , ESWT SVF  $6.4 \pm 2.2\%$  and ESWT FAT  $6.8 \pm 2.0\%$ ). Similarly, there was no difference in the expression of the hematopoietic marker CD45 after ESWT on SVF cells or ESWT on adipose tissue compared with control (Figure 5; hematopoietic marker) with mean values of  $13.6 \pm 2.6\%$  for untreated cells,  $12.9 \pm 2.7\%$  for ESWT-treated SVF cells and  $12.3 \pm 2.8\%$  for SVF cells derived from ESWT-treated adipose tissue.

Because ESWT applied on adipose tissue revealed higher beneficial effects regarding ATP release and expression of stem cell-/progenitor marker compared with ESWT applied on SVF, we decided to focus on this approach.

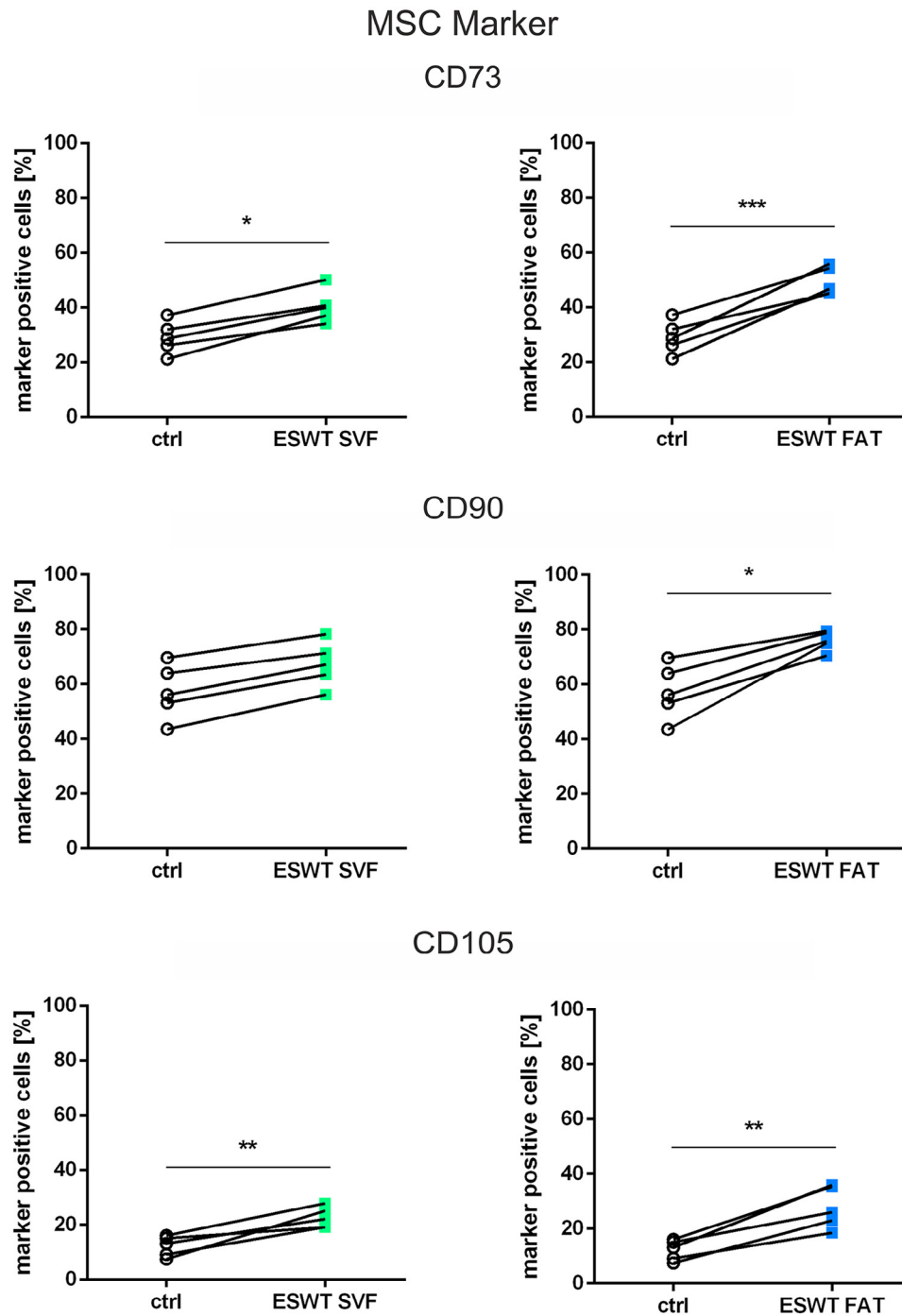


Figure 3. Immunophenotype of freshly isolated SVF: MSC marker. Freshly isolated ESWT-treated SVF cells and SVF cells derived from ESWT-treated adipose tissue were examined for cell surface marker expression and compared with untreated control. There was a significant increase in the mesenchymal stromal cell marker CD73 and CD105 after ESWT on SVF and a significant increase of CD73, CD90 and CD105 after ESWT on adipose tissue, with a higher percentage for cells derived from ESWT-treated adipose tissue. Data are shown as single values for each donor  $\pm$  ESWT. Asterisks indicate significant difference between the groups of  $n = 5$ . \* $P < 0.05$ ; \*\* $P < 0.01$ ; \*\*\* $P < 0.001$ .

#### Specific subpopulations present after ESWT on adipose tissue

Freshly isolated SVF cells from untreated and ESWT-treated adipose tissue were examined for the presence

of specific subpopulations. The percentage of EPC (CD45<sup>-</sup>/CD31<sup>+</sup>/CD34<sup>+</sup>) was similar with  $8.1 \pm 0.9\%$  for cells from untreated and  $10.1 \pm 2.9\%$  for cells from ESWT-treated adipose tissue (Figure 6a). There was a minor percentage of pericyte-like cells (CD45<sup>-</sup>/



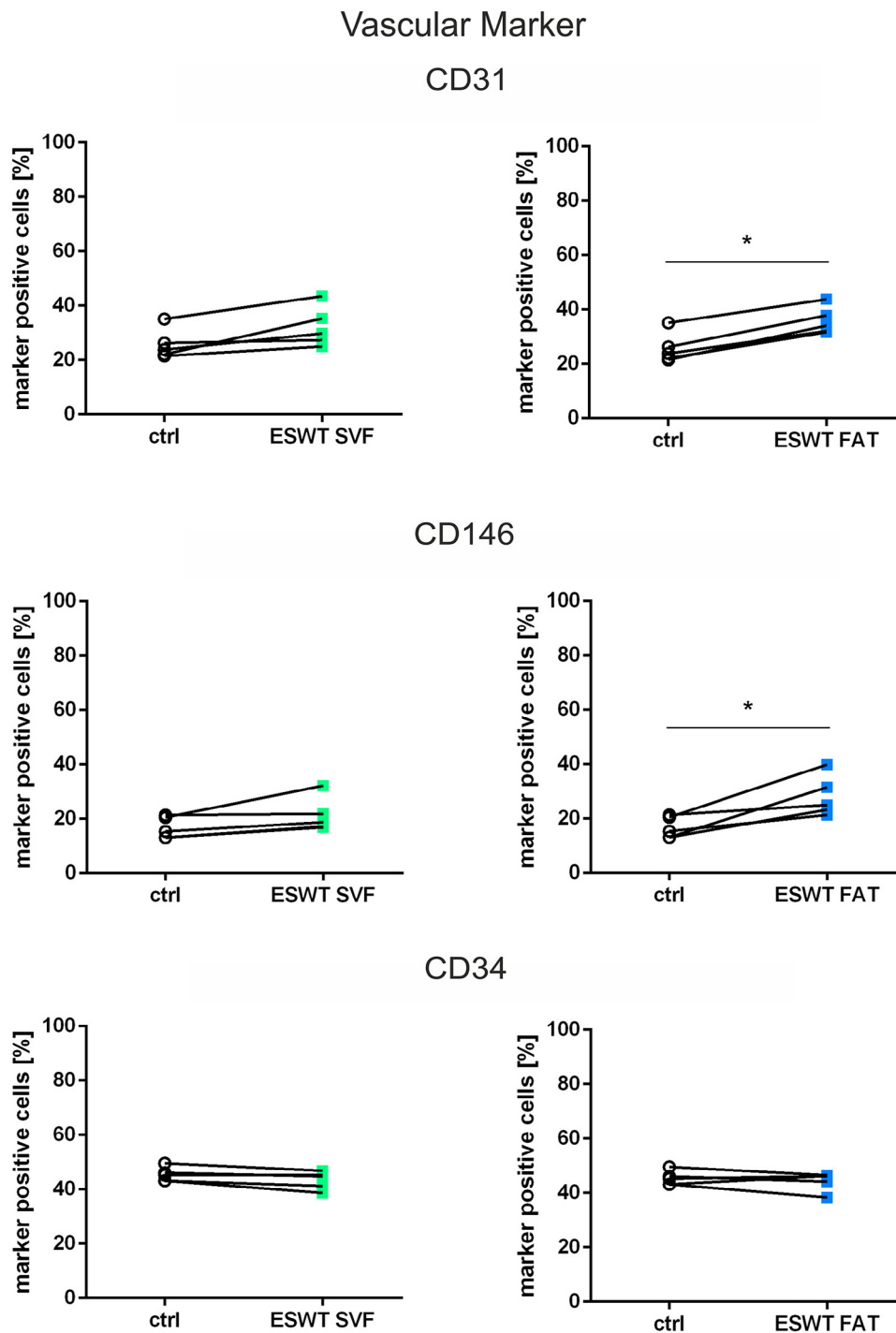


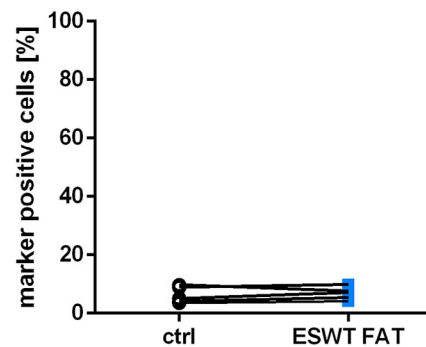
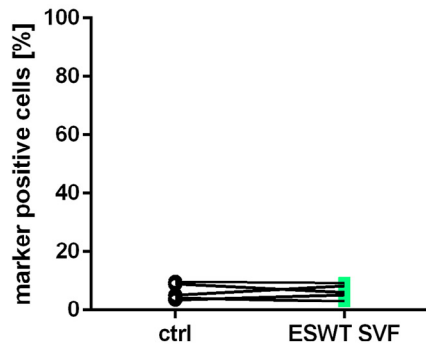
Figure 4. Immunophenotype of freshly isolated SVF: vascular marker. Freshly isolated ESWT-treated SVF cells and SVF cells derived from ESWT-treated adipose tissue were examined for cell surface marker expression and compared with untreated control. The hematopoietic progenitor/vascular endothelial marker CD34 was not affected after both ESWT treatments. The endothelial/pericytic marker CD146 and the endothelial marker CD31 were not affected after ESWT on SVF, but there was a significant increase after ESWT on adipose tissue. Data are shown as single values for each donor  $\pm$  ESWT. Asterisks indicate significant difference between the groups of  $n = 5$ .  $*P < 0.05$ .

CD31 $-$ /CD146 $+$ ) for both conditions ( $1.7 \pm 0.4\%$  versus  $1.5 \pm 0.6\%$ ). The number of SA-ASC (CD45 $-$ /CD31 $-$ /CD146 $-$ /CD34 $+$ ;  $13.5 \pm 4.2\%$  versus  $11.6 \pm 3.4\%$ ) and of the CD90 $+$ /CD146 $+$  mesenchymal/pericytic subset ( $48.0 \pm 5.5\%$  versus

$50.0 \pm 8.5\%$ ) was also not affected by ESWT treatment (Figure 6a). The total cell number of the EPC subpopulation ( $3.0 \pm 0.9 \times 10^6$  versus  $6.4 \pm 2.6 \times 10^6$ ), the SA-ASC ( $5.0 \pm 2.5 \times 10^6$  versus  $7.9 \pm 4.5 \times 10^6$ ) and the CD90 $+$ /CD146 $+$  mesenchymal/pericytic subset

## Hematopoietic Marker

## CD14



## CD45

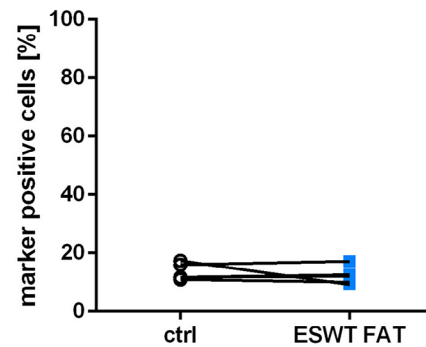
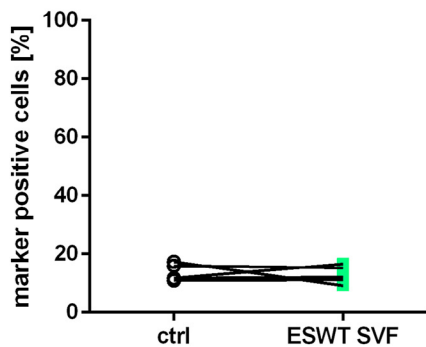


Figure 5. Immunophenotype of freshly isolated SVF: hematopoietic marker. Freshly isolated ESWT-treated SVF cells and SVF cells derived from ESWT-treated adipose tissue were examined for cell surface marker expression and compared with untreated control. There was a minimal percentage of cells positive for the monocyte/macrophage marker CD14 and the hematopoietic marker CD45 and no difference between the groups. Data are shown as single values for each donor  $\pm$  ESWT.  $n = 5$ .

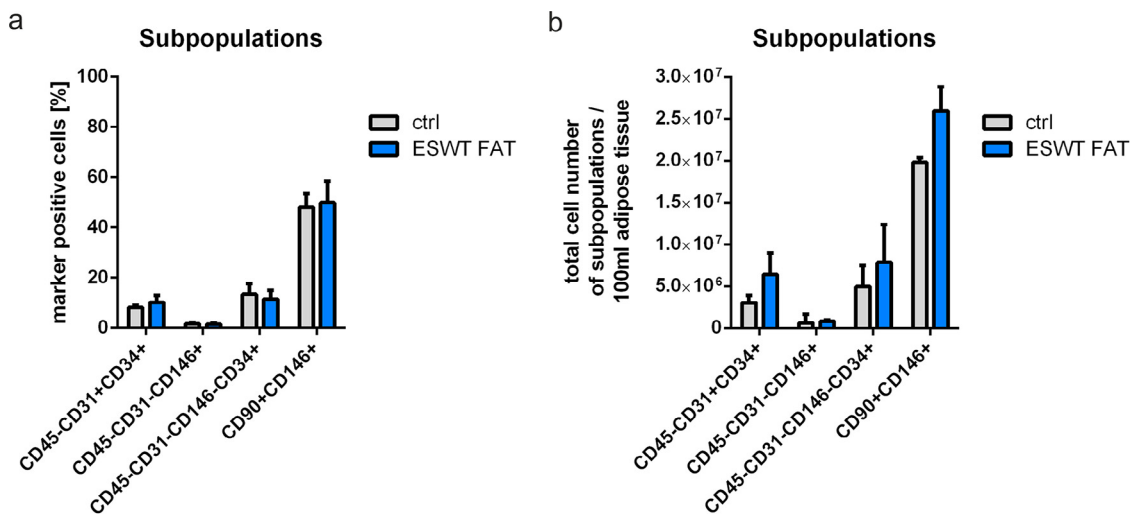


Figure 6. Subpopulations of freshly isolated SVF after ESWT on adipose tissue. SVF cell composition after ESWT on adipose tissue was analyzed for specific subpopulations. The percentage of EPC (CD45-/CD31+/CD34+), pericyte-like cells (CD45-/CD31-/CD146+), SA-ASC (CD45-/CD31-/CD146-/CD34+) and a mesenchymal/pericytic subset (CD90+/CD146+) was not affected after ESWT on adipose tissue (a). When analyzing the total cell number of subpopulations there was a minor but not significant increase of EPC, SA-ASC and the CD90+/CD146+ mesenchymal/pericytic subset. The number of pericyte-like cells was not changed (b). Data are shown as mean  $\pm$  SD.  $n = 3$ .

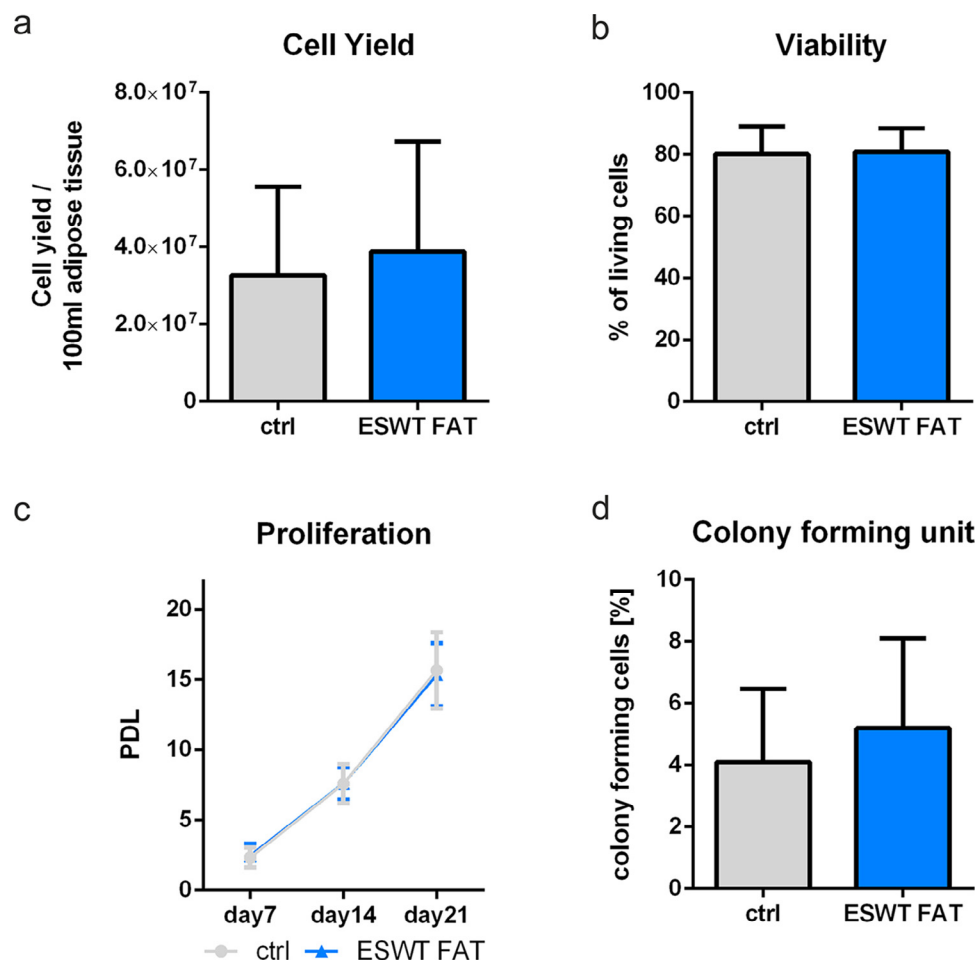


Figure 7. Cell yield, viability, proliferation and colony-forming potential of freshly isolated SVF cells after ESWT on adipose tissue. SVF obtained from ESWT-treated adipose tissue showed a slightly but not significantly increased cell yield compared with control  $n = 14$  (a). Cell viability  $n = 13$  (b) and PDL  $n = 8$  (c) were not affected after ESWT. The colony-forming potential was slightly but not significantly enhanced after ESWT on adipose tissue  $n = 4$  (d). Data are shown as mean  $\pm$  SD.  $n = 4$ –14.

( $2.0 \pm 0.1 \times 10^7$  versus  $2.6 \pm 0.3 \times 10^7$ ) was increased, however, not significantly, after ESWT. The number of pericyte-like cells (CD45 $^-$ /CD31 $^-$ /CD146 $^+$ ) was not changed after ESWT treatment ( $6.4 \pm 10.1 \times 10^3$  versus  $8.3 \pm 1.7 \times 10^3$ ; Figure 6b).

#### Cell yield, viability and proliferation after ESWT on adipose tissue

After application of ESWT on adipose tissue, the isolated cell yield was slightly but not significantly increased from  $3.3 \pm 2.3 \times 10^7$  to  $3.9 \pm 2.9 \times 10^7$  cells (Figure 7a). Viability of the freshly isolated SVF cells was similar for untreated cells and cells derived from ESWT-treated adipose tissue with  $80.1 \pm 9.0\%$  and  $80.9 \pm 7.6\%$  living cells compared with total cell number (Figure 7b). Similarly, there was no effect of ESWT on the proliferation potential of cultured ASC derived from the SVF. Cells isolated from ESWT-treated adipose tissue showed similar PDL compared with untreated cells after 7 days

( $2.3 \pm 0.7$  versus  $2.5 \pm 0.8$ ), 14 days ( $7.6 \pm 1.4$  versus  $7.6 \pm 1.2$ ) and 21 days ( $15.7 \pm 2.7$  versus  $15.4 \pm 2.3$ ; Figure 7c). Analysis of the colony-forming capacity of the cells revealed a slightly but not significantly enhanced frequency after ESWT treatment on adipose tissue from  $4.1 \pm 2.4\%$  for control to  $5.2 \pm 2.9\%$  for ESWT (Figure 7d). The effect of ESWT on SVF regarding cell yield, viability and proliferation is provided as a supplemental figure (Supplemental Figure S1).

#### Multilineage differentiation potential after ESWT on adipose tissue

ASC cultures derived from untreated and ESWT-treated adipose tissue and SVF were analyzed for their *in vitro* osteogenic, adipogenic and chondrogenic differentiation potential. Upon osteogenic induction, increase in ALP activity showed similar values for cells from untreated adipose tissue and cells derived from ESWT-treated adipose tissue ( $485 \pm 201 \mu\text{mol/L}$  versus

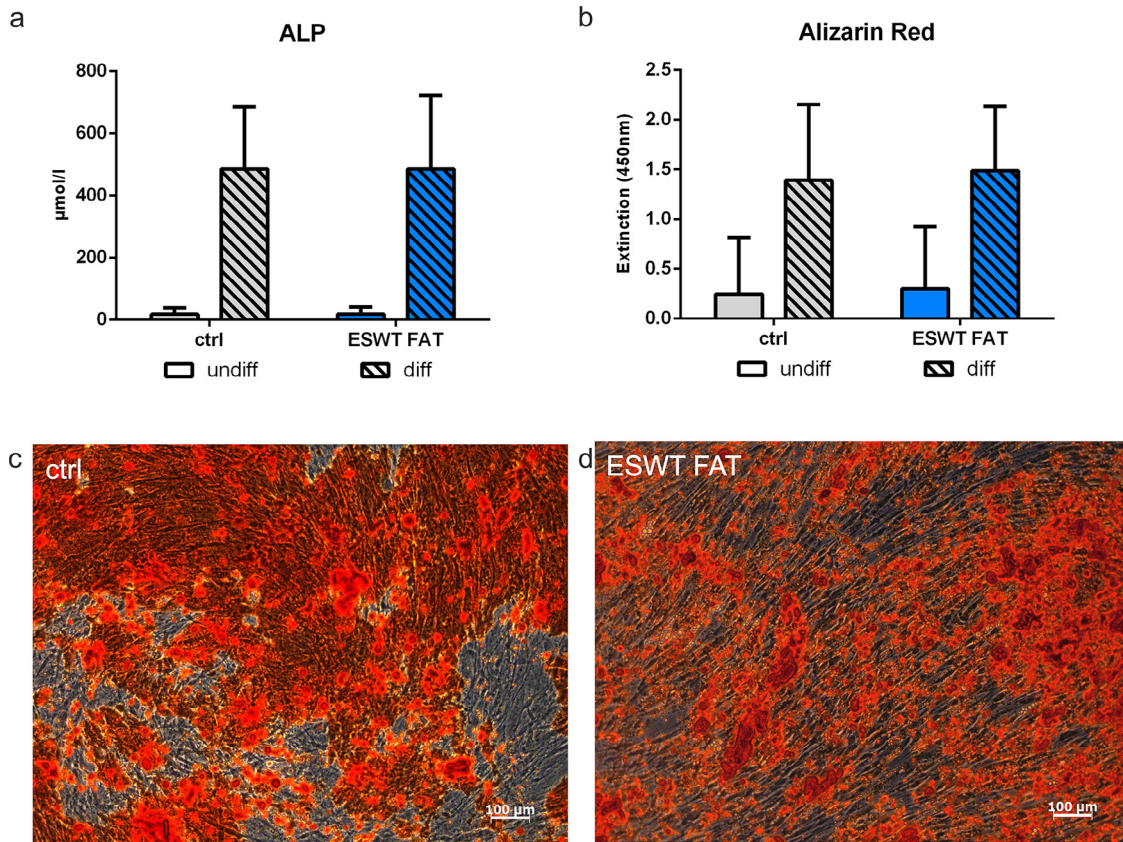


Figure 8. Osteogenic differentiation potential after ESWT on adipose tissue. Cells derived from ESWT-treated adipose tissue were analyzed for their osteogenic differentiation potential with ALP (a) and alizarin red staining (b–d) and compared with untreated control. The increase in ALP activity was similar for control and ESWT on adipose tissue  $n = 10$  (a). Alizarin red staining demonstrated similar mineralization for control (c) and cells derived from ESWT-treated adipose tissue (d), which was confirmed by quantitative analysis  $n = 9$  (b). Regarding quantitative analyses of differentiation, all conditions showed a significant enhancement of differentiated cells compared with undifferentiated cells (a, b). undiff, cells in control media without growth factors and stimuli; diff, cells in osteogenic differentiation media. Data are shown as mean  $\pm$  SD.  $n = 9$ –10. Size bar = 100  $\mu\text{m}$ .

$485 \pm 238 \mu\text{mol/L}$ ; Figure 8a). Qualitative analysis of osteogenic differentiation with alizarin red staining showed similar mineralization and calcification for both conditions (Figure 8c and 8d). This observation was confirmed by quantification of alizarin red staining by showing an extinction of  $1.4 \pm 0.8$  for untreated cells and  $1.5 \pm 0.7$  after ESWT on adipose tissue (Figure 8b). Adipogenic differentiation analyzed by oil red O staining also showed a similarly high intensity after ESWT on adipose tissue (Figure 9b and 9c), which was verified by quantitative analysis ( $0.58 \pm 0.15$  versus  $0.63 \pm 0.14$ ; Figure 9a). Figure 10 shows 3-D micromass pellets from three representative donors with high chondrogenic differentiation potential, demonstrated by strong alcian blue and collagen type II staining, but no difference was visible between control and ESWT treatment (Figure 10). The effects on the three lineage differentiation potentials after ESWT on SVF are provided as supplemental figures (Supplemental Figures S2–S4).

#### Secretory protein profile after ESWT on adipose tissue

To explore which molecular mechanisms are involved in the ESWT-induced changes supernatants of SVF cells were collected 24 h after isolation and protein expression was analyzed. All analyzed proteins (Figure 11 and Supplemental Figure S5) from the following families were expressed in the supernatant of SVF cells after ESWT treatment and without treatment (Figure 11a–11i): nerve growth factor (NGF), TGF $\beta$ , epidermal growth factor (EGF), colony-stimulating factor (CSF), platelet-derived growth factor (PDGF), fibroblast growth factor (FGF), vascular endothelial growth factor (VEGF) and insulin-like growth factor (IGF) family. There were only two of the 41 analyzed proteins significantly enhanced after ESWT treatment, otherwise only minimal changes in the protein expression between untreated and ESWT-treated supernatants were determined. Namely, the expression of placental growth factor (PLGF) was

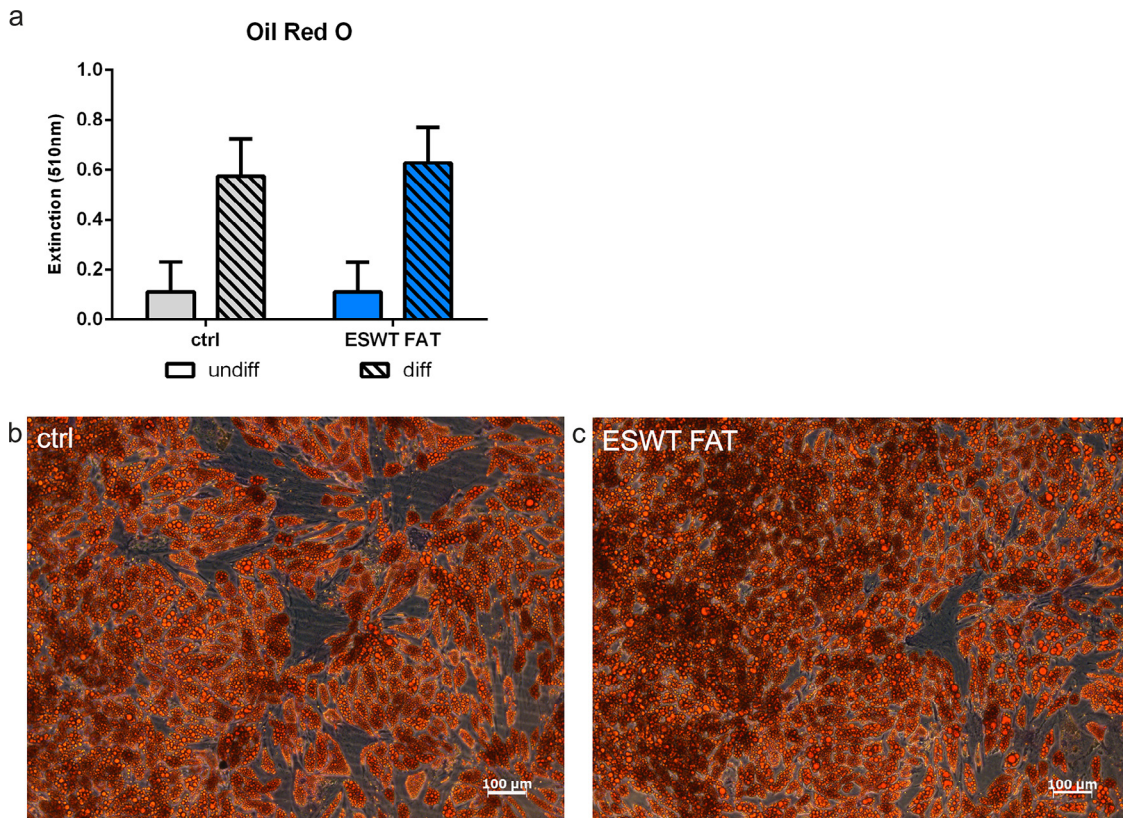


Figure 9. Adipogenic differentiation potential after ESWT on adipose tissue. Cells derived from ESWT-treated adipose tissue were analyzed for their adipogenic differentiation potential with oil red O staining and compared with untreated control. Oil red O staining demonstrated similar lipid droplet formation for cells derived from untreated (b) and ESWT-treated adipose tissue (c), which was confirmed using quantitative analysis (a). Regarding quantitative analysis of differentiation, all conditions showed a significant enhancement of differentiated cells compared with undifferentiated cells (a). undiff, cells in control media without growth factors and stimuli; diff, cells in adipogenic differentiation media. Data are shown as mean  $\pm$  SD.  $n = 10$ . Size bar = 100  $\mu\text{m}$ .

enhanced from  $0.20 \pm 0.08$  to  $0.34 \pm 0.16$ -fold after ESWT treatment (Figure 11g). The expression of IGF-1 was increased from  $0.14 \pm 0.08$  to  $0.32 \pm 0.11$ -fold after ESWT treatment (Figure 11i).

## Discussion

Based on our previous studies, application of low-energy ESWT is promising for promoting the regenerative quality of stem cells. Recently we have shown that shock wave treatment at an energy level of  $0.09 \text{ mJ}/\text{mm}^2$  enhanced adipogenic, osteogenic and Schwann-like cell differentiation of human ASC [43]. We have shown that shock waves at  $0.1 \text{ mJ}/\text{mm}^2$  and 300 impulses improve skin flap survival through neovascularization and early upregulation of angiogenesis-related growth factors in a rodent ischemic epigastric flap model [40]. In previous studies, we and others could observe enhanced VEGF expression after ESWT *in vitro* and *in vivo* (Holfeld *et al.* [49]; Peng *et al.* [50]; Mittermayr *et al.* [51]). Shock wave treatment further demonstrated enhanced proliferation by release of cellular ATP in the C3H10T1/2

mouse MSC line and human ASC in an energy-dependent manner. ATP release subsequently activates purinergic receptors and finally enhances proliferation via downstream Erk1/2 signaling [44]. This is supported by our current findings that ESWT increases cellular ATP concentration in the isolated SVF, which remained at higher levels throughout culture (of ASC) compared with untreated cells (data not shown). Viability of SVF cells was not negatively influenced by ESWT treatment. This is consistent with studies from Sun *et al.* [52] and Yu *et al.* [53] that describe that at our chosen shock wave settings (low energy, low pulses) the effect of ESWT on ATP concentration did not impact viability of the cells.

The efficacy of shock wave treatment depends on various parameters including shock wave settings, number and time points of treatment and used cell type or material. To meet the requirements of the regulatory agencies and to receive the classification “minimally manipulated” medicinal product, to be run under the legislation of tissue banks (e.g., in Europe) for the translation of cells and tissues into clinics, adipose tissue should not be further processed

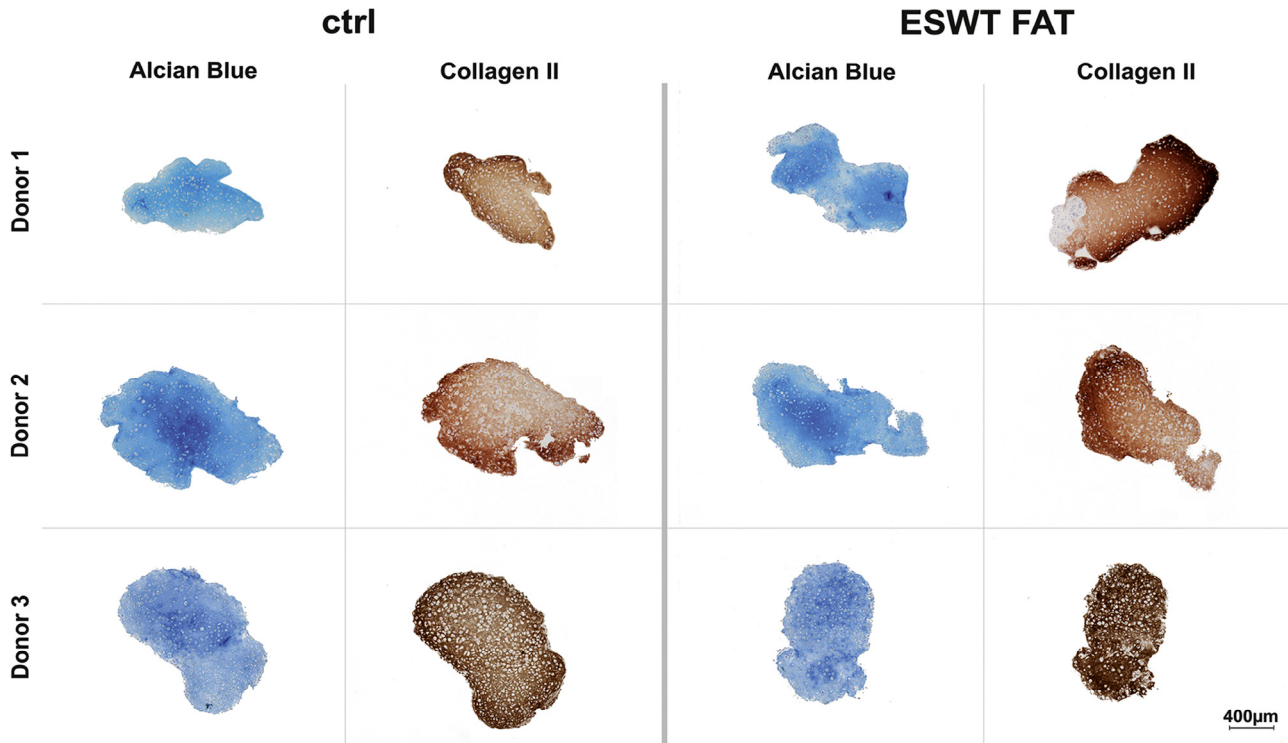


Figure 10. Chondrogenic differentiation potential after ESWT on adipose tissue. Cells derived from ESWT-treated adipose tissue were analyzed for their chondrogenic differentiation potential with alcian blue and collagen type II staining and compared with untreated control. Alcian blue and collagen type II staining demonstrated similar intensity for control and cells derived from ESWT-treated adipose tissue. Images show three representative donors.  $n = 10$ . Size bar = 200  $\mu\text{m}$ .

[51,54-57]. Therefore, we analyzed the effect of ESWT directly on adipose tissue for improvement of the cells within the graft. Furthermore, the treatment was performed in a blood bag, which is also compatible with a closed sterile isolation process and allows direct application of ESWT. The set-up described here avoids open processes and substantial manipulation and should hence be in accordance with GMP setting and potentially a one-step procedure within the operation theater.

To ensure highest possible cell quality for a successful transplantation we analyzed the isolated SVF cells immediately after isolation. We could demonstrate that ESWT applied on adipose tissue resulted in an activated cell population with higher cellular ATP content and higher percentage of a mesenchymal stem/stromal, endothelial and pericyte-like immunophenotype. Taking these cells into culture (as such defined as ASC) we could corroborate the MSC character that is defined by IFATS and ISCT [26] in assessment of the trilineage differentiation potential toward the adipo-, osteo- and chondrogenic lineage. Our improved isolation protocol generates cells with a high *in vitro* differentiation potential with and without ESWT.

Additionally, isolated SVF cells in suspension were treated with ESWT (previously described by Schuh

*et al.* [43] for adherence selected propagated ASC). ESWT-treated cells showed enhanced stem cell marker profile, which is consistent with the findings of Schuh *et al.* However, ESWT applied on adipose tissue provides cells with higher ATP content compared with ESWT applied on the isolated SVF thereof. This may be explained by the presence of surrounding tissue during treatment, which may protect the cells from the reflected waves. Furthermore, the tissue microenvironment including ECM and cellular context might contribute to the beneficial effect of ESWT within a native tissue. Immunophenotype analysis revealed cell populations with an enhanced percentage of single mesenchymal and vascular marker, suggesting more therapeutically relevant cells after ESWT. Analysis of percentages of specific subpopulations in SVF showed no effect of ESWT on adipose tissue. The total cell number of EPC, SA-ASC and mesenchymal/pericytic subset was elevated, although not significantly. Differentiation potential toward the osteo-, adipo- and chondrogenic lineage of cells derived from shock wave-treated adipose tissue was as high as for untreated cells. In the present study we could not detect a substantial influence of ESWT treatment on the secretion of human growth factors from freshly isolated SVF. Only two of the analyzed proteins showed a significantly

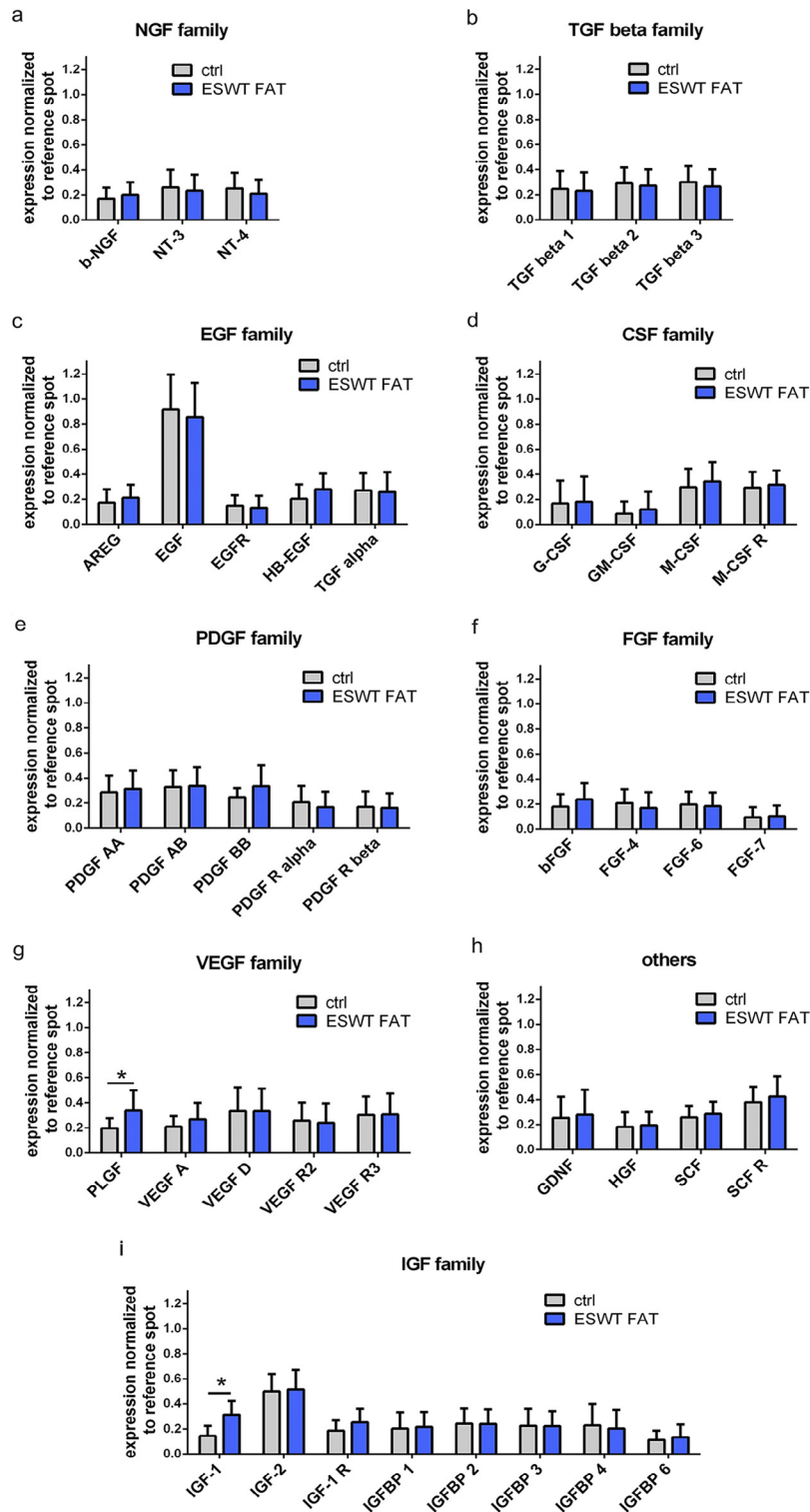


Figure 11. Secretory profile of freshly isolated SVF cells after ESWT on adipose tissue. ESWT treatment showed no substantial changes in the expression of all analyzed protein families (a-i). Only two of 41 analyzed proteins demonstrated a significantly enhanced expression after ESWT treatment: placental growth factor (PLGF) (g) and insulin-like growth factor-1 (IGF-1) (i). Data are shown as mean  $\pm$  SD.  $n = 6$ . \* $P < 0.05$ .

enhanced expression after ESWT treatment: PLGF, belonging to the VEGF family, and IGF-1. This suggests that the positive effect of ESWT on adipose tissue might probably not be due to a substantial change in trophic factor secretion. Cells isolated from shock wave-treated adipose tissue exhibit a higher cellular ATP turnover compared with shock wave-treated SVF cells or untreated cells. Although shock wave treatment on cells in culture triggers an immediate ATP release and a subsequent proliferation as demonstrated by Weihs *et al.* [44], we did not observe increased proliferation of cell cultures derived from shock wave-treated tissue, which, however, represents a different experimental set-up. The clinical success of ESWT in wound healing has already been demonstrated [41,51]. This effect is probably triggered through ATP release [44]. Wang *et al.* showed that intracellular ATP delivery promotes wound healing in a diabetic rat model [58]. Howard *et al.* [59] observed in an animal model devoid of skin contraction reduced wound healing times and accelerated new tissue growth after delivery of ATP. Hence, a higher ATP content of the cell could potentially be beneficial for transplantation and integration of the cell material inside the surrounding tissue, which is still a major challenge. Shock wave-activated adipose tissue could be used as a source material for cells that meet the standard of cell therapeutics. This follows the concept of bringing autologous cells such as SVF back into the patient without further processing within a one-step procedure. Limitation of potential risk factors during cell processing is also the prerequisite for classification of a cell product as “minimally manipulated” according to the regulatory framework as defined by the European Medicines Agency (EMA) [60]. Ongoing SVF and ASC transplantation studies have so far shown heterogeneous results regarding stem cell potency and efficacy. This is dependent on many factors such as tissue processing [61,62], cell isolation [25,63,64], patients' health [65,66], body mass index [45,67] or age [68-70]. We have shown that cells isolated from shock wave-treated adipose tissue responded to an external stimulus, leading to higher levels of ATP and enhanced expression of single mesenchymal and vascular marker. Hence, these cells have the potential to produce a higher amount of ATP, which could have a positive impact on the transplantation process even though the cell identity could not reach uniformity after ESWT. Because the effectiveness of autologous cell therapy is dependent on the potency of the patient's own cells, this technology might raise the number of patients eligible for autologous cell transplantation.

### Acknowledgments

We thank Dr. Matthias Sandhofer for providing liposuction material. Financial support from the Austrian

Research Promotion Agency (FFG) project Liporegeneration (846062) and the FFG project Disease Tissue (845443) is gratefully acknowledged.

**Disclosure of interests:** We exclude any conflict of interest and guarantee that all authors are in complete agreement with the contents and submission of this article. Furthermore, we declare that our work is original research, unpublished and not submitted to another journal.

### References

- [1] Neuber FF. Bericht über die Verhandlungen der Deutschen Gesellschaft fuer Chirurgie. Zentrabl Chir 1893;22:66.
- [2] Coleman SR. Structural fat grafting: more than a permanent filler. *Plast Reconstr Surg* 2006;118:108s–20s. doi:10.1097/01.prs.0000234610.81672.e7.
- [3] Gimble JM, Guilak F, Bunnell BA. Clinical and preclinical translation of cell-based therapies using adipose tissue-derived cells. *Stem Cell Res Ther* 2010;1:19. doi:10.1186/scrt19.
- [4] Rigotti G, Marchi A, Galie M, Baroni G, Benati D, Krampera M, et al. Clinical treatment of radiotherapy tissue damage by lipospirote transplant: a healing process mediated by adipose-derived adult stem cells. *Plast Reconstr Surg* 2007;119:1409–22, discussion 23–4. doi:10.1097/01.prs.0000256047.47909.71.
- [5] Cawthorn WP, Scheller EL, MacDougald OA. Adipose tissue stem cells meet preadipocyte commitment: going back to the future. *J Lipid Res* 2012;53:227–46. doi:10.1194/jlr.R021089.
- [6] Cousin B, Andre M, Arnaud E, Penicaud L, Casteilla L. Reconstitution of lethally irradiated mice by cells isolated from adipose tissue. *Biochem Biophys Res Commun* 2003;301:1016–22. doi:10.1016/S0006-291X(03)00061-5.
- [7] Han J, Koh YJ, Moon HR, Ryoo HG, Cho CH, Kim I, et al. Adipose tissue is an extramedullary reservoir for functional hematopoietic stem and progenitor cells. *Blood* 2010;115:957–64. doi:10.1182/blood-2009-05-219923.
- [8] McIntosh K, Zvonic S, Garrett S, Mitchell JB, Floyd ZE, Hammill L, et al. The immunogenicity of human adipose-derived cells: temporal changes *in vitro*. *Stem Cells* 2006;24:1246–53. doi:10.1634/stemcells.2005-0235.
- [9] Zimmerlin L, Donnenberg VS, Pfeifer ME, Meyer EM, Peault B, Rubin JP, et al. Stromal vascular progenitors in adult human adipose tissue. *Cytometry A* 2010;77:22–30. doi:10.1002/cyto.a.20813.
- [10] Zuk PA, Zhu M, Mizuno H, Huang J, Futrell JW, Katz AJ, et al. Multilineage cells from human adipose tissue: implications for cell-based therapies. *Tissue Eng* 2001;7:211–28. doi:10.1089/107632701300062859.
- [11] Sterodimas A, de Faria J, Nicaretta B, Boriani F. Autologous fat transplantation versus adipose-derived stem cell-enriched lipografts: a study. *Aesthet Surg J* 2011;31:682–93. doi:10.1177/1090820x11415976.
- [12] Tanikawa DY, Agueno M, Bueno DF, Passos-Bueno MR, Alonso N. Fat grafts supplemented with adipose-derived stromal cells in the rehabilitation of patients with craniofacial microsomia. *Plast Reconstr Surg* 2013;132:141–52. doi:10.1097/PRS.0b013e3182910a82.
- [13] Yoshimura K, Asano Y, Aoi N, Kurita M, Oshima Y, Sato K, et al. Progenitor-enriched adipose tissue transplantation as rescue for breast implant complications. *Breast J* 2010;16:169–75. doi:10.1111/j.1524-4741.2009.00873.x.
- [14] Yoshimura K, Sato K, Aoi N, Kurita M, Hirohi T, Harii K. Cell-assisted lipotransfer for cosmetic breast augmentation:



- supportive use of adipose-derived stem/stromal cells. *Aesthetic Plast Surg* 2008;32:48–55, discussion 6–7. doi:10.1007/s00266-007-9019-4.
- [15] Lendeckel S, Jodicke A, Christophis P, Heidinger K, Wolff J, Fraser JK, et al. Autologous stem cells (adipose) and fibrin glue used to treat widespread traumatic calvarial defects: case report. *J Craniomaxillofac Surg* 2004;32:370–3. doi:10.1016/j.jcms.2004.06.002.
- [16] Mesimaki K, Lindroos B, Tornwall J, Mauno J, Lindqvist C, Kontio R, et al. Novel maxillary reconstruction with ectopic bone formation by GMP adipose stem cells. *Int J Oral Maxillofac Surg* 2009;38:201–9. doi:10.1016/j.ijom.2009.01.001.
- [17] Michalek J, Moster R, Lukac L, Proefrock K, Petrasovic M, Rybar J, et al. Autologous adipose tissue-derived stromal vascular fraction cells application in patients with osteoarthritis. *Cell Transplant* 2015;doi:10.3727/096368915x686760.
- [18] Sandor GK, Numminen J, Wolff J, Thesleff T, Miettinen A, Tuovinen VJ, et al. Adipose stem cells used to reconstruct 13 cases with craniomaxillofacial hard-tissue defects. *Stem Cells Transl Med* 2014;3:530–40. doi:10.5966/sctm.2013-0173.
- [19] Thesleff T, Lehtimäki K, Niskakangas T, Mannerstrom B, Miettinen S, Suuronen R, et al. Cranioplasty with adipose-derived stem cells and biomaterial: a novel method for cranial reconstruction. *Neurosurgery* 2011;68:1535–40. doi:10.1227/NEU.0b013e31820ee24e.
- [20] Cho YB, Park KJ, Yoon SN, Song KH, Kim DS, Jung SH, et al. Long-term results of adipose-derived stem cell therapy for the treatment of Crohn's fistula. *Stem Cells Transl Med* 2015;4(5):532–7. doi:10.5966/sctm.2014-0199.
- [21] Ra JC, Kang SK, Shin IS, Park HG, Joo SA, Kim JG, et al. Stem cell treatment for patients with autoimmune disease by systemic infusion of culture-expanded autologous adipose tissue derived mesenchymal stem cells. *J Transl Med* 2011;9:181. doi:10.1186/1479-5876-9-181.
- [22] Sergeevicheva V, Kruchkova I, Chernykh E, Shevela E, Kulagin A, Gilevich A, et al. Rapid recovery from chronic PRCA by MSC infusion in patient after major ABO-mismatched alloSCT. *Case Rep Med* 2012;2012:862721. doi:10.1155/2012/862721.
- [23] Riordan NH, Ichim TE, Min WP, Wang H, Solano F, Lara F, et al. Non-expanded adipose stromal vascular fraction cell therapy for multiple sclerosis. *J Transl Med* 2009;7:29. doi:10.1186/1479-5876-7-29.
- [24] Bura A, Planat-Benard V, Bourin P, Silvestre JS, Gross F, Grolleau JL, et al. Phase I trial: the use of autologous cultured adipose-derived stroma/stem cells to treat patients with non-revascularizable critical limb ischemia. *Cytotherapy* 2014;16:245–57. doi:10.1016/j.jcyt.2013.11.011.
- [25] Oberbauer E, Steffenhagen C, Wurzer C, Gabriel C, Redl H, Wolbank S. Enzymatic and non-enzymatic isolation systems for adipose tissue-derived cells: current state of the art. *Cell Regen (Lond)* 2015;4:7. doi:10.1186/s13619-015-0020-0.
- [26] Bourin P, Bunnell BA, Casteilla L, Dominici M, Katz AJ, March KL, et al. Stromal cells from the adipose tissue-derived stromal vascular fraction and culture expanded adipose tissue-derived stromal/stem cells: a joint statement of the International Federation for Adipose Therapeutics and Science (IFATS) and the International Society for Cellular Therapy (ISCT). *Cytotherapy* 2013;15:641–8. doi:10.1016/j.jcyt.2013.02.006.
- [27] Park IS, Chung PS, Ahn JC. Enhancement of ischemic wound healing by spheroid grafting of human adipose-derived stem cells treated with low-level light irradiation. *PLoS ONE* 2015;10:e0122776. doi:10.1371/journal.pone.0122776.
- [28] Park IS, Mondal A, Chung PS, Ahn JC. Vascular regeneration effect of adipose-derived stem cells with light-emitting diode phototherapy in ischemic tissue. *Lasers Med Sci* 2015;30:533–41. doi:10.1007/s10103-014-1699-9.
- [29] Teuschl A, Balmayor ER, Redl H, van Griensven M, Dungal P. Phototherapy with LED light modulates healing processes in an *in vitro* scratch-wound model using 3 different cell types. *Dermatol Surg* 2015;41:261–8. doi:10.1097/dss.0000000000000266.
- [30] Paspaliaris B, Thornton JAF. Methods and apparatuses for isolating and preparing stem cells. 2014. US 20140093482 A1.
- [31] Tzouveleki A, Koliakos G, Ntoliou P, Baira I, Bouros E, Oikonomou A, et al. Stem cell therapy for idiopathic pulmonary fibrosis: a protocol proposal. *J Transl Med* 2011;9:182. doi:10.1186/1479-5876-9-182.
- [32] Maioli M, Rinaldi S, Santaniello S, Castagna A, Pigliaru G, Delitala A, et al. Radioelectric asymmetric conveyed fields and human adipose-derived stem cells obtained with a nonenzymatic method and device: a novel approach to multipotency. *Cell Transplant* 2014;23:1489–500. doi:10.3727/096368913x672037.
- [33] Gentile P, Orlandi A, Scioli MG, Di Pasquali C, Bocchini I, Curcio CB, et al. A comparative translational study: the combined use of enhanced stromal vascular fraction and platelet-rich plasma improves fat grafting maintenance in breast reconstruction. *Stem Cells Transl Med* 2012;1:341–51. doi:10.5966/sctm.2011-0065.
- [34] Van Pham P, Bui KHT, Ngo DQ, Vu NB, Truong NH, Phan NLC, et al. Activated platelet-rich plasma improves adipose-derived stem cell transplantation efficiency in injured articular cartilage. *Stem Cell Res Ther* 2013;4:91. doi:10.1186/scrt277.
- [35] Hamed S, Egozi D, Kruchevsky D, Teot L, Gilhar A, Ullmann Y. Erythropoietin improves the survival of fat tissue after its transplantation in nude mice. *PLoS ONE* 2010;5:e13986. doi:10.1371/journal.pone.0013986.
- [36] Ogden JA, Toth-Kischkat A, Schultheiss R. Principles of shock wave therapy. *Clin Orthop Relat Res* 2001;387:8–17.
- [37] Schaden W, Fischer A, Sailler A. Extracorporeal shock wave therapy of nonunion or delayed osseous union. *Clin Orthop Relat Res* 2001;387:90–4.
- [38] Furia JP, Juliano PJ, Wade AM, Schaden W, Mittermayr R. Shock wave therapy compared with intramedullary screw fixation for nonunion of proximal fifth metatarsal metaphyseal-diaphyseal fractures. *J Bone Joint Surg Am* 2010;92:846–54. doi:10.2106/jbjs.i.00653.
- [39] Elster EA, Stojadinovic A, Forsberg J, Shawen S, Andersen RC, Schaden W. Extracorporeal shock wave therapy for nonunion of the tibia. *J Orthop Trauma* 2010;24:133–41. doi:10.1097/BOT.0b013e3181b26470.
- [40] Mittermayr R, Hartinger J, Antonic V, Meinel A, Pfeifer S, Stojadinovic A, et al. Extracorporeal shock wave therapy (ESWT) minimizes ischemic tissue necrosis irrespective of application time and promotes tissue revascularization by stimulating angiogenesis. *Ann Surg* 2011;253:1024–32. doi:10.1097/SLA.0b013e3182121d6e.
- [41] Schaden W, Thiele R, Kolpl C, Pusch M, Nissan A, Attinger CE, et al. Shock wave therapy for acute and chronic soft tissue wounds: a feasibility study. *J Surg Res* 2007;143:1–12. doi:10.1016/j.jss.2007.01.009.
- [42] Saggini R, Figus A, Troccola A, Cocco V, Saggini A, Scuderi N. Extracorporeal shock wave therapy for management of chronic ulcers in the lower extremities. *Ultrasound Med Biol* 2008;34:1261–71. doi:10.1016/j.ultrasmedbio.2008.01.010.
- [43] Schuh CM, Heher P, Weihs AM, Banerjee A, Fuchs C, Gabriel C, et al. *In vitro* extracorporeal shock wave treatment enhances stemness and preserves multipotency of rat and human adipose-derived stem cells. *Cytotherapy* 2014;16(12):1666–78. doi:10.1016/j.jcyt.2014.07.005.


- [44] Weihs AM, Fuchs C, Teuschl AH, Hartinger J, Slezak P, Mittermayr R, et al. Shock wave treatment enhances cell proliferation and improves wound healing by ATP release-coupled extracellular signal-regulated kinase (ERK) activation. *J Biol Chem* 2014;289:27090–104. doi:10.1074/jbc.M114.580936.
- [45] Frazier TP, Gimble JM, Devay JW, Tucker HA, Chiu ES, Rowan BG. Body mass index affects proliferation and osteogenic differentiation of human subcutaneous adipose tissue-derived stem cells. *BMC Cell Biol* 2013;14:34. doi:10.1186/1471-2121-14-34.
- [46] Tobita M, Orbay H, Mizuno H. Adipose-derived stem cells: current findings and future perspectives. *Discov Med* 2011;11:160–70.
- [47] Wolbank S, Peterbauer A, Fahrner M, Hennerbichler S, van Griensven M, Stadler G, et al. Dose-dependent immunomodulatory effect of human stem cells from amniotic membrane: a comparison with human mesenchymal stem cells from adipose tissue. *Tissue Eng* 2007;13:1173–83. doi:10.1089/ten.2006.0313.
- [48] Holfeld J, Tepekoylu C, Kozaryn R, Urbschat A, Zacharowski K, Grimm M, et al. Shockwave therapy differentially stimulates endothelial cells: implications on the control of inflammation via toll-Like receptor 3. *Inflammation* 2014;37:65–70. doi:10.1007/s10753-013-9712-1.
- [49] Holfeld J, Tepekoylu C, Blunder S, Lobenwein D, Kirchmair E, Dietl M, et al. Low energy shock wave therapy induces angiogenesis in acute hind-limb ischemia via VEGF receptor 2 phosphorylation. *PLoS ONE* 2014;9:e103982. doi:10.1371/journal.pone.0103982.
- [50] Peng YZ, Zheng K, Yang P, Wang Y, Li RJ, Li L, et al. Shock wave treatment enhances endothelial proliferation via autocrine vascular endothelial growth factor. *Genet Mol Res* 2015;14:19203–10. doi:10.4238/2015.December.29.30.
- [51] Mittermayr R, Antonic V, Hartinger J, Kaufmann H, Redl H, Teot L, et al. Extracorporeal shock wave therapy (ESWT) for wound healing: technology, mechanisms, and clinical efficacy. *Wound Repair Regen* 2012;20:456–65. doi:10.1111/j.1524-475X.2012.00796.x.
- [52] Sun D, Junger WG, Yuan C, Zhang W, Bao Y, Qin D, et al. Shockwaves induce osteogenic differentiation of human mesenchymal stem cells through ATP release and activation of P2X7 receptors. *Stem Cells* 2013;31:1170–80. doi:10.1002/stem.1356.
- [53] Yu T, Junger WG, Yuan C, Jin A, Zhao Y, Zheng X, et al. Shockwaves increase T-cell proliferation and IL-2 expression through ATP release, P2X7 receptors, and FAK activation. *Am J Physiol Cell Physiol* 2010;298:C457–64. doi:10.1152/ajpcell.00342.2009.
- [54] Aarya Hari SG. Production of good manufacturing practice grade equine adiposederived mesenchymal stem cells for therapeutic use. *J Stem Cell Res Ther* 2013;3:2157–7633. doi:10.4172/2157-7633.1000154.
- [55] Sensebe L, Gadelorge M, Fleury-Cappellesso S. Production of mesenchymal stromal/stem cells according to good manufacturing practices: a review. *Stem Cell Res Ther* 2013;4:66. doi:10.1186/scrt217.
- [56] EudraLex. Clinical trial guidelines; 2010. Available from: [https://ec.europa.eu/health/documents/eudralex/vol-10\\_en](https://ec.europa.eu/health/documents/eudralex/vol-10_en). [Accessed 12 July 2017].
- [57] EudraLex. Good manufacturing practice (GMP); 2015. Available from: [https://ec.europa.eu/health/documents/eudralex/vol-4\\_en](https://ec.europa.eu/health/documents/eudralex/vol-4_en). [Accessed 12 July 2017].
- [58] Wang J, Wan R, Mo Y, Li M, Zhang Q, Chien S. Intracellular delivery of adenosine triphosphate enhanced healing process in full-thickness skin wounds in diabetic rabbits. *Am J Surg* 2010;199:823–32. doi:10.1016/j.amjsurg.2009.05.040.
- [59] Howard JD, Sarojini H, Wan R, Chien S. Rapid granulation tissue regeneration by intracellular ATP delivery—a comparison with Regranex. *PLoS ONE* 2014;9:e91787. doi:10.1371/journal.pone.0091787.
- [60] European Medicines Agency. Scientific recommendation on classification of advanced therapy medicinal products. EMA/500673/2012 ed; 2012. Available from: [http://www.ema.europa.eu/docs/en\\_GB/document\\_library/Report/2012/10/WC500134163.pdf](http://www.ema.europa.eu/docs/en_GB/document_library/Report/2012/10/WC500134163.pdf). [Accessed 12 July 2017].
- [61] Fisher C, Grahovac TL, Schafer ME, Shippert RD, Marra KG, Rubin JP. Comparison of harvest and processing techniques for fat grafting and adipose stem cell isolation. *Plast Reconstr Surg* 2013;132:351–61. doi:10.1097/PRS.0b013e3182958796.
- [62] Tuin AJ, Domerchie PN, Schepers RH, Willemsen JC, Dijkstra PU, Spijkervet FK, et al. What is the current optimal fat grafting processing technique? A systematic review. *J Craniomaxillofac Surg* 2015;44(1):45–55. doi:10.1016/j.jcms.2015.10.021.
- [63] Aronowitz JA, Lockhart RA, Hakakian CS. Mechanical versus enzymatic isolation of stromal vascular fraction cells from adipose tissue. *Springerplus* 2015;4:713. doi:10.1186/s40064-015-1509-2.
- [64] Faustini M, Bucco M, Chlapanidas T, Lucconi G, Marazzi M, Tosca MC, et al. Nonexpanded mesenchymal stem cells for regenerative medicine: yield in stromal vascular fraction from adipose tissues. *Tissue Eng Part C Methods* 2010;16:1515–21. doi:10.1089/ten.TEC.2010.0214.
- [65] Fortini C, Cesselli D, Beltrami AP, Bergamin N, Caragnano A, Moretti L, et al. Alteration of Notch signaling and functionality of adipose tissue derived mesenchymal stem cells in heart failure. *Int J Cardiol* 2014;174:119–26. doi:10.1016/j.ijcard.2014.03.173.
- [66] Yamanaka S, Yokote S, Yamada A, Katsuoka Y, Izuhara L, Shimada Y, et al. Adipose tissue-derived mesenchymal stem cells in long-term dialysis patients display downregulation of PCAF expression and poor angiogenesis activation. *PLoS ONE* 2014;9:e102311. doi:10.1371/journal.pone.0102311.
- [67] Yang HJ, Kim KJ, Kim MK, Lee SJ, Ryu YH, Seo BF, et al. The stem cell potential and multipotency of human adipose tissue-derived stem cells vary by cell donor and are different from those of other types of stem cells. *Cells Tissues Organs* 2014;199:373–83. doi:10.1159/000369969.
- [68] Choudhery MS, Badowski M, Muise A, Pierce J, Harris DT. Donor age negatively impacts adipose tissue-derived mesenchymal stem cell expansion and differentiation. *J Transl Med* 2014;12:8. doi:10.1186/1479-5876-12-8.
- [69] Dos-Anjos Vilaboa S, Navarro-Palou M, Llull R. Age influence on stromal vascular fraction cell yield obtained from human lipoaspirates. *Cytotherapy* 2014;16:1092–7. doi:10.1016/j.jcyt.2014.02.007.
- [70] Madonna R, Renna FV, Cellini C, Cotellesse R, Picardi N, Francomano F, et al. Age-dependent impairment of number and angiogenic potential of adipose tissue-derived progenitor cells. *Eur J Clin Invest* 2011;41:126–33. doi:10.1111/j.1365-2362.2010.02384.x.

## Appendix: Supplementary material

Supplementary data to this article can be found online at doi:10.1016/j.jcyt.2017.05.010.

## RESEARCH ARTICLE

# Extracorporeal shock wave therapy *in situ* – novel approach to obtain an activated fat graft

E. Priglinger<sup>1,2</sup>  | M. Sandhofer<sup>3</sup> | A. Peterbauer<sup>2,4</sup> | C. Wurzer<sup>1,2,5</sup> | C. Steffenhagen<sup>1,2</sup> | J. Maier<sup>1,2</sup> | W. Holthoner<sup>1,2</sup> | S. Nuernberger<sup>2,6,7</sup> | H. Redl<sup>1,2</sup> | S. Wolbank<sup>1,2</sup>

<sup>1</sup>Ludwig Boltzmann Institute for Experimental and Clinical Traumatology, AUVA Research Center, Linz/Vienna, Austria

<sup>2</sup>Austrian Cluster for Tissue Regeneration, Vienna, Austria

<sup>3</sup>Austrian Academy of Cosmetic Surgery and Aesthetic Medicine, Linz, Austria

<sup>4</sup>Red Cross Blood Transfusion Service of Upper Austria, Linz, Austria

<sup>5</sup>Liporegena GmbH, Austria

<sup>6</sup>Bernhard Gottlieb University Clinic of Dentistry, Universitätsklinik für Zahn-, Mund- und Kieferheilkunde Ges.m.b.H, Vienna, Austria

<sup>7</sup>Medical University of Vienna, Department of Trauma Surgery, Vienna, Austria

## Correspondence

Eleni Priglinger (formerly Eleni Oberbauer), Ludwig Boltzmann Institute for Experimental and Clinical Traumatology, Krankenhausstraße 7, 4010 Linz, Austria.

Email: eleni.priglinger@trauma.lbg.ac.at

## Abstract

One of the mainstays of facial rejuvenation strategies is volume restoration, which can be achieved by autologous fat grafting. In our novel approach, we treated the adipose tissue harvest site with extracorporeal shock wave therapy (ESWT) in order to improve the quality of the regenerative cells *in situ*. The latter was demonstrated by characterizing the cells of the stromal vascular fraction (SVF) in the harvested liposuction material regarding cell yield, adenosine triphosphate (ATP) content, proliferative capacity, surface marker profile, differentiation potential and secretory protein profile. Although the SVF cell yield was only slightly enhanced, viability and ATP concentration of freshly isolated cells as well as proliferation doublings after 3 weeks in culture were significantly increased in the ESWT compared with the untreated group. Likewise, cells expressing mesenchymal and endothelial/pericytic markers were significantly elevated concomitant with an improved differentiation capacity towards the adipogenic lineage and enhancement in specific angiogenic proteins. Hence, *in situ* ESWT might be applied in the future to promote cell fitness, adipogenesis and angiogenesis within the fat graft for successful facial rejuvenation strategies with potential long-term graft survival.

## KEYWORDS

adipogenesis, adipose tissue, angiogenesis, autologous fat grafting, extracorporeal shock wave therapy (ESWT), stromal vascular fraction (SVF)

## 1 | INTRODUCTION

The shape of the human face depends on many factors: the osseous facial skeleton, muscles, fat, connective tissue and skin. Nevertheless, adipose tissue together with the superficial fascia builds up the basic structure and contour of the human face. During facial aging, volume loss due to adipose and connective tissue atrophy occurs, followed by the sagging of structures and the formation of wrinkles (Amar & Fox, 2011; Sandhofer & Schauer, 2015). Hence, restoring volume by the injection of fillers is one of the mainstays of facial rejuvenation strategies. In contrast to traditional fillers, including hyaluronic acid and carboxymethylcellulose, which act only temporarily, autologous adipose tissue has the potential for permanent restoration combined with the additional advantage of improved quality of the overlying skin (Coleman & Katzel, 2015).

Autologous fat grafting was described for the first time in 1893 by Gustav A. Neuber (Neuber, 1893). Recently it has experienced a comeback in cosmetic and plastic surgery due to its relative ease of application associated with comparatively low risks (Gir, Oni, Brown, Mojallal, & Rohrich, 2012). The beneficial effect of autologous fat grafting could not only be shown for facial rejuvenation but also for body contour improvement and breast augmentation after mastectomies (Calabrese, Orzalesi, Casella, & Cataliotti, 2009; Gentile et al., 2012; Jiang, Li, Duan, Dong, & Wang, 2015; Luo et al., 2013). Although fat grafting has been constantly developed, certain drawbacks, such as fat resorption, limited survival of the graft followed by partial necrosis, fibrosis and calcification have to be faced in the clinics (Luo et al., 2013). Some of them might be attributed to improper harvesting and processing techniques and can be partially circumvented by adhering to the following principles: gentle harvesting of fat to preserve the adipose tissue structure, centrifugation to remove non-viable components and to concentrate the fat, and delivery of adipose tissue in small aliquots to facilitate adequate blood supply and thus maximize graft take and

Authors contributed equally.

graft retention up to 65% (Coleman & Katzel, 2015). However, standard protocols regarding fat harvesting (cannula size, manual, machine-assisted), processing (aspiration, infiltration), purification and transplantation are still missing (Gir et al., 2012; Suszynski, Sieber, Van Beek, & Cunningham, 2015). Furthermore, the main factor influencing long-term graft survival is still a matter of debate. Whereas older studies concentrated on the viability of mature adipocytes in the graft, there has been a shift towards the interaction among the different components of fat grafts, including adipose stem and precursor cells, endothelial cells and their precursors, as well as the cells' secretome influencing graft survival. Whether these recently proposed laboratory parameters are really correlated with graft survival and, hence, volume retention in humans has still to be proven (Tuin et al., 2016).

In 2006, a novel approach, known as cell assisted lipotransfer, was implemented. Supplementing the fat graft with therapeutic cells derived from adipose tissue, such as the stromal vascular fraction (SVF), which includes the adipose-derived stromal/stem cells (ASC), can improve the survival rate of transplanted fat grafts (Yoshimura et al., 2008). It has been shown that cell assisted lipotransfer can reduce postoperative atrophy in breast augmentation (Salgarello, Visconti, & Farallo, 2010) and enhance angiogenesis of the grafts (Gentile et al., 2012; Jiang et al., 2015). The latter is an important feature as early and abundant vascularization is a prerequisite for nutrition supply and integration inside the surrounding tissue (Garza et al., 2014; Luo et al., 2013). As cell properties might change with isolation procedure, the comparison of the outcome of clinical trials may be difficult. In our novel approach, we hypothesize that application of extracorporeal shock wave therapy (ESWT) at the adipose tissue harvest site might precondition the cells inside the fat graft in such a way that the regenerative potential is enhanced.

ESWT was clinically implemented 30 years ago as an effective treatment to disintegrate urinary stones. In contrast to stone disintegration, ESWT for modulating regeneration is performed with lower energy (Tandan & Reddy, 2011). However, this technology has also emerged as an effective non-invasive treatment approach for several other indications, including musculoskeletal disorders such as tendinopathies and bone defects (delayed/non-union of bone fractures, avascular necrosis of the femoral head) (Saggini et al., 2008), problematic soft tissue wounds (Antonic, Mittermayr, Schaden, & Stojadinovic, 2011) or erectile dysfunction (Lei et al., 2013). Potential regenerative mechanisms exerted as biological responses to therapeutic shock waves include initialization of neovascularization, recruitment of mesenchymal stem cells, stimulating cell proliferation and differentiation, anti-inflammatory and anti-microbial effects, as well as suppression of nociception (Mittermayr et al., 2012).

Also, in cosmetic and aesthetic medicine, ESWT has been discovered for the treatment of patients with cellulite, lipoedema and lymphoedema (Cebicci et al., 2016; Sandhofer, 2015; Siems, Grune, Voss, & Brenke, 2005). In cellulite and lipoedema patients, ESWT significantly improved the biomechanical skin properties, leading to smoothing of the dermis and hypodermis surface (Siems et al., 2005). This effect is, among others, caused by remodelling of collagen in the ESWT-treated regions (Angehrn, Kuhn, & Voss, 2007).

Concerning cells, ESWT has been shown to positively affect cell viability and proliferation of various cell types, including mesenchymal

stem cells from adipose tissue and bone marrow, primary tendon cells and endothelial progenitors (de Girolamo et al., 2014; Peng et al., 2008; Raabe et al., 2013; Weihs et al., 2014; Zhao et al., 2013). This effect is triggered through immediate adenosine triphosphate (ATP) release that subsequently binds to purinergic receptors acting via downstream Erk1/2 signalling on cell proliferation (Chen et al., 2004; Weihs et al., 2014). Apart from increased growth potential, enhanced differentiation from progenitors into mature cell types has also been observed (Chen et al., 2004; Leone et al., 2016; Muzio et al., 2014; Schuh et al., 2016; Zhai et al., 2016). By contrast, Raabe and co-workers (Raabe et al., 2013) did not find an effect of ESWT on the differentiation potential of equine ASC. The positive effect of ESWT on cells might also be attributed to increased expression and secretion of growth factors playing a role in regeneration settings (de Girolamo et al., 2014; Muzio et al., 2014; Peng et al., 2015; Zhao et al., 2013). On top of that, ESWT has not only been demonstrated to improve the quality of cells, but also to enhance cell yield when the nerve tissue was treated with ESWT before isolating cells, which might also be crucial for realizing cellular therapies (Schuh et al., 2016).

For this study, seven female patients undergoing routine liposuction were treated with ESWT before the actual procedure. Subsequently, from the liposuction material, the SVF was isolated and analysed regarding cell yield, ATP content, proliferative capacity, surface marker profile, differentiation potential and secretory protein profile. Within this study, SVF and derived cultured cells were used as an indicator for the functionality of future fat grafting approaches for facial rejuvenation using ESWT on the harvesting site. We hypothesized that *in situ* ESWT might positively affect the cell yield and the cell quality.

## 2 | MATERIALS AND METHODS

### 2.1 | Radial ESWT *in situ*

Seven female donors were treated locally below the iliac crest 1 week and 1 h before liposuction with radial ESWT (Z WavePro, Zimmer, Neu-Ulm, Germany) using two doses of 2000 pulses with 120 mJ/cm<sup>2</sup> and 16 Hz (Figure 1). The donors were treated on their left side with ESWT and remained untreated on their right side (control). The use of human adipose tissue was approved by the local ethical board with patient's consent. Subcutaneous adipose tissue was obtained during routine outpatient liposuction procedures under local tumescence anaesthesia. Afterwards, isolation of SVF from the liposuction waste was continued with enzymatic digestion. Briefly, 100 ml liposuction material was transferred to a blood bag (400 ml; Macopharma, Langen, Germany) and washed with an equal volume of phosphate-buffered saline (PBS) to remove blood and tumescence solution. Afterwards, for tissue digestion, PBS was replaced with 0.2 U/ml collagenase NB4 (Serva, Vienna, Austria) dissolved in 100 ml PBS containing Ca<sup>2+</sup>/Mg<sup>2+</sup> and 25 mM N-2-hydroxyethylpiperazine-N0-2-ethanesulfonic acid (HEPES; Sigma, Vienna, Austria) and the blood bag was incubated at 37 °C under moderate shaking (180 rpm) for 1 h. The digested tissue was transferred into 50 ml tubes. After centrifugation at 1200×g for 7 min the cell pellet was incubated with 100 ml erythrocyte lysis buffer [154 mM ammonium chloride (Sigma), 10 mM potassium



**FIGURE 1** Extracorporeal shock wave therapy (ESWT) *in situ*. Seven patients were treated on their left side below the iliac crest 1 week and 1 h before liposuction with a Zimmer Z WavePro radial extracorporeal shock wave using two times 2000 pulses with  $120 \text{ mJ/cm}^2$  and 16 Hz. The right side remained untreated (control). Afterwards, enzymatic isolation of the stromal vascular fraction (SVF) from liposuction waste material was performed

bicarbonate (Sigma), 0.1 mM ethylenediamine-tetraacetic acid (EDTA; Biochrom, Vienna, Austria) in aqua dest] for 3 min at  $37^\circ\text{C}$  to eliminate red blood cells. The supernatant was aspirated after centrifugation for 5 min at  $500\times g$ . The pellet was washed with PBS and filtered through a  $100 \mu\text{m}$  cell strainer (Greiner, Kremsmünster, Austria). After another centrifugation step at  $500\times g$  for 5 min the supernatant was removed and the isolated SVF cells were cultured at  $37^\circ\text{C}$ , 5%  $\text{CO}_2$  and 95% air humidity in endothelial growth medium (EGM-2; Lonza, Vienna, Austria) containing 2% fetal bovine serum, hydrocortisone, human fibroblast growth factor, vascular endothelial growth factor (VEGF), R3-insulin-like growth factor-1 (R3-IGF-1), ascorbic acid, human epidermal growth factor (hEGF), GA-1000 and heparin or resuspended in EGM-2 for further analyses.

## 2.2 | Cell yield and viability

Cell number was determined using trypan blue exclusion and quantification in a cell counter (TC-20, Biorad, Vienna, Austria). For measuring cell viability, the percentage of living cells compared with the total cell count was analysed with the cell counter.

## 2.3 | Cellular ATP

To determine the cellular ATP concentration, a CellTiter-Glo® Luminescent Cell Viability Assay (Promega, Mannheim, Germany) was

used and performed according to the manufacturer's instructions. Freshly isolated SVF cells were seeded at a density of  $1 \times 10^4$  cells per well in a black 96-well plate (Greiner) in  $100 \mu\text{l}$  EGM-2. After 2 h,  $100 \mu\text{l}$  CellTiter-Glo® Reagent were added to each well and the plate was gently agitated on a shaker for 2 min. The plate was then incubated for 10 min in the dark. The luminescent signal was detected with an Infinite® M200 Multimode Microplate Reader (Tecan, Grödig, Austria) at an exposure time of 2 s and compared with an ATP standard curve.

## 2.4 | Proliferation

The proliferation potential was analysed by determining the population doubling level (PDL) with the following formulas:

$$k = \frac{\ln N - \ln N_0}{t_1 - t_0}$$

$$t_2 = \frac{\ln 2}{k}$$

$$\text{PDL} = \frac{t_1}{t_2}$$

where  $k$  is the growth constant,  $N_0$  is the number of seeded cells,  $N$  is the number of cells after passing,  $t_0$  is the time of seeding,  $t_1$  is the time of passing and  $t_2$  is the generation time.

Freshly isolated SVF cells were seeded at a density of  $5 \times 10^5$  cells per T-25 culture flask in EGM-2 and the medium was changed every 3–4 days. When cells had reached a subconfluent state, they were passaged and the cell number was determined as described above. For the analysis of the PDL from passage 1 to 3, ASC were seeded at a density of  $5 \times 10^4$  per T-25 culture flask and the cell number determined at each passage.

## 2.5 | Flow cytometry analysis

Freshly isolated SVF cells were characterized using the following antibodies: HLA-DR-PE (eBiosciences, Vienna, Austria), CD73-FITC (BD, Schwechat, Austria), CD90-PE (eBiosciences), CD105-PE (eBiosciences), CD14-FITC (BD), CD45-PerCP (BD), CD31-FITC (eBiosciences), CD34-APC (BD) and CD146-PerCP (R&D, Wiesbaden-Nordenstadt, Germany). For staining,  $5 \times 10^5$  cells in 50  $\mu$ l PBS with 1% fetal calf serum (FCS; PAA, Pasching, Austria) were incubated with 5  $\mu$ l primary labelled antibodies at room temperature for 15 min in the dark. Cells were washed with 1.5 ml Cell Wash™ (BD) and centrifuged for 5 min at 400 $\times$ g. The supernatant was discarded and the cell pellet resuspended in 300  $\mu$ l  $1 \times$  Cell Fix™ (BD; diluted 1:10 with aqua dest). Samples were analysed on a FACSCalibur (BD).

## 2.6 | Adipogenic differentiation and detection

For adipogenic differentiation, ASC after 1 week in culture (passage 0) were plated at a density of  $1.4 \times 10^4$  cells per well in a 24-well plate in EGM-2 and incubated overnight. The next day, the medium was changed to adipogenic differentiation medium [DMEM high glucose (Lonza) containing 10% FCS, 2 mM L-glutamine (PAA), 100 U/ml penicillin/streptomycin (Lonza), 1  $\mu$ M dexamethasone (Sigma), 0.5 mM 3-isobutyl-1-methylxanthine (IBMX; Sigma), 10  $\mu$ g/ml insulin (Sigma) and 100  $\mu$ M indomethacin (Sigma)] or control medium (DMEM:F12/L-glutamine (Lonza) with 10% FCS and 100 U/ml penicillin/streptomycin). The medium was changed every 3–4 days. After 21 days, adipogenic differentiation was analysed with Oil Red O staining and quantification. Cells were fixed with 4% formaldehyde for 1 h. After washing with aqua dest, the cells were rinsed with 70% ethanol for 2 min and stained for 5–15 min with Oil Red O solution (Sigma). The cells were then washed with aqua dest, counterstained for 1–3 min with haematoxylin solution and blued with tap water. For quantitative detection of Oil Red O staining, the supernatant was discarded and 500  $\mu$ l isopropanol were added to each well. After resuspension, the mixture of cells and isopropanol was transferred to a transparent 96-well plate (100  $\mu$ l per well). The absorbance was measured at 510 nm with an Infinite® M200 Multimode Microplate Reader.

## 2.7 | Osteogenic differentiation and detection

For osteogenic differentiation, ASC after 1 week in culture (passage 0) were seeded at a density of  $2 \times 10^3$  cells per well in a 24-well plate in EGM-2 and incubated overnight. On the next day, medium was changed to osteogenic differentiation medium [DMEM low glucose (Lonza) containing 10% FCS, 2 mM L-glutamine, 100 U/ml penicillin/streptomycin, 10 nM dexamethasone, 150  $\mu$ M ascorbate-2-phosphate (Sigma), 10 mM  $\beta$ -glycerophosphate (StemCell Technologies, Cologne,

Germany) and 10 nM dihydroxy-vitamin D3 (Sigma)] or control medium [DMEM: F12/L-glutamine with 10% FCS and 100 U/ml penicillin/streptomycin]. The medium was changed every 3–4 days. After 21 days, osteogenic differentiation was analysed with Alizarin Red staining and quantification, as well as the determination of intracellular alkaline phosphatase (ALP) activity. For Alizarin Red staining of calcified structures, cells were fixed for 1 h with 70% ethanol at  $-20^\circ\text{C}$  and stained with Alizarin Red solution (Merck, Vienna, Austria) for 15 min. For quantitative analysis of Alizarin Red staining, the supernatant was discarded and the cells were incubated with 500  $\mu$ l 20% methanol and 10% acidic acid (diluted in aqua dest) for 15 min. After resuspension, the mixture of cells and methanol/acidic acid was transferred to a transparent 96-well plate (100  $\mu$ l per well). The absorbance was measured at 450 nm with an Infinite® M200 Multimode Microplate Reader. The second method to analyse osteogenic differentiation was the detection of intracellular ALP activity. Cells were incubated with 100  $\mu$ l PBS for 1 h at  $-20^\circ\text{C}$ . Cells were then lysed for 1 h by the addition of 100  $\mu$ l PBS containing 0.5% TritonX-100 (Sigma). For quantitative detection of ALP activity, 100  $\mu$ l substrate solution (4-nitrophenylphosphate) were added in each well and incubated for 1 h in the dark. Finally, the solution was transferred to a transparent 96-well plate (100  $\mu$ l per well) and absorbance was measured at 405 nm, together with a reference wavelength of 620 nm in an Infinite® M200 Multimode Microplate Reader. By creating a standard curve with known *p*-nitrophenol concentrations diluted in a solution containing 0.5% TritonX-100 diluted in PBS 1:2 and measuring the corresponding absorption, the ALP activity of the samples was calculated.

## 2.8 | Chondrogenic differentiation and detection

For chondrogenic differentiation in three-dimensional micromass pellet cultures,  $3 \times 10^5$  ASC after 1 week in culture (passage 0) were centrifuged in chondrogenic differentiation medium [hMSC Chondro BulletKit (Lonza) containing 10 ng/ml BMP-6 (R&D) and 10 ng/ml TGF- $\beta$ 3 (Lonza)] in screw cap microtubes. The tubes were placed in an incubator with slightly open caps for gas exchange. After 2 days, the pellets were transferred to 96-well U-bottom plates (Greiner) with fresh medium. The medium was changed every 2–3 days. After 35 days of differentiation, micromass pellets were fixed in 4% phosphate-buffered formalin overnight for histological analysis (Alcian Blue, collagen type II) (Oberbauer et al., 2016). The next day the pellets were washed in  $1 \times$  PBS and dehydrated in increasing concentrations of alcohol. After rinsing the pellets in xylol and infiltration with paraffin, deparaffinized sections were stained with Alcian Blue for 30 min and counterstained for 2 min with haematoxylin. For collagen type II staining, sections were treated with pepsin for 10 minutes at  $37^\circ\text{C}$  (AP-9007 RTU, Thermo Scientific, Vienna, Austria). Endogenous peroxidase was quenched with freshly prepared 3%  $\text{H}_2\text{O}_2$  for 10 min at room temperature, followed by normal horse serum 2.5% (Vector RTU) to block unspecific binding. Sections were incubated for 1 h with monoclonal anti-collagen type II (MS-306 P0 Thermo Scientific) at 1:100. After washing with Tris-buffered saline (TBS), sections were incubated with the secondary antibody (anti-mouse DAKO EnVision+ System horseradish peroxidase (HRP) labelled Polymer, Dako, Vienna,

Austria) for 30 min and rinsed in TBS again. Bindings were visualized using Nova Red (SK4800 Vector Labs, Vienna, Austria) for 6 min. Counterstaining was performed with haematoxylin for 2 min.

## 2.9 | Secretory profile

Freshly isolated SVF cells ( $5 \times 10^5$ ) were seeded in 2.5 ml EGM-2 in a T-25 flask for conditioning of the medium. After incubation for 2 h in EGM-2, the medium was changed to serum-free medium (DMEM low glucose with 2 mM L-glutamine). To also include non-adherent suspension cells, EGM-2 was withdrawn, collected and centrifuged at  $300 \times g$  for 5 min to obtain a pellet of suspension cells. The supernatant was discarded after centrifugation and suspension cells were resolved in 500  $\mu$ l serum-free medium and returned to the original culture flask. The adherent cells were meanwhile provided with 2 ml serum-free medium. Twenty-four hours after seeding the supernatant was collected and stored at  $-80^\circ\text{C}$  until analysis.

For the analysis of secreted angiogenic proteins, a Human Angiogenesis Array (RayBio, Georgia, USA) was used according to the manufacturer's instructions. Briefly, the membrane was blocked with a blocking buffer for 30 min prior to sample incubation for 5 h at room temperature. Every incubation and washing step excluding the incubation of detection buffer was performed under gentle rotation (0.8 cycles/s). After washing, the biotinylated antibody was incubated overnight at  $4^\circ\text{C}$  and membrane was washed again afterwards. HRP-conjugated streptavidin was incubated for 2 h at room temperature and membrane was washed again. Signals were detected by enhanced chemiluminescence and recorded on an X-ray

film (Figure S1). Signals were densitometrically quantified using ImageJ (NIH, Bethesda, MD, USA).

## 2.10 | Statistical analysis

Data are presented as box-plots (described as median in the text) or mean  $\pm$  standard deviation. A statistical analysis was performed using PRISM6 (GraphPad, San Diego, CA, USA), parametric two-tailed *t*-test or one-way ANOVA Tukey's post-hoc. *p*-values  $< 0.05$  were considered to be significant.

## 3 | RESULTS

### 3.1 | Increased cell viability and proliferation after ESWT

Cells obtained from the untreated and ESWT-treated side were evaluated for their cell yield, viability and proliferation. After ESWT treatment,  $5.2 \times 10^5$  cells were obtained compared with  $4.6 \times 10^5$  cells from the untreated side (Figure 2a). The viability of the freshly isolated cells was significantly increased after ESWT treatment, with 88.4% living cells compared with 80.0% for the untreated side (Figure 2b). Similarly, ESWT treatment significantly enhanced the ATP concentration of freshly isolated cells from 331 nmol/l for the untreated side to 473 nmol/l for the ESWT-treated side (Figure 2c). Cells obtained from ESWT-treated and -untreated sides showed similar proliferation, calculated as PDL, after 7 days ( $1.8 \pm 1.2$  vs.  $2.1 \pm 1.1$ ) and 14 days ( $7.3 \pm 1.9$  vs.

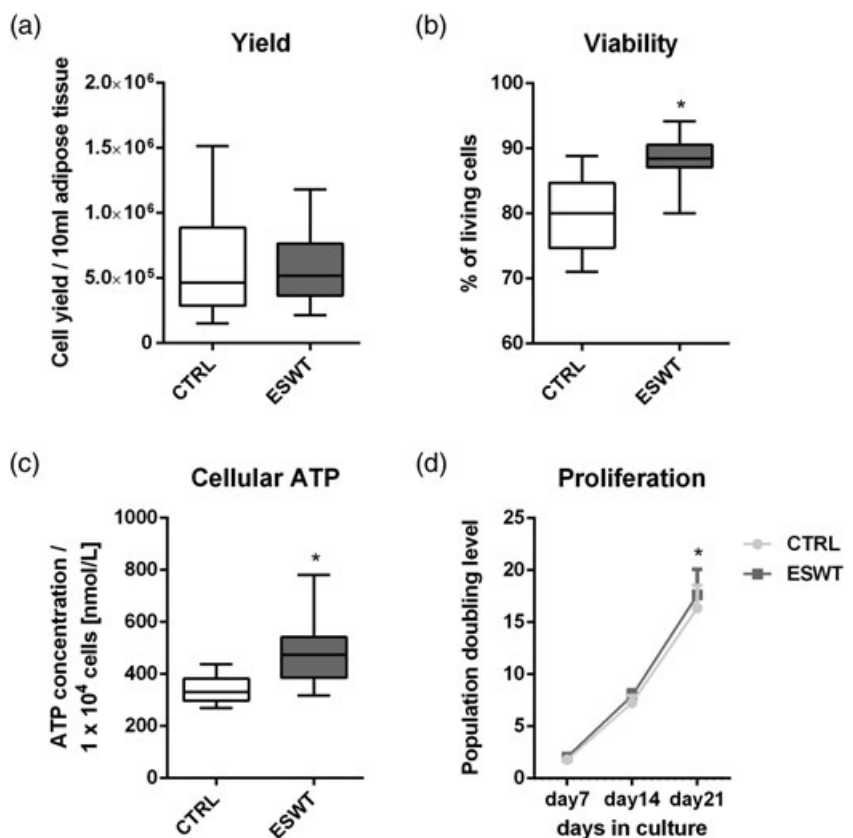


**FIGURE 2** Extracorporeal shock wave therapy (ESWT) *in situ* maintains yield, enhances viability, adenosine triphosphate (ATP) concentration and proliferation of isolated cells. The cell yield was not affected by ESWT treatment (a), whereas there was a significant increase in viability (b) and ATP concentration (c). ESWT treatment enhanced the population doubling level of isolated cells after 21 days in culture (d). Data are presented as box-plots (a–c) or mean  $\pm$  standard deviation (d). \**p*  $< 0.05$

$7.9 \pm 1.6$ ), but a significant increase after 21 days in culture ( $16.4 \pm 6.2$  vs.  $17.6 \pm 6.9$ ) (Figure 2d).

### 3.2 | SVF surface marker expression after ESWT

For analysis of the cellular composition of the isolated SVF cells, the surface marker expression was investigated. ESWT treatment significantly

reduced the number of cells expressing the histocompatibility marker HLA-DR from 45.2% for the untreated side to 41.2% for the treated side (Figure 3). Expression of mesenchymal markers CD73, CD90 and CD105 was significantly increased after ESWT treatment (Figure 3). ESWT treatment resulted in 55.1% CD73-, 64.0% CD90- and 48.5% CD105-positive cells for the treated side compared with the untreated side with 29.4% CD73-, 44.8% CD90- and 21.8% CD105-positive cells.

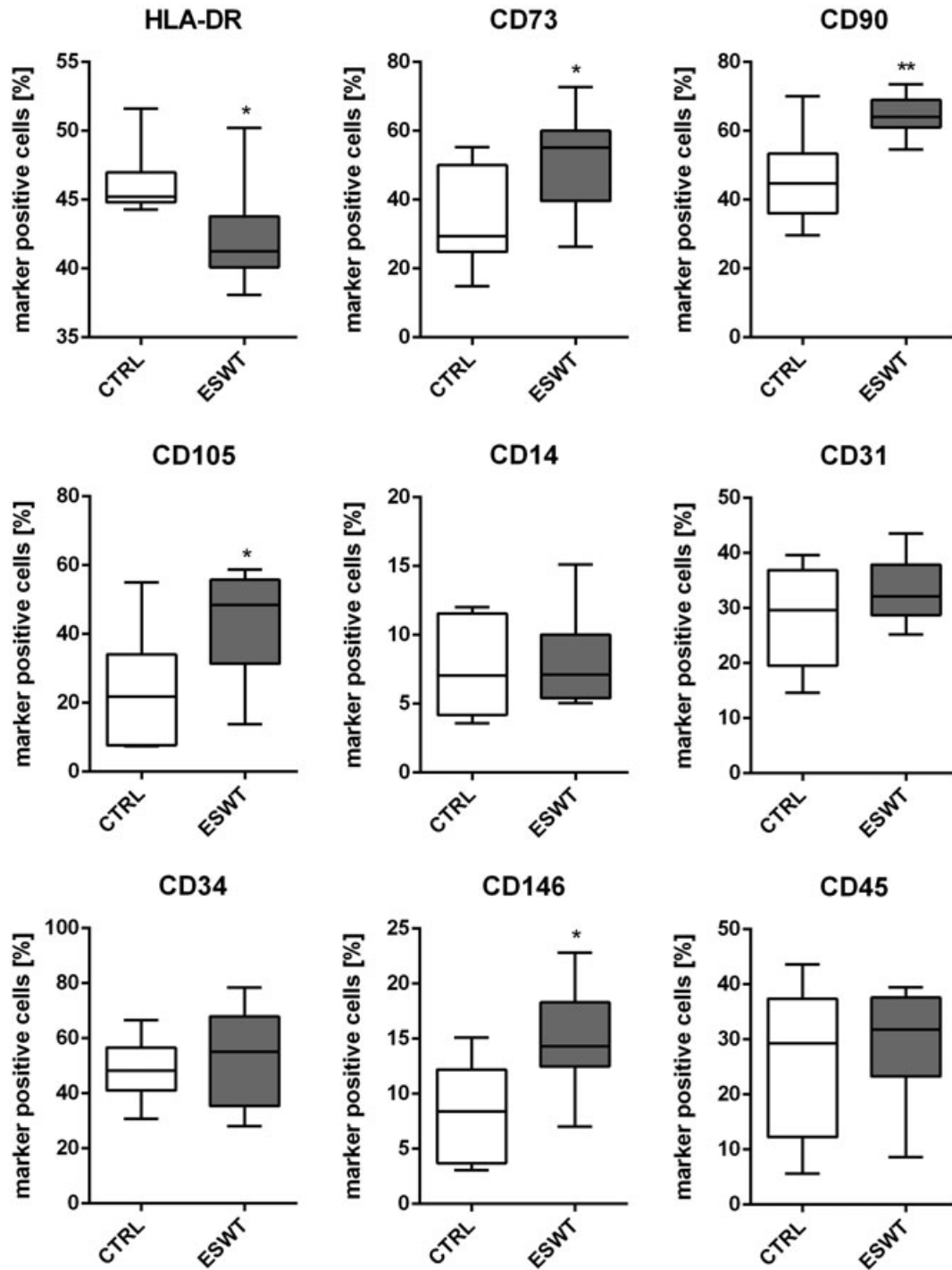


**FIGURE 3** Extracorporeal shock wave therapy (ESWT) *in situ* positively affects the surface marker profile of isolated cells. After ESWT treatment there was a significant downregulation of the histocompatibility marker HLA-DR. The mesenchymal stem cell markers CD73, CD90 and CD105 were significantly enhanced after ESWT treatment. The monocyte/macrophage marker CD14, the endothelial marker CD31, the haematopoietic progenitor/vascular endothelial marker CD34 and the haematopoietic marker CD45 were not affected through ESWT treatment, whereas the expression of the endothelial/pericytic marker CD146 was significantly increased compared with the untreated side. Data are presented as box-plots.  $n = 7$  for all tested markers except HLA-DR ( $n = 4$ ). \* $p < 0.05$ , \*\* $p < 0.01$



ESWT treatment did not affect the number of cells positive for the monocyte/macrophage marker CD14, with 7.1% for both untreated and ESWT-treated sides (Figure 3). Also, expression of the endothelial marker CD31, the haematopoietic progenitor/vascular endothelial marker CD34 and the haematopoietic marker CD45 was not significantly affected after ESWT treatment (Figure 3). Cells derived from the ESWT-treated side showed an expression of 32.1% CD31, 55.2% CD34 and 31.7% CD45, whereas cells derived from the untreated side showed an expression of 29.7% CD31, 48.3% CD34 and 29.3% CD45. By contrast, the endothelial/pericytic marker CD146 was significantly increased after ESWT treatment, with an expression of 14.3% compared with 8.4% for cells obtained from the untreated side (Figure 3).

### 3.3 | Enhanced differentiation potential after ESWT

Adipose tissue-derived cells from untreated and ESWT-treated sides were analysed for their *in vitro* adipogenic, osteogenic and chondrogenic differentiation potential. Upon adipogenic induction, cells obtained from the ESWT-treated side clearly showed more lipid droplet formation, analysed by Oil Red O staining (Figure 4a, b). This observation was confirmed by quantitative analysis, which demonstrated a significant difference between the untreated side with an extinction of 0.9 and the ESWT-treated side with 1.2 (Figure 4c). Osteogenic differentiation potential analysed by Alizarin Red staining for mineralization was also slightly enhanced after ESWT treatment, which is reflected in the quantitative analysis with an extinction of 1.4 for the untreated side and 1.8 for the ESWT-treated side (Figure 5a–c). Similarly, ALP activity was increased upon osteogenic

induction after ESWT treatment, with 427  $\mu\text{mol/l}$  compared with the untreated side with 379  $\mu\text{mol/l}$  (Figure 5d). Moreover, cells derived from the ESWT-treated side demonstrated a stronger chondrogenic differentiation potential, illustrated by intense Alcian Blue (glycosaminoglycans) (Figure 6a, b) and collagen type II staining compared with the untreated side (Figure 6c, d). The diameter area of the three-dimensional micromass pellets was similar after 7 days ( $1.1 \pm 0.1 \text{ mm}^2$  vs.  $1.2 \pm 0.3 \text{ mm}^2$ ), 14 days ( $1.0 \pm 0.1 \text{ mm}^2$  vs.  $0.9 \pm 0.2 \text{ mm}^2$ ), 21 days ( $0.9 \pm 0.2 \text{ mm}^2$  vs.  $0.8 \pm 0.3 \text{ mm}^2$ ) and 28 days ( $0.9 \pm 0.3 \text{ mm}^2$  vs.  $1.0 \pm 0.6 \text{ mm}^2$ ), but slightly increased after 35 days of chondrogenic induction ( $1.1 \pm 0.5 \text{ mm}^2$  vs.  $1.3 \pm 1.0 \text{ mm}^2$ ) for cells obtained from the ESWT-treated side (Figure 6e).

### 3.4 | Secretory protein profile after ESWT

In order to explore angiogenic proteins that might be involved in the ESWT-induced changes, supernatants of SVF cells were collected 24 h after isolation and protein expression was analysed. ESWT treatment showed substantial changes in the secretion of angiogenesis-related proteins. Cells derived from the ESWT-treated site showed a significantly enhanced expression of interleukin-6 (IL-6), monocyte chemoattractant protein-1 (MCP-1) and tissue inhibitor of metalloproteinase 1 (TIMP-1) (Figure 7). The expression of IL-6 was increased from 0.62- to 0.91-fold, MCP-1 from 0.74- to 0.93-fold and TIMP-1 from 0.47- to 0.68-fold. There was also a clear but not significant increase in the expression of EGF, IL-8, TIMP-2, urokinase-type plasminogen activator receptor (uPAR), IGF-1, leptin, thrombopoietin (TPO), VEGF-A and VEGF-D. All other analysed proteins did not show significant changes after ESWT treatment (Figure S2) and are summarized in Figure S1.

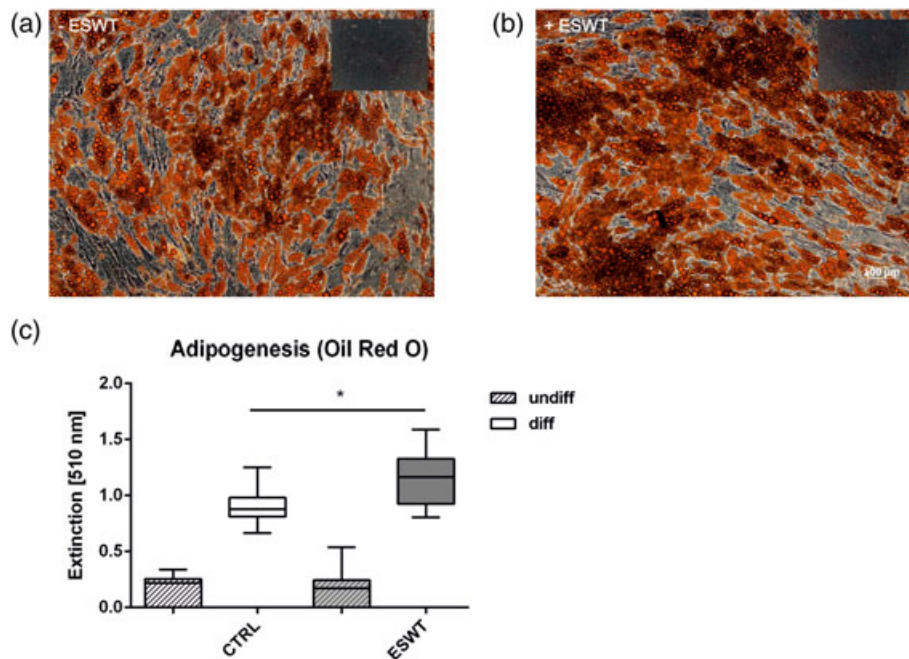


**FIGURE 4** Extracorporeal shock wave therapy (ESWT) *in situ* increases the adipogenic differentiation potential of isolated cells. Adipogenic induction resulted in a stronger Oil Red O staining of cells obtained from the ESWT-treated side compared with the untreated side (a, b), which was confirmed through quantitative analysis (c). Images show representative pictures, small inserts show cells in control medium without growth factors and stimuli (a, b). Regarding quantitative analysis of differentiation, all conditions showed a significant enhancement of differentiated cells compared with undifferentiated cells (c). undiff, cells in control medium without growth factors and stimuli; diff, cells in differentiation medium. Data are presented as box-plots (c).  $n = 4$  in triplicate. \* $p < 0.05$

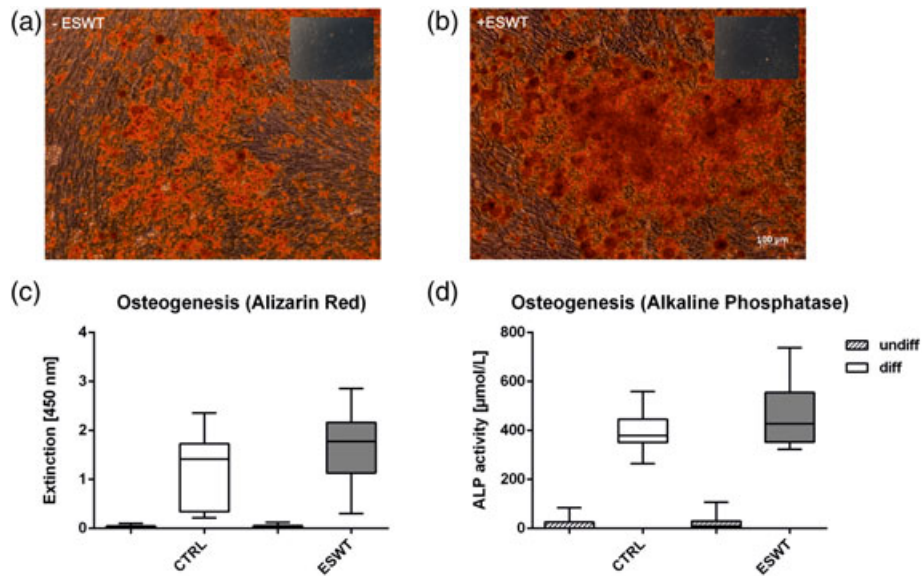


**FIGURE 5** Extracorporeal shock wave therapy (ESWT) *in situ* maintains the osteogenic differentiation potential of isolated cells. Osteogenic differentiation analysed by Alizarin Red staining was slightly enhanced after ESWT treatment (a, b), which was confirmed through quantitative analysis of the staining (c) as well as ALP activity (d). Images show representative pictures, small inserts show cells in control medium without growth factors and stimuli (a, b). Regarding quantitative analysis of differentiation, all conditions showed a significant enhancement of differentiated cells compared with undifferentiated cells (c, d). undiff, cells in control medium without growth factors and stimuli; diff, cells in differentiation medium. Data are presented as box-plots (c, d).  $n = 4$  in triplicate

## 4 | DISCUSSION

We have previously shown that the application of low-energy ESWT is promising for promoting stem cell properties in isolated cells derived from adipose tissue (Schuh et al., 2014; Schuh et al., 2016). Hence, the effect of ESWT applied to adipose tissue *in situ* on the regenerative cell populations present within their tissue microenvironment is worthwhile investigating.

In the present study we focused on the cell properties and functionality after shock wave treatment directly on the harvesting site in patients. Here we could demonstrate that ESWT applied *in situ* 1 week and 1 h before harvest resulted in significantly enhanced cell viability and ATP content in the isolated cell population, although the total cell yield remained unaffected. In a previous study, we demonstrated that ESWT on explanted rat sciatic nerves before isolation of Schwann cells significantly increased extracellular ATP. Subsequently, a number of effects were observed in culture: higher Schwann cell yield, higher cell purity and increased proliferation rate (Schuh et al., 2016). The release of ATP is triggered by ESWT, which could be proven in murine mesenchymal progenitor cells, primary human ASC and a human Jurkat T cell line *in vitro*. ATP release subsequently activates purinergic receptors and finally enhances proliferation via downstream Erk1/2 signalling (Weihs et al., 2014). ESWT-treated equine ASC showed increased proliferation, expression of Cx43, a gap junction protein and significant activation of Erk1/2, whereas no significant effect on the differentiation potential was observed (Raabe et al., 2013). Mitogen-activated protein kinases, including Erk1/2, regulate the stimulation of biophysical ESWT, thereby triggering mitogenic and osteogenic responses (Chen et al., 2004).

The proliferative activity of rat endothelial progenitor cells was optimally supported when cells were treated with ESWT within the

range of 0.10–0.13 mJ/mm<sup>2</sup> and 200–300 impulses, whereas higher-energy ESWT led to cell apoptosis (Zhang, Yan, Wang, Tang, & Chai, 2014). However, others have observed that ESWT with an energy intensity of 0.0016 mJ/mm<sup>2</sup> (at 4 kV) and 2000 pulses is able to disrupt pig adipose tissue (Liang, Chang, & Yang, 2014). Interestingly, we could corroborate an increase in proliferative potential after ESWT *in situ* with significant enhancement after 21 days in culture using an energy level of 120 mJ/cm<sup>2</sup> and two times 2000 impulses. The different outcomes can be explained by the type of shock waves (electrohydraulic, piezoelectric, electromagnetic, radial), applied energy (focused or unfocused, dose-dependent), the field of application (*in vitro*, *in vivo*, *in situ*) and the frequency of application (Ke et al., 2016; Lohrer, Nauck, Dorn-Lange, Scholl, & Vester, 2010; Lohrer, Nauck, Korakakis, & Malliaropoulos, 2016).

Furthermore, our ESWT *in situ* setting might activate stem and progenitor cells within their niches, leading to a significant higher amount of isolated cell populations expressing mesenchymal and endothelial/pericytic marker, while downregulating HLA-DR. In our previous study, ESWT in culture led to maintenance and significant elevation of mesenchymal markers (CD73, CD90, CD105) in human and rat ASC, accompanied by significantly increased differentiation capacity towards the osteogenic and adipogenic lineage as well as towards Schwann-cell like cells even after extended passaging, thus preserving multipotency of ASC *in vitro* (Schuh et al., 2014).

In this study, ESWT *in situ* increased significantly the adipogenic differentiation potential of isolated cells while osteogenic and chondrogenic differentiation was slightly enhanced. As the differentiation potential was analysed with a defined cell number, the adipogenic potential might not correlate to the cell yield obtained after isolation. This could, however, support the assumption that ESWT *in situ* targets a distinct subpopulation highly susceptible for adipogenic induction.

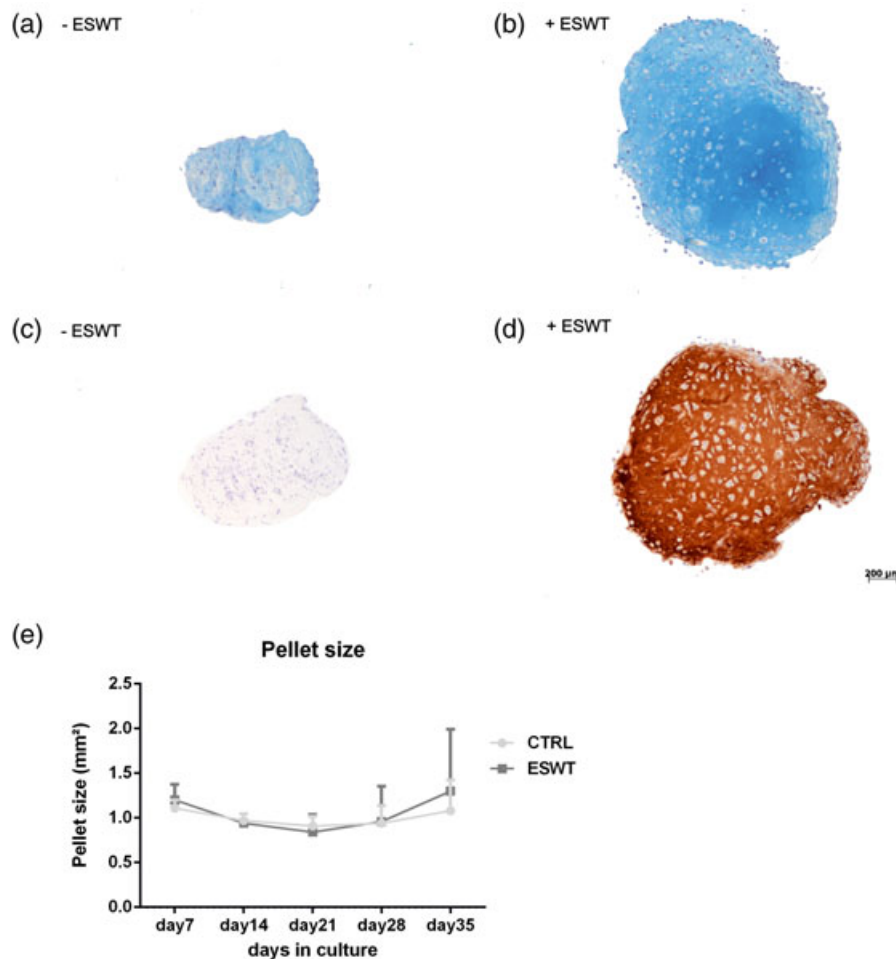


**FIGURE 6** Extracorporeal shock wave therapy (ESWT) *in situ* increases the chondrogenic differentiation potential of isolated cells. ESWT treatment increased chondrogenic differentiation resulting in stronger staining of Alcian Blue (a, b) and collagen type II (c, d) after 35 days, as well as a slightly increased diameter area of the three-dimensional micromass pellets after 35 days of chondrogenic induction (e). Images show representative pictures (a–d). Data are presented as mean  $\pm$  standard deviation (e).  $n = 3$

Dissimilar properties have been shown for ESWT-treated bone marrow mesenchymal stromal/stem cells (BMSC) from patients with avascular necrosis of the femoral head with induced osteoblast differentiation and concurrently inhibited adipogenic differentiation (Zhai et al., 2016). ESWT has also been shown to induce osteogenic activity of MG-63 cells seeded onto glass-ceramic scaffolds mediated by increased expression of bone morphogenetic proteins (Muzio et al., 2014). Apart from the mesodermal trilineage differentiation, ESWT treatment led to significantly accelerated human tendon-derived stem/progenitor cell differentiation *in vitro* (Leone et al., 2016).

A prerequisite in fat grafting is an early and abundant vascularization for nutrition supply and integration inside the surrounding tissue (Garza et al., 2014; Luo et al., 2013). ESWT may play a critical role in this manner as demonstrated in a previous study with enhanced lymphangiogenesis (Rohringer et al., 2014). ESWT induced VEGF expression in human umbilical vein endothelial cells (Holfeld et al., 2014). VEGF was secreted to culture medium and enhanced endothelial cell proliferation in an autocrine manner (Peng et al., 2015). Proliferation of rat BMSC and secretion of growth factors playing a role in regeneration settings as well as promotion of angiogenesis and nerve regeneration *in vitro* were enhanced by the application of ESWT (Zhao et al., 2013). In the present study we could

detect a substantial influence of ESWT treatment on the secretion of specific angiogenic proteins, such as IL-6, MCP-1 and TIMP-1. There was also a clear, although not significant, increase in the expression of EGF, IL-8, TIMP-2, uPAR, IGF-1, leptin, TPO, VEGF-A and VEGF-D. These factors might also have a paracrine impact on adipogenic differentiation of ASC. The pro-adipogenic impact of IGF-1 in SVF populations has been demonstrated previously (Hu et al., 2015). Leptin and IL-6 are also important markers in adipocyte differentiation (Vicennati, Vottero, Friedman, & Papanicolaou, 2002).

Within this study we could demonstrate the positive effect of ESWT applied *in situ* leading to enhanced cell properties, adipogenesis and angiogenesis *in vitro*. This set-up could reflect a clinical situation of a one-step procedure, avoiding risk factors such as a water bath, which is the prerequisite for ESWT *in vitro*, tissue processing, which requires a sterile workbench, collagenase, which might have a negative impact on cell efficacy, expansion of cells (ASC), which would be classified as advanced therapy medicinal product and would require central market authorization associated with high costs and stricter conditions. Conclusively, the use of ESWT *in situ* might be a promising tool to enhance the quality of fat grafts and in consequence a successful transplantation with long-term graft survival.

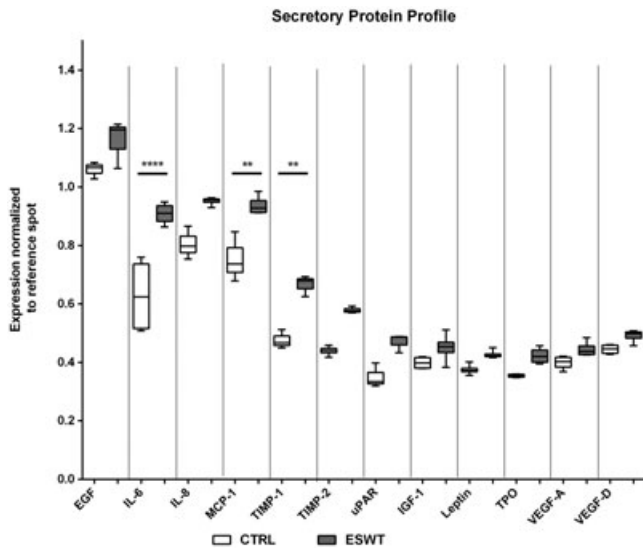


**FIGURE 7** Extracorporeal shock wave therapy (ESWT) *in situ* changes the secreted angiogenic protein profile of isolated cells. ESWT treatment showed substantial changes in the expression of angiogenesis-related proteins. Three analysed proteins demonstrated a significantly enhanced expression after ESWT treatment: interleukin-6 (IL-6), monocyte chemoattractant protein-1 (MCP-1) and tissue inhibitor of metalloproteinase 1 (TIMP-1). The expression of the following proteins was clearly but not significantly increased after ESWT: epidermal growth factor (EGF), IL-8, TIMP-2, urokinase-type plasminogen activator receptor (uPAR), insulin-like growth factor 1 (IGF-1), leptin, thrombopoietin (TPO), vascular endothelial growth factor A (VEGF-A) and VEGF-D. Data are presented as box-plots and represent duplicate measurements of two independent donors. \*\* $p < 0.01$ , \*\*\*\* $p < 0.0001$

## ACKNOWLEDGEMENTS

We would like to acknowledge Susanne Suessner and Christina M. A. P. Schuh for excellent technical support and flow cytometric analysis.

## CONFLICT OF INTEREST

We exclude any conflict of interest and guarantee that all authors are in complete agreement with the contents and submission of this manuscript. Furthermore, we declare that our work is original research, unpublished and not submitted to another journal.

## REFERENCES

- Amar, R. E., & Fox, D. M. (2011). The facial autologous muscular injection (FAMI) procedure: An anatomically targeted deep multiplane autologous fat-grafting technique using principles of facial fat injection. *Aesthetic Plastic Surgery*, 35(4), 502–510.
- Anghern, F., Kuhn, C., & Voss, A. (2007). Can cellulite be treated with low-energy extracorporeal shock wave therapy? *Clinical Interventions in Aging*, 2(4), 623–630.
- Antonic, V., Mittermayr, R., Schaden, W., & Stojadinovic, A. (2011). Evidence supporting extracorporeal shock wave therapy for acute and chronic soft tissue wounds. *Wounds*, 23(7), 204–215.
- Calabrese, C., Orzalesi, L., Casella, D., & Cataliotti, L. (2009). Breast reconstruction after nipple/areola-sparing mastectomy using cell-enhanced fat grafting. *Eccancermedicalscience*, 3, 116.
- Cebicci, M. A., Sutbeyaz, S. T., Goksu, S. S., Hocaoglu, S., Oguz, A., & Atilabey, A. (2016). Extracorporeal shock wave therapy for breast cancer related lymphedema: A pilot study. *Archives of Physical Medicine and Rehabilitation*, 97(9), 1520–1525.

- Chen, Y. J., Kuo, Y. R., Yang, K. D., Wang, C. J., Sheen Chen, S. M., Huang, H. C., ... Wang, F. S. (2004). Activation of extracellular signal-regulated kinase (ERK) and p38 kinase in shock wave-promoted bone formation of segmental defect in rats. *Bone*, 34(3), 466–477.
- Coleman, S. R., & Katzel, E. B. (2015). Fat grafting for facial filling and regeneration. *Clinics in Plastic Surgery*, 42(3), 289–300, vii.
- de Girolamo, L., Stanco, D., Galliera, E., Vigano, M., Lovati, A. B., Marazzi, M. G., ... Sansone, V. (2014). Soft-focused extracorporeal shock waves increase the expression of tendon-specific markers and the release of anti-inflammatory cytokines in an adherent culture model of primary human tendon cells. *Ultrasound in Medicine & Biology*, 40(6), 1204–1215.
- Garza, R. M., Paik, K. J., Chung, M. T., Duscher, D., Gurtner, G. C., Longaker, M. T., & Wan, D. C. (2014). Studies in fat grafting: Part III. Fat grafting irradiated tissue-improved skin quality and decreased fat graft retention. *Plastic and Reconstructive Surgery*, 134(2), 249–257.
- Gentile, P., Orlandi, A., Scioli, M. G., Di Pasquali, C., Bocchini, I., Curcio, C. B., ... Cervell, V. (2012). A comparative translational study: The combined use of enhanced stromal vascular fraction and platelet-rich plasma improves fat grafting maintenance in breast reconstruction. *Stem Cells Translational Medicine*, 1(4), 341–351.
- Gir, P., Oni, G., Brown, S. A., Mojallal, A., & Rohrich, R. J. (2012). Human adipose stem cells: Current clinical applications. *Plastic and Reconstructive Surgery*, 129(6), 1277–1290.
- Holfeld, J., Tepekoylu, C., Blunder, S., Lobenwein, D., Kirchmair, E., Dietl, M., ... Grimm, M. (2014). Low energy shock wave therapy induces angiogenesis in acute hind-limb ischemia via VEGF receptor 2 phosphorylation. *PLoS One*, 9(8), e103982.
- Hu, L., Yang, G., Hagg, D., Sun, G., Ahn, J. M., Jiang, N., ... Mao, J. J. (2015). IGF1 promotes adipogenesis by a lineage bias of endogenous adipose stem/progenitor cells. *Stem Cells*, 33(8), 2483–2495.
- Jiang, A., Li, M., Duan, W., Dong, Y., & Wang, Y. (2015). Improvement of the survival of human autologous fat transplantation by adipose-derived stem-cells-assisted lipotransfer combined with bFGF. *Scientific World Journal*, 2015, 968057.
- Ke, M. J., Chen, L. C., Chou, Y. C., Li, T. Y., Chu, H. Y., Tsai, C. K., & Wu, Y. T. (2016). The dose-dependent efficiency of radial shock wave therapy for patients with carpal tunnel syndrome: A prospective, randomized, single-blind, placebo-controlled trial. *Scientific Reports*, 6, 38344.
- Lei, H., Liu, J., Li, H., Wang, L., Xu, Y., Tian, W., ... Xin, Z. (2013). Low-intensity shock wave therapy and its application to erectile dysfunction. *World Journal of Men's Health*, 31(3), 208–214.
- Leone, L., Raffa, S., Vetrano, M., Ranieri, D., Malisan, F., Scrofani, C., ... Visco, V. (2016). Extracorporeal shock wave treatment (ESWT) enhances the *in vitro*-induced differentiation of human tendon-derived stem/progenitor cells (hTSPCs). *Oncotarget*, 7(6), 6410–6423.
- Liang, S. M., Chang, M. H., & Yang, Z. Y. (2014). Development and performance evaluation of an electromagnetic-type shock wave generator for lipolysis. *Review of Scientific Instruments*, 85(1), 015113.
- Lohrer, H., Nauck, T., Dorn-Lange, N. V., Scholl, J., & Vester, J. C. (2010). Comparison of radial versus focused extracorporeal shock waves in plantar fasciitis using functional measures. *Foot and Ankle International*, 31(1), 1–9.
- Lohrer, H., Nauck, T., Korakakis, V., & Malliaropoulos, N. (2016). Historical ESWT paradigms are overcome: A narrative review. *Biomed Research International*, 2016, 3850461
- †Luo, S., Hao, L., Li, X., Yu, D., Diao, Z., Ren, L., & Xu, H. (2013). Adipose tissue-derived stem cells treated with estradiol enhance survival of autologous fat transplants. *Tohoku Journal of Experimental Medicine*, 231(2), 101–110.
- Mittermayr, R., Antonic, V., Hartinger, J., Kaufmann, H., Redl, H., Teot, L., ... Schaden, W. (2012). Extracorporeal shock wave therapy (ESWT) for wound healing: Technology, mechanisms, and clinical efficacy. *Wound Repair and Regeneration*, 20(4), 456–465.
- Muzio, G., Martinasso, G., Baino, F., Frairia, R., Vitale-Brovarene, C., & Canuto, R. A. (2014). Key role of the expression of bone morphogenetic proteins in increasing the osteogenic activity of osteoblast-like cells

- exposed to shock waves and seeded on bioactive glass-ceramic scaffolds for bone tissue engineering. *Journal of Biomaterials Applications*, 29(5), 728–736.
- Neuber, F. F. (1893). Bericht über die Verhandlungen der Deutschen Gesellschaft fuer Chirurgie. *Zentralblatt für Chirurgie*, 22, 66.
- Oberbauer, E., Steffenhagen, C., Feichtinger, G., Hildner, F., Hacobian, A., Danzer, M., ... Wolbank, S. (2016). A luciferase-based quick potency assay to predict chondrogenic differentiation. *Tissue Engineering Part C Methods*, 22(5), 487–495.
- Peng, L., Jia, Z., Yin, X., Zhang, X., Liu, Y., Chen, P., ... Zhou, C. (2008). Comparative analysis of mesenchymal stem cells from bone marrow, cartilage, and adipose tissue. *Stem Cells and Development*, 17(4), 761–773.
- Peng, Y. Z., Zheng, K., Yang, P., Wang, Y., Li, R. J., Li, L., ... Guo, T. (2015). Shock wave treatment enhances endothelial proliferation via autocrine vascular endothelial growth factor. *Genetics and Molecular Research*, 14(4), 19203–19210.
- Raabe, O., Shell, K., Goessl, A., Crispens, C., Delhasse, Y., Eva, A., ... Arnhold, S. (2013). Effect of extracorporeal shock wave on proliferation and differentiation of equine adipose tissue-derived mesenchymal stem cells in vitro. *American Journal of Stem Cells*, 2(1), 62–73.
- Rohringer, S., Holthoner, W., Hackl, M., Weihs, A. M., Runzler, D., Skalicky, S., ... Redl, H. (2014). Molecular and cellular effects of in vitro shockwave treatment on lymphatic endothelial cells. *PLoS One*, 9(12), e114806.
- Saggini, R., Figus, A., Troccola, A., Cocco, V., Saggini, A., & Scuderi, N. (2008). Extracorporeal shock wave therapy for management of chronic ulcers in the lower extremities. *Ultrasound in Medicine & Biology*, 34(8), 1261–1271.
- Salgarello, M., Visconti, G., & Farallo, E. (2010). Autologous fat graft in radiated tissue prior to alloplastic reconstruction of the breast: Report of two cases. *Aesthetic Plastic Surgery*, 34(1), 5–10.
- Sandhofer, M. (2015). Radial shockwave therapy after cryolipolysis™ in cellulite and lymphedema - A field report. *Cosmetic Medicine*, 36, 12–13.
- Sandhofer, M., & Schauer, P. (2015). Niche-specific fat transfer in the face. *Journal für Ästhetische Chirurgie*, 8(3), 129–132.
- Schuh, C. M., Heher, P., Weihs, A. M., Banerjee, A., Fuchs, C., Gabriel, C., ... Teuschl, A. H. (2014). In vitro extracorporeal shock wave treatment enhances stemness and preserves multipotency of rat and human adipose-derived stem cells. *Cytotherapy*, 16(12), 1666–1678.
- Schuh, C. M., Hercher, D., Stainer, M., Hopf, R., Teuschl, A. H., Schmidhammer, R., & Redl, H. (2016). Extracorporeal shockwave treatment: A novel tool to improve Schwann cell isolation and culture. *Cytotherapy*, 18(6), 760–770.
- Siems, W., Grune, T., Voss, P., & Brenke, R. (2005). Anti-fibrosclerotic effects of shock wave therapy in lipedema and cellulite. *Biofactors*, 24(1–4), 275–282.
- Suszynski, T. M., Sieber, D. A., Van Beek, A. L., & Cunningham, B. L. (2015). Characterization of adipose tissue for autologous fat grafting. *Aesthetic Surgery Journal*, 35(2), 194–203.
- Tandan, M., & Reddy, D. N. (2011). Extracorporeal shock wave lithotripsy for pancreatic and large common bile duct stones. *World Journal of Gastroenterology*, 17(39), 4365–4371.
- Tuin, A. J., Domerchie, P. N., Schepers, R. H., Willemsen, J. C., Dijkstra, P. U., Spijkervet, F. K., ... Jansma, J. (2016). What is the current optimal fat grafting processing technique? A systematic review. *Journal of Craniomaxillofacial Surgery*, 44(1), 45–55.
- Vicennati, V., Vottero, A., Friedman, C., & Papanicolaou, D. A. (2002). Hormonal regulation of interleukin-6 production in human adipocytes. *International Journal of Obesity and Related Metabolic Disorders*, 26(7), 905–911.
- Weihs, A. M., Fuchs, C., Teuschl, A. H., Hartinger, J., Slezak, P., Mittermayr, R., ... Runzler, D. (2014). Shock wave treatment enhances cell proliferation and improves wound healing by ATP release-coupled extracellular signal-regulated kinase (ERK) activation. *Journal of Biological Chemistry*, 289(39), 27090–27104.
- Yoshimura, K., Sato, K., Aoi, N., Kurita, M., Hirohi, T., & Harii, K. (2008). Cell-assisted lipotransfer for cosmetic breast augmentation: Supportive use of adipose-derived stem/stromal cells. *Aesthetic Plastic Surgery*, 32(1), 48–55. discussion 56–47
- Zhai, L., Sun, N., Zhang, B., Liu, S. T., Zhao, Z., Jin, H. C., ... Xing, G. Y. (2016). Effects of focused extracorporeal shock waves on bone marrow mesenchymal stem cells in patients with avascular necrosis of the femoral head. *Ultrasound in Medicine & Biology*, 42(3), 753–762.
- Zhang, X., Yan, X., Wang, C., Tang, T., & Chai, Y. (2014). The dose-effect relationship in extracorporeal shock wave therapy: The optimal parameter for extracorporeal shock wave therapy. *Journal of Surgical Research*, 186(1), 484–492.
- Zhao, Y., Wang, J., Wang, M., Sun, P., Chen, J., Jin, X., & Zhang, H. (2013). Activation of bone marrow-derived mesenchymal stromal cells—a new mechanism of defocused low-energy shock wave in regenerative medicine. *Cytotherapy*, 15(12), 1449–1457.

## SUPPORTING INFORMATION

Additional Supporting Information may be found online in the supporting information tab for this article.

**Figure S1.** Overview of angiogenesis array membranes. Membranes include 43 different angiogenesis-related proteins, which are spotted in duplicates. Membranes were exposed to X-ray films and show different spot densities (a). Allocation of proteins throughout the membranes (b)

**Figure S2.** Angiogenic protein profiles of the angiogenesis array. ESWT treatment showed no significant changes in the expression of these angiogenesis-related proteins. Data are presented as box-plots and represent duplicate measurements of two independent donors

**How to cite this article:** Priglinger E, Sandhofer M, Peterbauer A, et al. Extracorporeal shock wave therapy *in situ* – novel approach to obtain an activated fat graft. *J Tissue Eng Regen Med*. 2017;1–11. <https://doi.org/10.1002/term.2467>



# Photobiomodulation of freshly isolated human adipose tissue-derived stromal vascular fraction cells by pulsed light-emitting diodes for direct clinical application

Short title: Light-emitting diodes modulate stromal vascular fraction

**Priglinger E.<sup>1,2\*</sup>, Maier J.<sup>1,2\*</sup>, Chaudary S.<sup>1,2</sup>, Lindner C.<sup>1,2</sup>, Wurzer C.<sup>1,2,3</sup>, Rieger S.<sup>1,2</sup>, Redl H.<sup>1,2</sup>, Wolbank S.<sup>1,2</sup>, Dungel P.<sup>1,2</sup>**

<sup>1</sup>Ludwig Boltzmann Institute for Experimental and Clinical Traumatology, AUVA Research Center, Linz/Vienna, Austria

<sup>2</sup>Austrian Cluster for Tissue Regeneration, Vienna, Austria

<sup>3</sup>Liporegena GmbH, Breitenfurt, Austria

**\*These authors contributed equally**

Keywords: Low Level Light Therapy, LED, Photostimulation, Photobiomodulation, Adipose Tissue, Stromal Vascular Fraction, Vascularization, VEGF

## **Corresponding Author:**

Dr. Eleni Priglinger

eleni.priglinger@trauma.lbg.ac.at

Ludwig Boltzmann Institute for Experimental and Clinical Traumatology

Donaueschingenstraße 13

A-1200 Vienna, Austria

Tel.: +43 (0) 5 93 93-41961

Fax: +43 (0) 5 93 93-41982

This article has been accepted for publication and undergone full peer review but has not been through the copyediting, typesetting, pagination and proofreading process which may lead to differences between this version and the Version of Record. Please cite this article as doi: 10.1002/term.2665

## Abstract

A highly interesting source for adult stem cells is adipose tissue, from which the stromal vascular fraction (SVF) - a heterogeneous cell population including the adipose-derived stromal/stem cells (ASC) - can be obtained. To enhance the regenerative potential of freshly isolated SVF cells low level light therapy (LLLT), was used. The effects of pulsed blue (475 nm), green (516 nm) and red light (635 nm) from light-emitting diodes (LEDs) applied on freshly isolated SVF were analyzed regarding cell phenotype, cell number, viability, adenosine triphosphate content, cytotoxicity and proliferation, but also osteogenic, adipogenic and pro-angiogenic differentiation potential. The colony-forming unit fibroblast assay revealed a significantly increased colony size after LLLT with red light compared to untreated cells, whereas the frequency of colony forming cells was not affected. LLLT with green and red light resulted in a stronger capacity to form vascular tubes by SVF when cultured within 3D fibrin matrices compared to untreated cells, which was corroborated by increased number and length of the single tubes and a significantly higher concentration of vascular endothelial growth factor. Our study showed beneficial effects after LLLT on the vascularization potential and proliferation capacity of SVF cells. Therefore, LLLT using pulsed LED light might represent a new approach for activation of freshly isolated SVF cells for direct clinical application.

## 1. Introduction

Clinical applications using mesenchymal stem cells (MSC) have become increasingly important over the past years. Their ability to differentiate into many lineages and support regeneration holds promise for a wide field of treatments ranging from wound healing (Kim et al., 2007), cardiac diseases (Faiella and Atoui, 2016), neurodegenerative disorders (Lindvall et al., 2004), leukemia (Lane et al., 2009) and other areas of tissue regeneration (Gimble et al., 2007). MSC, as one of the main investigated types of adult stem cells, can be isolated from many different sources such as adipose tissue, bone marrow, muscle, connective tissue, skin, placenta, blood, cord blood, synovium, periosteum and perichondrium (Arai et al., 2002; De Bari et al., 2001; In 't Anker et al., 2004; Parolini et al., 2008; Wakitani et al., 1994; Young et al., 2001; Zuk et al., 2001; Zvaifler et al., 2000). These cells have proven a wide range of differentiation into adipocytes, chondrocytes, osteocytes and myocytes (Pittenger et al., 1999), as well as pro-regenerative properties such as secretion of anti-apoptotic, anti-inflammatory, immunomodulatory, anti-fibrotic and pro-angiogenic factors (Kronsteiner et al., 2011; Rehman et al., 2004), which makes them an attractive option for development of clinical applications in regenerative medicine. One main source for MSC nowadays is adipose tissue, which can be easily processed from liposuction material. Adipose-derived stromal/stem cells (ASC) are a part of the stromal vascular fraction (SVF) (Lin et al., 2010), a heterogeneous cell population consisting of preadipocytes, fibroblasts, vascular smooth muscle cells, endothelial cells, endothelial progenitor cells, macrophages and lymphocytes among others (Bourin et al., 2013; Zimmerlin et al., 2010), which can be obtained from liposuction material. The adherent SVF cell fraction includes predominantly ASC, which allows selection and expansion of these cells on plastic surfaces in expansion media *in vitro*.



An advantage of using SVF cells is the direct clinical application after isolation in a one-step procedure. *In vitro* and *in vivo* studies have shown beneficial influence of ASC and their secretome in experimental settings of wound healing (Kapur and Katz, 2013). Examinations of ASC applied to skin wound and *in vitro* models revealed enhanced fibroblast proliferation, collagen secretion, re-epithelialization, macrophage polarization, skin blood perfusion, extracellular matrix production and angiogenesis (Ebrahimian et al., 2009; Kim et al., 2007; Lau et al., 2009), all important elements of wound healing.

Similar effects on wound healing processes were shown by applying low level light therapy (LLLT). Cellular functions, such as angiogenesis, macrophage activation, fibroblast proliferation, collagen deposition and tissue repair (Huang, 2009) were positively influenced by LLLT. Up to date, other clinical uses of LLLT include pain relief, treatment of neurological and chronic joint disorders and reducing inflammation (Chung et al., 2012). Several studies already aimed to investigate the effects of LLLT on stem cells on a cellular level. Investigations of low level lasers on MSC cultures derived from bone marrow or adipose tissue *in vitro* and *in vivo* revealed enhanced cell proliferation, viability, osteogenic differentiation and tissue regeneration (Kim et al., 2012; Mvula et al., 2010; Tuby et al., 2007).

The biological mechanisms of LLLT are not yet fully understood but are assumed to enhance metabolic activity involving adenosine triphosphate (ATP) production (Huang, 2009) leading to an enhanced regenerative potential for biological tissues. Within the electron transport chain cytochrome c oxidase has been identified as one responsible chromophore associated with light-induced increase in ATP production (Karu et al., 2004). Standard treatments on patients and animals are up to date performed with red and near-infrared light (Huang, 2009) leading to successful

influences on wound healing (Fekrazad et al., 2015; Rodrigo et al., 2009). Recently, we investigated the effects of blue light at 470 nm and found that it has comparable effects on wound healing and NO release *in vivo* (Adamskaya et al., 2011; Mittermayr et al., 2007). Additionally we showed that NO-inhibited mitochondria can be effectively reactivated with blue light by releasing NO from cytochrome oxidase and other mitochondrial heme proteins (Dungel et al., 2008). An alternative biological mechanism of LLLT seems to involve circadian clock proteins, which have been demonstrated to respond with translocation after LLLT (Kushibiki and Awazu, 2007; Kushibiki and Awazu, 2008).

Up to date LLLT is mostly performed with laser light, however light-emitting diodes (LEDs) represent an appropriate alternative without the laser's disadvantages such as local heat production, narrow beam width and high costs. Comparative studies using lasers and LEDs came to the conclusion that no significant differences were detectable in connection with wound healing, angiogenesis and proliferation (Corazza et al., 2007; de Vasconcelos Catao et al., 2015; Klebanov et al., 2005).

Within this study, we hypothesized that LLLT might be a suitable method to enhance the potential of cell therapeutics within a one-step procedure. Therefore, we investigated the effects of blue, green and red light emitted by LEDs directly on freshly isolated SVF from human liposuction material and analyzed cell phenotype, cell number, viability, ATP content, LDH cytotoxicity and proliferation, but also osteogenic, adipogenic and pro-angiogenic differentiation potential *in vitro*.

## 2. Methods

### 2.1. SVF isolation and cultivation

The collection of human adipose tissue was approved by the local ethical board with written patient's consent. Subcutaneous adipose tissue was obtained during routine outpatient liposuction procedures under local tumescence anaesthesia. All 13 patients were female at an age of  $45 \pm 11$  and with a BMI of  $29 \pm 6$ . For SVF isolation 100 ml liposuction material was transferred to a blood bag (Macopharma, Langen, Germany) and washed with an equal volume of phosphate buffered saline (PBS) to remove blood and tumescence solution. Afterwards, for tissue digestion PBS was replaced with 0.2 U/ml collagenase NB4 (Serva, Vienna, Austria) dissolved in 100 ml PBS containing  $\text{Ca}^{2+}/\text{Mg}^{2+}$  and 25 mM N-(2-hydroxyethyl)piperazine-N'-(2-ethanesulfonic acid) (HEPES; Sigma, Vienna, Austria) and the blood bag was incubated at  $37^{\circ}\text{C}$  under moderate shaking (180 rpm) for 1 hour. The digested tissue was transferred into 50 ml-tubes. After centrifugation at 1200 g for 7 minutes the cell pellet was incubated with 100 ml erythrocyte lysis buffer for 5 minutes at  $37^{\circ}\text{C}$  to eliminate red blood cells. The supernatant was aspirated after centrifugation for 5 minutes at 500 g. The pellet was washed with PBS and filtered through a 100- $\mu\text{m}$  cell strainer (Greiner, Kremsmünster, Austria). After another centrifugation step at 500 g for 5 minutes the supernatant was removed. The isolated SVF cells were resuspended in endothelial growth medium (EGM-2; Lonza, Vienna, Austria) for LLLT stimulation. After LLLT stimulation, SVF cells were used for further analyses or cultured in EGM-2 at  $37^{\circ}\text{C}$ , 5%  $\text{CO}_2$ , and 95% air humidity. After seeding the SVF cells on plastic surface in expansion medium (EGM-2), the adherent cell fraction including ASC can outgrow as an adherent monolayer. The cells were cultured to a subconfluent state and detached with 1x trypsin/EDTA at  $37^{\circ}\text{C}$ . Medium was changed every 3 to 4 days.

## **2.2. Low Level Light Therapy (LLLT)**

LED lamps for light therapy were provided by Repuls Lichtmedizintechnik GmbH, Vienna, Austria. Freshly isolated SVF cells were divided in 4 different tubes (Cryo.s, Greiner bio-one) with  $5 \times 10^6$  cells in 2 ml EGM-2. Cells were treated with pulsed LED light of either 475 nm (blue), 516 nm (green), 635 nm (red) at room temperature for 10 minutes from a distance of 7 cm while unstimulated controls were treated equally but protected from light. All LED devices had a peak irradiance intensity of  $80 \text{ mW/cm}^2$ , which was measured with a USB 2000 spectrometer (Ocean Optics, FL, USA). Given the pulse rate of 50% and a repetition frequency of 2.5 Hz, an average irradiance intensity of  $40 \text{ mW/cm}^2$  was used, resulting in a fluence of  $24 \text{ J/cm}^2$ .

## **2.3. Flow cytometry analysis**

Freshly isolated SVF cells were characterized using the following antibodies: cluster of differentiation (CD)31-FITC (eBiosciences, Vienna, Austria), CD34-APC (BD, Schwechat, Austria), CD45-PerCP (BD), CD73-FITC (eBiosciences), CD90-PE (eBiosciences), CD105-PE (eBiosciences), CD146-PerCP (R&D, Wiesbaden-Nordenstadt, Germany) and human leukocyte antigen-antigen D related (HLA-DR)-PE (eBiosciences). For staining,  $5 \times 10^5$  cells in 50  $\mu\text{L}$  PBS with 1% fetal calf serum (FCS; PAA, Pasching, Austria) were incubated with 5  $\mu\text{l}$  primary labeled antibodies at room temperature for 15 minutes in the dark. Cells were washed with 1.5 ml Cell Wash™ (BD) and centrifuged for 5 minutes at 400 g. The supernatant was discarded and the cell pellet resuspended in 300  $\mu\text{L}$  1 x Cell Fix™ (BD; diluted 1:10 with aqua dest). Samples were analyzed on a FACSCalibur (BD).

#### **2.4. Cytotoxicity by lactate dehydrogenase (LDH) release**

For quantification of LDH release, cellular supernatants were analyzed using Cytotoxicity Detection Kit (Roche, Vienna, Austria). Freshly isolated SVF cells were seeded at a density of  $2 \times 10^4$  in a 96-well plate in 200  $\mu\text{L}$  EGM-2 and incubated for 24 hours. SVF cells seeded in 100  $\mu\text{L}$  EGM-2 and 100  $\mu\text{L}$  Triton X-100 (Sigma) was used as control for 100 % dead cells. After an incubation of 24 hours 100  $\mu\text{L}$  of each supernatant was transferred into a new well and 100  $\mu\text{L}$  Reaction mixture was added for 0.5 hours. Absorbance was measured with an Infinite® M200 Multimode Microplate Reader (Tecan, Grödig, Austria) at 490 nm and after subtraction of a reference value at 650 nm it was normalized to positive control Triton X-100, which lyses the cells.

#### **2.5. Cell number and viability**

Cell number after LLLT was determined using trypan blue exclusion and quantification in a cell counter (TC-20, Biorad, Vienna, Austria). For measuring cell viability of freshly isolated SVF cells and cells after one week in culture, the percentage of living cells compared to total cell count was analyzed with the cell counter.

#### **2.6. Cellular ATP**

To determine the cellular ATP concentration, CellTiter-Glo® Luminescent Cell Viability Assay (Promega, Mannheim, Germany) was used and performed according to the manufacturer's instructions. Freshly isolated SVF cells and cells after one week in culture were seeded at a density of  $1 \times 10^4$  cells per well in a black 96-well plate (Greiner) in 100  $\mu\text{L}$  EGM-2 and ATP concentration was measured after 2 hours. For this purpose, 100  $\mu\text{L}$  CellTiter-Glo® Reagent were added to each well and the plate was gently agitated on a shaker for 2 minutes. Afterwards the plate was incubated for

10 minutes in the dark. The luminescent signal was detected with an Infinite® M200 Multimode Microplate Reader at an exposure time of 2 seconds and correlated to an ATP standard curve.

### **2.7. Colony-forming unit fibroblast (CFU-F) assay**

A defined number of SVF cells (4, 20, 100, 500, 2500, 12500) was seeded in each well of a 6-well plate and cells were cultured in EGM-2 for 14 days. Medium was changed on day 7 after cell seeding. After 14 days of culture, cells were fixed with 4% formaldehyde and stained with hematoxylin. Afterwards, the cells were washed with tap water and stained with eosin solution (Roth/Lactan, Graz, Austria). The percentage of cells that formed visible colonies was calculated and compared to the total number of seeded cells. The colony diameter was measured using ImageJ (NIH, Bethesda, Maryland, USA). The minimum colony size was defined with a diameter of >1mm.

### **2.8. Adipogenic differentiation and detection**

For adipogenic differentiation, cells were seeded at a density of  $1.4 \times 10^4$  cells per well in a 24-well plate in EGM-2 and incubated over night. On the next day, medium was changed to adipogenic differentiation medium DMEM-high glucose (Lonza) containing 10% FCS, 2 mM L-glutamine (PAA), 100 U/ml Pen/Strep (Lonza), 1  $\mu$ M dexamethasone (Sigma), 0.5 mM 3-isobutyl-1-methylxanthine (IBMX; Sigma), 10  $\mu$ g/ml insulin (Sigma) and 100  $\mu$ M indomethacin (Sigma) or control medium consisting of DMEM:F12 / L-glutamine (Lonza) with 10% FCS and 100 U/ml Pen/Strep. Medium was changed every 3 to 4 days. After 21 days, adipogenic differentiation was analyzed with Oil Red O staining and quantification. Cells were fixed with 4% formaldehyde for 1 hour. After washing with aqua dest, the cells were rinsed with 70% ethanol for 2

minutes and stained for 5-15 minutes with Oil Red O solution (Sigma). Then the cells were washed with aqua dest, counterstained for 1-3 minutes with hematoxylin solution and blued with tap water. For quantitative detection of Oil Red O staining, the supernatant was discarded and 500 µl isopropanol were added in each well. After resuspension, the mixture of cells and isopropanol was transferred to a transparent 96-well plate (100 µl per well). The absorbance was measured at 510 nm with an Infinite® M200 Multimode Microplate Reader.

### **2.9. Osteogenic differentiation and detection**

For osteogenic differentiation, cells were seeded at a density of  $2 \times 10^3$  cells per well in a 24-well plate in EGM-2 and incubated over night. On the next day, medium was changed to osteogenic differentiation medium DMEM-low glucose (Lonza) containing 10% FCS, 2 mM L-glutamine, 100 U/ml Pen/Strep, 10 nM dexamethasone, 150 µM ascorbat-2-phosphate (Sigma), 10 mM β-glycerophosphate (StemCell Technologies, Cologne, Germany) and 10 nM dihydroxy-vitamin D3 (Sigma) or control medium consisting of DMEM:F12 / L-glutamine with 10% FCS and 100 U/ml Pen/Strep. Medium was changed every 3 to 4 days. After 21 days, osteogenic differentiation was analyzed with Alizarin Red staining and quantification, as well as determination of intracellular alkaline phosphatase (ALP) activity. For Alizarin Red staining of calcified structures, cells were fixed for 1 hour with 70% ethanol at -20°C and stained with Alizarin Red solution (Merck, Vienna, Austria) for 15 minutes. For quantitative analysis of Alizarin Red staining, the supernatant was discarded and the cells were incubated with 500 µl 20% methanol and 10% acidic acid (diluted in aqua dest) for 15 minutes. After resuspension, the mixture of cells and methanol / acidic acid was transferred to a transparent 96-well plate (100 µl per well). The absorbance was measured at 450

nm with an Infinite® M200 Multimode Microplate Reader. The second method to analyze osteogenic differentiation is the detection of the activity of intracellular ALP. Cells were incubated with 100 µl PBS for 1 hour at -20°C. Afterwards, the cells were lysed for 1 hour by addition of 100 µl PBS containing 0.5% TritonX-100 (Sigma). For quantitative detection of ALP activity, 100 µl substrate solution (4-nitrophenylphosphate) were added in each well and incubated for 1 hour in the dark. Finally, the solution was transferred to a transparent 96-well plate (100 µl per well) and absorbance was measured at 405 nm together with a reference wavelength of 620 nm in an Infinite® M200 Multimode Microplate Reader. By creating a standard curve with known p-nitrophenol concentrations diluted in a solution containing 0.5% TritonX-100 diluted in PBS 1:2 and measuring the corresponding absorption, the ALP activity of the samples was calculated.

### **2.10. Vascularization induction and detection**

For determination of the vascularization potential of SVF cells, a fibrin clot culture was performed (Holthoner et al., 2015).  $4 \times 10^5$  SVF cells were mixed with fibrinogen (2.5 mg/mL; Baxter, Vienna, Austria) and thrombin (0.2 U/mL; Baxter) for clot formation and pipetted on coverslips in 12-well plates. Clots were polymerized at 37°C for 30 minutes and cultured for 2 weeks in EGM-2 containing aprotinin (100 KIU/mL; Baxter). Medium was changed every 3-4 days. After cultivation clots were fixed with 4% paraformaldehyde (PFA), washed with PBS and incubated with a FITC-conjugated monoclonal mouse anti-human CD31 antibody (1:50 dilution in PBS/1%BSA; BD Biosciences) for 12 hours in the dark. Clots were again washed with PBS and images were taken on a fluorescence microscope (Axiovert 200; Zeiss, Vienna, Austria).



Number of vascular tubes per picture was counted and length of tubes was measured using ImageJ.

### **2.11. Vascular endothelial growth factor (VEGF) concentration**

For analysis of human VEGF, the supernatant of SVF cells in fibrin clot cultures was analyzed after 2 weeks with a DuoSet ELISA Development System kit (R&D Systems). Supernatant was collected and stored at  $-80^{\circ}\text{C}$  until analysis. The DuoSet ELISA Development System kit was performed according to the manufacturer's instructions. Briefly, a 96-well plate was coated with the Capture Antibody and incubated overnight. After blocking the plates with 1% BSA in PBS for 1 hour the samples were added and incubated for 2 hours. Afterwards, the plate was incubated for 2 hours with the Detection Antibody followed by addition of Streptavidin-HRP and incubation in the dark for 20 minutes. Each of the described steps was followed by a washing step with 0.05% Tween20 in PBS. Then, the plate was incubated in the dark for 20 minutes with a mixture of Color Reagent A ( $\text{H}_2\text{O}_2$ ) and Color Reagent B (Tetramethylbenzidine) before directly adding 2N  $\text{H}_2\text{SO}_4$  to stop the reaction. Immediately afterwards, absorbance was measured at 450 nm together with a reference wavelength of 540 nm in an Infinite® M200 Multimode Microplate Reader and correlated to a VEGF standard curve.

### **2.12. Statistical analysis**

Data are presented as scatter plots showing observations from single donors and mean lines or mean  $\pm$  standard deviation (SD). The dashed line represents the control condition, mean of untreated cells from all donors. Statistical analysis was performed using PRISM6 (GraphPad, San Diego, CA, USA), one-way ANOVA Tukey's post hoc,

or two-way ANOVA Tukey's post hoc for flow cytometry analysis. P values of < 0.05 were considered to be significant.

### **3. Results**

#### ***3.1. SVF cell characterization after LLLT***

Analysis of the cellular phenotype, i.e. expression of vascular, mesenchymal, pericytic and hematopoietic markers as well as combinations of them, in the SVF showed a similar cellular composition after LLLT with blue, green and red light and without LLLT treatment (Figure 1, Supplementary Figure 1). Approximately 40% of the cells were positive for the endothelial marker CD31. A similar number of cells was positive for the endothelial/pericytic marker CD146, whereas the number of CD34 (hematopoietic progenitor/vascular endothelial marker) positive cells was higher with approximately 60%. The percentage of mesenchymal marker was > 45% for CD73 and CD105 and > 55% for CD90. Less than 40% of the cells expressed the hematopoietic marker CD45 and approximately 50% the histocompatibility marker HLA-DR. Pairwise combination of CD markers showed no difference between LLLT with blue, green and red light and without LLLT treatment (Supplementary Figure 1).

#### ***3.2. SVF cell vitality after LLLT***

In order to exclude that LLLT has a negative impact on cell vitality we analyzed the cell cytotoxicity, cell number, viability and cellular ATP concentration. Blue, green and red LLLT did not show a cytotoxic effect as analyzed by the release of LDH (Figure 2a). LDH release was similar for blue, green and red light as well as untreated control cells (dashed line) but significantly reduced for all conditions compared to positive

control Triton X-100 ( $p < 0.0001$ ), which lyses all cells. There was a slightly but not significantly higher cell number ( $\sim 1.2$ -fold) after LLLT with blue ( $p=0.86$ ), green ( $p=0.90$ ) and red ( $p=0.91$ ) light compared to untreated control cells (dashed line) (Figure 2b). The viability was in a high range after LLLT with blue, green and red light with approximately 80% living cells and untreated control cells (dashed line) with 74% (Figure 2c). After one week in culture, viability was slightly increased (80-85% living cells) but did not show any differences between the conditions (Figure 2d). Since it has been shown that LLLT positively impacts ATP, an indicator for energy production and cell viability, we analyzed cellular ATP concentration. However, cellular ATP concentrations of both - freshly isolated cells and cells after one week in culture - were not affected by LLLT treatment (Figure 2e,f).

### **3.3. SVF properties after LLLT**

Morphology of the SVF cells was analyzed one day after isolation (Figure 3a). Untreated control cells as well as cells after LLLT had started to adhere to the plastic surface showing characteristic ASC spindle-shaped cell morphology. In all conditions lymphatic endothelial cells aggregated as small lymphatic islands. Analysis of the colony forming capacity of the cells demonstrated that untreated control and LLLT treated SVF cells were able to form colonies (Figure 3b). Although there were some variations in the number of colony forming cells within the conditions, quantitative analysis revealed equally high mean frequencies for the untreated control cells (dashed line) and red LLLT and only slightly lower frequencies after LLLT with blue ( $p=0.93$ ) and green ( $p=0.93$ ) light (0.8-fold) (Figure 3c). In contrast, LLLT with red light significantly enhanced the size of the formed colonies compared to untreated control cells (dashed line) (1.6-fold,  $p=0.04$ ; Figure 3d). After LLLT with blue light, colony size

was also increased 1.5-fold ( $p=0.14$ ) compared to untreated control cells (dashed line), although not reaching significance.

### **3.4. SVF differentiation capacity after LLLT**

Untreated and LLLT treated cells were analyzed for their *in vitro* adipogenic and osteogenic differentiation potential. Upon adipogenic induction, cells from all light conditions and untreated control cells (dashed line) showed equally high levels of lipid droplet formation, which was verified through quantitative analysis (Figure 4a,c). In contrast, LLLT with red light tended to increase the osteogenic differentiation potential compared to untreated control cells (dashed line). Despite high variations between the single donors, the mean level of Alizarin Red staining was slightly enhanced after LLLT with red light (1.2-fold,  $p=1.00$ ; Figure 4b,d). In comparison, slightly reduced levels of Alizarin Red staining were observed after LLLT with blue ( $p=0.98$ ) and green ( $p=0.92$ ) light (0.8-fold compared to control).

### **3.5. SVF vascular tube formation after LLLT**

Freshly isolated SVF cells were examined in 3D fibrin matrices for their potential to form vascular tubes *in vitro*. After 2 weeks incubation in expansion medium, gels were stained with the endothelial marker CD31 to visualize tube-like structures. The staining demonstrated that cells after LLLT with red and green light showed a stronger capacity to form tube-like structures compared to untreated cells and blue LLLT (Figure 5a). This observation was verified through quantitative analysis of vascular tube length. Tubes formed after LLLT with red light were significantly prolonged compared to

untreated control cells (dashed line) (1.5-fold,  $p=0.01$ ; Figure 5b). Moreover, the number of vascular tubes was also enhanced 1.2-fold ( $p=0.55$ ) after LLLT with red light compared to untreated control cells (dashed line), but this increase did not reach significance (Figure 5c). There was also a slight but not significant increase in the vascular tube length after green LLLT compared to untreated control cells (dashed line) (1.4-fold,  $p=0.06$ ). We further verified our observations by analyzing the VEGF concentration within the supernatants of the fibrin clot cultures (Figure 5d). VEGF concentration was significantly increased after LLLT with red (4-fold,  $p=0.0002$ ) and green light (4-fold,  $p=0.0005$ ) compared to untreated control cells (dashed line). After LLLT with blue light there was also a clear but not significant enhancement in VEGF concentration compared to untreated control cells (dashed line) (2-fold,  $p=0.16$ ).

#### 4. Discussion

Since adipose tissue is a highly vascularized tissue and a dynamic endocrine organ (Harwood, 2012) consisting of multiple regenerative cell types represented by the SVF (Bourin et al., 2013), we hypothesized, that application of LLLT might enhance its regenerative cell potential. Within the present study, we focused on the impact of single LLLT by pulsed LED light with 475 nm, 516 nm and 635 nm on freshly isolated SVF cell properties and their functionality. We were able to demonstrate beneficial properties after LLLT including enhanced vascularization potential and proliferation capacity of SVF cells.

Recently we could show that single application of extracorporeal shock wave therapy (ESWT) demonstrates beneficial effects on adipose tissue-derived SVF cells

(Priglinger et al., 2017). Therefore, a single light application could be preferable to repeated applications for future cell-therapies in a one-step procedure.

In contrast to our previous studies, where the number of mesenchymal and vascular endothelial cells was enhanced after a single application of ESWT on adipose tissue or freshly isolated SVF cells (Priglinger et al., 2017), a single application of LLLT on freshly isolated SVF cells had no effect on cell number, regardless of the used wavelength. The number of cells positive for CD34, CD73, CD90, CD105 and CD45 corroborate the percentages of the joint statement of IFATS and ISCT, only the number of cells positive for the vascular marker CD31 is with approximately 40% higher compared to <20% in the guidelines. Analysis of combined CD marker showed no difference between the applied wavelengths (Bourin et al., 2013; van Dongen et al., 2017). Paspaliaris et al. developed a cell isolation and activation device with lasers for SVF stimulation after the isolation process. They could demonstrate an increased number of SVF cells after the treatment with Adistem laser (green, yellow and red) (Paspaliaris and Thornton, 2014). Here, we could also observe a slightly higher cell count after LLLT with blue, green and red light compared to untreated cells, although not significant.

Further, we analyzed the cytotoxic impact of our single LLLT dose on SVF cells showing no difference between untreated cells and cells undergoing LLLT. Lugongolo et al. 2017 made an interesting observation after application of laser irradiation to infected (HIV-1) and uninfected cells, demonstrating no inhibitory effect on uninfected cells but induced cell damage in the HIV-1 infected cells in a dose dependent manner (Lugongolo et al., 2017). Another study was performed using the effect of photobiomodulation on endothelial cells where the LDH release was decreased and the viability increased after red and near-infrared laser treatment (Franco et al., 2016).

Within our setting, the viability of our freshly isolated SVF cells was still in a high range after 10 minutes exposure to blue, green and red LLLT compared to untreated cells.

In contrast to literature where LLLT was found to trigger ATP production in cells (Mvula et al., 2010; Ong et al., 2013), we could not see enhanced ATP concentration independently of the applied wavelength. This difference might be due to our set-up using one single application of LLLT after SVF isolation. Li et al. reported that multiple stimuli of LLLT are required to promote cell growth, whereas Hawkings et al. showed that the application of a single dose is more beneficial to restore cell function than multiple doses (Hawkins and Abrahamse, 2007; Li et al., 2010). In addition, LLLT is known to trigger alternative mechanisms involving circadian clock proteins and the circadian transcriptional and post-translational apparatus in cells. Kushibiki et al. demonstrated that blue laser irradiation of mouse MSC promotes the translocation of circadian rhythm protein cryptochrome 1 (CRY1) from the cytoplasm to the nucleus and enhances osteogenesis at the expense of adipogenesis (Kushibiki and Awazu, 2007; Kushibiki and Awazu, 2008). Different wavelengths are associated with re-setting the body's biological clock, while short wavelengths seem to be more effective (Duffy and Czeisler, 2009).

Cell proliferation can be positively influenced by LLLT as already shown in various studies (Emelyanov and Kiryanova, 2015; Li et al., 2013; Lipovsky et al., 2013; Min et al., 2015). This is in consistence with our findings of increased sizes of colonies in the CFU-F assay. While the number of colonies indicated equal numbers of stem cells, the increased size of the colonies represents a higher proliferation potential after single red LLLT. This is exactly opposite to the study of Khan et al. where the size of the colonies was not affected by different red light sources but the number of colonies was significantly elevated (Khan and Arany, 2016). In this study, however, a 810nm laser

at fluences of 1-3 J/cm<sup>2</sup> was used. A positive impact of LLLT on CFU-F was also reported by Li et al. where bone marrow MSC (BM-MSc) showed a gradual increase in the number of colonies from single to daily red light irradiation in a dose-dependent manner (Li et al., 2006). Wang et al. demonstrated that red and near-infrared light stimulate proliferation and increase cellular ATP concentration of human ASC, but blue and green light inhibit proliferation and reduce ATP concentration (Wang et al., 2017). One of the well-described positive effects of LLLT is an increase in osteogenic differentiation using red/infrared light (Amid et al., 2014). The majority of these studies were using BM-MSc or osteoblasts alone (Bouvet-Gerbettaz et al., 2009; Li et al., 2006; Li et al., 2010; Saygun et al., 2012) or in combination with scaffolds (Crisan et al., 2015; Khadra, 2005). This might depend to the origin-dependent lineage commitment of BM-MSc. Nonetheless, Choi et al., 2013 showed a rapid bone formation in athymic nude mice by applying daily doses of red light on ASC for 56 days (Choi et al., 2013). In contrast, our single LLLT application on SVF cells did not affect differentiation capacity towards the osteogenic and adipogenic lineage, however, red light showed a tendency for enhanced osteoblast differentiation.

Another positive and very important effect of LLLT for tissue regeneration is the stimulation of angiogenesis and vasculogenesis as reported in several *in vivo* studies after red light irradiation (Corazza et al., 2007; Tuby et al., 2006). In this context we previously showed that also blue light can significantly enhance angiogenesis (Dungel et al., 2014). Within the present study, SVF cells treated with green and red light, embedded in a fibrin matrix, revealed a stronger capacity to form vascular tubes compared to blue light and untreated cells. These morphological observations were corroborated by quantification of the number and length of the single vascular tubes. Cells treated with red light showed significantly prolonged vascular tubes compared to



untreated cells. The enhanced vascularization potential of irradiated SVF cells can potentially be corroborated with the increased proliferation capacity after red light irradiation. Szymanska et al. (2013) reported that increased cell proliferation after light stimulation is mediated by an increase of VEGF and transforming growth factor beta (TGF- $\beta$ ) level (Szymanska et al., 2013). This is in line with our data by analyzing VEGF in cell supernatants as potential mediator for vascular tube formation of SVF cells in a fibrin matrix. VEGF protein concentration of the fibrin clot culture supernatants was fourfold higher from red and green light treated cells compared to untreated cells. The study performed by Cury et al. demonstrated an enhanced VEGF mRNA expression in a dose dependent manner after red and infrared irradiation (Cury et al., 2013). A detailed study about vascular regeneration after LLLT on spheroid ASC in hind limb ischemia mice was performed by the group of Park, who demonstrated enhanced secretion of angiogenic growth factors and improved functional recovery (Park et al., 2014; Park et al., 2015; Park et al., 2017; Park et al., 2017; Park et al., 2015).

Although the donor-dependent variability in primary SVF cell differentiation is a challenge in *in vitro* cultures (Priglinger et al., 2017) we could observe higher proliferation, stronger vascular tube formation, enhanced VEGF secretion and a tendency to higher osteogenic differentiation using red light. The differences between our effects and current literature might be due to the different treatment parameters such as light intensity, fluence, wavelengths, number of treatments, cell sources and cell types. Most of the studies were using cultures of BM-MSC or ASC for LLLT, which requires *in vitro* expansion or further processing. While these cultures may represent homogeneous populations of cells highly enriched in MSC, their use complicates regulatory authorization and translation into clinics. In contrast, we were using SVF cells, which are not further processed and also proven for their therapeutic effect in

many clinical studies. Within our study we were able to show beneficial effects after LLLT which are important for wound healing suggesting that for a clinical application it is not mandatory to use a set-up requiring multiple irradiations or a specific cell type.

## **5. Conclusion**

In the present work, we demonstrated that the impact of LLLT on isolated SVF cells resulted in enhanced vascularization potential with high VEGF production, which might potentially be associated with the increased SVF proliferation capacity. Since the cell composition of SVF cells and also the CFU frequency did not change after LLLT, it suggests that there is not a distinct stem/precursor cell type responsible for this effect, but rather a combination of interacting cells which are activated by specific wavelengths. This study provides a new approach for activation of freshly isolated SVF cells for direct clinical application with a well-described and non-invasive method: LLLT using pulsed LED light.

## **6. Acknowledgements**

We would like to acknowledge Susanne Suessner for flow cytometric analysis and Carina Wagner for data analysis. This study was supported by FFG BRIDGE grant #3925263.

## **7. Disclosure of Interest**

We exclude any conflict of interest and guarantee that all authors are in complete agreement with the contents and submission of this manuscript. Furthermore, we declare that our work is original research, unpublished, and not submitted to another journal.

## 8. Authors contributions

EP and PD made substantial contributions to conception and design, enquired and drafted the manuscript. JM and SC helped to write the manuscript. JM, SC, CL and CW performed the experiments. CW and SR analyzed data. PD, HR and SW have given final approval and revised the manuscript critically. All authors read and approved the final manuscript.

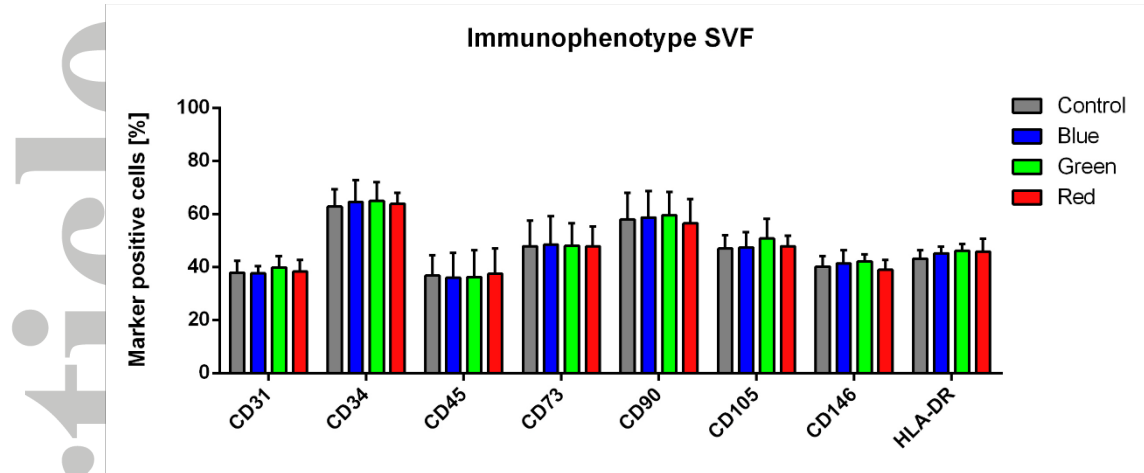
## 9. References

- Adamskaya N, Dungal P, Mittermayr R et al. 2011; Light therapy by blue LED improves wound healing in an excision model in rats. *Injury* **42**: 917-921.
- Amid R, Kadkhodazadeh M, Ahsaie MG, Hakakzadeh A. 2014; Effect of low level laser therapy on proliferation and differentiation of the cells contributing in bone regeneration. *J Lasers Med Sci* **5**: 163-170.
- Arai F, Ohneda O, Miyamoto T, Zhang XQ, Suda T. 2002; Mesenchymal stem cells in perichondrium express activated leukocyte cell adhesion molecule and participate in bone marrow formation. *J Exp Med* **195**: 1549-1563.
- Bourin P, Bunnell BA, Casteilla L et al. 2013; Stromal cells from the adipose tissue-derived stromal vascular fraction and culture expanded adipose tissue-derived stromal/stem cells: a joint statement of the International Federation for Adipose Therapeutics and Science (IFATS) and the International Society for Cellular Therapy (ISCT). *Cytotherapy* **15**: 641-648.
- Bouvet-Gerbetaz S, Merigo E, Rocca JP, Carle GF, Rochet N. 2009; Effects of low-level laser therapy on proliferation and differentiation of murine bone marrow cells into osteoblasts and osteoclasts. *Lasers Surg Med* **41**: 291-297.
- Choi K, Kang BJ, Kim H et al. 2013; Low-level laser therapy promotes the osteogenic potential of adipose-derived mesenchymal stem cells seeded on an acellular dermal matrix. *J Biomed Mater Res B Appl Biomater* **101**: 919-928.
- Chung H, Dai T, Sharma SK, Huang YY, Carroll JD, Hamblin MR. 2012; The nuts and bolts of low-level laser (light) therapy. *Ann Biomed Eng* **40**: 516-533.
- Corazza AV, Jorge J, Kurachi C, Bagnato VS. 2007; Photobiomodulation on the angiogenesis of skin wounds in rats using different light sources. *Photomed Laser Surg* **25**: 102-106.
- Crisan L, Soritau O, Baciut M, Baciut G, Crisan BV. 2015; The influence of laser radiation on human osteoblasts cultured on nanostructured composite substrates. *Clujul Med* **88**: 224-232.
- Cury V, Moretti AI, Assis L et al. 2013; Low level laser therapy increases angiogenesis in a model of ischemic skin flap in rats mediated by VEGF, HIF-1 $\alpha$  and MMP-2. *J Photochem Photobiol B* **125**: 164-170.
- De Bari C, Dell'Accio F, Tylzanowski P, Luyten FP. 2001; Multipotent mesenchymal stem cells from adult human synovial membrane. *Arthritis Rheum* **44**: 1928-1942.
- de Vasconcelos Catao MH, Nonaka CF, de Albuquerque RL, Jr., Bento PM, de Oliveira Costa R. 2015; Effects of red laser, infrared, photodynamic therapy, and green LED on the healing process of third-degree burns: clinical and histological study in rats. *Lasers Med Sci* **30**: 421-428.
- Duffy JF, Czeisler CA. 2009; Effect of Light on Human Circadian Physiology. *Sleep Med Clin* **4**: 165-177.

- Dungel P, Hartinger J, Chaudary S et al. 2014; Low level light therapy by LED of different wavelength induces angiogenesis and improves ischemic wound healing. *Lasers Surg Med* **46**: 773-780.
- Dungel P, Mittermayr R, Haindl S et al. 2008; Illumination with blue light reactivates respiratory activity of mitochondria inhibited by nitric oxide, but not by glycerol trinitrate. *Arch Biochem Biophys* **471**: 109-115.
- Ebrahimian TG, Pouzoulet F, Squiban C et al. 2009; Cell therapy based on adipose tissue-derived stromal cells promotes physiological and pathological wound healing. *Arterioscler Thromb Vasc Biol* **29**: 503-510.
- Emelyanov AN, Kiryanova VV. 2015; Photomodulation of proliferation and differentiation of stem cells by the visible and infrared light. *Photomed Laser Surg* **33**: 164-174.
- Faiella W, Atoui R. 2016; Therapeutic use of stem cells for cardiovascular disease. *Clin Transl Med* **5**: 34.
- Fekrazad R, Mirmoezzi A, Kalhori KA, Arany P. 2015; The effect of red, green and blue lasers on healing of oral wounds in diabetic rats. *J Photochem Photobiol B* **148**: 242-245.
- Franco AT, Silva LM, Costa MS et al. 2016; Effect of photobiomodulation on endothelial cell exposed to Bothrops jararaca venom. *Lasers Med Sci* **31**: 1017-1025.
- Gimble JM, Katz AJ, Bunnell BA. 2007; Adipose-derived stem cells for regenerative medicine. *Circ Res* **100**: 1249-1260.
- Harwood HJ, Jr. 2012; The adipocyte as an endocrine organ in the regulation of metabolic homeostasis. *Neuropharmacology* **63**: 57-75.
- Holnthoner W, Hohenegger K, Husa AM et al. 2015; Adipose-derived stem cells induce vascular tube formation of outgrowth endothelial cells in a fibrin matrix. *J Tissue Eng Regen Med* **9**: 127-136.
- Huang Y-Y. 2009; Low-level laser therapy: an emerging clinical paradigm. *SPIE Newsroom* **9**: 1-3.
- In 't Anker PS, Scherjon SA, Kleijburg-van der Keur C et al. 2004; Isolation of mesenchymal stem cells of fetal or maternal origin from human placenta. *Stem Cells* **22**: 1338-1345.
- Kapur SK, Katz AJ. 2013; Review of the adipose derived stem cell secretome. *Biochimie* **95**: 2222-2228.
- Karu TI, Pyatibrat LV, Afanasyeva NI. 2004; A novel mitochondrial signaling pathway activated by visible-to-near infrared radiation. *Photochem Photobiol* **80**: 366-372.
- Khadra M. 2005; The effect of low level laser irradiation on implant-tissue interaction. In vivo and in vitro studies. *Swed Dent J Suppl*: 1-63.
- Khan I, Arany PR. 2016; Photobiomodulation Therapy Promotes Expansion of Epithelial Colony Forming Units. *Photomed Laser Surg* **34**: 550-555.
- Kim H, Choi K, Kweon OK, Kim WH. 2012; Enhanced wound healing effect of canine adipose-derived mesenchymal stem cells with low-level laser therapy in athymic mice. *J Dermatol Sci* **68**: 149-156.
- Kim WS, Park BS, Sung JH et al. 2007; Wound healing effect of adipose-derived stem cells: a critical role of secretory factors on human dermal fibroblasts. *J Dermatol Sci* **48**: 15-24.
- Klebanov GI, Shuraeva N, Chichuk TV et al. 2005; [A comparative study of the effects of laser and light-emitting diode irradiation on the wound healing and functional activity of wound exudate leukocytes]. *Biofizika* **50**: 1137-1144.
- Kronsteiner B, Wolbank S, Peterbauer A et al. 2011; Human mesenchymal stem cells from adipose tissue and amnion influence T-cells depending on stimulation method and presence of other immune cells. *Stem Cells Dev* **20**: 2115-2126.
- Kushibiki T, Awazu K. 2007; *A blue-violet laser irradiation stimulates bone nodule formation of mesenchymal stromal cells by the control of the circadian clock protein - art. no. 64351B.*
- Kushibiki T, Awazu K. 2008; Controlling osteogenesis and adipogenesis of mesenchymal stromal cells by regulating a circadian clock protein with laser irradiation. *Int J Med Sci* **5**: 319-326.
- Lane SW, Scadden DT, Gilliland DG. 2009; The leukemic stem cell niche: current concepts and therapeutic opportunities. *Blood* **114**: 1150-1157.

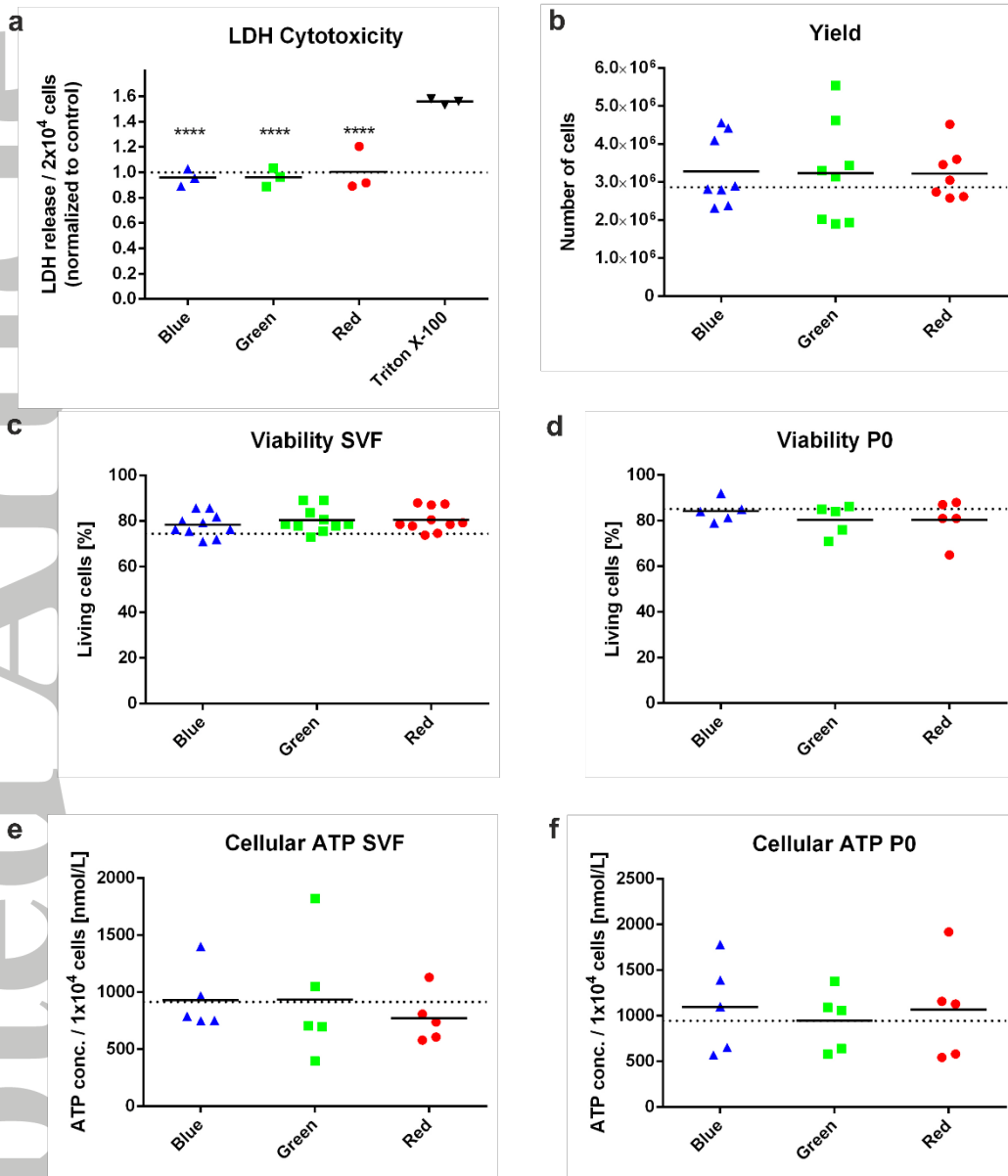
- Lau K, Paus R, Tiede S, Day P, Bayat A. 2009; Exploring the role of stem cells in cutaneous wound healing. *Exp Dermatol* **18**: 921-933.
- Li W-T, Chen H-L, Wang C-T. 2006; Effect of Light Emitting Diode Irradiation on Proliferation of Human Bone Marrow Mesenchymal Stem Cells. *Journal of Medical and Biological Engineering* **26**.
- Li WT, Chen CW, Huang PY. 2013; Effects of low level light irradiation on the migration of mesenchymal stem cells derived from rat bone marrow. *Conf Proc IEEE Eng Med Biol Soc* **2013**: 4121-4124.
- Li WT, Leu YC, Wu JL. 2010; Red-light light-emitting diode irradiation increases the proliferation and osteogenic differentiation of rat bone marrow mesenchymal stem cells. *Photomed Laser Surg* **28 Suppl 1**: S157-165.
- Lin CS, Xin ZC, Deng CH, Ning H, Lin G, Lue TF. 2010; Defining adipose tissue-derived stem cells in tissue and in culture. *Histol Histopathol* **25**: 807-815.
- Lindvall O, Kokaia Z, Martinez-Serrano A. 2004; Stem cell therapy for human neurodegenerative disorders-how to make it work. *Nat Med* **10 Suppl**: S42-50.
- Lipovsky A, Oron U, Gedanken A, Lubart R. 2013; Low-level visible light (LLVL) irradiation promotes proliferation of mesenchymal stem cells. *Lasers Med Sci* **28**: 1113-1117.
- Lugongolo MY, Manoto SL, Ombinda-Lemboumba S, Maaza M, Mthunzi-Kufa P. 2017; The effects of low level laser therapy on both HIV-1 infected and uninfected TZM-bl cells. *J Biophotonics* **10**: 1335-1344.
- Min KH, Byun JH, Heo CY, Kim EH, Choi HY, Pak CS. 2015; Effect of Low-Level Laser Therapy on Human Adipose-Derived Stem Cells: In Vitro and In Vivo Studies. *Aesthetic Plast Surg* **39**: 778-782.
- Mittermayr R, Osipov A, Piskernik C et al. 2007; Blue laser light increases perfusion of a skin flap via release of nitric oxide from hemoglobin. *Mol Med* **13**: 22-29.
- Mvula B, Moore TJ, Abrahamse H. 2010; Effect of low-level laser irradiation and epidermal growth factor on adult human adipose-derived stem cells. *Lasers Med Sci* **25**: 33-39.
- Ong WK, Chen HF, Tsai CT et al. 2013; The activation of directional stem cell motility by green light-emitting diode irradiation. *Biomaterials* **34**: 1911-1920.
- Park IS, Chung PS, Ahn JC. 2014; Enhanced angiogenic effect of adipose-derived stromal cell spheroid with low-level light therapy in hind limb ischemia mice. *Biomaterials* **35**: 9280-9289.
- Park IS, Chung PS, Ahn JC. 2015; Adipose-derived stromal cell cluster with light therapy enhance angiogenesis and skin wound healing in mice. *Biochem Biophys Res Commun* **462**: 171-177.
- Park IS, Chung PS, Ahn JC. 2017; Adipose-derived stem cell spheroid treated with low-level light irradiation accelerates spontaneous angiogenesis in mouse model of hindlimb ischemia. *Cytotherapy* **19**: 1070-1078.
- Park IS, Chung PS, Ahn JC, Leproux A. 2017; Human adipose-derived stem cell spheroid treated with photobiomodulation irradiation accelerates tissue regeneration in mouse model of skin flap ischemia. *Lasers Med Sci* **32**: 1737-1746.
- Park IS, Mondal A, Chung PS, Ahn JC. 2015; Vascular regeneration effect of adipose-derived stem cells with light-emitting diode phototherapy in ischemic tissue. *Lasers Med Sci* **30**: 533-541.
- Parolini O, Alviano F, Bagnara GP et al. 2008; Concise review: isolation and characterization of cells from human term placenta: outcome of the first international Workshop on Placenta Derived Stem Cells. *Stem Cells* **26**: 300-311.
- Paspaliaris B, Thornton JAF. 2014; Methods and apparatuses for isolating and preparing stem cells. **US 20140093482 A1**.
- Pittenger MF, Mackay AM, Beck SC et al. 1999; Multilineage potential of adult human mesenchymal stem cells. *Science* **284**: 143-147.
- Priglinger E, Schuh C, Steffenhagen C et al. 2017; Improvement of adipose tissue-derived cells by low-energy extracorporeal shock wave therapy. *Cytotherapy* **19**: 1079-1095.
- Rehman J, Traktuev D, Li J et al. 2004; Secretion of angiogenic and antiapoptotic factors by human adipose stromal cells. *Circulation* **109**: 1292-1298.
- Rodrigo SM, Cunha A, Pozza DH et al. 2009; Analysis of the systemic effect of red and infrared laser therapy on wound repair. *Photomed Laser Surg* **27**: 929-935.

- Saygun I, Nizam N, Ural AU, Serdar MA, Avcu F, Tozum TF. 2012; Low-level laser irradiation affects the release of basic fibroblast growth factor (bFGF), insulin-like growth factor-I (IGF-I), and receptor of IGF-I (IGFBP3) from osteoblasts. *Photomed Laser Surg* **30**: 149-154.
- Szymanska J, Goralczyk K, Klawe JJ et al. 2013; Phototherapy with low-level laser influences the proliferation of endothelial cells and vascular endothelial growth factor and transforming growth factor-beta secretion. *J Physiol Pharmacol* **64**: 387-391.
- Tuby H, Maltz L, Oron U. 2006; Modulations of VEGF and iNOS in the rat heart by low level laser therapy are associated with cardioprotection and enhanced angiogenesis. *Lasers Surg Med* **38**: 682-688.
- Tuby H, Maltz L, Oron U. 2007; Low-level laser irradiation (LLLI) promotes proliferation of mesenchymal and cardiac stem cells in culture. *Lasers Surg Med* **39**: 373-378.
- van Dongen JA, Tuin AJ, Spiekman M, Jansma J, van der Lei B, Harmsen MC. 2017; Comparison of intraoperative procedures for isolation of clinical grade stromal vascular fraction for regenerative purposes: a systematic review. *J Tissue Eng Regen Med*.
- Wakitani S, Goto T, Pineda SJ et al. 1994; Mesenchymal cell-based repair of large, full-thickness defects of articular cartilage. *J Bone Joint Surg Am* **76**: 579-592.
- Wang Y, Huang YY, Wang Y, Lyu P, Hamblin MR. 2017; Red (660 nm) or near-infrared (810 nm) photobiomodulation stimulates, while blue (415 nm), green (540 nm) light inhibits proliferation in human adipose-derived stem cells. *Sci Rep* **7**: 7781.
- Young HE, Steele TA, Bray RA et al. 2001; Human reserve pluripotent mesenchymal stem cells are present in the connective tissues of skeletal muscle and dermis derived from fetal, adult, and geriatric donors. *Anat Rec* **264**: 51-62.
- Zimmerlin L, Donnenberg VS, Pfeifer ME et al. 2010; Stromal vascular progenitors in adult human adipose tissue. *Cytometry A* **77**: 22-30.
- Zuk PA, Zhu M, Mizuno H et al. 2001; Multilineage cells from human adipose tissue: implications for cell-based therapies. *Tissue Eng* **7**: 211-228.
- Zvaifler NJ, Marinova-Mutafchieva L, Adams G et al. 2000; Mesenchymal precursor cells in the blood of normal individuals. *Arthritis Res* **2**: 477-488.



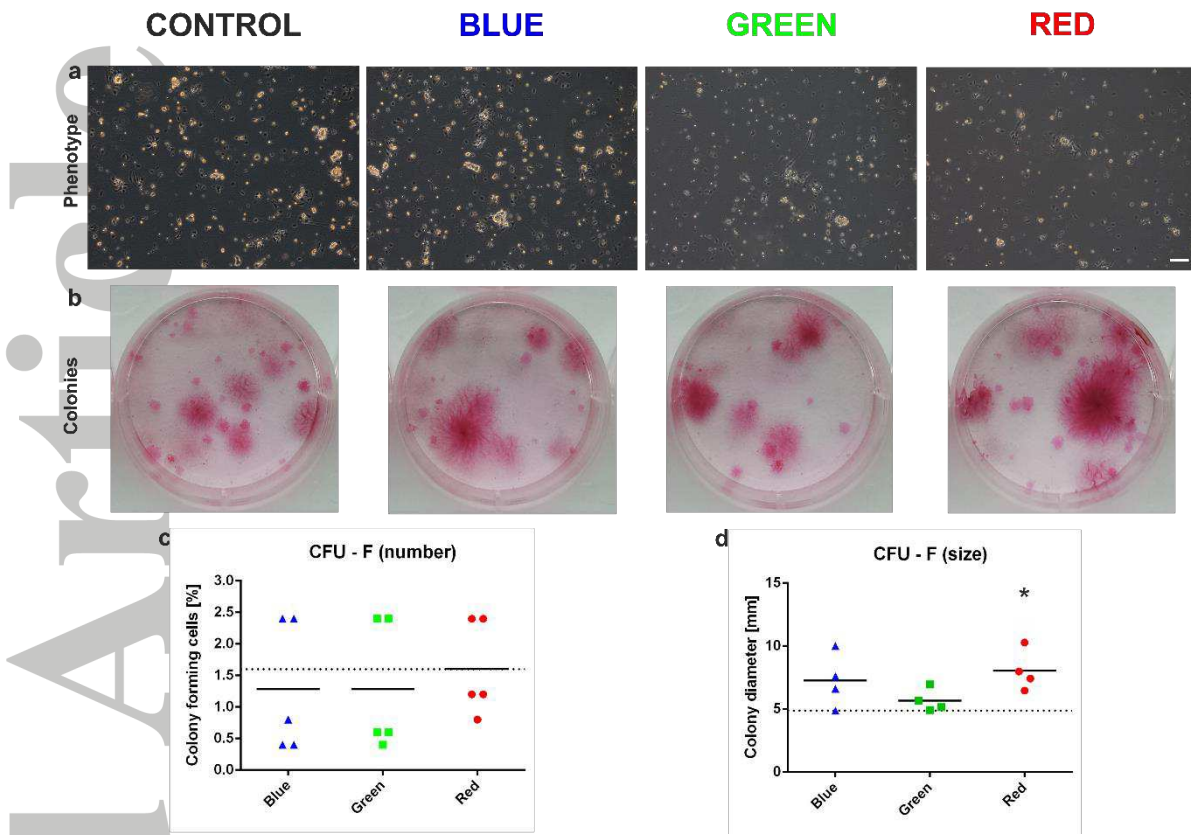
**Figure 1. SVF cell characterization after LLLT.** Flow cytometry analysis of untreated and LLLT treated SVF cells (n=5) represented as percent cells expressing specific marker.

Fig. 2



**Figure 2. SVF cell vitality after LLLT.** (a) Analysis of cell cytotoxicity represented by LDH release from untreated and LLLT treated SVF cells. Asterisks indicate significant differences compared to positive control Triton X-100. \*\*\*\* $p < 0.0001$ .  $n=3$  (b-f) Analysis of cell number  $n=7-8$  (b), viability SVF  $n=10$  (c) and viability P0  $n=5$  (d), cellular ATP SVF  $n=5$  (e) and cellular ATP P0  $n=5$  (f) from untreated and LLLT treated SVF cells. Each point represents one donor. The dashed line represents the control condition, mean of untreated cells from all donors.





**Figure 3. SVF properties after LLLT.** (a) Representative images of untreated and LLLT treated SVF cells one day after isolation. (b) Representative images of colonies derived from untreated and LLLT treated SVF cells after 2 weeks cultivation and staining with hematoxylin/eosin. Size bar = 100µm. (c,d) Quantification of colony formation represented as number n=5 (c) and average size n=4 (d) of colonies. Each point represents one donor. The dashed line represents the control condition, mean of untreated cells from all donors. \*p < 0.05.

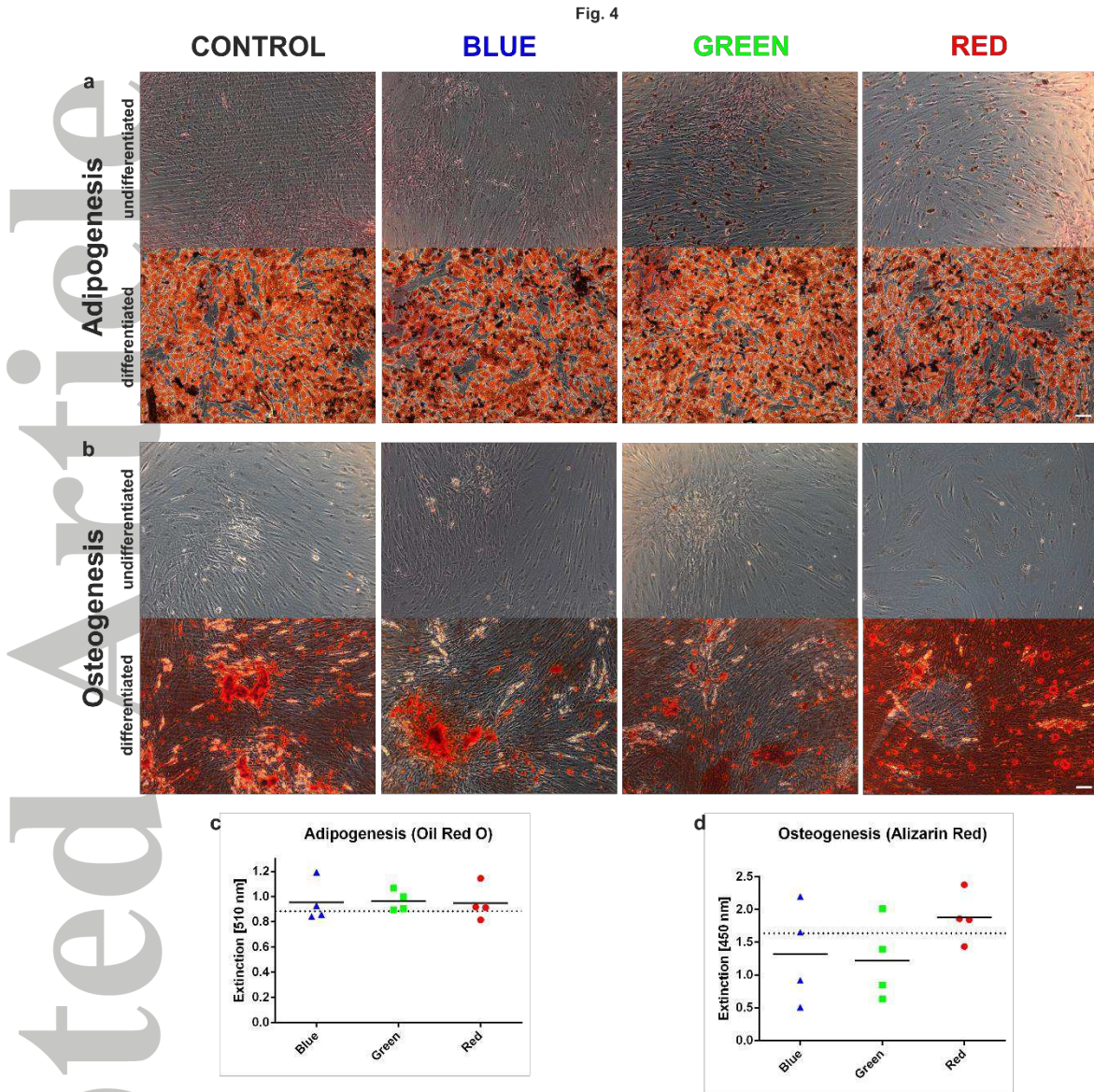


**Figure 4. SVF differentiation capacity after LLLT.** (a) Representative images of untreated and LLLT treated cells after 21 days without growth factors and stimuli (undifferentiated) and upon adipogenic induction (differentiated), stained with Oil Red O. (b) Representative images of untreated and LLLT treated cells after 21 days without growth factors and stimuli (undifferentiated) and upon osteogenic induction (differentiated), stained with Alizarin Red. Size bar = 100µm. (c,d) Quantification of Oil Red O staining n=4 (c) and Alizarin Red staining n=4 (d). All conditions showed a significant enhancement of differentiated cells compared to undifferentiated cells. Each point represents one donor. The dashed line represents the control condition, mean of untreated cells from all donors.

Fig. 5

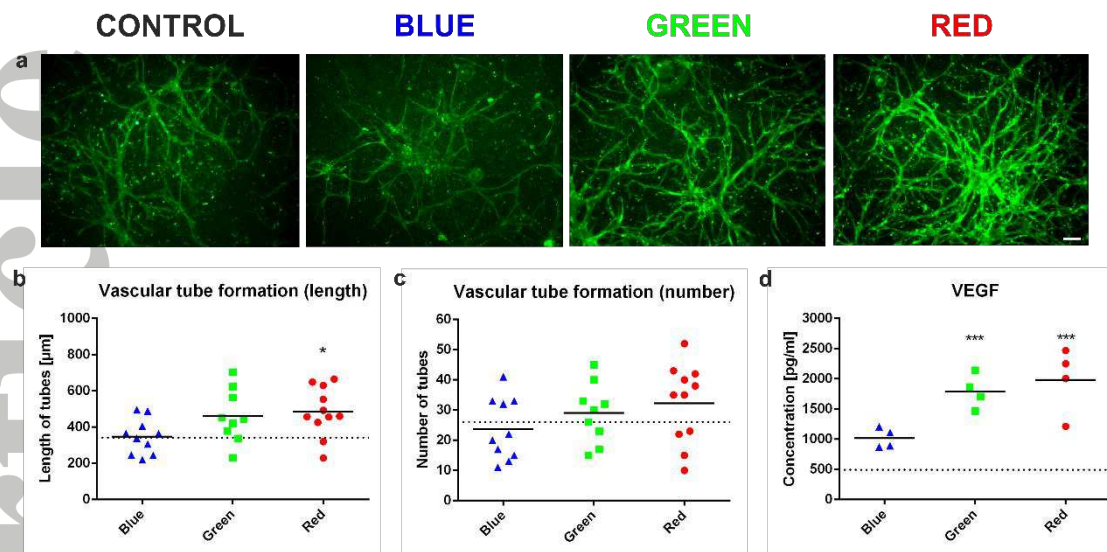


**Figure 5. SVF vascular tube formation after LLLT.** (a) Representative images of formed vascular tubes derived from untreated and LLLT treated SVF cells after 2 weeks cultivation in 3D fibrin matrices and staining with the endothelial marker CD31. Size bar = 100µm. (b,c) Quantification of vascular tube formation represented as average length (b) and number (c) of tubes n=9-11. (d) Analysis of VEGF concentration within supernatants from fibrin clot cultures n=4. Each point represents one donor. The dashed line represents the control condition, mean of untreated cells from all donors. \*p < 0.05; \*\*\*p < 0.001.



## ADIPOSE TISSUE CELLS

**The adipose tissue–derived stromal vascular fraction cells from lipedema patients: Are they different?**

ELENI PRIGLINGER<sup>1,2</sup>, CHRISTOPH WURZER<sup>1,2,3</sup>, CAROLIN STEFFENHAGEN<sup>1,2</sup>,  
JULIA MAIER<sup>1,2</sup>, VICTORIA HOFER<sup>4,5</sup>, ANJA PETERBAUER<sup>2,6</sup>,  
SYLVIA NUERNBERGER<sup>2,7,8</sup>, HEINZ REDL<sup>1,2</sup>, SUSANNE WOLBANK<sup>1,2,†</sup> &  
MATTHIAS SANDHOFER<sup>5,†</sup>

<sup>1</sup>AUVA Research Center, Ludwig Boltzmann Institute for Experimental and Clinical Traumatology, Linz, Austria, <sup>2</sup>Austrian Cluster for Tissue Regeneration, Vienna, Austria, <sup>3</sup>Liporegena GmbH, Breitenfurt, Austria, <sup>4</sup>Faculty of Medicine/Dental Medicine, Danube Private University, Krems-Stein, Austria, <sup>5</sup>Austrian Academy of Cosmetic Surgery and Aesthetic Medicine, Linz, Austria, <sup>6</sup>Red Cross Blood Transfusion Service of Upper Austria, Linz, Austria, <sup>7</sup>Bernhard Gottlieb University Clinic of Dentistry, Universitätsklinik für Zahn-, Mund- und Kieferheilkunde Ges.m.b.H, Vienna, Austria, and <sup>8</sup>Department of Trauma Surgery, Medical University of Vienna, Vienna, Austria

**Abstract**

**Background aims.** Lipedema is a hormone-related disease of women characterized by enlargement of the extremities caused by subcutaneous deposition of adipose tissue. In healthy patients application of autologous adipose tissue–derived cells has shown great potential in several clinical studies for engrafting of soft tissue reconstruction in recent decades. The majority of these studies have used the stromal vascular fraction (SVF), a heterogeneous cell population containing adipose-derived stromal/stem cells (ASC), among others. Because cell identity and regenerative properties might be affected by the health condition of patients, we characterized the SVF cells of 30 lipedema patients in comparison to 22 healthy patients. **Methods.** SVF cells were analyzed regarding cell yield, viability, adenosine triphosphate content, colony forming units and proliferative capacity, as well as surface marker profile and differentiation potential in vitro. **Results.** Our results demonstrated a significantly enhanced SVF cell yield isolated from lipedema compared with healthy patients. In contrast, the adipogenic differentiation potential of SVF cells isolated from lipedema patients was significantly reduced compared with healthy patients. Interestingly, expression of the mesenchymal marker CD90 and the endothelial/pericytic marker CD146 was significantly enhanced when isolated from lipedema patients. **Discussion.** The enhanced number of CD90<sup>+</sup> and CD146<sup>+</sup> cells could explain the increased cell yield because the other tested surface marker were not reduced in lipedema patients. Because the cellular mechanism and composition in lipedema is largely unknown, our findings might contribute to a better understanding of its etiology.

**Key Words:** adipogenesis, adipose tissue, adult stem cells, CD146, lipedema, stromal vascular fraction

**Introduction**

Lipedema is a progressive disease characterized by subcutaneous bilateral deposition of adipose tissue in the extremities and buttocks [1,2]. In 60% of lipedema cases, genetic background with familial predisposition has been described [3]. In a recent study, we observed that 89% of lipedema patients had maternal and paternal predisposition over three generations

[4]. The genetic background of lipedema was demonstrated in a clinical report with 330 family members, although the involved genes have not been completely identified [5]. Patients suffer for a long time because their symptoms, such as reduced joint mobility, hematoma, and edema, are frequently misdiagnosed with adipositas or lipohypertrophy [6–8]. In fact, the increase in fatty tissue is a consequence of adipocyte hypertrophy and hyperplasia [9] accentuated by

†These authors contributed equally.

Correspondence: Eleni Priglinger, PhD, Ludwig Boltzmann Institute for Experimental and Clinical Traumatology, Krankenhausstraße 7, 4010 Linz, Austria.  
E-mail: Eleni.Priglinger@trauma.lbg.ac.at

(Received 17 January 2017; accepted 21 March 2017)

alterations of the connective tissue [10]. Furthermore, the enhanced adipocyte growth leads to capillary permeability and insufficient lymphatic backflow associated with hematoma [11]. Lipedema symptoms have primarily been treated with compression [12] or lymph drainage [13–15]. Because lipedema does not respond to diets, drugs or physical activity, the only efficient treatment option with demonstrated long-term benefit to date [16] is micro-cannular liposuction in tumescent anesthesia [17–20]. Additionally, radial shockwave therapy is able to enhance lymphatic decongestion in lipedema after micro-cannular liposuction [19], and water-jet-assisted liposuction provides long-term improvement by preserving lymph vessels in lipedema [21].

Lipedema is a hormone-related disease mainly affecting women starting in puberty, after pregnancy or during menopause [5,22]. Estrogen contributes to decreased lipolysis in the gluteal, compared with the abdominal, region due to a distinct pattern of estrogen receptors [23]. Moreover, estrogen regulates bone morphogenetic protein (BMP)-2, which can stimulate adipogenesis but inhibits it by knockdown PPARgamma2; thus, PPARgamma2 may play a role in BMP-induced adipogenesis [24]. However, the exact etiopathogenesis of this disorder is still largely unknown. Examination of adipose tissue of lipedema patients exhibit differences in adipocyte morphology. Suga *et al.* analyzed adipose tissue of lipedema patients and observed infiltration of macrophages and the presence of necrotizing adipocytes. In parallel, enhanced proliferation capacity of adipose-derived stem/progenitor/stromal cells (Ki67<sup>+</sup>CD34<sup>+</sup> cells) was described, which seems to promote adipogenesis [25]. Additionally, hypertrophy-induced hypoxia and subsequently enhanced angiogenesis of pathologic vessels might contribute to capillary permeability [26,27]. This would explain the fluid increase in the interstitium and consequently the emerging orthostatic edema.

All in all, little is known about the cell composition including the properties of adult stem and precursor cells in lipedema. The aim of this study was to investigate adipose tissue-derived cells obtained from lipedema patients by liposuction compared with healthy patients. Because adipose tissue is a highly vascularized tissue containing a broad variety of regenerative cells, we concentrated on the adipose-derived stromal vascular fraction (SVF) including adipose-derived stromal/stem cells (ASC). Cells isolated from liposuction material from healthy and lipedema patients were analyzed regarding phenotypic and functional criteria for the identification of adipose-derived cells as defined in the statement of the International Federation for Adipose Therapeutics and Science (IFATS) together with the International Society for Cellular Therapy (ISCT) [28].

Table I. Characteristics of healthy and lipedema patients.

Characteristics	Healthy	Lipedema
N	22	30
Sex	Female	Female
Age (years)	42 ± 10	41 ± 13
Weight (kg)	75 ± 17	91 ± 18
BMI (kg/m <sup>2</sup> )	27 ± 6	33 ± 7
Type II	—	3%
Type III	—	5%
Type I–III	—	10%
Type I–IV	—	82%
Stage 2	—	55%
Stage 2–3	—	24%
Stage 3	—	21%

## Methods

### Liposuction

The collection of human adipose tissue was approved by the local ethical board with patients' written consent. Dermal and subcutaneous white adipose tissue was obtained during routine outpatient liposuction procedures from the hips and outer thighs ("saddlebags") under local tumescence anaesthesia. Table I provides patient characteristics. Tumescent solution contained one vial Volon-A 10 mg (Dermapharm), three vials Suprarenin 1 mg/mL (Sanofi), 45 mL bicarbonate 8.4% (Fresenius Kabi) and 60 mL Xylocaine 2% including Lidocaine 0.04% (Astra Zeneca). The harvesting cannulas were triport and 4 mm in diameter (MicroAire System power-assisted liposuction).

### SVF/ASC isolation

SVF isolation was performed as modified from Wolbank *et al.* [29]. Briefly, 100 mL of liposuction material was transferred to a blood bag (Macopharma) and washed with an equal volume of phosphate-buffered saline (PBS) to remove blood and tumescence solution. Afterward, for tissue digestion PBS was replaced with 0.2 U/mL collagenase NB4 (Serva) dissolved in 100 mL PBS containing Ca<sup>2+</sup>/Mg<sup>2+</sup> and 25 mmol/L N-2-hydroxyethylpiperazine-N0-2-ethanesulfonic acid (HEPES; Sigma), and the blood bag was incubated at 37°C under moderate shaking (180 rpm) for 1 h. The digested tissue was transferred into 50-mL tubes. After centrifugation at 1200 g for 7 min, the cell pellet was incubated with 100 mL erythrocyte lysis buffer for 5 min at 37°C to eliminate red blood cells. The supernatant was aspirated after centrifugation for 5 min at 500 g. The pellet was washed with PBS and filtered through a 100-µm cell strainer (Greiner). After another centrifugation step at 500 g for 5 min, the supernatant was removed, and the isolated SVF cells were cultured in endothelial growth medium (EGM-2) at 37°C, 5% CO<sub>2</sub> and 95% air humidity or

resuspended in EGM-2 for further analyses. After seeding the SVF on plastic surface in expansion medium (EGM-2), the adherent cell fraction including ASC could outgrow as an adherent monolayer and was cultured to a subconfluent state. Medium was changed every 3–4 days. Cells were detached with  $1 \times$  trypsin/EDTA at  $37^\circ\text{C}$  and collected in a tube. After centrifugation, the pellet was resuspended in EGM-2 medium, and cells were quantified with trypan blue exclusion in a cell counter (TC-20, Bio-Rad). Adherent SVF from passage 0 were used for analysis of the adenosine triphosphate (ATP) concentration and immunophenotype of cells after 1 week in culture as well as the differentiation potential, whereas freshly isolated SVF was used for all other experiments.

#### *Cell yield and viability*

Cell number was determined using trypan blue exclusion and quantification in a cell counter (TC-20, Bio-Rad). For measuring cell viability, the percentage of living cells compared with total cell count was analyzed with the cell counter.

#### *Cellular ATP*

To determine the cellular ATP concentration CellTiter-Glo Luminescent Cell Viability Assay (Promega) was used and performed according to the manufacturer's instructions. Freshly isolated SVF and cells after 1 week in culture were seeded at a density of  $1 \times 10^4$  cells per well in a black 96-well plate (Greiner) in  $100 \mu\text{L}$  EGM-2 medium. After 2 h,  $100 \mu\text{L}$  CellTiter-Glo Reagent were added to each well, and the plate was gently agitated on a shaker for 2 min. Afterward, the plate was incubated for 10 min in the dark. The luminescent signal was detected with an Infinite M200 Multimode Microplate Reader (Tecan) at an exposure time of 2000 ms and correlated to an ATP standard curve.

#### *Colony-forming unit fibroblast assay*

A defined number of SVF cells (4, 20, 100, 500, 2500, 12 500) was seeded in each well of a six-well plate (Sarstedt) and cells were cultured in EGM-2 for 14 days. Medium was changed on day 7 after cell seeding. After 14 days of culture, cells were fixed with 4% formaldehyde and stained with hematoxylin. The cells were then washed with tap water and stained with eosin solution (Roth/Lactan). The percentage of cells that formed visible colonies was calculated and compared with the total number of seeded cells.

#### *Proliferation*

Proliferation potential was analyzed by determining the population doubling level (PDL). Freshly iso-

lated SVF cells were seeded at a density of  $5 \times 10^5$  cells per T-25 culture flask and cultured in EGM-2 medium. Medium was changed every 3–4 days. When cells had reached a subconfluent state, they were passaged, and cell number was determined as described earlier. For further analysis of PDL, ASC were seeded at a density of  $5 \times 10^4$  in T-25 culture flasks and cultured until passage 3. Cell number was determined after each passage.

#### *Flow cytometry analysis*

Freshly isolated SVF cells and after 1 week in culture were characterized using the following antibodies: CD14-FITC (BD), CD31-FITC (eBiosciences), CD34-APC (BD), CD45-PerCP (BD), CD73-FITC (eBiosciences), CD90-PE (eBiosciences), CD105-PE (eBiosciences) and CD146-PerCP (R&D). For staining,  $5 \times 10^5$  cells in  $50 \mu\text{L}$  PBS with 1% fetal calf serum (FCS; PAA) were incubated with  $5 \mu\text{L}$  primary labeled antibodies at room temperature for 15 min in the dark. Cells were washed with 1.5 ml Cell Wash (BD) and centrifuged for 5 min at  $400 g$ . The supernatant was discarded and the cell pellet resuspended in  $300 \mu\text{L}$   $1 \times$  Cell Fix (BD; diluted 1:10 with aqua dest). Samples were analyzed on a FACSCalibur (BD).

#### *Osteogenic differentiation and detection*

For osteogenic differentiation, cells were seeded at a density of  $2 \times 10^3$  cells per well in a 24-well plate in EGM-2 medium and incubated over night. The next day, medium was changed to osteogenic differentiation medium Dulbecco's Modified Eagle's Medium (DMEM)-low glucose (Lonza) containing 10% FCS, 2 mmol/L L-glutamine (PAA), 100 U/mL penicillin/streptomycin (Lonza), 10 nmol/L dexamethasone (Sigma), 150  $\mu\text{mol/L}$  ascorbat-2-phosphate (Sigma), 10 mmol/L  $\beta$ -glycerophosphate (StemCell Technologies) and 10 nmol/L dihydroxy vitamin D3 (Sigma) or control medium consisting of DMEM/F12/L-glutamine (Lonza) with 10% FCS and 100 U/mL penicillin/streptomycin. Medium was changed every 3–4 days. After 21 days, osteogenic differentiation was analyzed with alizarin red staining and quantification, as well as determination of intracellular alkaline phosphatase (ALP) activity. For alizarin red staining of calcified structures, cells were fixed for 1 h with 70% ethanol at  $-20^\circ\text{C}$  and stained with alizarin red solution (Merck) for 15 min. For quantitative analysis of alizarin red staining, the supernatant was discarded, and the cells were incubated with  $500 \mu\text{L}$  20% methanol and 10% acidic acid (diluted in aqua dest) for 15 min. After resuspension, the mixture of cells and methanol/acidic acid was transferred to a transparent

96-well plate (100  $\mu$ L per well). The absorbance was measured at 450 nm with an Infinite M200 Multimode Microplate Reader. The second method to analyze osteogenic differentiation is the detection of the activity of intracellular ALP. Cells were incubated with 100  $\mu$ L PBS for 1 h at  $-20^{\circ}\text{C}$ . The cells were then lysed for 1 h with the addition of 100  $\mu$ L PBS containing 0.5% TritonX-100 (Sigma). For quantitative detection of ALP activity, 100  $\mu$ L of substrate solution (4-nitrophenylphosphate) were added in each well and incubated for 1 h in the dark. Finally, the solution was transferred to a transparent 96-well plate (100  $\mu$ L per well), and absorbance was measured at 405 nm together with a reference wavelength of 620 nm in an Infinite M200 Multimode Microplate Reader. By creating a standard curve with known p-nitrophenol concentrations diluted in a solution containing 0.5% TritonX-100 diluted in PBS 1:2 and

measuring the corresponding absorption, the ALP activity of the samples was calculated.

#### Adipogenic differentiation and detection

For adipogenic differentiation, cells were seeded at a density of  $1.4 \times 10^4$  cells per well in a 24-well plate in EGM-2 medium and incubated over night. The next day, medium was changed to adipogenic differentiation medium DMEM-high glucose (Lonza) containing 10% FCS, 2 mmol/L L-glutamine, 100 U/mL penicillin/streptomycin, 1  $\mu$ mol/L dexamethasone, 0.5 mmol/L 3-isobutyl-1-methylxanthine (IBMX; Sigma), 10  $\mu$ g/mL insulin (Sigma) and 100  $\mu$ mol/L indomethacin (Sigma) or control medium consisting of DMEM/F12/L-glutamine with 10% FCS and 100 U/mL penicillin/streptomycin. Medium was changed every 3–4 days. After 21 days, adipogenic differentiation was analyzed

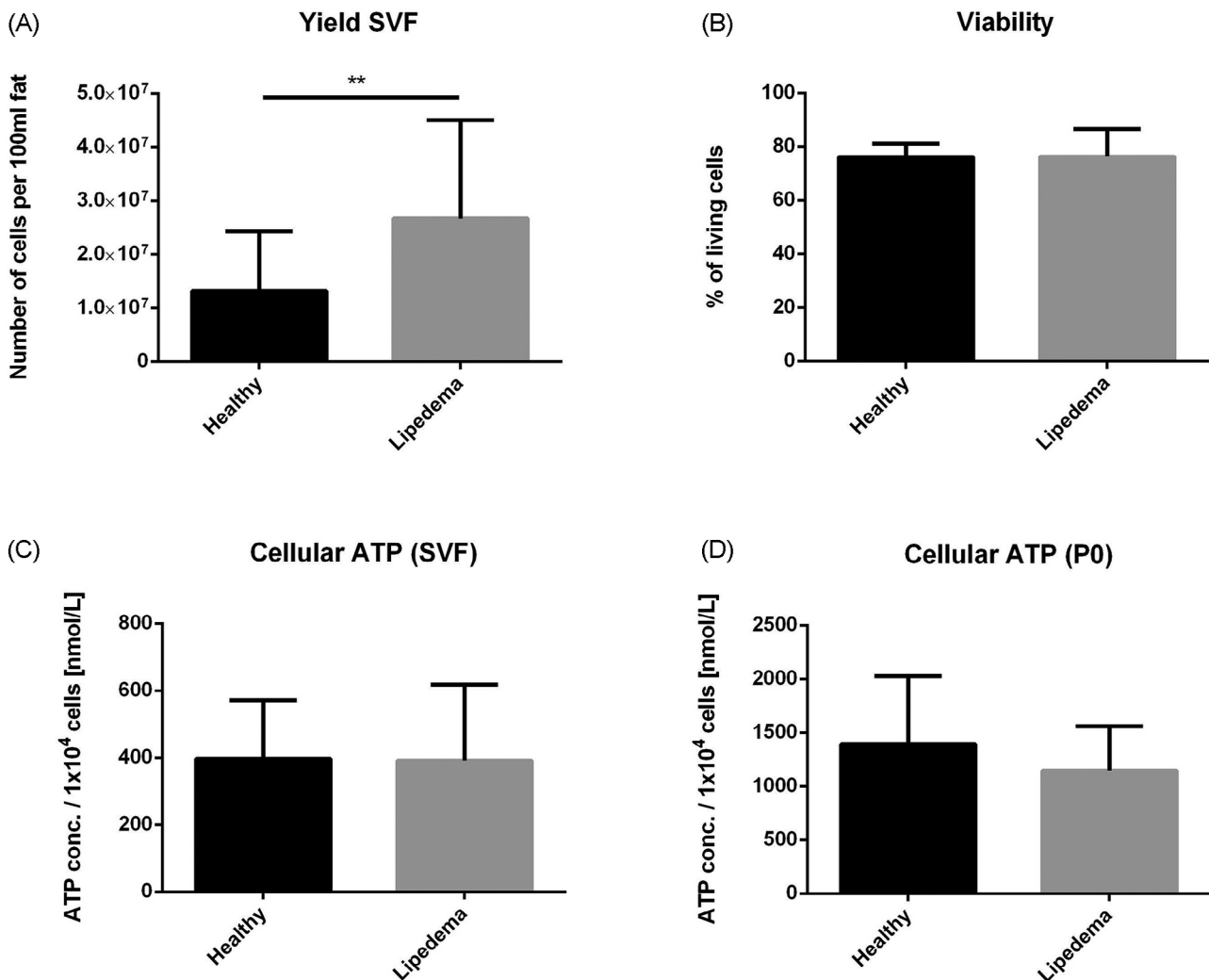


Figure 1. Cell yield, viability and ATP concentration. The SVF cell yield from liposuction material was significantly enhanced for lipedema patients compared with healthy patients (A) ( $n = 22$  and  $30$ ), whereas there was no difference in viability (B) ( $n = 19$  and  $29$ ) and ATP concentration of cells directly after isolation (C) ( $n = 13$  and  $19$ ) and after 1 week in culture (D) ( $n = 9$  and  $12$ ).  $**P < 0.01$ .

with oil red O staining and quantification. Cells were fixed with 4% formaldehyde for 1 h. After washing with aqua dest, the cells were rinsed with 70% ethanol for 2 min and stained for 5–15 min with oil red O solution (Sigma). Then the cells were washed with aqua dest, counterstained for 1–3 min with hematoxylin solution and blued with tap water. For quantitative detection of oil red O staining, the supernatant was discarded, and 500  $\mu$ L isopropanol were added in each well. After resuspension, the mixture of cells and isopropanol was transferred to a transparent 96-well plate (100  $\mu$ L per well). The absorbance was measured at 510 nm with an Infinite M200 Multimode Microplate Reader.

#### Chondrogenic differentiation and detection

For chondrogenic differentiation and three-dimensional micromass pellet cultures,  $3 \times 10^5$  cells were centrifuged in chondrogenic differentiation medium consisting of hMSC Chondro BulletKit (Lonza) with 10 ng/mL BMP-6 (R&D) and 10 ng/mL transforming growth factor- $\beta$ 3 (Lonza) in screw cap microtubes. The tubes were placed in an incubator at 37°C, 5% CO<sub>2</sub>, and 95% humidity with slightly open

cap for gas exchange. After 2 days, the pellets were transferred to 96-well U-bottom plates (Greiner) with fresh medium. Medium was changed every 2–3 days. After 35 days of differentiation, micromass pellets were fixed in 4% phosphate-buffered formalin overnight for histological analysis. The next day, the pellets were washed in 1 $\times$  PBS and dehydrated in increasing concentrations of alcohol. After rinsing the pellets in xylol and infiltration with paraffin, deparaffinized sections were stained with alcian blue for 30 min and counterstained for 2 min with hematoxylin. For collagen type II staining, sections were treated with pepsin for 10 min at 37°C (AP-9007 RTU, Thermo Scientific). Endogenous peroxidase was quenched with freshly prepared 3% H<sub>2</sub>O<sub>2</sub> for 10 min at room temperature, followed by normal horse serum 2.5% (Vector RTU) to block unspecific binding. Sections were incubated 1 h with monoclonal anti-collagen type II (MS-306 P0 Thermo Scientific) at 1:100. After washing with TBS, sections were incubated with the secondary antibody (anti-mouse DAKO EnVision + System HRP-labeled Polymer, Dako) for 30 min and rinsed in TBS again. Bindings were visualized using Nova Red (SK4800 Vector Labs) for 6 min. Counterstaining was performed with hematoxylin for 2 min.

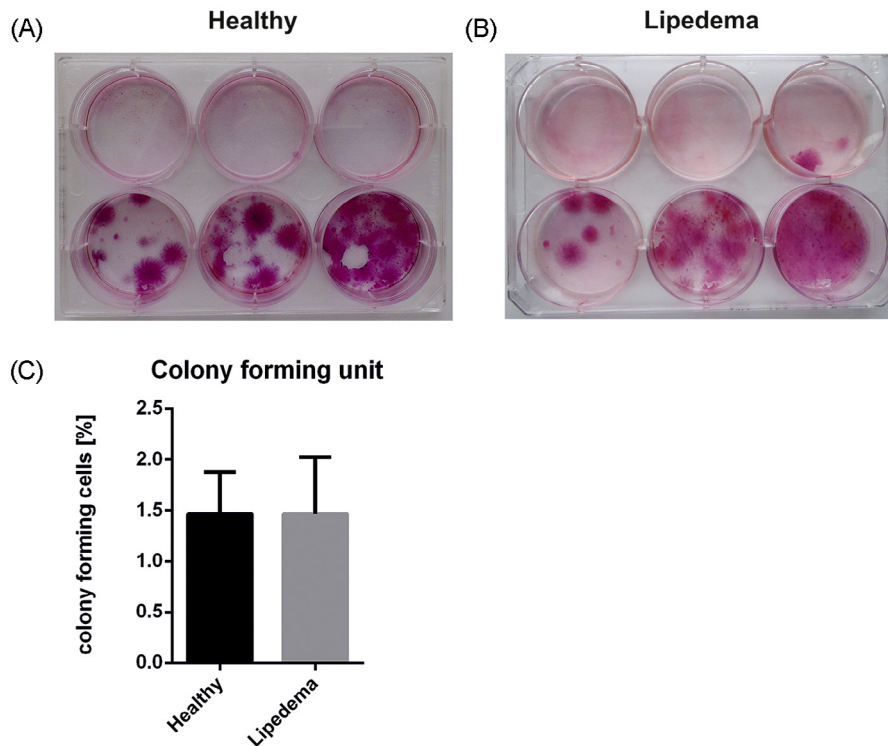


Figure 2. Colony-forming unit fibroblast assay. SVF cells derived from healthy and lipedema patients were seeded at defined numbers of cells (4, 20, 100, 500, 2500, 12 500), and the resulting colonies after 2 weeks cultivation were stained with hematoxylin/eosin (representative pictures) (A, B). Quantitative analysis revealed no difference in the colony-forming potential of cells from healthy and lipedema patients (C). n = 3 and 9.



*Adipose tissue biopsies*

Adipose tissue biopsies were excised from healthy and lipedema patients and stored in fixation buffer. Dehydration, paraffin embedding and staining with hematoxylin and eosin (H/E) were performed by the lab Dr. Edith Beck, institute for cytological, histological and bacteriological investigations (Linz, Austria).

*Statistical analysis*

Data are presented as mean  $\pm$  SD and statistical analysis was performed using PRISM6 (GraphPad), parametric two-tailed *t*-test or one-way analysis of variance Tukey's post hoc. *P* values < 0.05 were considered to be significant.

**Results***SVF isolation from lipedema patients results in a higher cell yield*

Comparison of the SVF cell yield per 100 mL of liposuction material revealed a significantly increased cell number when isolated from lipedema patients. Adipose tissue from lipedema patients yielded double the amount of cells compared with adipose tissue from healthy patients (Figure 1A). Viability of the freshly isolated cells was similar for healthy and lipedema patients (Figure 1B). ATP concentration of freshly isolated cells (Figure 1C) and after 1 week in culture (Figure 1D) was also similar for healthy and lipedema patients, but higher after 1 week in culture. Analysis of the

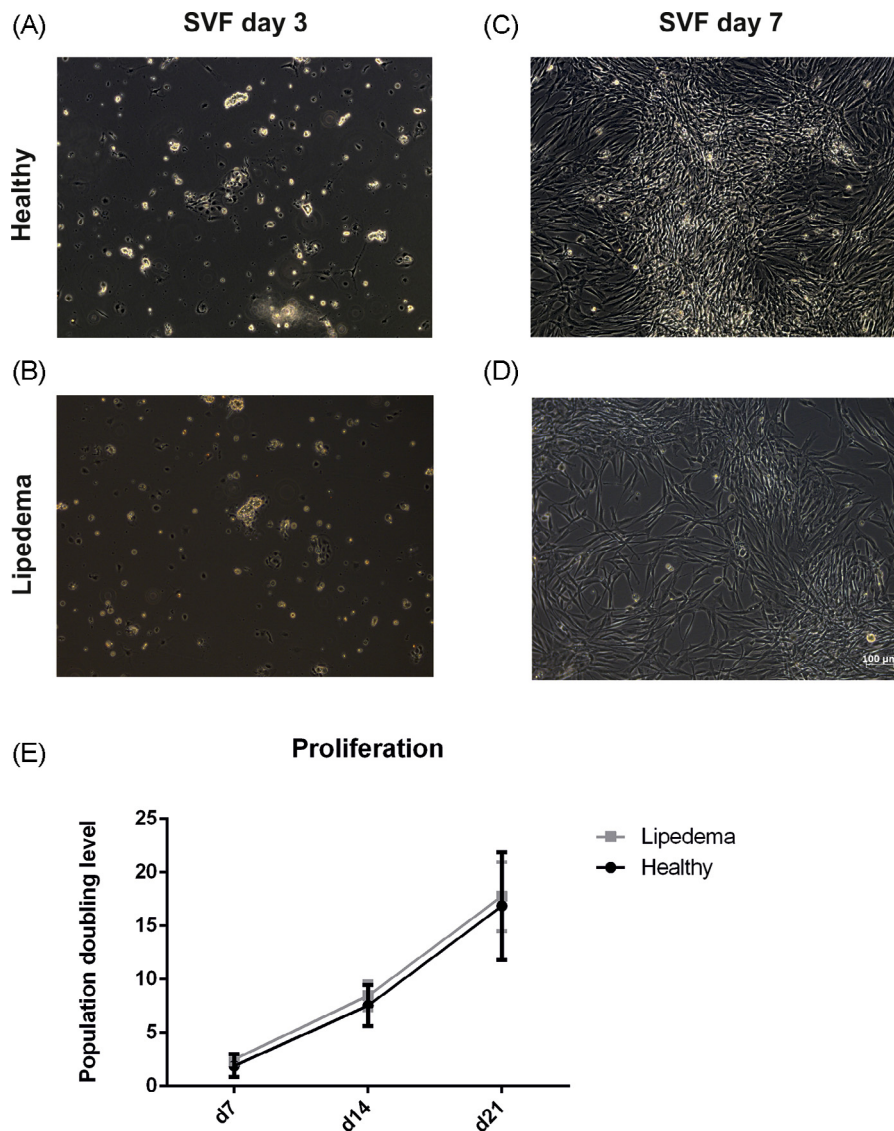


Figure 3. Morphology and proliferation potential. SVF cells derived from healthy and lipedema patients were examined by light microscopy after 3 (A, B) and 7 days (C, D) in expansion medium. Cells from both healthy and lipedema patients adhered to the plastic surface and showed spindle-shaped cell morphology. Size bar = 100  $\mu$ m (A–D). Analysis of the proliferation potential after 7, 14 and 21 days in expansion medium showed similar PDL of cells derived from healthy and lipedema patients (E). *n* = 12 and 11.

colony-forming capacity after 2 weeks in proliferation medium revealed no difference between cells derived from healthy or lipedema patients (Figure 2A–C).

Morphology of the isolated SVF cells was analyzed on day 3 (Figure 3A,B) and on day 7 (Figure 3C,D) of culture. Both cells from healthy and lipedema patients were able to adhere to the plastic surface and showed characteristic ASC spindle-shaped cell morphology on day 7 (Figure 3A–D). Cells from lipedema patients showed a minor but not significant increase of the PDL after 7, 14 and 21 days (Figure 3E).

#### *Immunophenotype is similar for healthy and lipedema patients*

The composition of the cellular phenotype in the SVF was similar for healthy and lipedema patients as analyzed by surface marker expression (Figure 4A).

Directly after SVF isolation, there was a minimal percentage of the monocyte/macrophage marker CD14 for healthy and lipedema patients. A higher percentage of SVF cells expressed the endothelial marker CD31 and the hematopoietic progenitor/vascular endothelial marker CD34. Less than 32% of SVF cells were positive for the hematopoietic marker CD45 for healthy and lipedema patients.

The percentage of mesenchymal marker was >30% for CD73 and CD105 and >50% for CD90 for SVF cells derived from healthy and lipedema patients. The expression levels of CD73 and CD105 were similar for healthy and lipedema patients. However, the number of CD90 cells was 12% higher for lipedema patients compared with healthy patients. Similarly, the expression level of the endothelial/pericytic marker CD146 was 20% higher for lipedema patients compared with healthy patients.

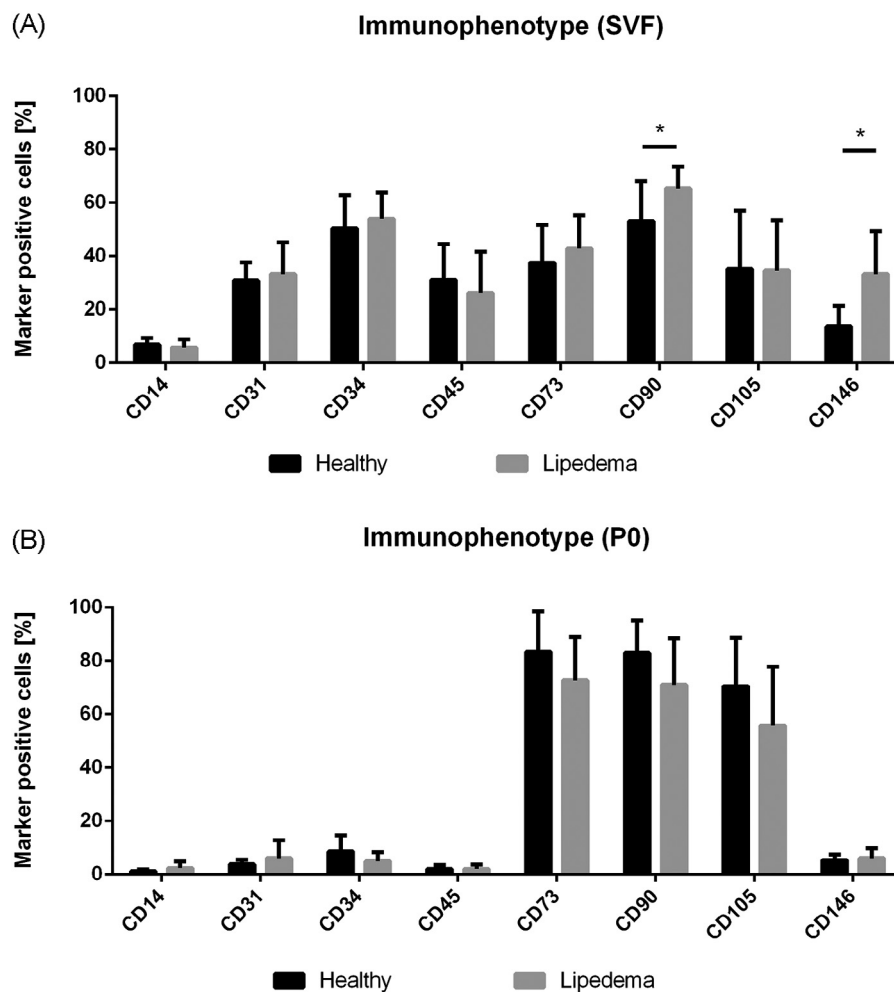


Figure 4. Surface marker profile of isolated cells. The composition of the cellular phenotype of SVF cells was similar between healthy and lipedema patients directly after isolation (A) ( $n = 3$  and  $20$ ) and after 1 week in culture (B) ( $n = 3$  and  $5$ ) as analyzed by flow cytometry of surface marker expression. The percentages of the mesenchymal stromal cell marker CD90 and the endothelial/pericytic marker CD146 were significantly increased in freshly isolated cells from lipedema patients compared with healthy patients (A). \* $P < 0.05$ .

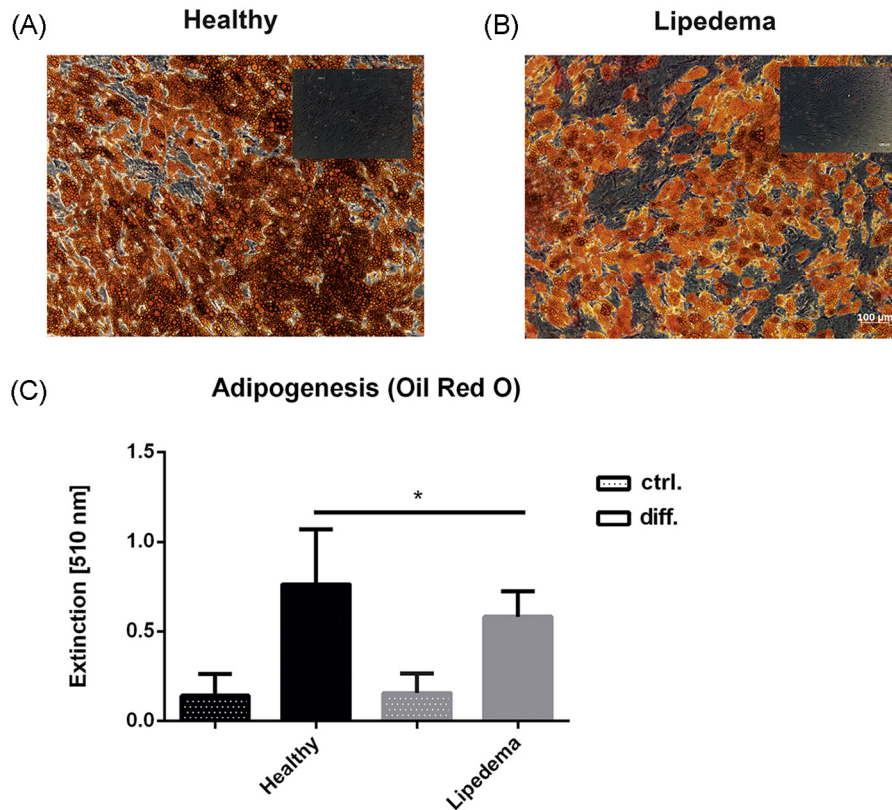


Figure 5. Adipogenic differentiation potential of isolated cells. *In vitro* adipogenic differentiation analyzed by oil red O staining 3 weeks after adipogenic induction was lower for lipedema patients compared to healthy patients (A, B), which was confirmed through quantitative analysis of the staining (C). Under differentiation conditions, the degree of lipid accumulation was significantly reduced in cells from lipedema patients compared with cultures from healthy patients. Small inserts show cells in control media (A, B). Cells in differentiation conditions showed a significant enhancement compared with undifferentiated cells in control media (C). ctrl., cells in control media without growth factors and stimuli; diff., cells in differentiation media. Size bar = 100  $\mu$ m; n = 11 and 13. \* $P < 0.05$ . (For interpretation of the references to colour in this figure legend, the reader is referred to the web version of this article.)

After 1 week in culture, the composition of the cellular phenotype was also similar for healthy and lipedema patients (Figure 4B). There was still a minimal percentage of cells positive for the monocyte/macrophage marker CD14 for healthy and lipedema patients. The endothelial marker CD31 and the hematopoietic progenitor/vascular endothelial marker CD34 were both reduced in regard to freshly isolated cells for healthy and lipedema patients. A minimal percentage of cells derived from healthy and lipedema patients expressed the hematopoietic marker CD45 after 1 week in culture.

In contrast to freshly isolated cells the percentage of mesenchymal stromal cell marker was clearly enhanced. For healthy patients, more than 80% of cells were positive for CD73 and CD90 and approximately 70% expressed CD105. For lipedema patients, more than 70% of cells expressed CD73 and CD90 and approximately 55% were positive for CD105. In contrast, the expression level of the endothelial/pericytic marker CD146 was reduced after 1 week in culture for healthy and lipedema patients.

#### Differentiation potential of cells derived from lipedema patients

Cells from healthy and lipedema patients were analyzed for their *in vitro* adipogenic, osteogenic and chondrogenic differentiation potential. Interestingly, cells from lipedema patients showed a reduced potential for adipogenic differentiation analyzed by oil red O staining (Figure 5A,B). This observation was confirmed by quantitative analysis of the staining with a significantly higher extinction for healthy patients than for lipedema patients (Figure 5C). Upon osteogenic induction, cells from healthy and lipedema patients showed equally high levels of alizarin red staining (Figure 6A,B), which was verified through quantitative analysis (Figure 6C). Similarly, analysis of ALP activity did not show a difference between healthy and lipedema patients (Figure 6D). Moreover, cells derived from both healthy and lipedema patients demonstrated a high chondrogenic differentiation potential illustrated by strong collagen type II and alcian blue staining of micromass

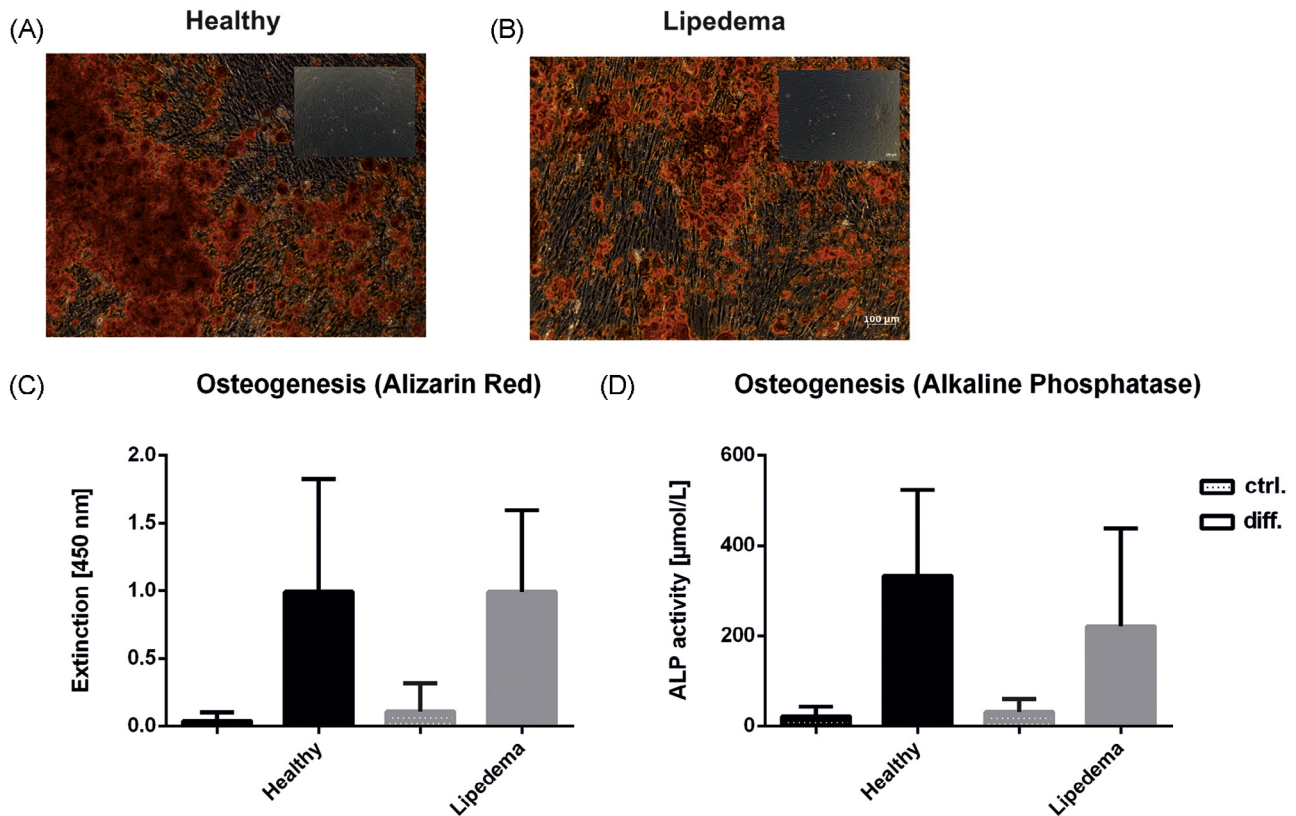


Figure 6. Osteogenic differentiation potential of isolated cells. *In vitro* osteogenic differentiation analyzed by alizarin red staining after 3 weeks of induction was similar for healthy and lipedema patients (A, B), which was confirmed through quantitative analysis of the staining (C) (n = 11 and 14) and alkaline phosphatase activity (D) (n = 11 and 13). Small inserts show cells in control media (A, B). Cells in differentiation conditions showed a significant enhancement compared to undifferentiated cells in control media (C, D). ctrl., cells in control media without growth factors and stimuli; diff., cells in differentiation media. Size bar = 100 µm. (For interpretation of the references to colour in this figure legend, the reader is referred to the web version of this article.)

pellets (Figure 7A–D). Analysis of the diameter area of the three-dimensional micromass pellets after 7, 14, 21, 28 and 35 days did not show significant differences for healthy and lipedema patients (Figure 7E).

#### Adipose tissue biopsies from healthy and lipedema patients

Adipose tissue biopsies were excised from healthy and lipedema patients and analyzed for their structure. H/E staining of adipose tissue biopsies from lipedema patients shows typical crown-like structures (Figure 8B) compared with biopsies from healthy patients (Figure 8A).

#### Discussion

Investigating the cell composition and property of lipedema compared with healthy adipose tissue might provide further understanding of this disease and insights into the possible etiology. In this comparison study, liposuction material from 52 women was

enzymatically digested and the SVF isolated. Comparison of the SVF cell yield revealed a significantly increased cell number when isolated from lipedema patients, whereas viability and ATP concentration showed no difference compared with healthy patients.

The potential of ASC to differentiate into the adipogenic, osteogenic and chondrogenic lineage (as defined by IFATS and ISCT) [28] could be demonstrated with cells from lipedema as well as healthy patients. However, regarding the adipogenic differentiation potential the degree of lipid vesicle accumulation upon adipogenic induction was significantly reduced in lipedema patients compared with healthy patients. Within the yielded SVF of lipedema patients, significantly higher cell numbers expressing the mesenchymal stromal cell marker CD90 and the endothelial/pericytic marker CD146 were found. In particular, approximately half of these cells are double positive expressing CD90<sup>+</sup>CD146<sup>+</sup> (data not shown) indicating the presence of a subpopulation of adipose stem cells originating from perivascular cells [30] and approximately 20% of these cells are CD146<sup>+</sup>CD31<sup>-</sup>CD45<sup>-</sup> (data not shown),

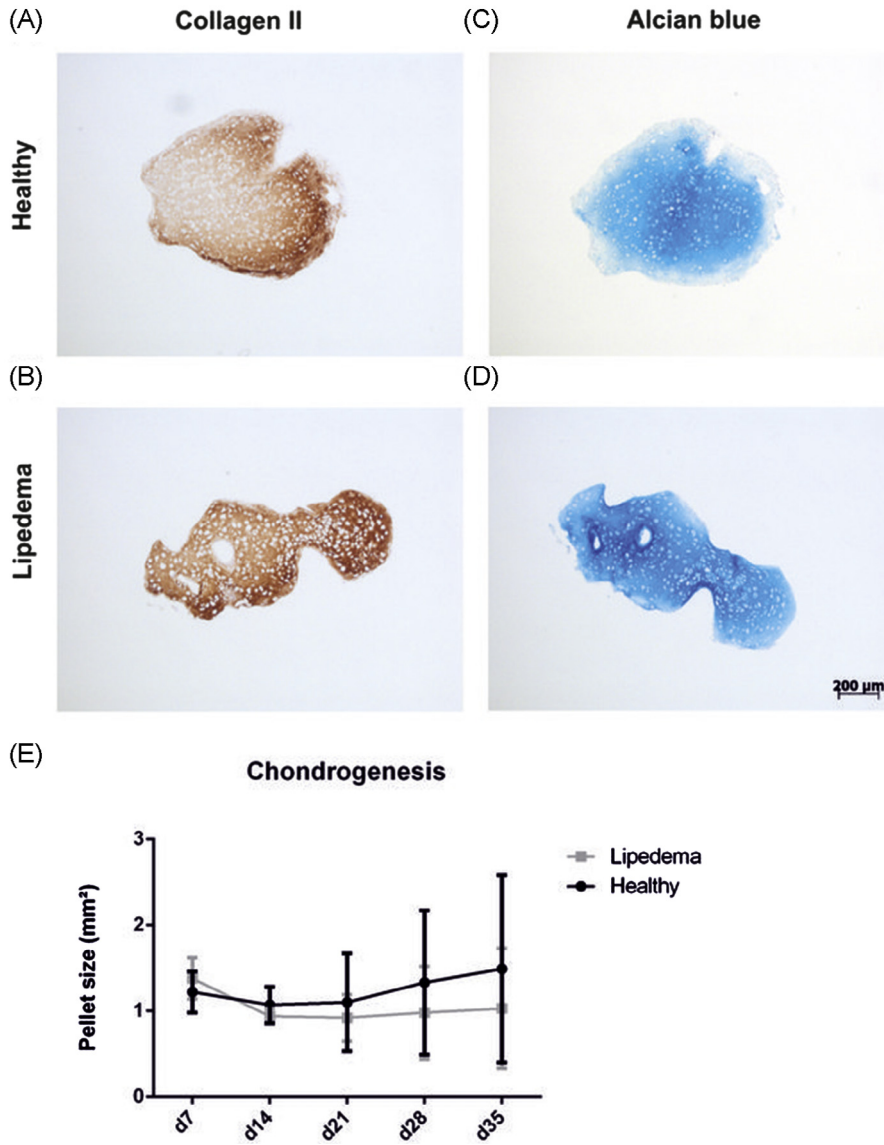


Figure 7. Chondrogenic differentiation potential of isolated cells. Cells derived from both healthy and lipedema patients showed a high chondrogenic differentiation potential when cultured in micromass pellets under inductive conditions for 5 weeks, as illustrated by strong collagen type II (A, B) and Alcian blue (C, D) staining. Analysis of the diameter area of the 3D micromass pellets after 7, 14, 21, 28 and 35 days did not show significant differences for healthy and lipedema patients (E). Size bar = 100  $\mu\text{m}$ ; n = 8. (For interpretation of the references to colour in this figure legend, the reader is referred to the web version of this article.)

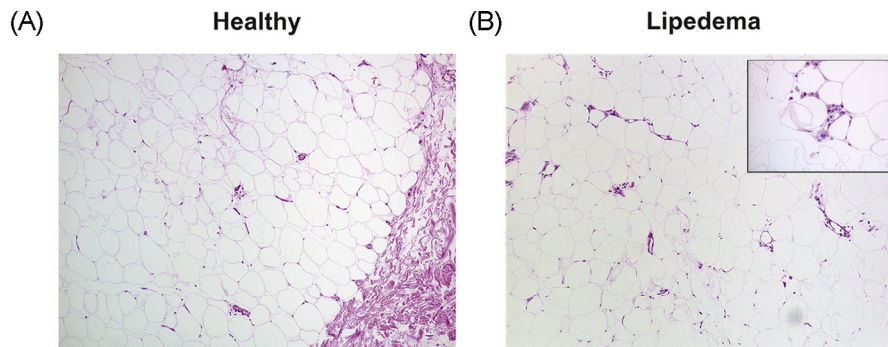


Figure 8. Adipose tissue from healthy and lipedema patients. H/E staining of adipose tissue biopsies from lipedema patients shows typical crown-like structures (B) compared with biopsies from healthy patients (A). Main images are 40 $\times$  magnification; the small insert is 100 $\times$  magnification.

a set of markers representing pericyte-like cells [31]. The enhanced number of CD90<sup>+</sup> and CD146<sup>+</sup> cells might explain the increased cell yield because the other tested surface marker were not reduced in lipedema patients.

Li *et al.* previously demonstrated that CD146<sup>+</sup> cells (pericyte subpopulation) exhibit a very low adipogenic differentiation potential compared with CD31<sup>-</sup>/CD34<sup>+</sup> cells (preadipocyte subpopulation) from adipose tissue [32]. Similarly, Hu *et al.* observed that the CD146<sup>+</sup> subpopulation of CD31<sup>-</sup>/CD34<sup>+</sup> cells (CD31<sup>-</sup>/CD34<sup>+</sup>/CD146<sup>+</sup>) showed a lower adipogenic potential compared with the CD146<sup>-</sup> subpopulation (CD31<sup>-</sup>/CD34<sup>+</sup>/CD146<sup>-</sup>) [33]. In contrast, James *et al.* found a higher osteogenic differentiation potential when sorting the SVF for CD146<sup>+</sup> cells from adipose tissue of healthy patients [34].

Adipocyte death and subsequent macrophage infiltration in lipedema could be explained by hypertrophy-induced hypoxia [25]. Bilkovski *et al.* also showed in human adipose tissue biopsies that adipocytes are surrounded by macrophages in crown-like structures. These observations were also found in our analyzed lipedema tissue biopsies showing typical crown-like structures. Moreover, macrophages were also found responsible for inhibiting adipogenesis of a mesenchymal precursor cell line via Wnt signaling molecules [35]. CD146 is up-regulated by enhanced tumor necrosis factor (TNF)-alpha level [36], which is secreted by macrophages and adipocytes shown in obese patients [37]. This is consistent with our findings about the increased number of CD146<sup>+</sup> cells and enhancement of crown-like structures in adipose tissue biopsies of lipedema patients.

These observations might be due to the fact that edematous tissue contains leaky lymphatic vessels. This leads to enhanced interstitial lymphatic fluid concomitant adipocyte growth, resulting in hypoxia and then microangiopathy, microaneurysm and lymphedema [38–41]. It has long been known that TNF-alpha and interleukin-6 are associated with obesity and type 2 diabetes by suppressing the insulin pathway [42]. Lipedema is a chronic injury of the capillaries that could be demonstrated by enhanced pericyte-like markers, which are responsible for repair of vessel damage after injuries [43].

In conclusion, we demonstrate that SVF cells from lipedema patients meet the characterization criteria for adipose tissue-derived cells postulated by ISCT and IFATS [28]. These cells may hence be a suitable option for autologous tissue regeneration strategies in lipedema patients.

**Disclosure of interest:** The authors have no commercial, proprietary, or financial interest in the products or companies described in this article.

## References

- [1] Allen E, Hines E. Mayo Clinic staff meetings: vascular clinics. Lipedema of the legs: a syndrome characterized by fat legs and orthostatic edema. *Proc Staff Meet Mayo Clin* 1940;15:184–7.
- [2] Wold LE, Hines JEA, Allen EV. Lipedema of the legs: a syndrome characterized by fat legs and edema. *Ann Intern Med* 1951;34:1243–50.
- [3] Fife CE, Maus EA, Carter MJ. Lipedema: a frequently misdiagnosed and misunderstood fatty deposition syndrome. *Adv Skin Wound Care* 2010;23:81–92, quiz 93–94.
- [4] Sandhofer M, Sandhofer M, Werner M, Marion L, Hofer V, Schauer P. The lipedema—when the subcutaneous fat rebels. *Kosmet Med* 2016;1:16.
- [5] Child AH, Gordon KD, Sharpe P, Brice G, Ostergaard P, Jeffery S, et al. Lipedema: an inherited condition. *Am J Med Genet A* 2010;152a:970–6.
- [6] Herbst KL. Rare adipose disorders (RADs) masquerading as obesity. *Acta Pharmacol Sin* 2012;33:155–72.
- [7] Herpertz U. Ödeme und Lymphdrainage: Diagnose und Therapie—Lehrbuch der Ödematologie. 5th Aufl. Stuttgart: Schattauer; 2014.
- [8] Okhovat JP, Alavi A. Lipedema: a review of the literature. *Int J Low Extrem Wounds* 2015;14:262–7.
- [9] Kaiserling E. Morphologische Befunde beim Lymphödem, Lipödem, Lipolymphödem. In: Földi M, Földi E, Kubik S, editors. *Lehrbuch der Lymphologie*. Stuttgart, New York: Gustav Fischer; 2005. p. 374–8.
- [10] Brenner E. Plasma—interstitielle Flüssigkeit—Lymph. *Lymphforsch* 2009;13:25–7.
- [11] Harwood CA, Bull RH, Evans J, Mortimer PS. Lymphatic and venous function in lipoedema. *Br J Dermatol* 1996;134:1–6.
- [12] Beninson J, Edelglass JW. Lipedema—the non-lymphatic masquerader. *Angiology* 1984;35:506–10.
- [13] Herpertz U. Krankheitsspektrum des Lipödems an einer Lymphologischen Fachklinik—Erscheinungsformen, Mischbilder und Behandlungsmöglichkeiten. *Vasomed* 1997;5:301–7.
- [14] Szolnoky G, Borsos B, Barsony K, Balogh M, Kemeny L. Complete decongestive physiotherapy with and without pneumatic compression for treatment of lipedema: a pilot study. *Lymphology* 2008;41:40–4.
- [15] Szolnoky G, Nagy N, Kovacs RK, Dosa-Racz E, Szabo A, Barsony K, et al. Complex decongestive physiotherapy decreases capillary fragility in lipedema. *Lymphology* 2008; 41:161–6.
- [16] Baumgartner A, Hueppe M, Schmeller W. Long-term benefit of liposuction in patients with lipoedema: a follow-up study after an average of 4 and 8 years. *Br J Dermatol* 2016;174:1061–7.
- [17] Peled AW, Slavin SA, Brorson H. Long-term outcome after surgical treatment of lipedema. *Ann Plast Surg* 2012;68:303–7.
- [18] Rappich S, Dingler A, Podda M. Liposuction is an effective treatment for lipedema—results of a study with 25 patients. *J Dtsch Dermatol Ges* 2011;9:33–40.
- [19] Sandhofer M. Radial shockwave therapy after cryolipolysis™ in cellulite and lymphedema—a field report. *Cosmet Med* 2015;12–13.
- [20] Schmeller W, Hüppe M, Meier-Vollrath I. Liposuction in lipoedema yields good longterm results. *Br J Dermatol* 2012;166:161–8.
- [21] Stutz JJ, Krahl D. Water jet-assisted liposuction for patients with lipoedema: histologic and immunohistologic analysis of the aspirates of 30 lipoedema patients. *Aesthetic Plast Surg* 2009;33:153–62.

- [22] Mayes JS, Watson GH. Direct effects of sex steroid hormones on adipose tissues and obesity. *Obes Rev* 2004;5:197–216.
- [23] Gavin KM, Cooper EE, Hickner RC. Estrogen receptor protein content is different in abdominal than gluteal subcutaneous adipose tissue of overweight-to-obese premenopausal women. *Metabolism* 2013;62:1180–8.
- [24] Kang Q, Song WX, Luo Q, Tang N, Luo J, Luo X, et al. A comprehensive analysis of the dual roles of BMPs in regulating adipogenic and osteogenic differentiation of mesenchymal progenitor cells. *Stem Cells Dev* 2009;18:545–59.
- [25] Suga H, Araki J, Aoi N, Kato H, Higashino T, Yoshimura K. Adipose tissue remodeling in lipedema: adipocyte death and concurrent regeneration. *J Cutan Pathol* 2009;36:1293–8.
- [26] Földi M, Földi E, Kubik S. *Lehrbuch der Lymphologie*. Stuttgart, New York: Gustav Fischer; 2005.
- [27] Szolnoky G, Nemes A, Gavaller H, Forster T, Kemeny L. Lipedema is associated with increased aortic stiffness. *Lymphology* 2012;45:71–9.
- [28] Bourin P, Bunnell BA, Casteilla L, Dominici M, Katz AJ, March KL, et al. Stromal cells from the adipose tissue-derived stromal vascular fraction and culture expanded adipose tissue-derived stromal/stem cells: a joint statement of the International Federation for Adipose Therapeutics and Science (IFATS) and the International Society for Cellular Therapy (ISCT). *Cytotherapy* 2013;15:641–8.
- [29] Wolbank S, Peterbauer A, Fahrner M, Hennerbichler S, van Griensven M, Stadler G, et al. Dose-dependent immunomodulatory effect of human stem cells from amniotic membrane: a comparison with human mesenchymal stem cells from adipose tissue. *Tissue Eng* 2007;13:1173–83.
- [30] Cai X, Lin Y, Hauschka PV, Grottkau BE. Adipose stem cells originate from perivascular cells. *Biol Cell* 2011;103:435–47.
- [31] Zimmerlin L, Donnenberg VS, Pfeifer ME, Meyer EM, Peault B, Rubin JP, et al. Stromal vascular progenitors in adult human adipose tissue. *Cytometry A* 2010;77:22–30.
- [32] Li H, Zimmerlin L, Marra KG, Donnenberg VS, Donnenberg AD, Rubin JP. Adipogenic potential of adipose stem cell subpopulations. *Plast Reconstr Surg* 2011;128:663–72.
- [33] Hu L, Yang G, Hagg D, Sun G, Ahn JM, Jiang N, et al. IGF1 promotes adipogenesis by a lineage bias of endogenous adipose stem/progenitor cells. *Stem Cells* 2015;33:2483–95.
- [34] James AW, Zara JN, Zhang X, Askarinam A, Goyal R, Chiang M, et al. Perivascular stem cells: a prospectively purified mesenchymal stem cell population for bone tissue engineering. *Stem Cells Transl Med* 2012;1:510–19.
- [35] Bilkovski R, Schulte DM, Oberhauser F, Mauer J, Hampel B, Gutschow C, et al. Adipose tissue macrophages inhibit adipogenesis of mesenchymal precursor cells via wnt-5a in humans. *Int J Obes (Lond)* 2011;35:1450–4.
- [36] Ueda M, Fujisawa T, Ono M, Hara ES, Pham HT, Nakajima R, et al. A short-term treatment with tumor necrosis factor- $\alpha$  enhances stem cell phenotype of human dental pulp cells. *Stem Cell Res Ther* 2014;5:31.
- [37] Vachharajani V, Vital S. Obesity and sepsis. *J Intensive Care Med* 2006;21:287–95.
- [38] Harvey NL, Srinivasan RS, Dillard ME, Johnson NC, Witte MH, Boyd K, et al. Lymphatic vascular defects promoted by Prox1 haploinsufficiency cause adult-onset obesity. *Nat Genet* 2005;37:1072–81.
- [39] Karkkainen MJ, Saaristo A, Jussila L, Karila KA, Lawrence EC, Pajusola K, et al. A model for gene therapy of human hereditary lymphedema. *Proc Natl Acad Sci USA* 2001;98:12677–82.
- [40] Schneider M, Conway EM, Carmeliet P. Lymph makes you fat. *Nat Genet* 2005;37:1023–4.
- [41] Szel E, Kemeny L, Groma G, Szolnoky G. Pathophysiological dilemmas of lipedema. *Med Hypotheses* 2014;83:599–606.
- [42] Dandona P, Aljada A, Bandyopadhyay A. Inflammation: the link between insulin resistance, obesity and diabetes. *Trends Immunol* 2004;25:4–7.
- [43] Tigges U, Komatsu M, Stallcup WB. Adventitial pericyte progenitor/mesenchymal stem cells participate in the restenotic response to arterial injury. *J Vasc Res* 2013;50:134–44.